AD-A066 543 ROCKWELL INTERNATIONAL CANOGA PARK CALIF ROCKETDYNE DIV F/G 21/5
INTEGRATED POWER UNIT.(U)
DEC 78 G S WONG, T I YU, J J WARD F33615-76-C-2054
UNCLASSIFIED RI/RD78-237 AFAPL-TR-78-98 NL

1 OF 3
AD
A066543

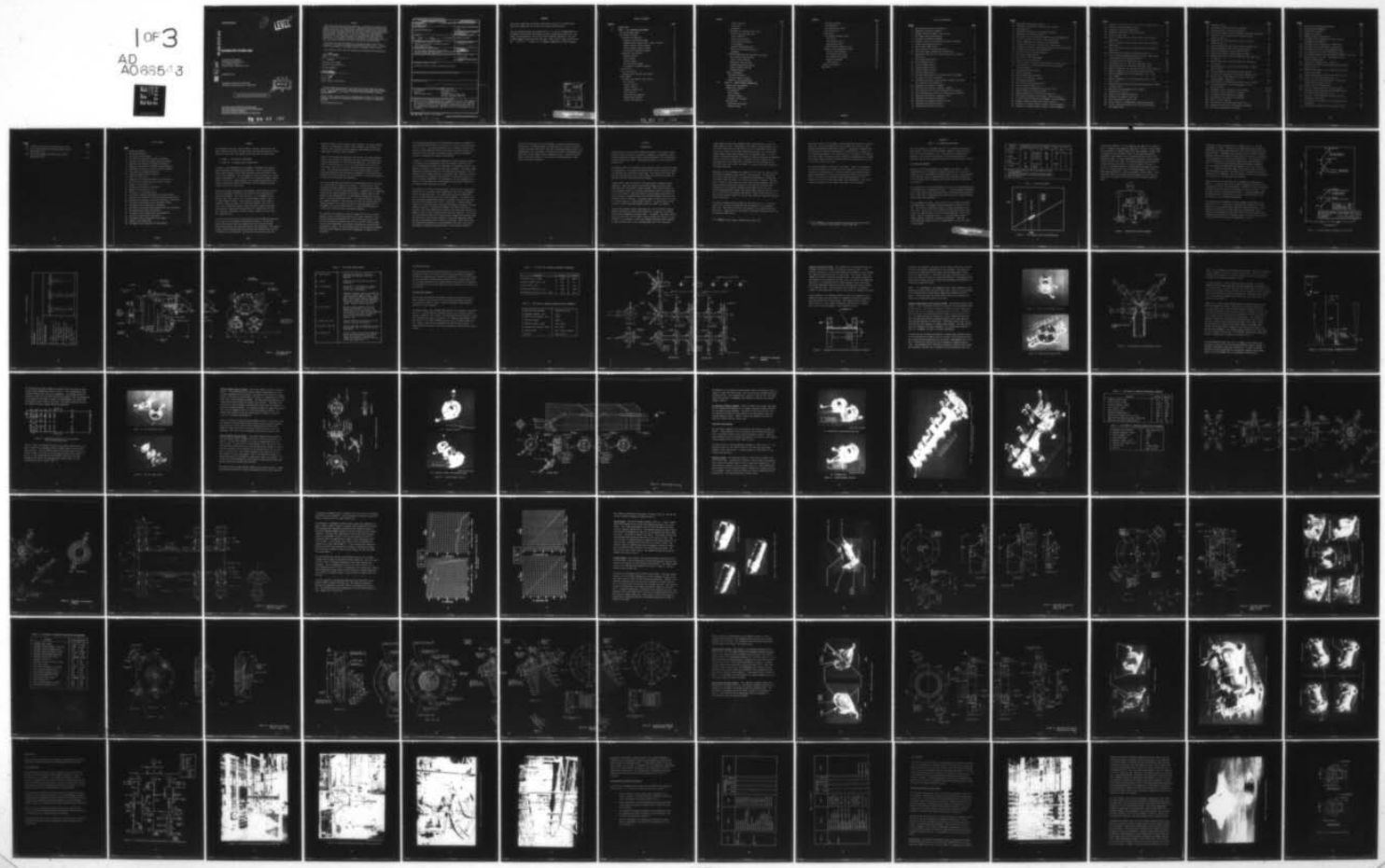

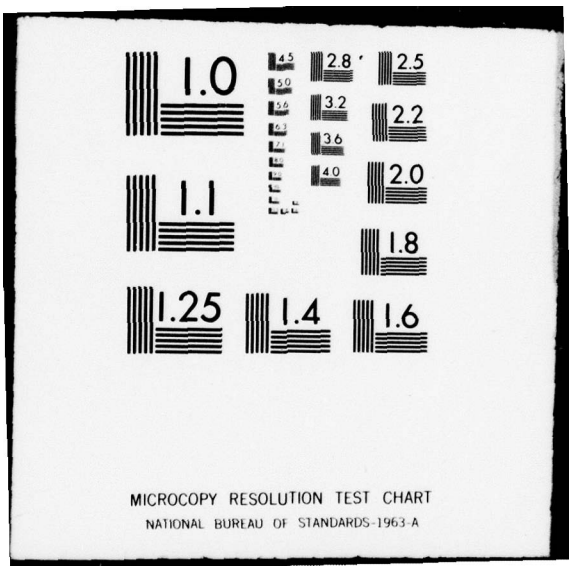
1.0
1.1
1.25
1.4
1.6
1.8
2.0
2.2
2.5
2.8
3.2
3.6
4.0
4.5
5.0
5.6
MICROCOPY RESOLUTION TEST CHART
NATIONAL BUREAU OF STANDARDS-1963-A

AFAPL-TR-78-98

LEVEL II

AD A066543

DDC FILE COPY

INTEGRATED POWER UNIT

ROCKETDYNE DIVISION
ROCKWELL INTERNATIONAL
6633 CANOGA AVENUE
CANOGA PARK, CALIFORNIA 91304

DECEMBER 1978

TECHNICAL REPORT AFAPL-TR-78-98
Final Report for Period April 1976 – August 1978

AIR FORCE AERO PROPULSION LABORATORY
AIR FORCE WRIGHT AERONAUTICAL LABORATORIES
AIR FORCE SYSTEMS COMMAND
WRIGHT-PATTERSON AIR FORCE BASE, OHIO 45433

NOTICE

When Government drawings, specifications, or other data are used for any purpose other than in connection with a definitely related Government procurement operation, the United States Government thereby incurs no responsibility nor any obligation whatsoever; and the fact that the government may have formulated, furnished, or in any way supplied the said drawings, specifications, or other data, is not to be regarded by implication or otherwise as in any manner licensing the holder or any other person or corporation, or conveying any rights or permission to manufacture, use, or sell any patented invention that may in any way be related thereto.

This report has been reviewed by the Information Office (OI) and is releasable to the National Technical Information Service (NTIS). At NTIS, it will be available to the general public, including foreign nations.

This technical report has been reviewed and is approved for publication.

B. L. McFadden

B. L. McFadden

Technical Area Manager

Auxiliary Power Generation

FOR THE COMMANDER

W. F. Bailey

W. F. Bailey

Major, USAF

Chief, Vehicle Power Branch

If your address has changed, if you wish to be removed from our mailing list, or if the addressee is no longer employed by your organization please notify AFAPL/POP *, W-PAFB, OH 45433 to help us maintain a current mailing list.*

Copies of this report should not be returned unless return is required by security considerations, contractual obligations, or notice on a specific document.

AIR FORCE/56780/22 March 1979 — 145

(9) Final rept. 16 Apr 76 - 31 Jul 78,

SECURITY CLASSIFICATION OF THIS PAGE (When Data Entered)

(19) **REPORT DOCUMENTATION PAGE**

READ INSTRUCTIONS BEFORE COMPLETING FORM

1. REPORT NUMBER (18) AFAPL-TR-78-98	2. GOVT ACCESSION NO.
3. RECIPIENT'S CATALOG NUMBER	
4. TITLE (and Subtitle) (4) INTEGRATED POWER UNIT,	5. TYPE OF REPORT & PERIOD COVERED: Final (16 April 1976 to 31 July 1978)
6. PERFORMING ORG. REPORT NUMBER (14) RI/RD78-237	
7. AUTHOR(s) (10) G. S. Wong, J. J. Ward, J. A. Williams, T. I. Yu, R. L. Binsley	8. CONTRACT OR GRANT NUMBER(s) (15) F33615-76-C-2054
9. PERFORMING ORGANIZATION NAME AND ADDRESS: Rockwell International, Rocketdyne Division, 6633 Canoga Avenue, Canoga Park, CA 91304	10. PROGRAM ELEMENT, PROJECT, TASK AREA & WORK UNIT NUMBERS (16) 3145 01 31 (17) 01
11. CONTROLLING OFFICE NAME AND ADDRESS: Air Force Aero Propulsion Laboratory/POP-1, Air Force Wright Aeronautical Laboratories (AFSC), Wright-Patterson AFB, Ohio 45433	12. REPORT DATE (11) December 1978
	13. NUMBER OF PAGES: 242
14. MONITORING AGENCY NAME & ADDRESS (if different from Controlling Office) (12) 255 P.	15. SECURITY CLASS. (of this report): Unclassified
	15a. DECLASSIFICATION/DOWNGRADING SCHEDULE

16. DISTRIBUTION STATEMENT (of this Report)

Approved for public release; distribution unlimited

17. DISTRIBUTION STATEMENT (of the abstract entered in Block 20, if different from Report)

18. SUPPLEMENTARY NOTES

Accessory Power Units (APU) and Emergency Power Units (EPU)

19. KEY WORDS (Continue on reverse side if necessary and identify by block number)

Gas Generator
GOX/JP-4
Aircraft Engine Starter
Propellant Injector
Gas Turbine
Aircraft Auxiliary Power Unit
Aircraft Integrated Power Unit

20. ABSTRACT (Continue on reverse side if necessary and identify by block number)

Results of a development program for an Integrated Power Unit (IPU) combining the functions of the ~~APU and EPU power units~~ for the aircraft are presented. The design and testing of two gas generators using gaseous oxygen (GOX) and JP-4 propellants are discussed. Subsequent design and test results for an IPU engine starter demonstrator that used one of the gas generators are also presented.

DD FORM 1 JAN 73 1473 EDITION OF 1 NOV 65 IS OBSOLETE

SECURITY CLASSIFICATION OF THIS PAGE (When Data Entered)

390 199

JOB

FOREWORD

This report summarizes the design, fabrication, and test of a LOX/JP-4 gas generator system which can be used for aircraft auxiliary power.

The work described herein was directed by Mr. A. D. Lucci, Program Manager, at Rocketdyne International's Rocketdyne Division, Canoga Park, California. The project was sponsored by the Air Force Aero-Propulsion Laboratory, Air Force Systems Command, Wright-Patterson AFB, Ohio, under Project, Task, and Work Unit No. 3145 01 31 with Mr. B. L. McFadden, AFAPL/POP, as Project Manager.

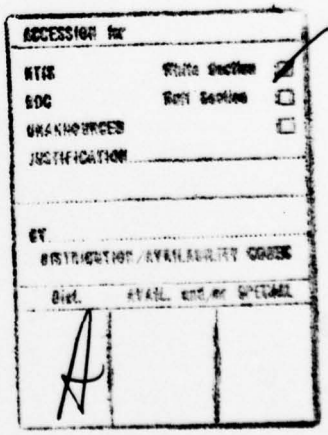

TABLE OF CONTENTS

SECTION PAGE

LIST OF ILLUSTRATIONS

LIST OF TABLES

SUMMARY

The Integrated Power Unit (IPU) program, to develop a LOX/JP-4 gas generator system for aircraft auxiliary power, was conducted between 16 April 1976 and 31 July 1978. The program was divided into two major phases:

- Phase I: Gas Generator Development
- Phase II: IPU Engine Starter Demonstrator

In Phase I, two gas generators were designed, fabricated, and tested to verify performance and demonstrate feasibility. The two gas generator units, when integrated into an auxiliary power system, provided a range of 10 to 300 horsepower. Each gas generator can be throttled over a power range of approximately 3 to 1 and operate at a combustion chamber pressure from 91 to 290 psia. Correspondingly, the low-power gas generator total flowrate varied from 0.089 to 0.280 lb/sec, and the high-power gas generator from 0.232 to 0.749 lb/sec.

During the low-power gas generator development, three different injector types were designed, fabricated, and tested with the gas generator to evaluate performance. The three types were: (1) an augmented spark ignition (ASI) type injector, (2) a triplet-element injector, and (3) a coaxial-element injector. Each injector was tested over a range of combustion chamber pressure (75 to 350 psia), mixture ratio (0.23 to 1.26), and two combustor lengths (6 and 10 inches), and the performance characteristics experimentally evaluated were: combustion efficiency (c*), ignition, combustion stability, carbon formation, and heat transfer characteristics.

A total of 311 hot-fire tests were achieved on the low-power gas generator for a total of 7035 seconds of steady-state operation. The ASI-type injector was found to have poor ignition and local heating problems. Both GOX-tube burnout and choke-ring erosion were encountered. The coaxial-element injector had good ignition and local heat problems which resulted in combustor wall burnthrough. High ignition energy was required for

ignition; however, carbon formation was a minimum. The triplet-element injector, in combination with the 10-inch combustor and increased contraction ratio, achieved reliable ignition, good combustion, uniform temperature, and modest carbon formation.

Based on the low-power gas generator test results, the triplet-element injector was selected for additional testing to determine ignition and combustion performances at the following conditions: cold propellants (GOX at -240 F and JP-4 at -60 F); hot propellants (135 F); low-cut (volatility) fuel (JP-8 or Jet A); and high-altitude condition (74,000 feet). The low-power gas generator with the triplet-element injector achieved good ignition and combustion performance at all the above environmental and fuel conditions, and was selected for further developmental testing with the high-power gas generator.

Test of the high-power gas generator was accomplished with 112 tests and over 1200 seconds of steady-state operation. Initial hot-fire tests encountered unstable combustion particularly at the throttled operating conditions (75 to 50% of normal power level). Although use of a purge-gas lead and choke ring eliminated the instability problem caused by poor mixing, direct modifications of the gas generator design were investigated. The three modifications were : (1) a partial sleeve to decrease the combustor diameter at the injector and reduce the recirculation of combustion gases; (2) a premix cup plate to increase mixing; and (3) enlargement of the GOX injector orifice to reduce the GOX injection velocity and increase the fuel penetration parameter.

The high-power gas generator, using the enlarged GOX orifice, triplet-element injector, achieved good ignition and stable combustion at all throttled operating conditions down to 50% normal power level. The c* efficiency obtained was greater than 90% over the full throttle range of operation investigated, and combustion temperatures correlated well with expected values. The design modification also resulted in formation of softer carbon deposits that did not accumulate, but tended to be stabilized.

The high-power gas generator also achieved good ignition and combustion with cold propellants (GOX at -170 F and JP-4 at -70 F) and low-cut fuels (JP-8 or Jet A). Localized overheating on the combustor wall near the injector was encountered (which was overcome by increased combustor coolant jacket flow) that must be resolved through further developmental efforts in optimizing the injector spray pattern.

In Phase II, fully utilizing the experimental results obtained in Phase I, a IPU engine starter demonstrator unit was designed, fabricated, and tested to demonstrate further the feasibility of utilizing a LOX/JP-4 gas generator reliably in an aircraft-type power equipment. The engine starter demonstrator assembly consisted of the high-power gas generator with the modified triplet-element injector; an available power turbine; an off-the-shelf gearbox; and a flywheel load simulator to simulate a typical aircraft jet engine (CFM56-2B). The demonstrator unit was designed with a capability of developing over 200 horsepower and attaining a gearbox output speed of 8000 rpm within 25 seconds.

The planned 10 hot-fire, full-acceleration start tests were successfully achieved by the IPU engine starter demonstrator unit with no disassembly and only normal inspection. An eleventh test was made to demonstrate that no afterburning occurred in the turbine exhaust. Full engine start was consistently demonstrated within 25.5 seconds, with output power and speed of 228 horsepower and 7777 rpm, respectively. Posttest hardware inspection of the gas generator and turbine revealed no anomalies and good hardware integrity. Gas generator combustor wall heat stains were as expected. Soft carbon deposits were found in the turbine nozzles and rotor blades, as well as those normally found within the combustor. The effects of carbon formation within the turbine nozzle passages was observed during the testing as a test-to-test "sawtooth" trace of gas generator chamber pressure, indicating alternate buildup and spalling. These effects were not considered detrimental to the performance of the unit, but further development consideration should be made to reduce carbon formation.

The overall objectives of the IPU program, to prove the feasibility and practicality of using available on-board LOX and JP-4 fuel for aircraft-mounted, auxiliary power units, have been successfully demonstrated by the experimental tests performed on the LOX/JP-4 low-power and high-power gas generators and the engine starter demonstrator unit. Continued development is indicated, however, in the areas of optimizing injector spray pattern and carbon formation.

SECTION I

INTRODUCTION

Modern military aircraft require significant amounts of "secondary" power. Such power may be electrical, hydraulic, pneumatic, or mechanical, and is directly provided by engine-driven accessory gearboxes or by air-breathing accessory power units (APU). Engine starting power is often provided by ground carts.

An important trend in providing aircraft secondary power is the drive toward self-sufficiency. This means that each aircraft will be completely capable of providing all its auxiliary power needs. The aircraft then could land and take off again from a "bare base" without the need for any ground cart services, and only refueling would be required.

Another recent trend in aircraft is the major need for emergency power capability. Many new aircraft are control-configured vehicles, which means they have "fly-by-wire" control systems. Such control systems require continuous supply of electrical and hydraulic power to maintain control of the aircraft. When any portion of the secondary power system is lost in flight, an immediate means for providing alternate electrical and hydraulic power is required. An extreme example of this would be the loss of the main engine in a single-engine fighter. To provide power at high altitude a nonair-breathing emergency power unit (EPU) is required.

Another major emergency power requirement has to do with modern engines. Windmill starting of a modern fanjet engine is, in general, not feasible without some supplementary starting power. In general, this power requirement is in the 100 to 200 hp range. Since an engine may flame out at any altitude, it is necessary to have this emergency starting power available at high altitudes where an air-breathing power unit is not practical.

A good example of all these emergency power characteristics is the F-16 single-engine aircraft. Restarting of the engine following flameout can be done below 20,000 feet altitude where the air is sufficiently dense that the jet fuel starter can provide enough starting power. At all altitudes engine flameout would cause complete loss of secondary power. For this reason a hydrazine-fueled EPU is provided to produce electrical and hydraulic power in the event of engine loss. This EPU also has a capability for providing power in the event that the engine is still operating but the secondary power system itself has failed. In that case the EPU operates on the engine bleed air.

Beginning in 1974, Rocketdyne was funded by the Air Force to study aircraft secondary and emergency power needs for future aircraft. The results of this study, presented in Ref. 1,* showed the desirability of integrating the various power functions of the aircraft as much as possible. The goal was to provide a single power unit which would provide emergency power for engine starting and aircraft operation at altitudes up to 80,000 feet. Comparison of the possible propellants which might be used for such a nonair-breathing machine showed that liquid oxygen (LOX) and jet fuel (JP-4, JP-5, or JP-8) were an excellent combination. These fluids, which are on many current aircraft and are in the Air Force logistics system, are therefore natural selections.

The present program was the followup to the study of Ref. 1. It has the objective of proving the feasibility and practicality of an integrated power unit (IPU) which can serve a dual purpose of the normal APU and EPU power units. Demonstration of low specific propellant consumption also was an important design factor.

---

* 1. Emergency Power Supply, AFAPL-TR-75-9, April 1975.

During the course of this program, a further advanced concept of an aircraft power unit, the Superintegrated Power Unit (SIPU), was conceived. This concept is described in more detail in Ref. 2. Basically it combines both air-breathing and nonair-breathing modes of operation into a single piece of multipurpose machinery. With this concept it is possible to consider an even wider range of possible aircraft secondary and emergency power systems. The present program therefore has developed basic data applicable not only to the IPU but also to the SIPU.

The present program was conducted in two phases. Phase I was initiated with systems analysis of a typical IPU which produced a set of design requirements for gas generators. This was followed by an extensive experimental demonstration of both low- and high-power LOX/JP-4 gas generators. Phase II consisted of the detailed design and experimental test of a demonstration IPU that would meet engine start requirements. This report presents the results of both Phase I and Phase II of the program.

2. B. L. McFadden, the Super-Integrated Power Unit--The Aircraft Power Unit of the Future, AIAA Paper No. 77-502, March 1977

SECTION II

PHASE I: GAS GENERATOR DEVELOPMENT

The IPU gas generator development phase of the program is presented in this section. The IPU system requirements leading to design specifications for two gas generators, viz., a low-power and a high-power gas generator, are discussed; the designs for both gas generators are presented; and the test programs and results for both are given in detail.

IPU SYSTEM REQUIREMENTS

The basic IPU design requirements are summarized in Table 1 . These requirements do not represent any specific aircraft, but rather are a composite of the requirements of several modern aircraft. They represent a wide possible range of required power levels and modes of operation. It is not likely that any single aircraft would require all these modes of operation.

The required duty cycle and operational life in each of the possible modes of operation also is summarized in Table 1. The environmental temperature and altitude ranges under which power must be provided are also presented there. This set of requirements then forms the basis for the preliminary system design work performed.

The requirements of Table 1 show a ratio of 12.5 between the minimum and maximum power requirements during gas generator operation of the IPU. This implies a throttling range on a single gas generator of at least 10:1. Since that is not a practicable range with today's technology, the approach taken is to use two gas generators to cover this range. This is illustrated in Fig. 1 . The total power range is divided between a high- and low-power gas generator. Thus, the throttling range required on each is approximately 3:1 on flow, which is practicable.

Modes of Operation	Output Shaft hp Required*	Run Time per Cycle	Endurance,** cycles	Altitude, feet	Temperature, F
Auxiliary					
Checkout	100	10 minutes	1000	<8,000	+500 to -65
	20	60 minutes	1000	↓	↓
Standby	85	60 minutes	1000	↓	↓
Engine Start	250	30 seconds	2000	↓	↓
Emergency					
In-Flight Start	150	20 seconds	10	<80,000	↓
Flyback	20	3 hours	10	↓	↓
	100***	3 hours	10	↓	↓

*Net output after deduction of all required parasitic loads, including heaters
**The endurance column above is defined as the total cycles in each mode that the IPU is to perform between major overhauls
***Bleed air operation

Table 1. Design Requirements

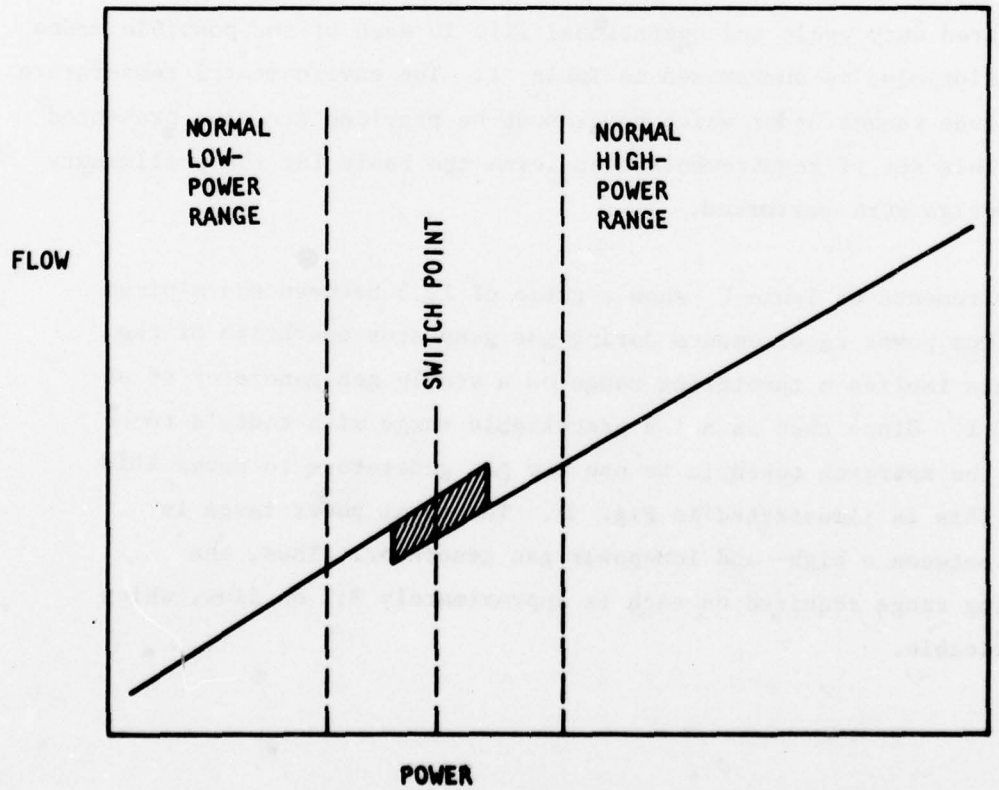

Figure 1. IPU Operation With Two Gas Generators

A simplified schematic of an IPU using two gas generators is shown in Fig. 2. Oxygen for gas generator operation is stored as liquid oxygen then vaporized in a turbine exhaust duct heat exchanger. Oxygen vapor is burned with fuel in either a high- or low-power gas generator, depending on power demand. Fuel is supplied initially either from a pressurized source or, after operation is initiated, it may be pumped from the aircraft fuel tank. The alternate engine bleed air mode of turbine operation (see Table 1) is also provided for in Fig. 2. In Fig. 2, the engine bleed air is shown passing through a different part of the turbine from that for the exhaust gases of the low- or high-power gas generator. This is discussed in detail below. In all operational modes, the turbine drives the engine for start and the accessories for hydraulic and electrical power through a gearbox as shown.

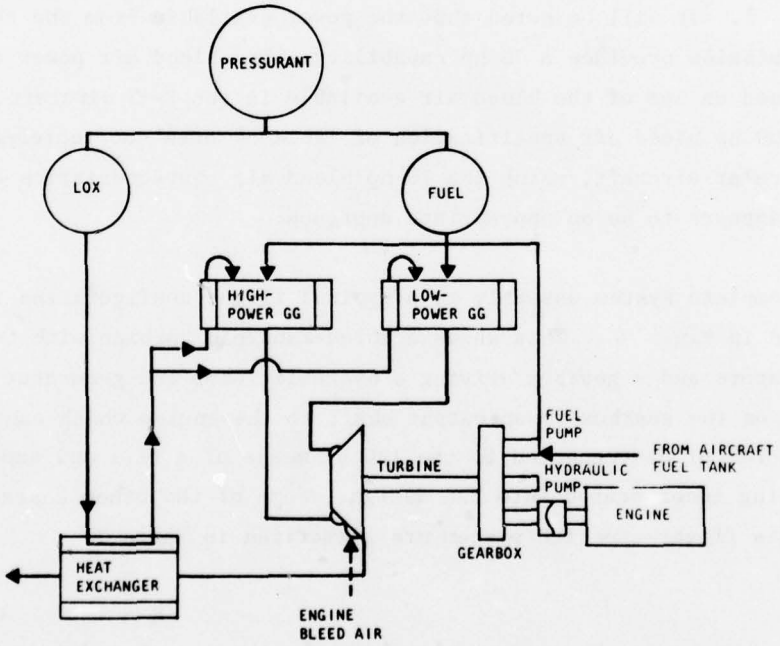

Figure 2. Simplified IPU System Schematic

Preliminary sizing calculations for the system of Fig. 2 and the requirements of Table 1 show that the turbine nozzle throat areas required for the two gas generators and for the bleed air operations were quite different. Therefore, three different sets of nozzles or arcs of admission within the turbine are used, which allow each arc of admission to be optimized for its particular energy source. The results of the system calculations on a three-arc-of-admission system are shown in Fig. 3 . The throttling performance during gas generator operation for the low-power and high-power gas generator arcs is also shown in Fig. 3 . The throat area data shown at the bottom of Fig. 3 indicate the requirements in terms of the bleed air arc of admission and the gas generator arcs of admission. The air requires a throat area approximately four times that of the high-power gas generator.

Design point data for the three arcs of admission are summarized in Table 2. It will be noted that the power available from the third arc of admission provides a 70 hp capability. The bleed air power calculation is based on use of the bleed air available in the F-16 aircraft. Since the 100 hp bleed air specification of Table 1 does not represent any particular aircraft, using the 70 hp bleed air characteristics of the F-16 appears to be an appropriate approach.

The complete system assembly in a typical flight configuration is presented in Fig. 4 . This shows a three-manifold turbine with two gas generators and a gearbox driving a hydraulic pump and generator. Also shown on the gearbox is an output shaft to the engine which can be connected or disconnected to the IPU by means of a fill and empty fluid coupling incorporated into the design. Some of the other characteristics of this flight-type IPU system are summarized in Table 3.

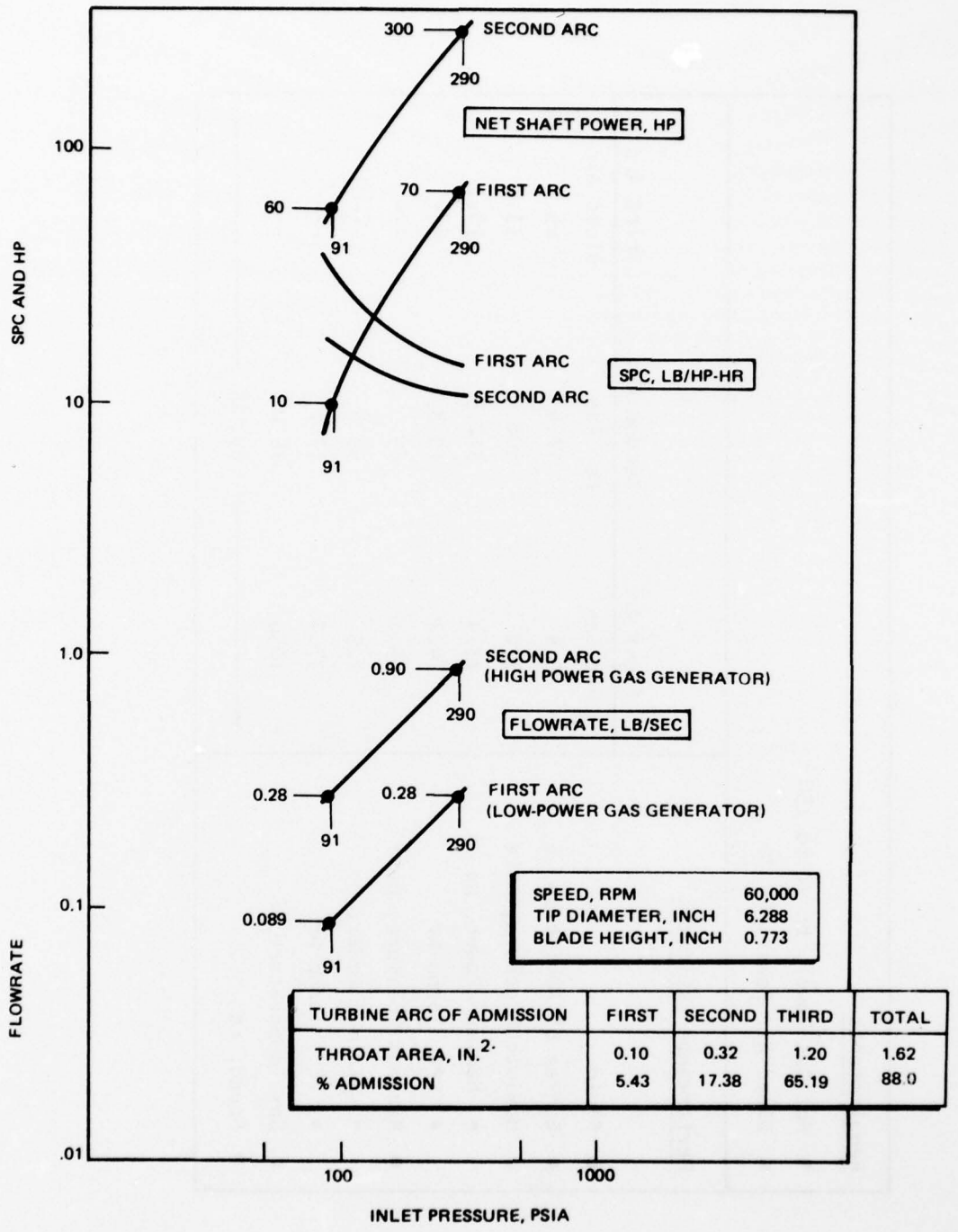

TURBINE ARC OF ADMISSION	FIRST	SECOND	THIRD	TOTAL
THROAT AREA, IN.^{2}	0.10	0.32	1.20	1.62
% ADMISSION	5.43	17.38	65.19	88.0

Figure 3 . Optimum Turbine Performance, Hot Gas Only

TABLE 2. IPU DESIGN PARAMETERS

Requirements

- Hot Gas Power, hp 20 to 250
- Bleed Air Power, hp 70

Performance Estimates

	First Arc	Second Arc	Third Arc
• Fluid	Hot Gas	Hot Gas	Bleed Air
• Degree of Admission, %	5.4	17.4	65.2
• Maximum Pressure, psia	300	300	33.5
• Maximum Power, hp	73.4	312.5	78.1
• SPC, lb/hp-hr	14.3	10.8	---
• Minimum Pressure, psia	85	85	---
• Minimum Power, hp	7.9	53.8	---
• SPC, lb/hp-hr	37.7	17.7	---
• Gas Temperature, F	1650	1650	---
• Speed, rpm	← 60,000 →		

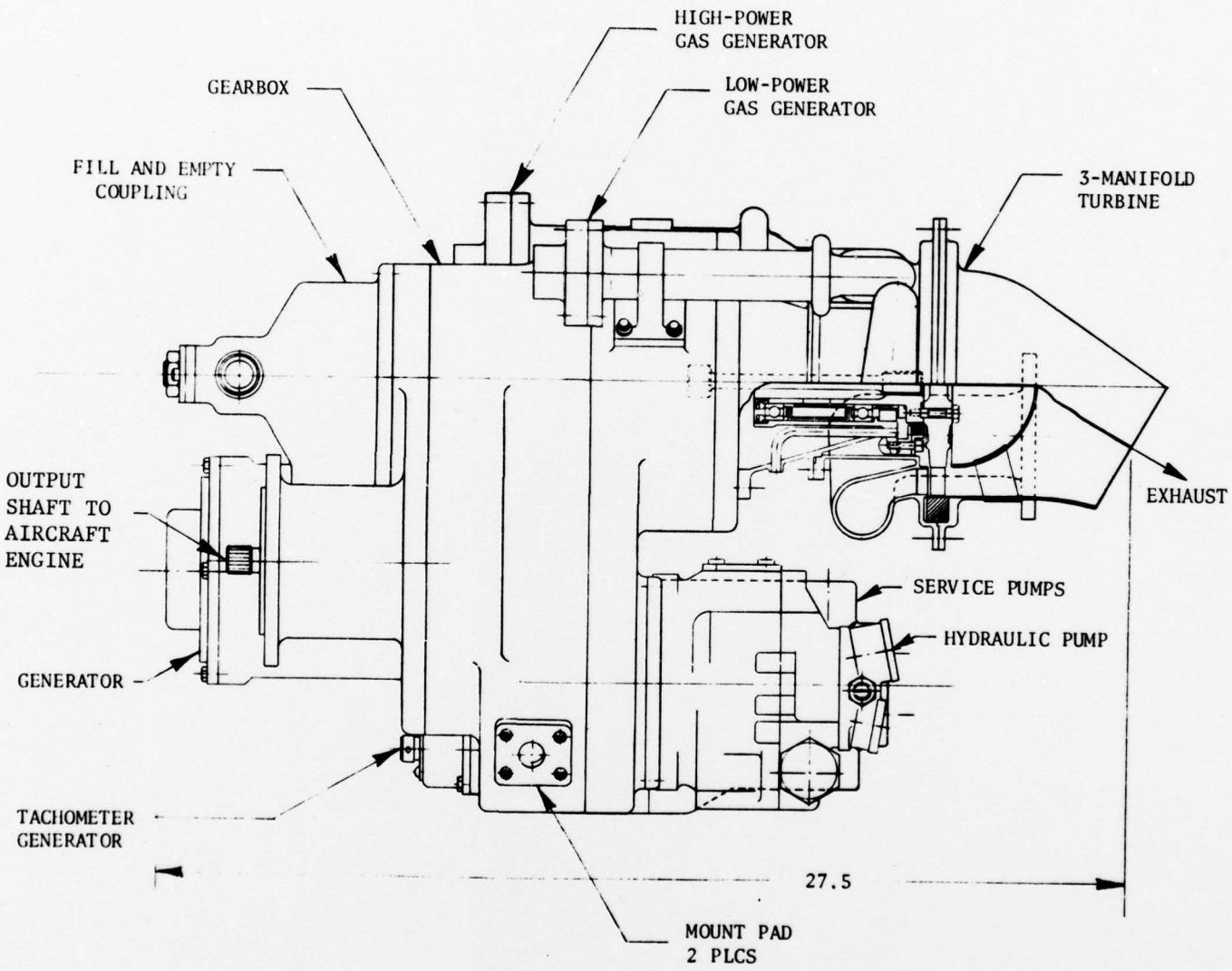
HIGH-POWER
GAS GENERATOR
GEARBOX
LOW-POWER
GAS GENERATOR
FILL AND EMPTY
COUPLING
3-MANIFOLD
TURBINE
OUTPUT
SHAFT TO
AIRCRAFT
ENGINE
EXHAUST
SERVICE PUMPS
HYDRAULIC PUMP
GENERATOR
TACHOMETER
GENERATOR
27.5
MOUNT PAD
2 PLCS

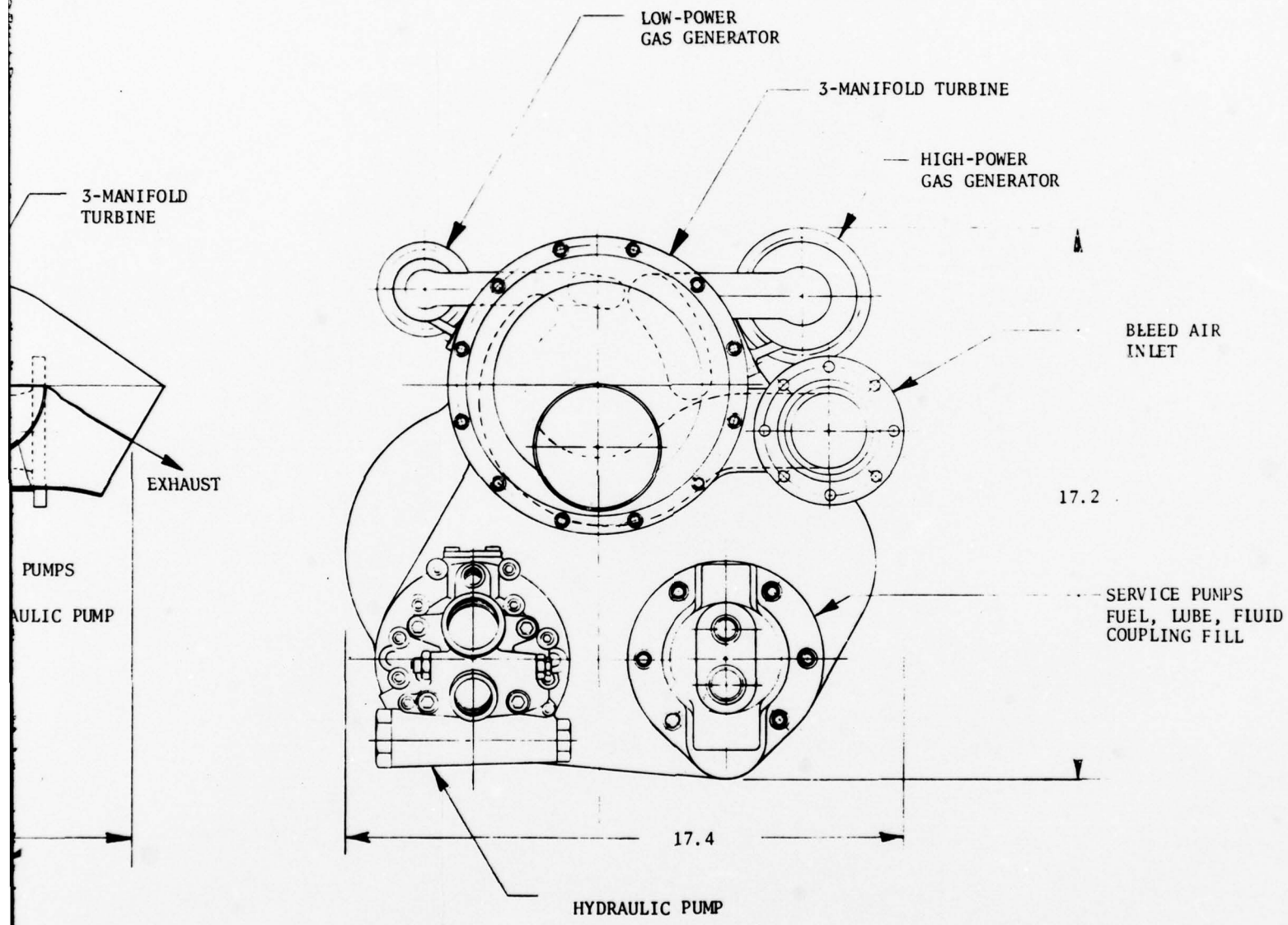

Figure 4 . IPU Flight System Configuration

2

TABLE 3. IPU FLIGHT SYSTEM PACKAGE

• Power Source	Low-Power Gas Generator (LOX/JP-4) High-Power Gas Generator (LOX/JP-4) Bleed Air
• Turbine	Three-Manifold Optimum Design 300 hp at 60,000 rpm
• Fluid Coupling	Pressure-fill, self-emptying, 250 hp at 15,000 rpm. Custom mount to provide direct drain into gearbox.
• Gearbox	Planetary reduction stage from 60,000 rpm turbine to 15,000 rpm main shaft. Single-stage reduction to 8400 rpm engine start pad. Multiple gear stages to accommodate speeds and locations of other components. Full-pressure lubrication with dry sump system. Integral system mount pads.
• Service Pumps	Multiple element assembly using four gerotor-type elements: one for lube scavenging, one for lube pressure, one for coupling fill and one for gas generator fuel. Custom mount pad to gearbox to provide direct scavenging without external line.
• Engine Start Pad	250 hp at 8400 rpm configuration to meet customer interface requirements.
• Hydraulic Pump Pad	57 hp at 3750 rpm, and 20002 pad for Abex model AP10V-7 pump or equivalent 30 gpm at 3000 psi.
• Generator Pad	9 hp at 12,000 rpm for IDG-type generator 5kva with constant-speed drive removed. Custom pad to provide front bearing support for generator (normally provided by constant-speed drive).

GAS GENERATOR DESIGN

The IPU system design requirements described in the previous section and presented in Table 1 were used to define the gas generator requirements for both the high-power and low-power gas generators. The initial designs for the low-power and high-power gas generators are presented below. Some of the design parameters were slightly modified during the test program for each gas generator, and these modifications are described in the respective test sections.

Low-Power Gas Generator

The low-power gas generator performance parameters are given in Table 4. These parameters are consistent with the system requirements discussed in the previous section. Table 5 gives the hardware design parameters selected for test evaluation.

The design layout of the low-power gas generator test hardware is presented in Fig. 5. The gas generator assembly consists of an injector, spark igniters, a combustor, and a nozzle. The gas generator was designed to accept the following three types of injectors: (1) augmented spark igniter (ASI) type injector, (2) triplet-element injector, and (3) coaxial-element injector. Figure 5 shows the unit assembled with the ASI-type injector. A bolted assembly was used to allow easy disassembly and modification during testing.

TABLE 4. LOW-POWER GAS GENERATOR PERFORMANCE PARAMETERS

Parameter	Maximum	Minimum
Flowrate (w_{tot}), lb/sec	0.280	0.089
Chamber Pressure (P_c), psia	290	91
Mixture Ratio (o/f)	0.54	0.62
Combustion Temperature (T_c), F	1650	1650
Characteristic Velocity (c*), ft/sec	3314	3314

TABLE 5. LOW-POWER GAS GENERATOR HARDWARE DESIGN PARAMETERS

Combustor Heat Exchanger	GOX Spiral Circuit
Combustor Diameter, inch	1.00
Nozzle Throat Diameter, inch	0.357
Contraction Ratio	7.85:1
Combustor Length, inches	6.00, 10.00
Characteristic Length, inches	47.1, 78.5
Injector Types	ASI, Triplet, Coaxial
Ignition	Spark Igniter

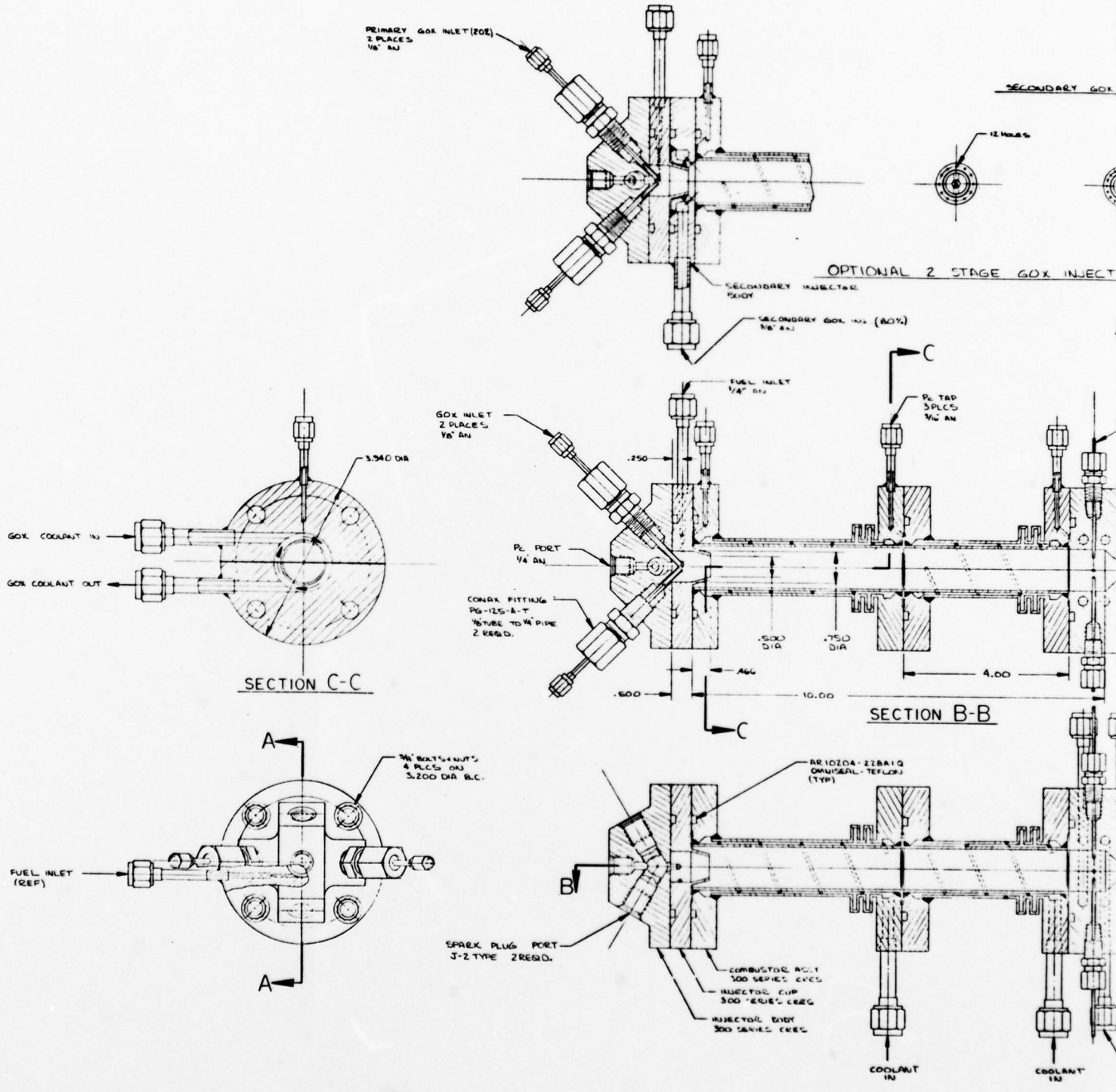
PRIMARY GOX INLET (FOR)
2 PLACES
1/8" AN
SECONDARY GOX
12 HOLES
OPTIONAL 2 STAGE GOX INJECT
SECONDARY INJECTOR BODY
SECONDARY GOX INJ (80%)
3/8" AN
C
FUEL INLET
1/4" AN
Pc TAP
3 PLCS
3/16" AN
GOX INLET
2 PLACES
1/8" AN
.250
3.540 DIA
GOX COOLANT IN
GOX COOLANT OUT
Pc PORT
1/4 AN
CONAX FITTING
PG-125-A-T
1/8 TUBE TO 1/4 PIPE
2 REQ'D.
.500 DIA
.750 DIA
.666
4.00
.500
10.00
C
SECTION C-C
SECTION B-B
A
3/8" BOLTS + NUTS
4 PLCS ON
3.200 DIA B.C.
FUEL INLET
(REF)
A
AR 1020A-22BA1Q
OMNISEAL-TEFLON
(TYP)
B
SPARK PLUG PORT
J-2 TYPE 2 REQ'D.
COMBUSTOR ASY
300 SERIES CRES
INJECTOR CUP
300 SERIES CRES
INJECTOR BODY
300 SERIES CRES
COOLANT IN
COOLANT IN
SECTION A-A

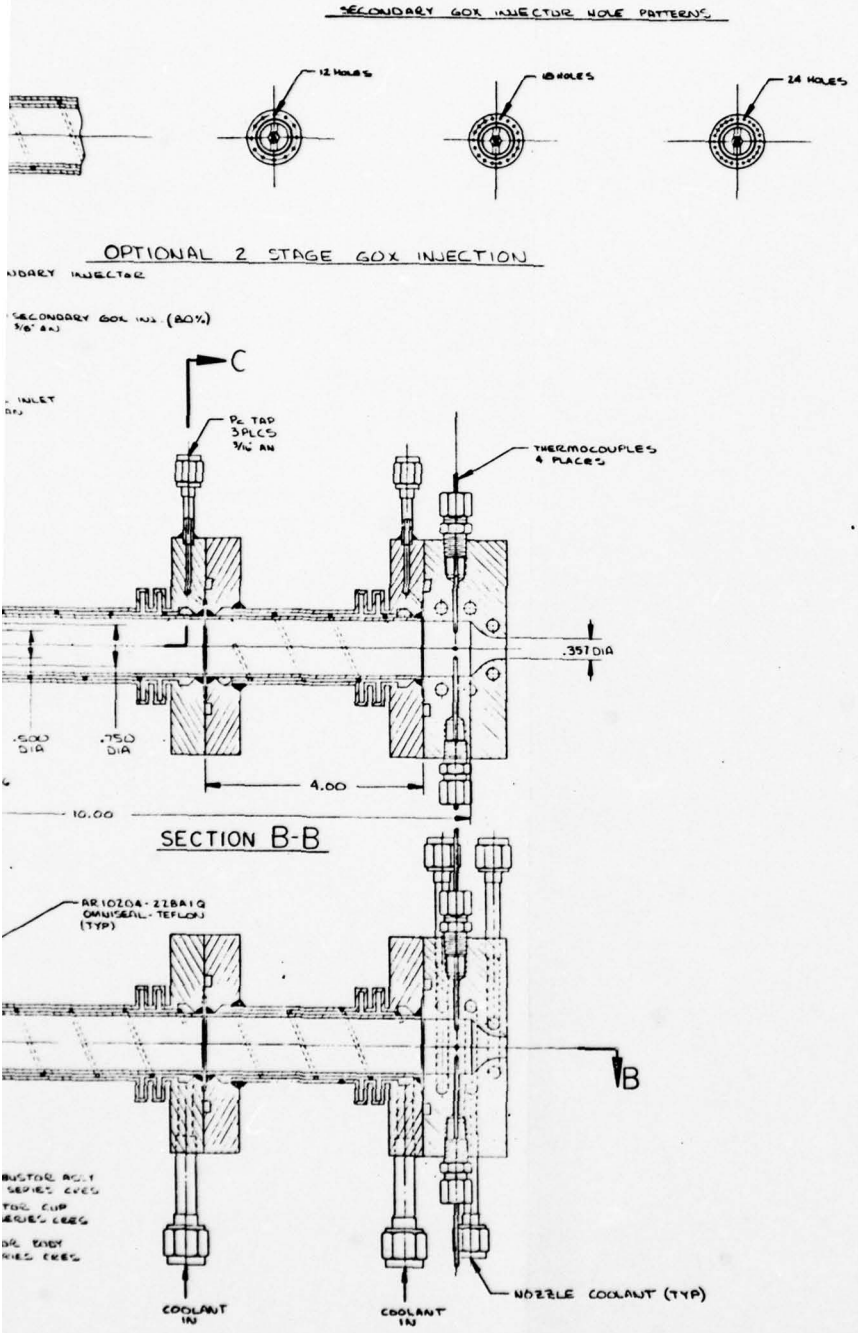

Figure 5. Low-Power Gas Generator Assembly

Combustor and Nozzle Designs. The combustor was a double-walled GOX heat exchanger design with a spiral coolant path as shown in Fig. 5. Two combustor sections of 4- and 6-inch lengths were designed to allow changing the combustor length from 6.00 to 10.00 inches. The coolant circuit and flanges were made of 300 series stainless steel. The spiral coolant path was formed by a wire brazed to the inner tube. The spiral flow scheme was retained in the flange manifolds by using tangential inlets and outlets. This scheme minimized pressure drop while providing good coolant velocity in the manifold areas. Pressure ports were provided in the combustor flanges to allow measurement of injector and nozzle end combustor pressures.

Stress analysis of the combustor showed the need for an expansion joint between the inner and outer shells to accommodate differential expansion and avoid buckling on the inner shell. This expansion joint, shown in detail in Fig. 6 , was a simple configuration machined as an integral part of one of the end flanges of each combustor section.

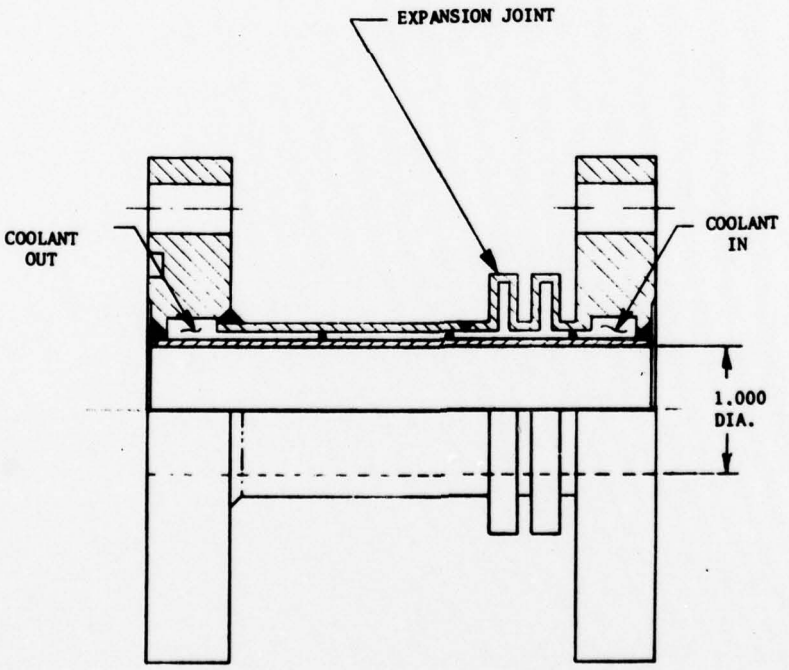

Figure 6. Expansion Joint for Low-Power Gas Generator Combustor

The nozzle was designed to simulate the IPU turbine nozzles and to provide a location for hot-gas thermocouples for test purposes. The nozzle was constructed of OFHC copper with a simple drilled passage water coolant circuit as shown in Fig. 5. The nozzle was sized to provide the IPU turbine nozzle area and to hold the hot gas thermocouples. Packing gland type thermocouple fittings are used to allow easy replacement and adjustment of thermocouple penetration depth.

Figure 7 is a photograph of the completed 6-inch cooled combustor section showing the coolant (GOX) inlet and outlet tubes. Figure 8 is a photograph of the completed water-cooled nozzle looking from upstream toward the throat. The coolant inlet and outlet tubes as well as the pressure and temperature instrumentation ports can be seen.

Augmented Spark Igniter (ASI) Injector Design. The ASI-type injector shown in Fig. 5 was a scaled-down version of a previously tested Rocketdyne GOX-RP ASI injector. The injector consists of a small cup with a single tangential fuel orifice providing a swirling flow on the walls. The GOX is injected through self-impinging tubular elements into the center of the cup. The spark igniters are recessed in a cavity beneath the GOX tubes. This configuration provides an ignitable mixture at the spark igniters while keeping them free of liquid fuel. Propellants from the ASI injector discharge into the combustor to complete their burning. The GOX injection tubes are designed to be easily replaced, or to permit their insertion depth to be changed, in order to optimize performance.

A modification to the basic ASI injector to promote more efficient mixing of fuel and oxidizer is shown at the top of Fig. 5 and in detail in Fig. 9 This design uses two-stage injection of the GOX. Approximately 20% of the GOX is injected into the ASI cup, still providing an ignitable mixture ratio. The remaining 80% of the GOX is injected in a ring of holes around the periphery of the ASI cup to impinge on the swirling hollow cone fuel

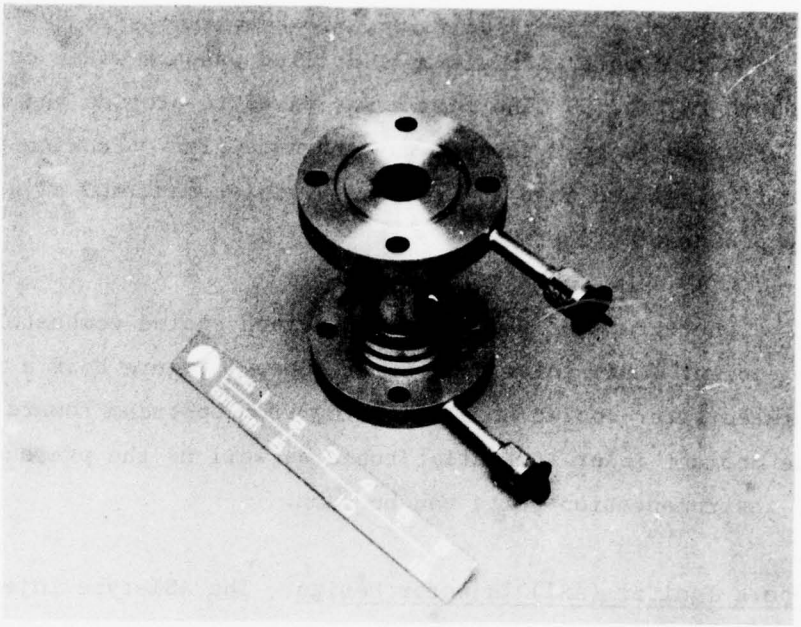

Figure 7. 6-Inch Cooled Combustor Section

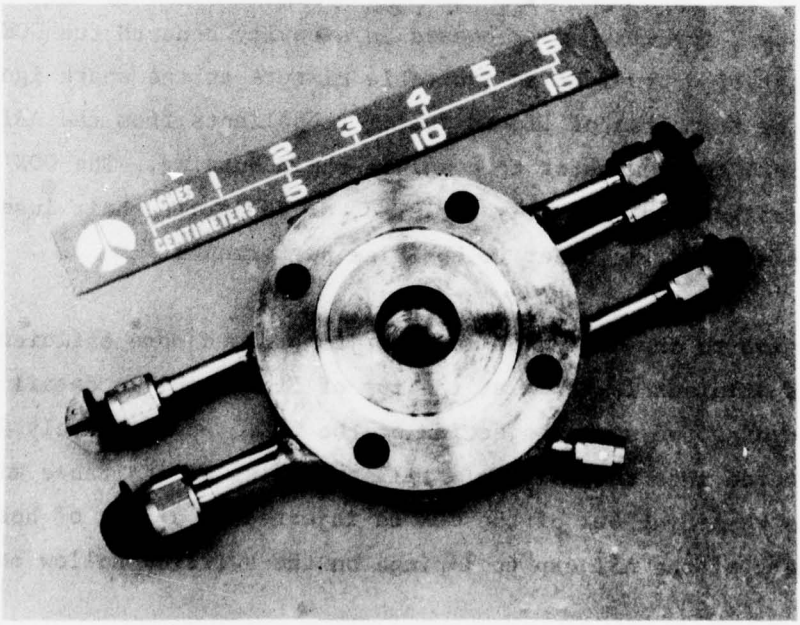

Figure 8. Water-Cooled Copper Nozzle

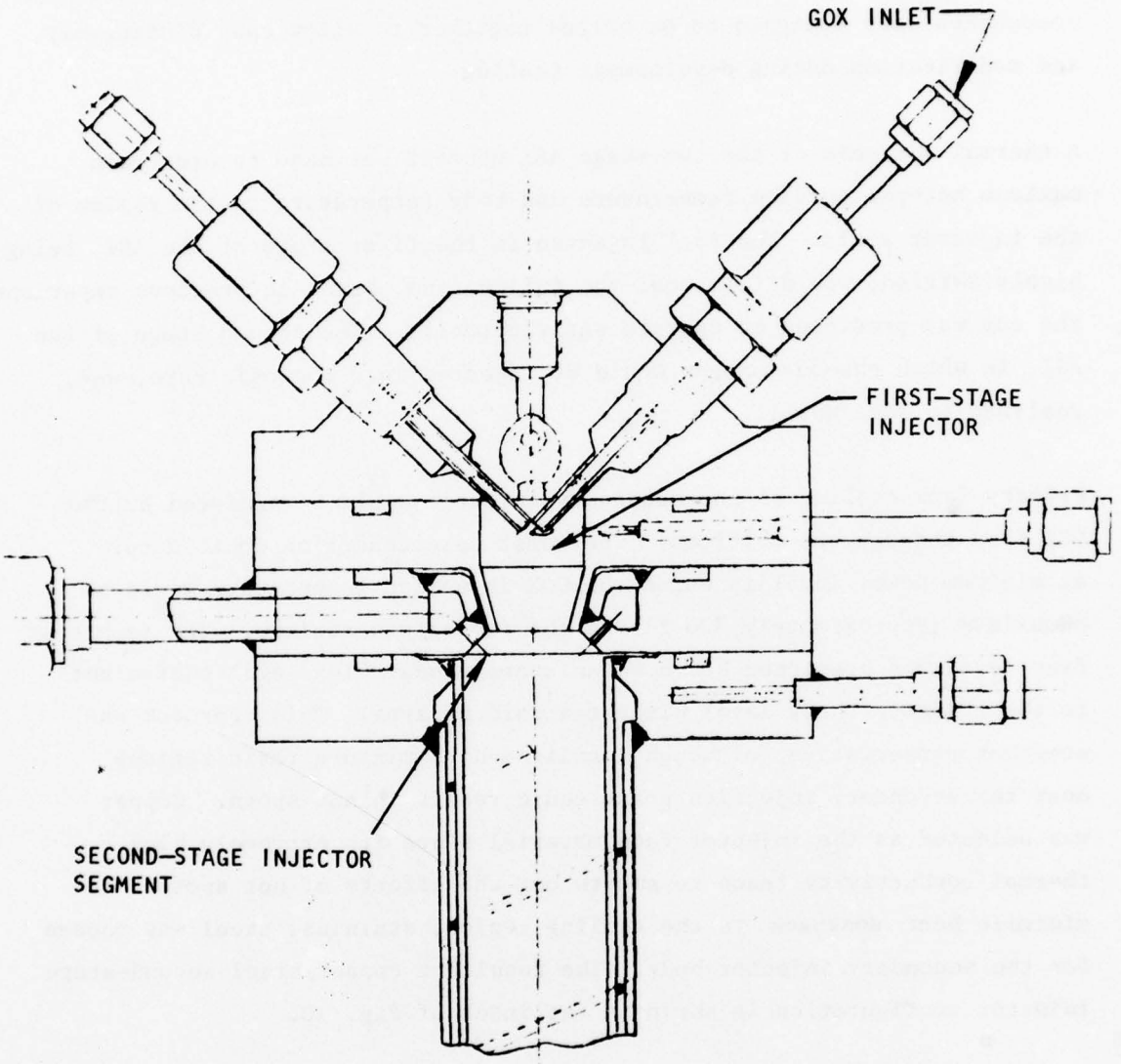

Figure 9. Cross Section of Two-Stage ASI Injector

spray. This configuration is achieved by providing a separate second-stage injector segment to mate with the basic ASI injector. All of the injector components were designed to be bolted together to allow easy disassembly and modification during development testing.

A thermal analysis of the two-stage ASI concept was made to ascertain maximum hot-gas surface temperature and body temperature in the region of the injector seals. The fuel injected in the first stage of the ASI, being highly swirled, would film cool the ASI cup and, based on previous experience, the cup was predicted to operate satisfactorily. The second stage of the ASI, in which gaseous oxygen would be injected into the main core, was, analyzed in some detail.

Primary face cooling of the secondary injector would be achieved by the GOX flow through the orifices. The worst case condition would occur at minimum power level in which the GOX injection temperature would be a maximum (approximately 200 F) and the flowrate a minimum. The face heat flux level was predicted based on an average heat flux level equivalent to the combustor body level without a carbon layer. This approach was somewhat conservative, although localized high mixture ratio regions near the secondary injection point could result in hot spots. Copper was selected as the injector face material since its extremely high thermal conductivity tends to smooth out the effects of hot spots. To minimize heat soakback to the sealing region, stainless steel was chosen for the secondary injector body. The resultant copper/steel second-stage injector configuration is shown in the inset of Fig. 10.

A three-dimensional model (Fig. 10) of a segment of the injector was utilized in conjunction with the Rocketdyne HEATING computer program to determine steady-state temperature distribution. Contact resistance between the second-stage injector and adjacent components was included based on a total clamping force of approximately 12,000 pounds.

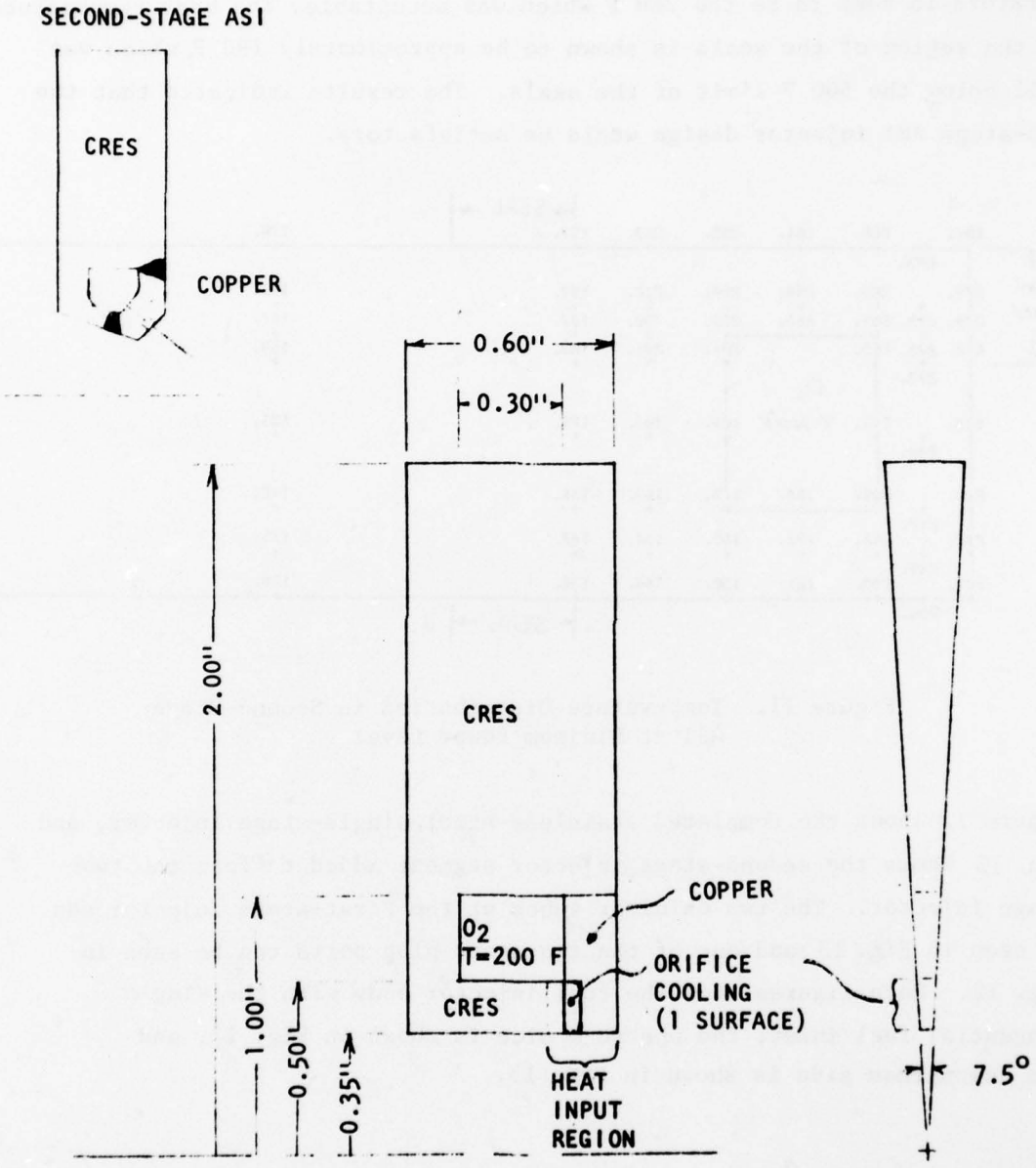

Figure 10. ASI Second Stage, 3-Dimensional Thermal Model

The resulting calculated temperature distribution in one plane is shown in the typical program CRT output of Fig. 11. The circumferential temperature variation was found to be negligible. The maximum copper temperature is seen to be the 280 F which was acceptable. The body temperature in the region of the seals is shown to be approximately 190 F, which was well below the 500 F limit of the seals. The results indicated that the two-stage ASI injector design would be satisfactory.

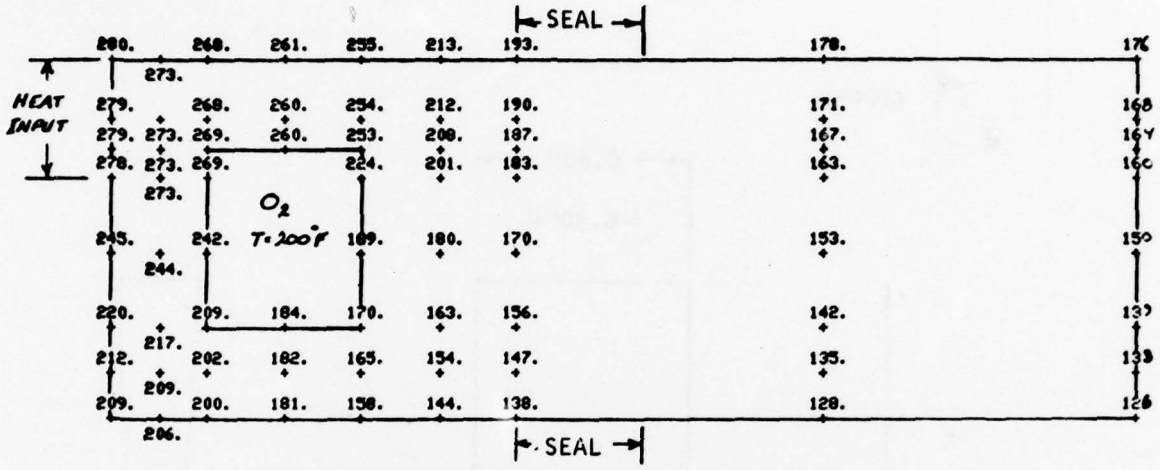

Figure 11. Temperature Distribution in Second-Stage ASI at Minimum Power Level

Figure 12 shows the completed stainless-steel, single-stage injector, and Fig. 13 shows the second-stage injector segment added to form the two-stage injector. The two oxidizer tubes of the first-stage injector can be seen in Fig. 13 and one of the two spark plug ports can be seen in Fig. 12. Both figures show the fuel injector body with the single tangential fuel inlet; the upstream side is shown in Fig. 12, and the downstream side is shown in Fig. 13.

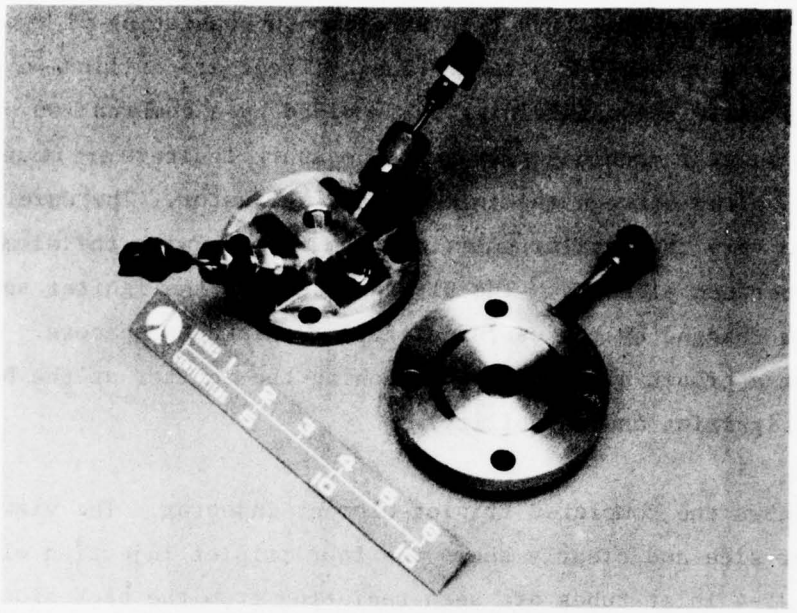

Figure 12. ASI Single-Stage Injector

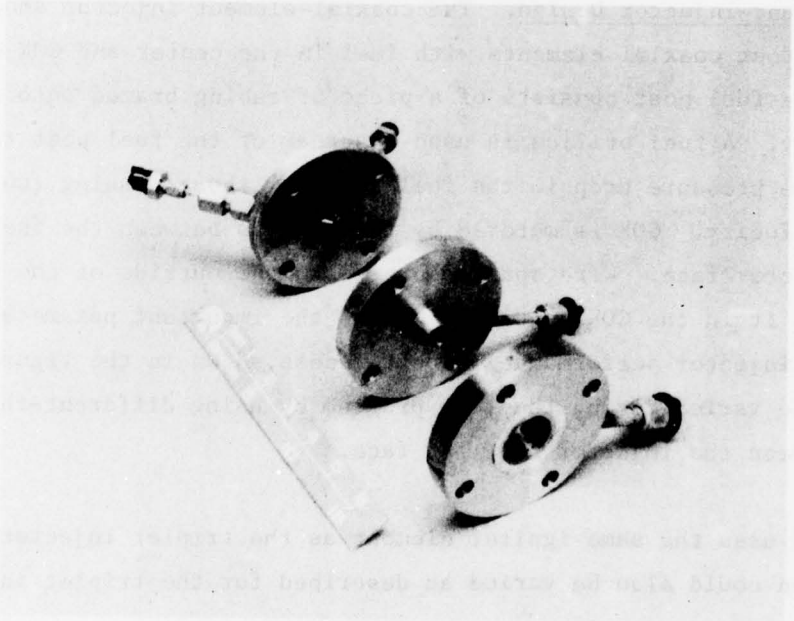

Figure 13. ASI Two-Stage Injector

Triplet-Element Injector Design. The triplet-element injector is shown in Fig. 14. This design uses four triplet elements consisting of two fuel streams impinging on one GOX stream. The orifices are drilled in a copper injector body while the manifolding is provided by a combination of drilled holes and an annular machined passage. The spark igniters are mounted in a cooled wafer bolted between the injector and combustor. The wafer could be rotated to vary the igniter position from in-line with the elements to half-way in-between elements. The distance between the igniter and injector face could be changed by the use of different-thickness spacers. The movable wafer approach allows for positioning the igniter at the best location for ignition and durability.

Figure 15a shows the completed triplet-element injector. The view is from the combustor side and clearly shows the four triplet injection elements. The GOX and JP-4 inlet tubes are seen radiating from the back side. Figure 15b shows the injector with one of the spacers used to set the sparkplug wafer (seen in the foreground) away from the injector face.

Coaxial-Element Injector Design. The coaxial-element injector shown on Fig. 16 uses four coaxial elements with fuel in the center and GOX on the outside. The fuel post consists of a piece of tubing brazed into the injector body. A fuel orifice is used upstream of the fuel post to provide adequate pressure drop in the fuel system without causing too high an injection velocity. GOX is metered by the annulus between the fuel post and the injector face. Wire spacers brazed to the outside of the fuel post centers it in the GOX annulus. One of the important parameters in determining injector performance is post recess shown in the figure. This recess can be varied during the test program by using different-thickness spacers between the injector body and face.

The injector uses the same igniter element as the triplet injector. Sparkplug position could also be varied as described for the triplet injector.

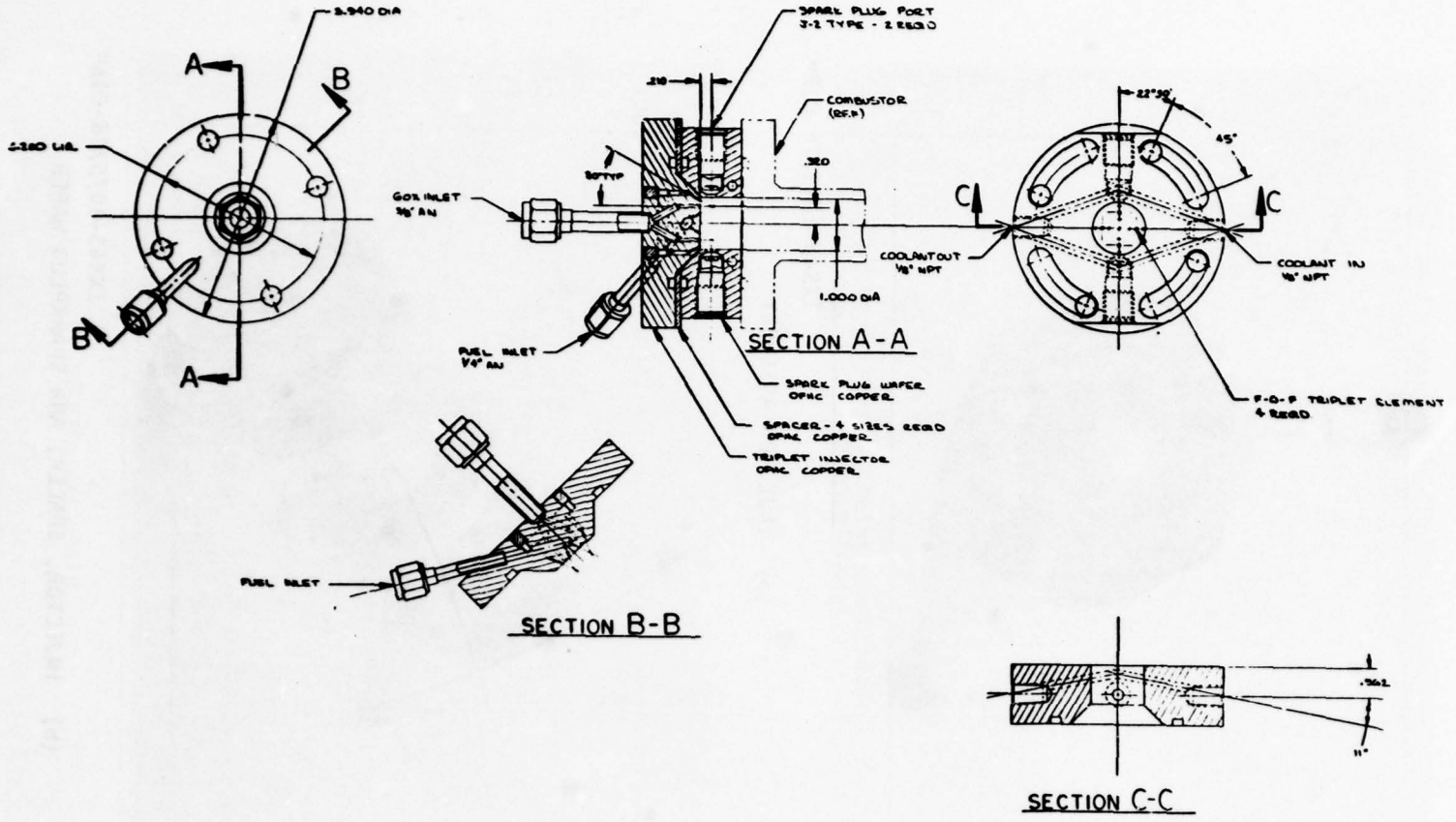

Figure 14. Triplet Element Injector

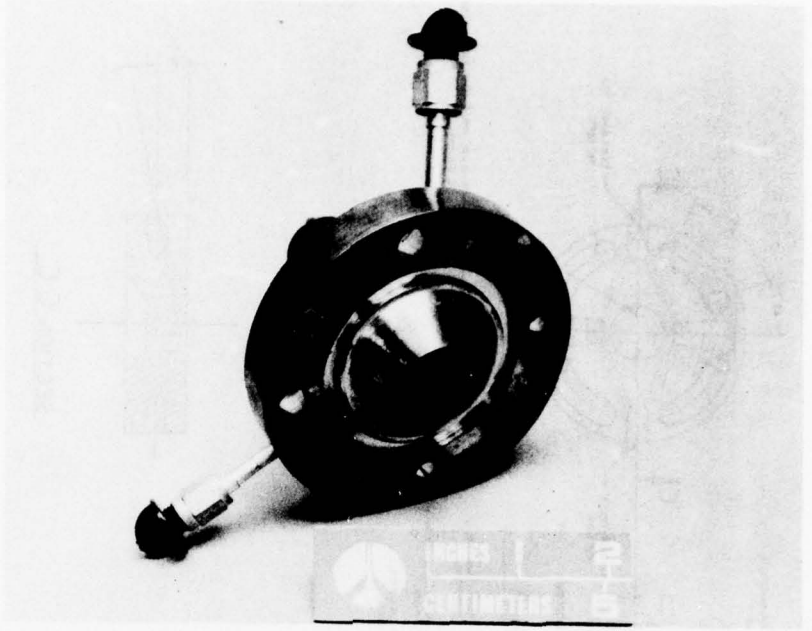

1XX45-10/5/76-C1E*

(a) INJECTOR ASSEMBLY

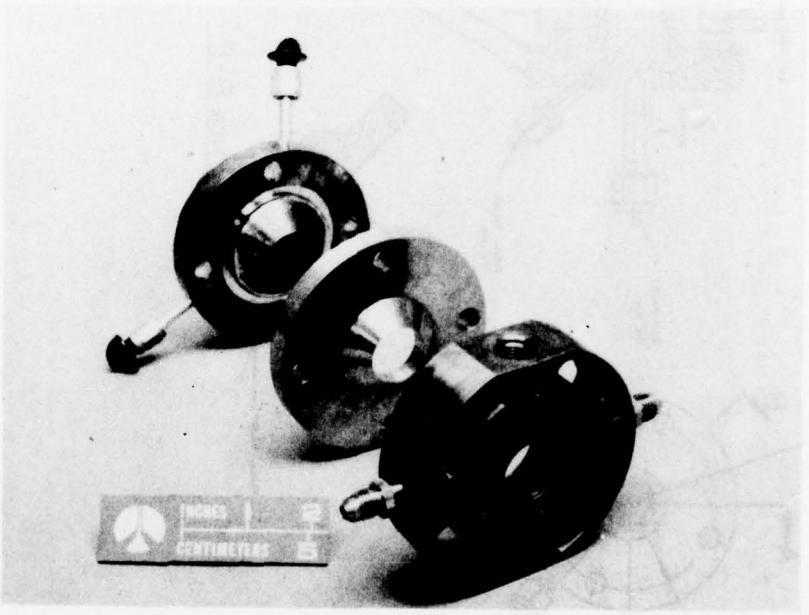

1XX45-10/5/76-C1A*

(b) INJECTOR, SPACER, AND SPARKPLUG WAFER

Figure 15. Triplet-Element Injector

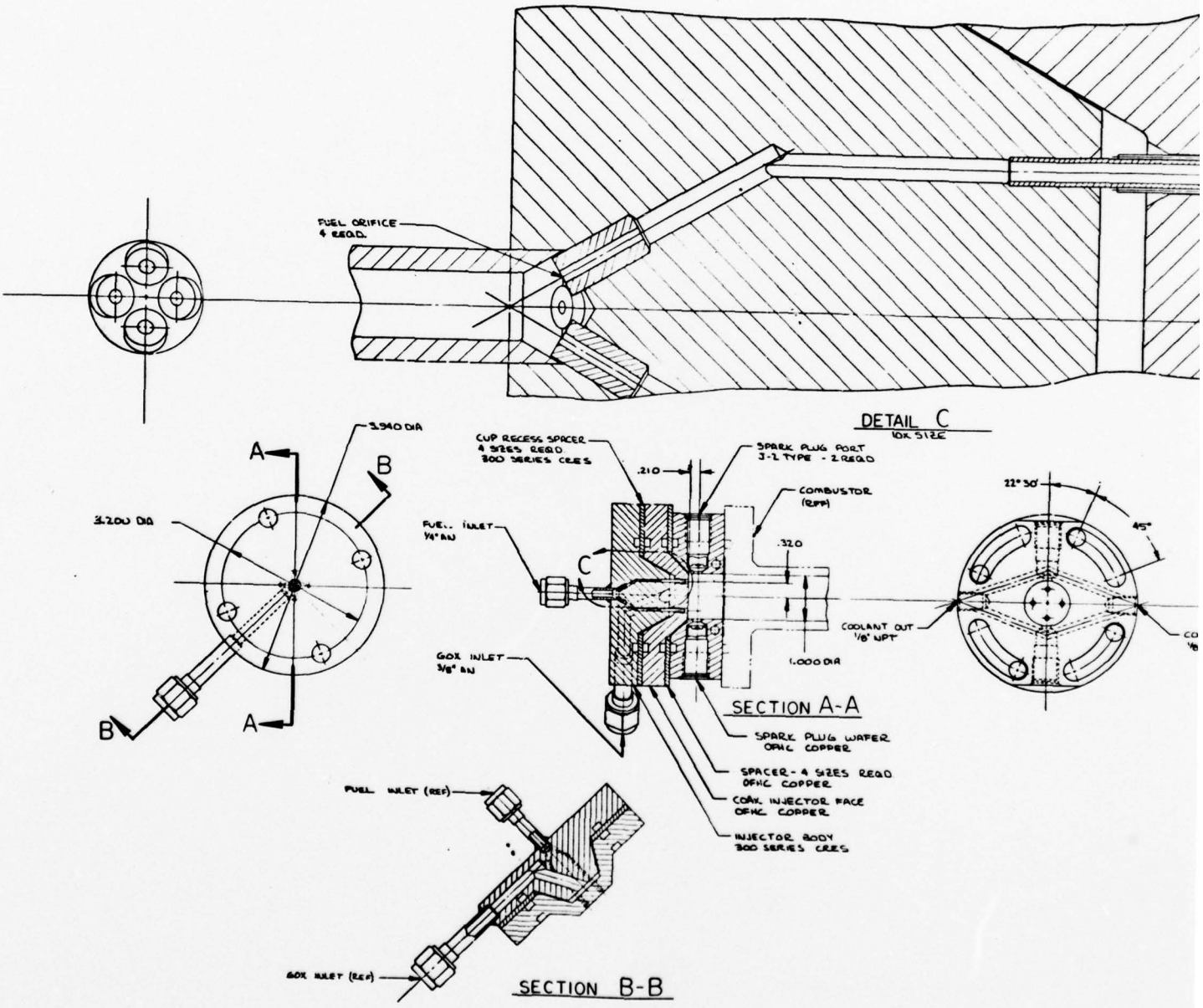
FUEL ORIFICE
4 REQD.
DETAIL C
10X SIZE
3.940 DIA
3.200 DIA
A
B
B
A
CUP RECESS SPACER
4 SIZES REQD
300 SERIES CRES
.210
SPARK PLUG PORT
J-1 TYPE - 2 REQD
COMBUSTOR
(REF)
FUEL INLET
1/4" AN
.320
C
1.000 DIA
GOX INLET
3/8" AN
22° 30'
45°
COOLANT OUT
1/8" NPT
SECTION A-A
SPARK PLUG WAFER
OFHC COPPER
SPACER - 4 SIZES REQD
OFHC COPPER
COAX INJECTOR FACE
OFHC COPPER
INJECTOR BODY
300 SERIES CRES
FUEL INLET (REF)
GOX INLET (REF)
SECTION B-B

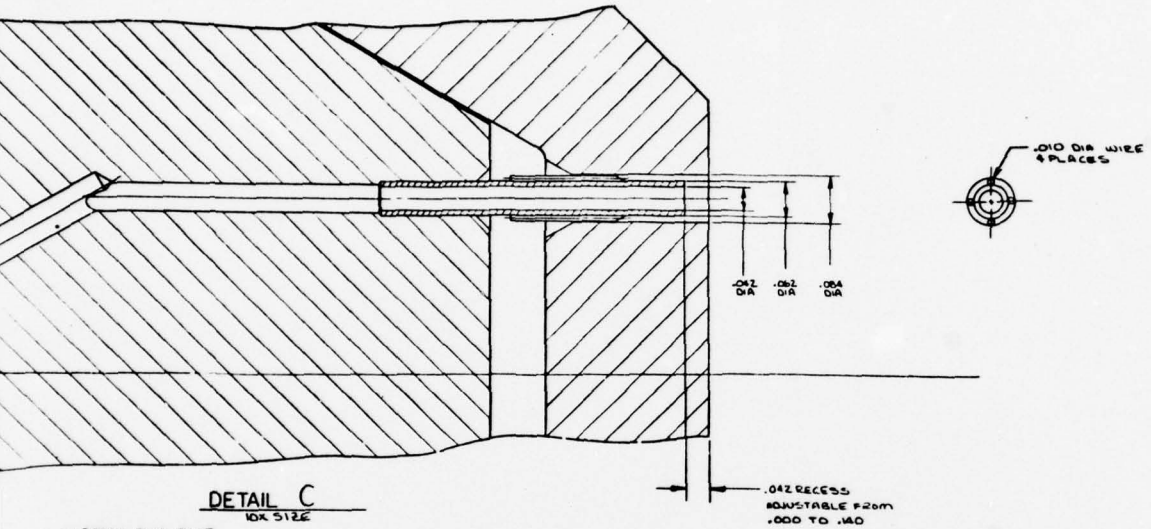

DETAIL C
10X SIZE

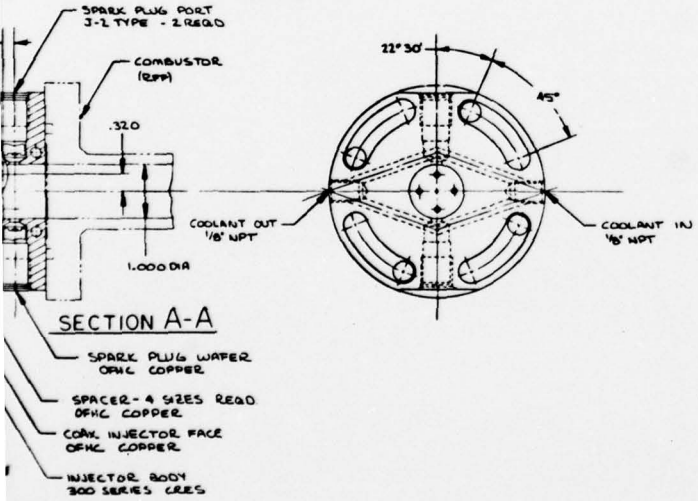

SECTION A-A

Figure 16. Coaxial-Element Injector

Photographs of the completed coaxial-element injector are shown in Fig. 17. Figure 17a shows the fuel section, with its four posts, separated from the oxidizer section. The assembled unit is shown in the Fig. 17b The spark-plug wafer and spacer arrangement are identical to that for the triplet-element injector.

Gas Generator Hardware Assembly. Figure 18 shows all the parts which make up the low-power gas generator in its longest (10-inch) buildup, and with the two-stage injector assembly. The view is from the nozzle end. The two combustor sections are turned around in the photograph to show the thermal expansion joints. Figure 19 shows the assembled unit with the same parts viewed from the injector end.

High-Power Gas Generator

The performance parameters for the high-power gas generator are given in Table 6. These parameter values are based on the IPU high-power gas generator requirements given in the system requirements section. Based on these parameters and the low-power gas generator test results, the hardware design parameters given in Table 7 were selected.

The design layout of the gas generator assembly is shown in Fig. 20. The assembly consists of the triplet injector, optional spark plug wafer, combustor, and cooled nozzle. A bolted assembly is used similar to the low-power gas generator.

Combustor Design. The combustor design is 3.260 inches in diameter and 10.00 inches long. Construction is similar to the low-power gas generator with a spiral GOX coolant path of 4-inch pitch within a double wall. The coolant path is formed by a wire as shown in Fig. 21. The end manifolds were improved from the low-power design to provide full cooling to the end of the chamber. Double inlets and outlets were used to provide good flow distribution to the low-pressure drop coolant circuit.

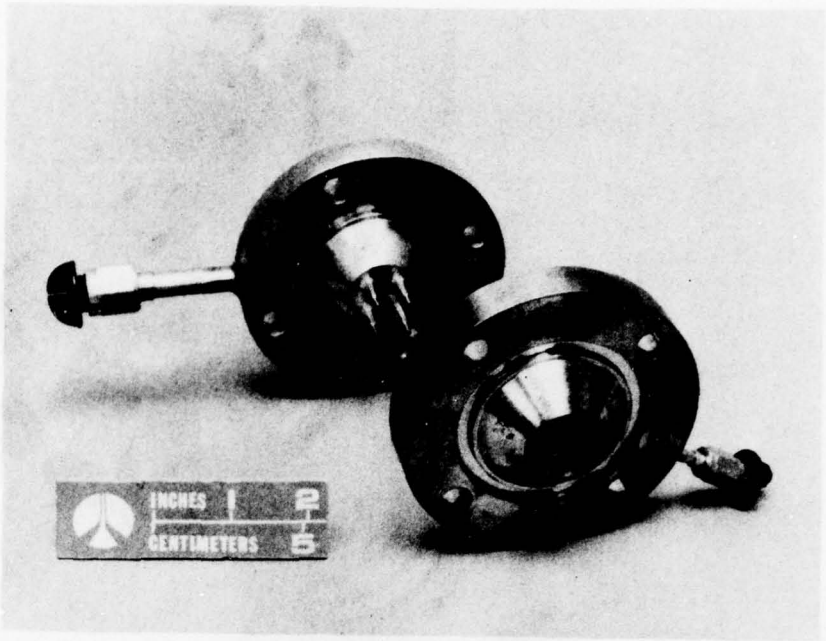

1XX45-10/5/76-C1D*

(a) SEPARATED FUEL AND OXIDIZER SECTIONS

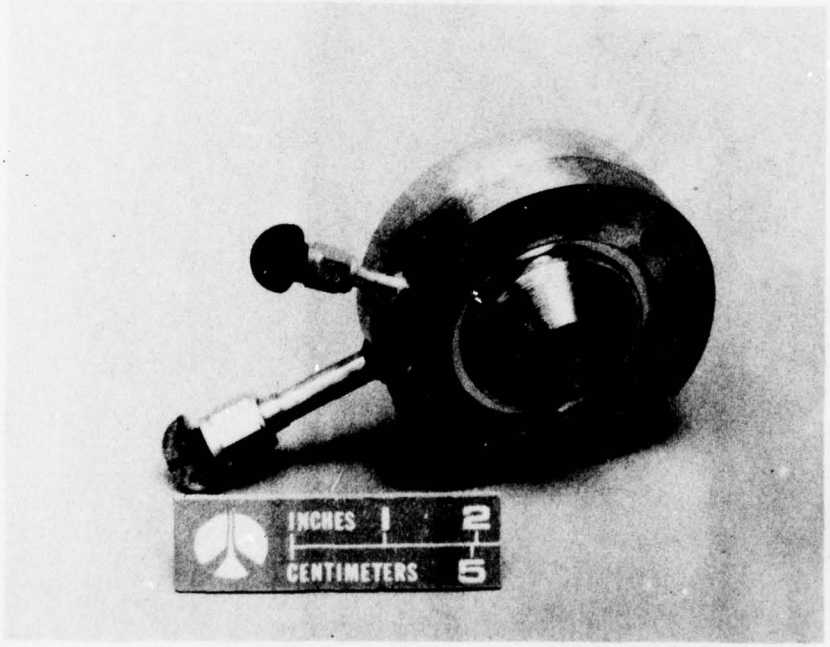

1XX45-10/5/76-C1B*

(b) ASSEMBLED UNIT

Figure 17. Coaxial-Element Injector

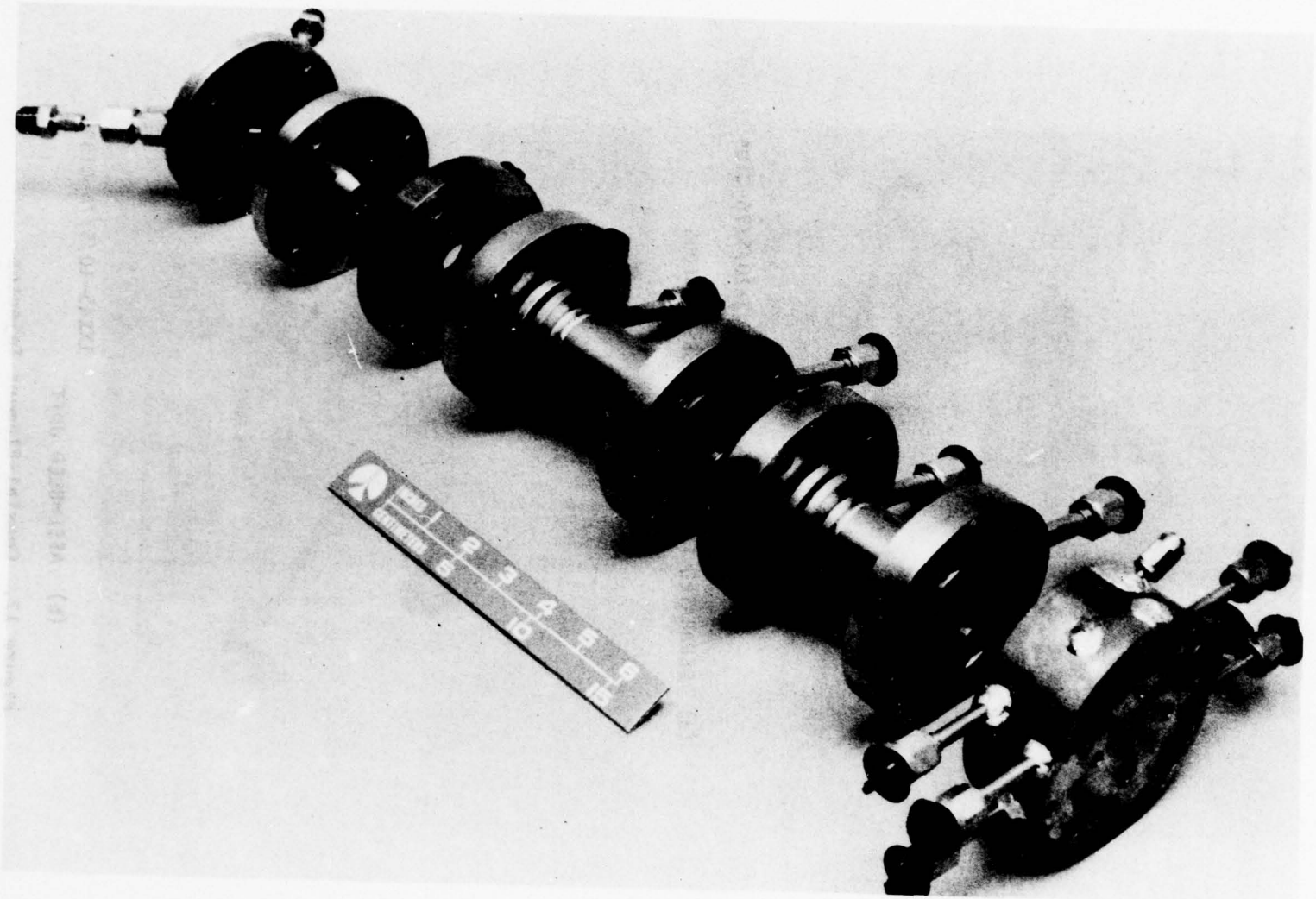

1XZ22-8/26/76-C1A*

Figure 18. Low-Power Gas Generator Test Hardware Parts (Two-Stage ASI Injector/10-Inch Combustor)

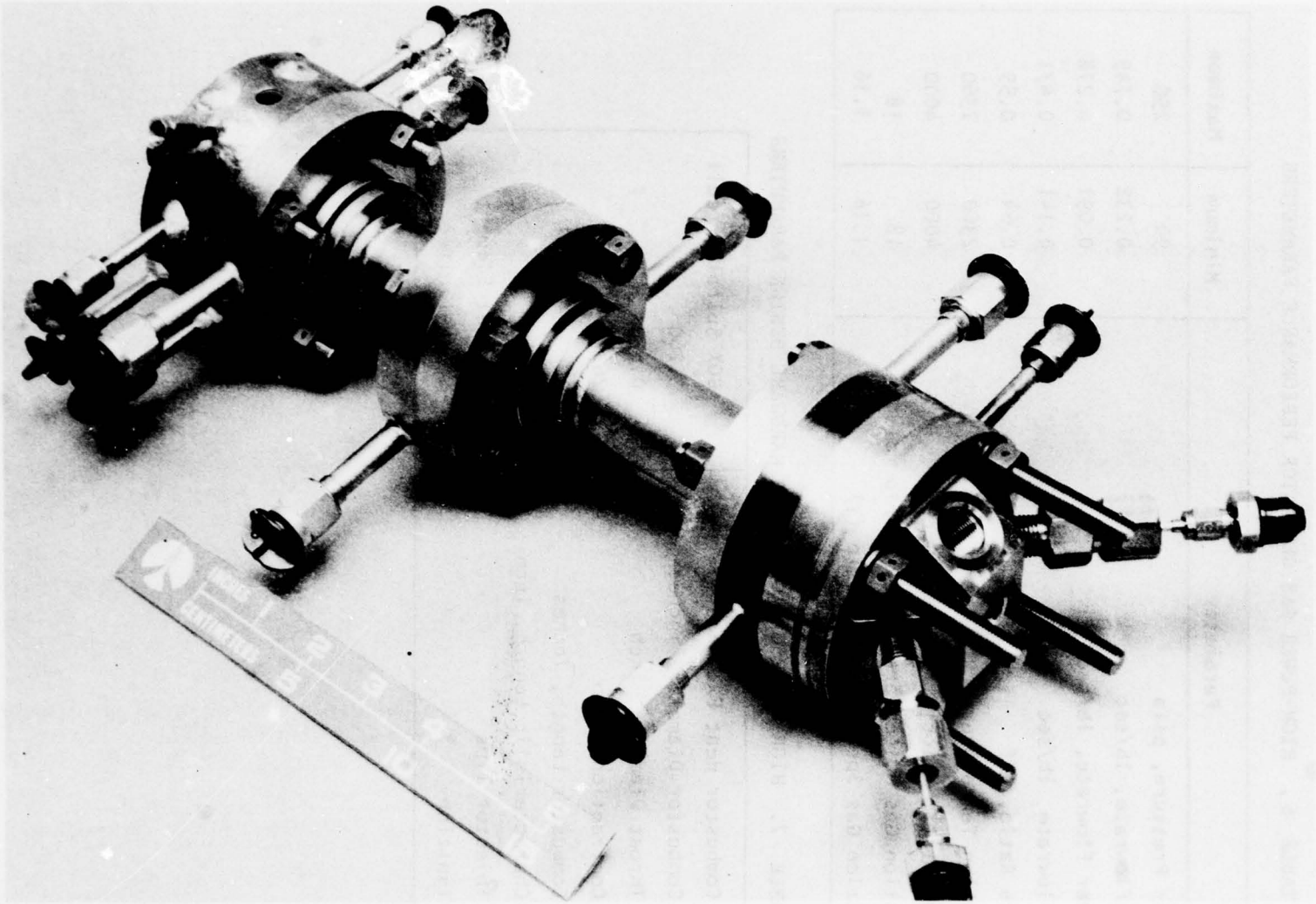

1XZ22-8/26/76-C1B*

Figure 19. Low-Power Gas Generator Test Hardware Assembly (Two-Stage ASI Injector/4 Inch Combustor)

TABLE 6. HIGH-POWER GAS GENERATOR PERFORMANCE PARAMETERS

Parameter	Minimum	Maximum
Chamber Pressure, psia	90	290
Total Flowrate, lb/sec	0.232	0.749
Oxidizer Flowrate, lb/sec	0.091	0.278
Fuel Flowrate, lb/sec	0.141	0.471
Mixture Ratio, o/f	0.64	0.59
Combustion Temperature, R	2360	2360
Characteristic Velocity (C*), ft/sec	4000	4000
Combustion Gas Molecular Weight, lbm/lb mole	18	18
Combustion Gas Specific Heat Ratio (γ)	1.16	1.16

TABLE 7. HIGH-POWER GAS GENERATOR HARDWARE DESIGN PARAMETERS

Combustor Heat Exchanger	GOX Spiral Circuit
Combustor Diameter, inches	3.260
Throat Diameter, inch	0.639
Contraction Ratio	26:1
Combustor Length, inches	10
Characteristic Length, inch	260
Injector Type	Triplet Element
Ignition	Spark Igniter

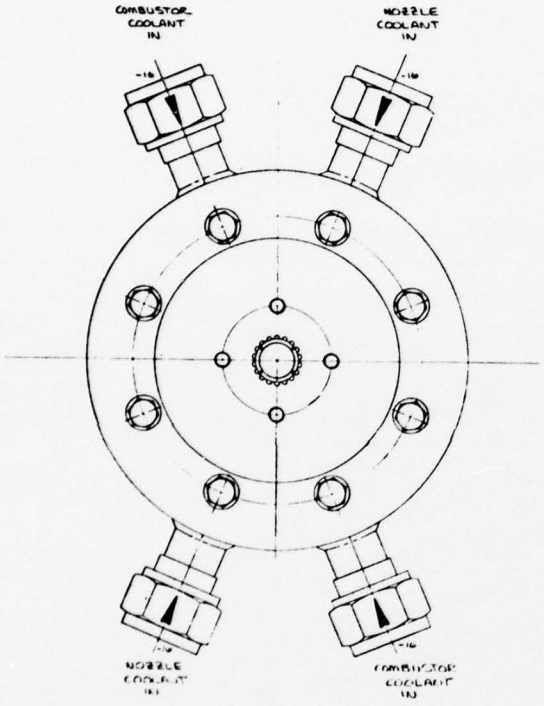
COMBUSTOR COOLANT IN
NOZZLE COOLANT IN
-16
-16
NOZZLE COOLANT IN
COMBUSTOR COOLANT IN

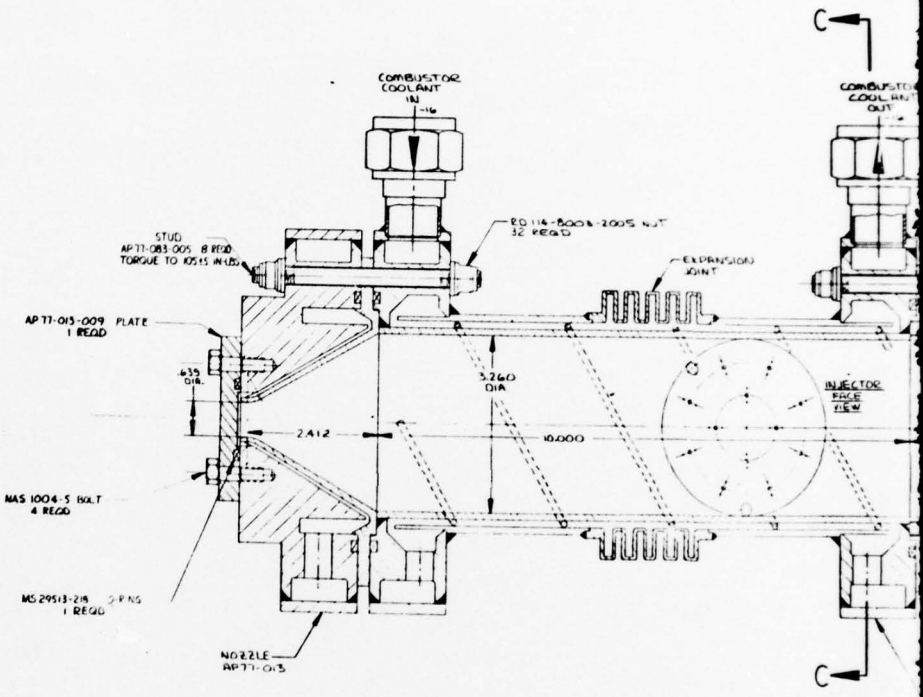
COMBUSTOR COOLANT IN
-16
COMBUSTOR COOLANT OUT
STUD AP77-083-005 8 REQD TORQUE TO 105±5 IN-LBS
RD 114-8008-2005 NUT 32 REQD
EXPANSION JOINT
AP77-013-009 PLATE 1 REQD
.639 DIA.
3.260 DIA
INJECTOR FACE VIEW
2.412
10.000
NAS 1004-5 BOLT 4 REQD
MS 29513-219 O-RING 1 REQD
NOZZLE AP77-013
C
C

SECTION A-A

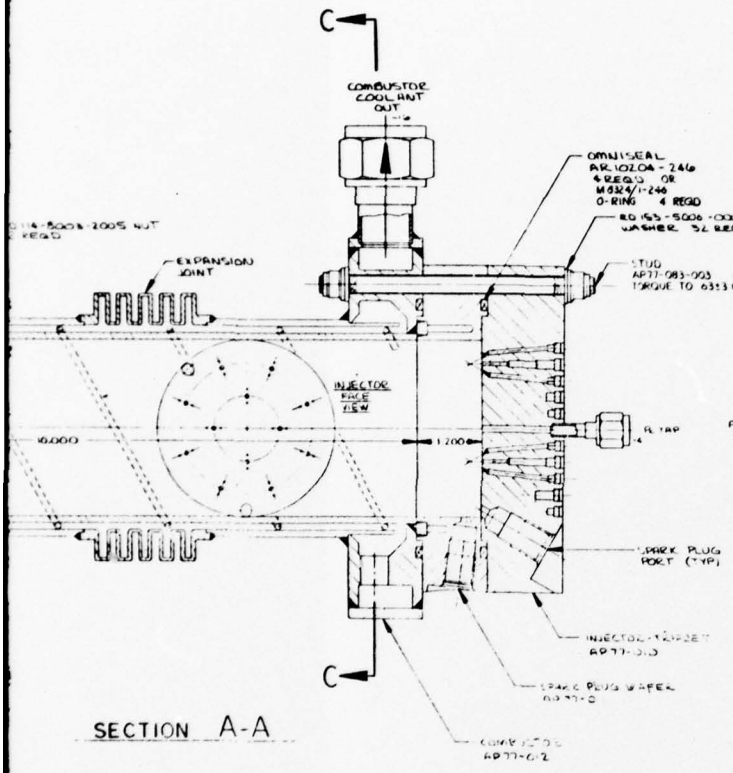

SECTION A-A

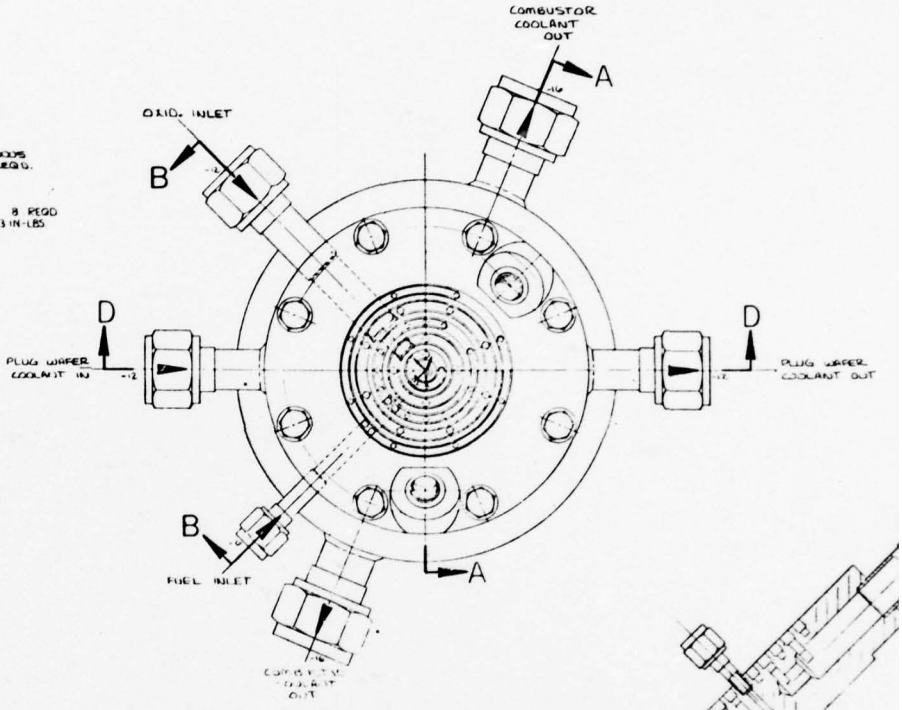

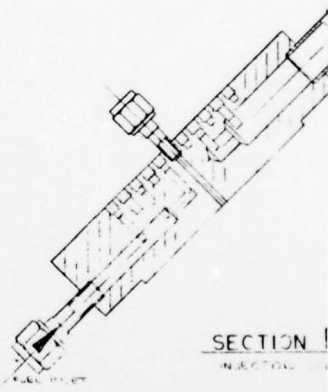

SECTION

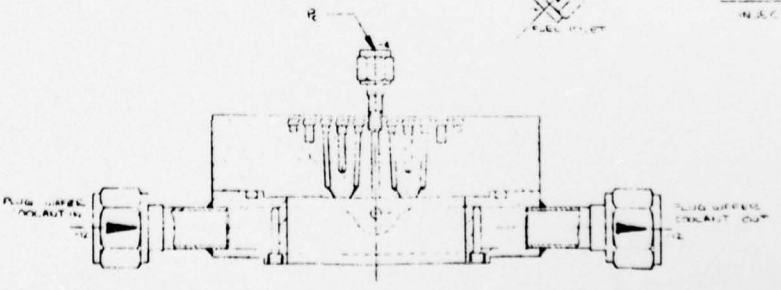

SECTION D-D

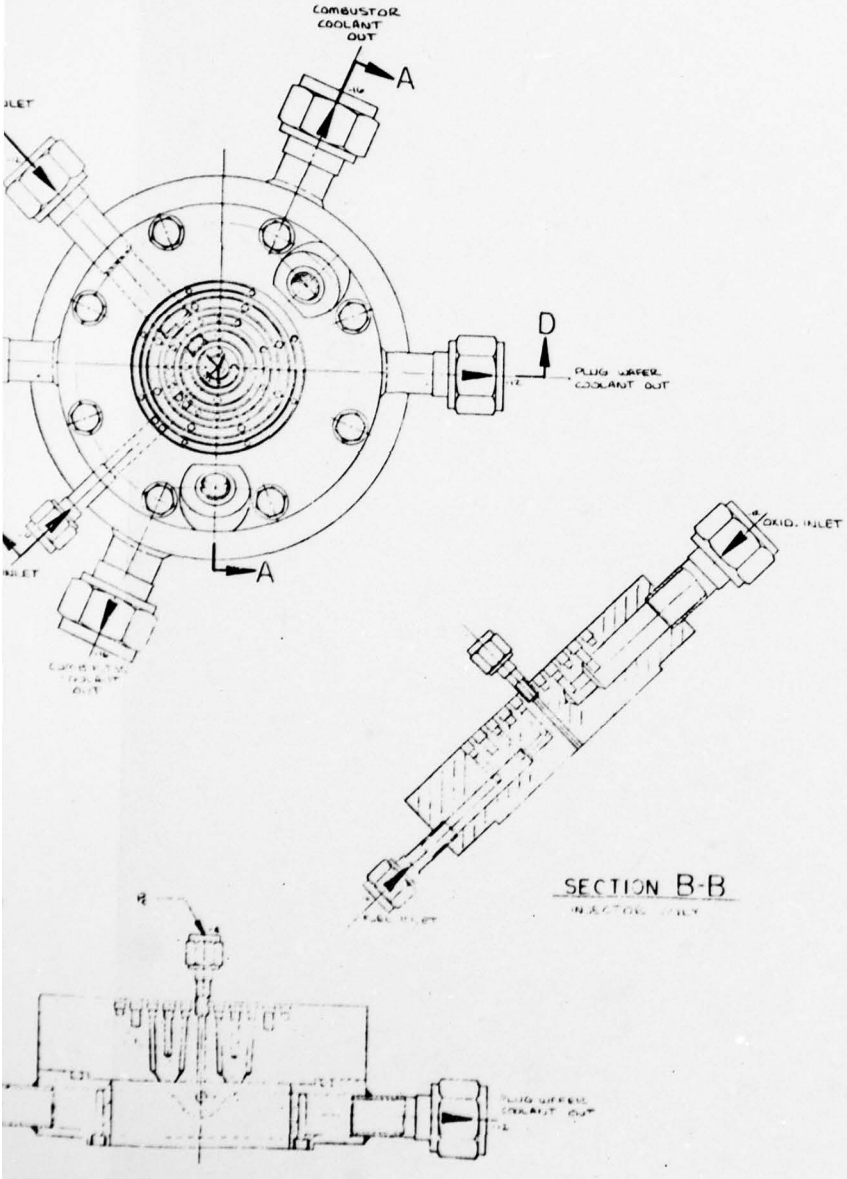

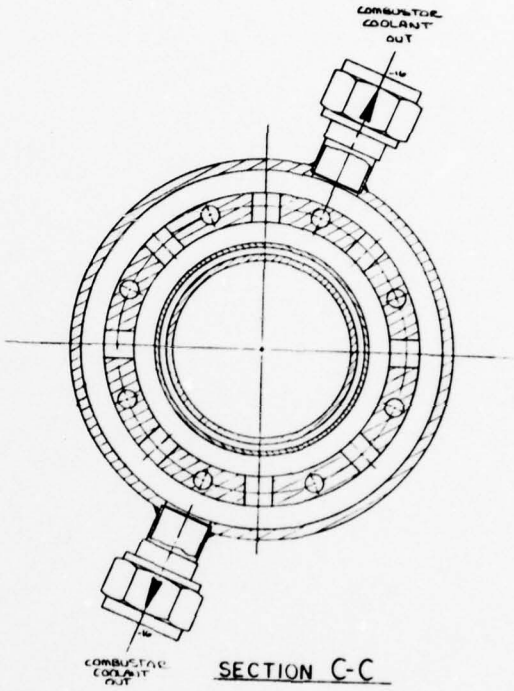

Figure 20, High-Power Gas Generator Assembly

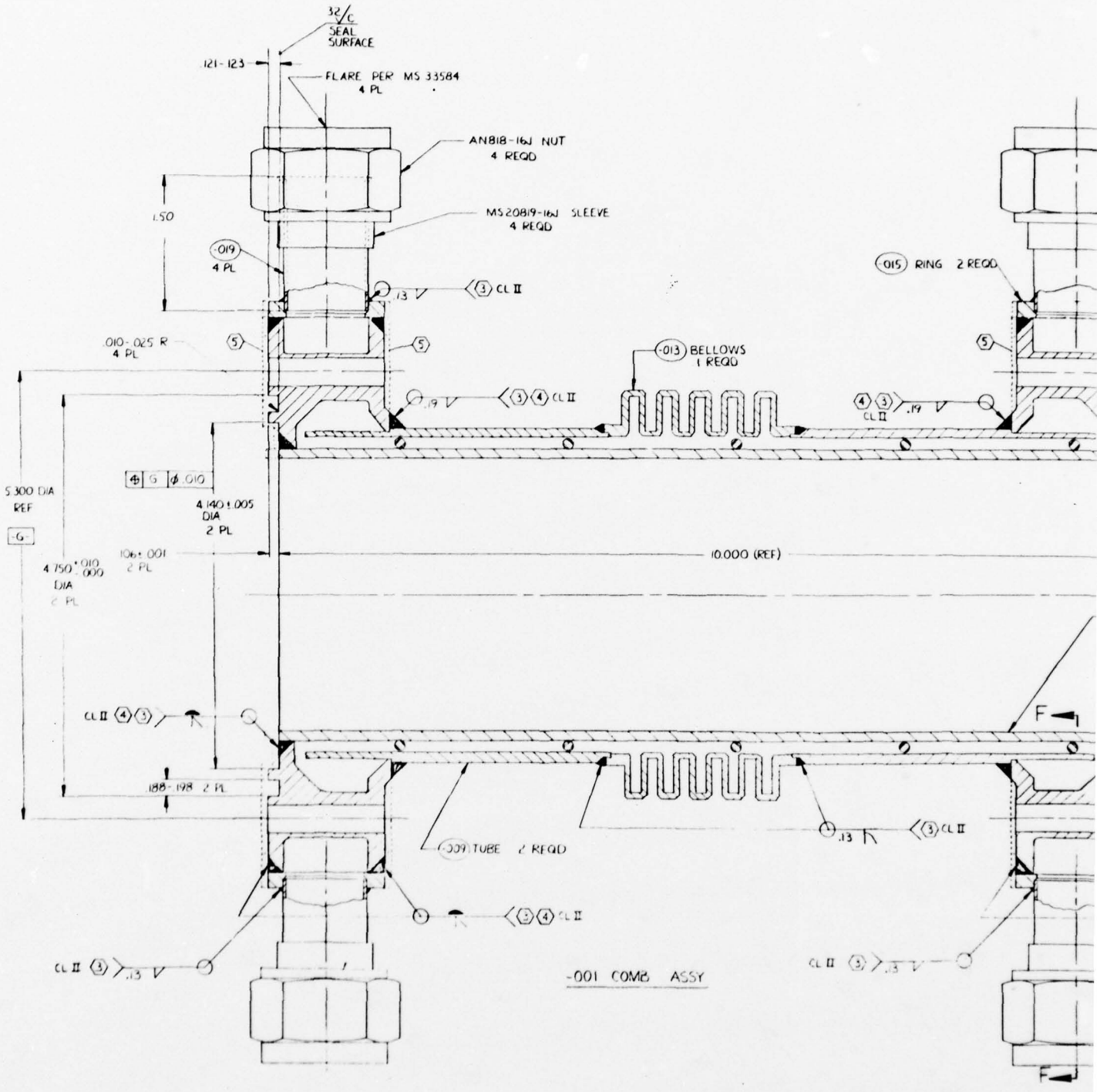
32/C
SEAL SURFACE
121-123
FLARE PER MS 33584
4 PL
AN818-16J NUT
4 REQD
MS20819-16J SLEEVE
4 REQD
.150
-019
4 PL
.13
CL II
-015 RING 2 REQD
.010-.025 R
4 PL
-013 BELLOWS
1 REQD
.19
CL II
5.300 DIA
REF
-G-
⌖ G Ø.010
4.140±.005
DIA
2 PL
4.750 +.010 -.000
DIA
2 PL
106±.001
2 PL
10.000 (REF)
188-198 2 PL
-009 TUBE 2 REQD
F
-001 COMB ASSY

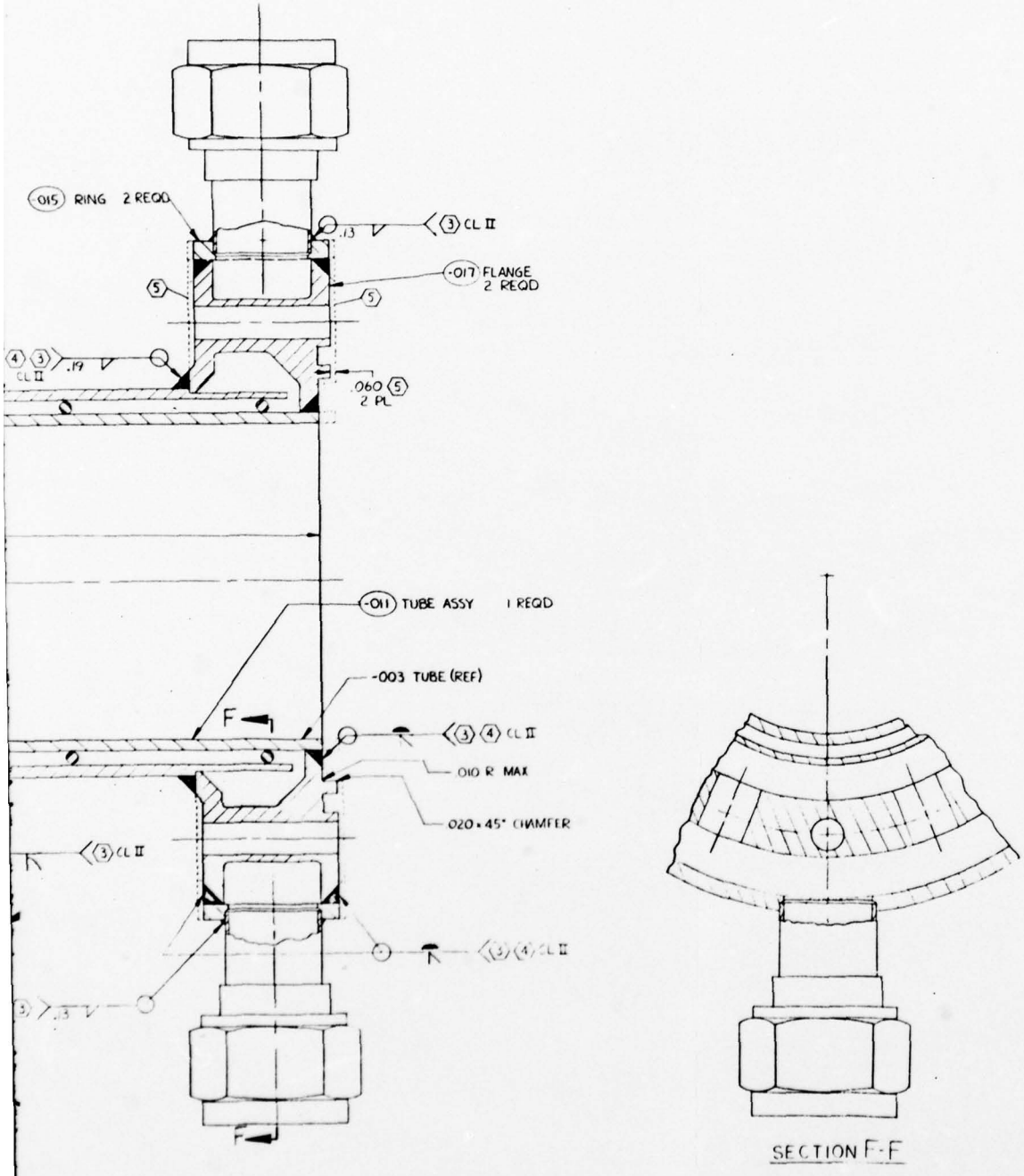

Figure 21. High-Power Gas Generator Combustor Assembly

A bellows-type expansion joint is placed in the outer tube to accommodate differential axial expansion. Five convolutions provided in the bellows ensure a fatigue life of at least 1000 cycles.

The combustor is designed to operate with an inner wall temperature of 1660 to 1860 R (1200 to 1400 F) to inhibit carbon formation on the wall. The predicted wall temperature profiles for the design are shown in Fig. 22a for maximum chamber pressure (290 psia) operation and no carbon formation. The lower wall temperature at the coolant inlet location (start of convergence) is due to the low GOX temperature (-190 F) in conjunction with the improved inlet region coolant enhancement factor ($\approx$15 to 30%). At the coolant exit (injector end) the maximum wall temperature is about 1900 R (1440 F). A more uniform axial temperture profile could have been achieved by utilizing a variable pitch and/or gap in the basic combustor coolant circuit design, but this was deemed to be unnecessary.

The corresponding GOX coolant bulk temperature profile for the high pressure case is shown in Fig. 23a (no carbon formation). The flow enters at 270 R (-190 F), assuming preheating in the turbine exhaust heat exchanger. The exit temperature is shown to be 420 R (-40 F), for a total temperature rise of 150 R. The existence of a carbon layer, however, would substantially reduce both the wall temperature and GOX temperature rise through the combustor jacket. Such an effect is shown in Fig. 22b and 23b.

A similar analysis of the baseline design was also conducted for the minimum chamber pressure (90 psia) case. The resulting predicted maximum wall temperature was 1290 R (830 F) occurring at the injector end. The predicted GOX outlet temperature was 770 R (310 F) based on an inlet temperature of 465 R (5 F).

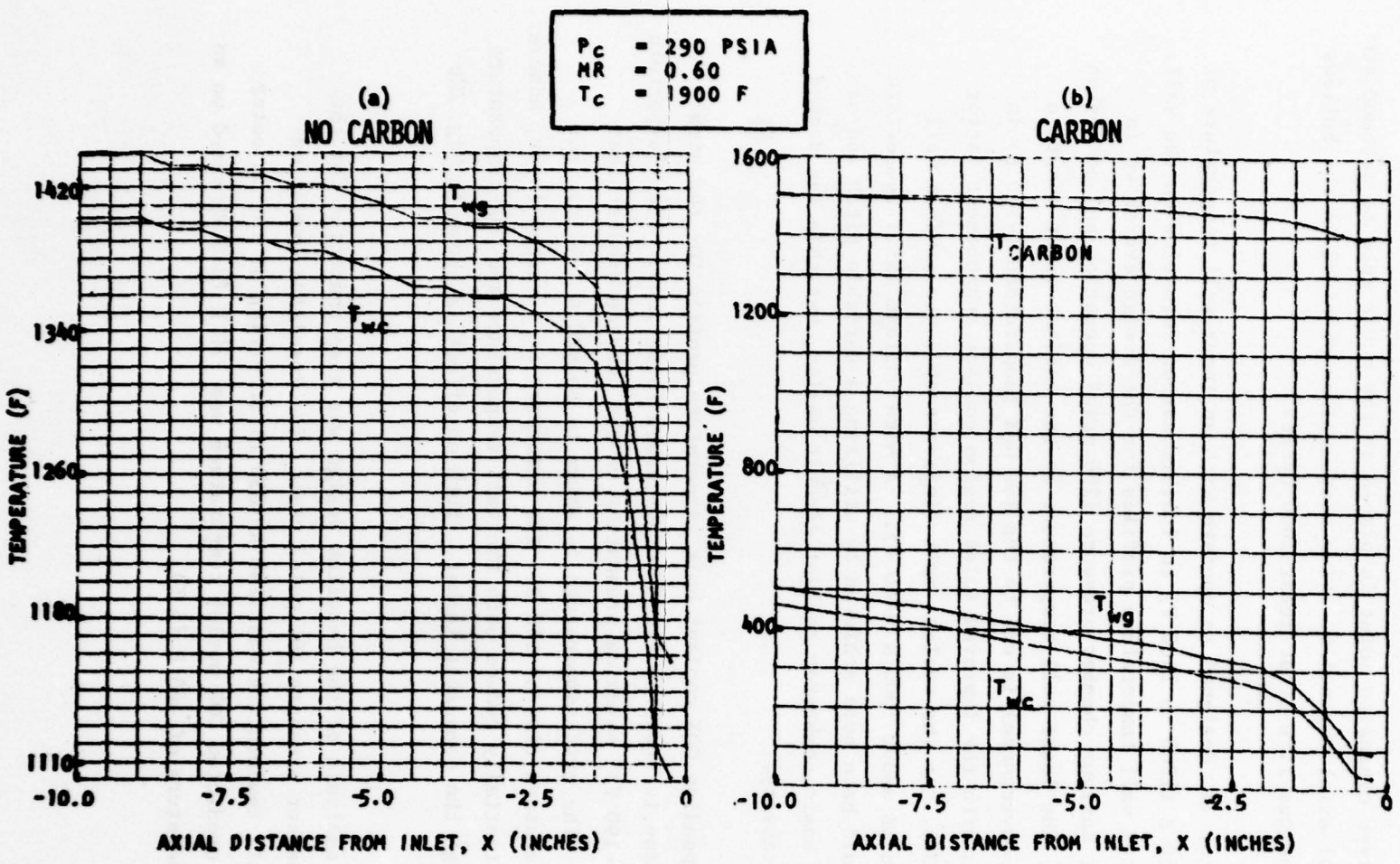

Figure 22. Wall Temperature Profiles for High-Power Gas Generator

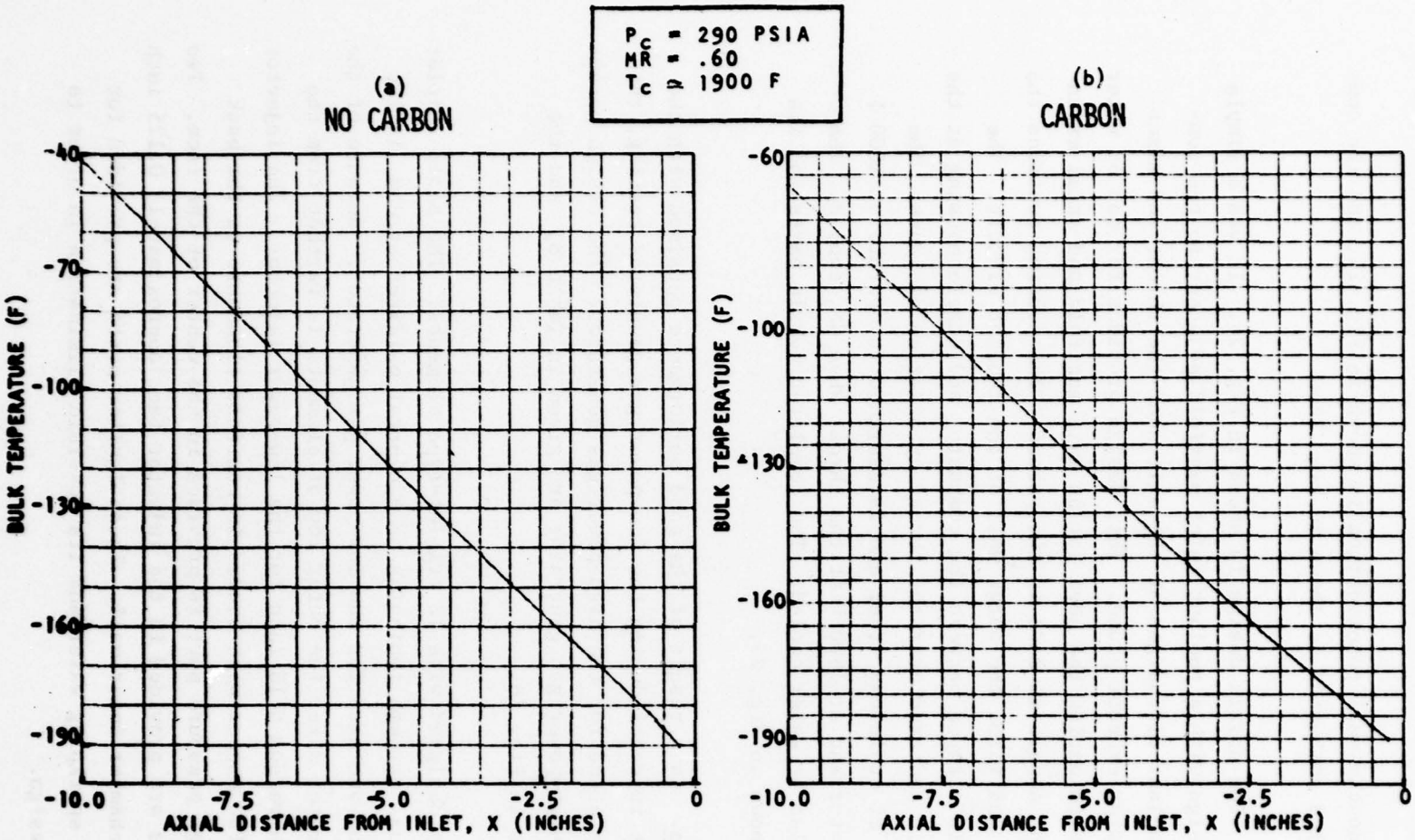

Figure 23. GOX Bulk Temperature Profile for High-Power Gas Generator

The combustor double wall construction is shown in Fig. 24, and the completely assembled combustor is shown in Fig. 25.

Nozzle Design. The nozzle design is shown in Fig. 26. It was a simple dump-cooled design with a coolant inlet manifold adjacent to the combustor. The coolant discharges at the exit near the throat and mixes with the combustor exhaust plume. This design provides for gas or water cooling while eliminating the need for an exit manifold and axial expansion joint. The nozzle is made in two pieces. The housing contains the inlet manifold and forms the outer wall of the coolant circuit. The conical liner is clamped between the combustor and nozzle housing at the inlet end and is centered near the throat by a series of lands. The nozzle is made of stainless steel and is designed to operate at 1000 F near the combustor and at 1600 F at the throat when GN_2 cooled. The nozzle could also be water cooled. The completed nozzle parts and its assembly are shown in Fig. 27.

Injector Design. As a result of the good performance obtained with the triplet-element injector during the low-power gas generator testing, this injector was selected for the high-power gas generator. The design parameters for the high-power gas generator are given in Table 8, and the design is shown in Fig. 28.

The injector is designed with 12 triplet-type elements. The basic triplet element, two fuel streams impinging on a central oxidizer stream, is the same size as the one used for the low-power gas generator. Because of the increased combustor size, the outer row of elements is farther from the wall, 0.43 inch versus 0.18 inch for the low-power injector. The injector is made from OFHC copper with brazed-in manifold closeouts on the back side. A chamber pressure port is provided in the center of the face. Two sparkplug ports are provided in the injector face approximately 0.125 inch away from the chamber inner wall. These igniter ports are provided for evaluating the sparkplug wafer and its possible elimination in order to simplify the design.

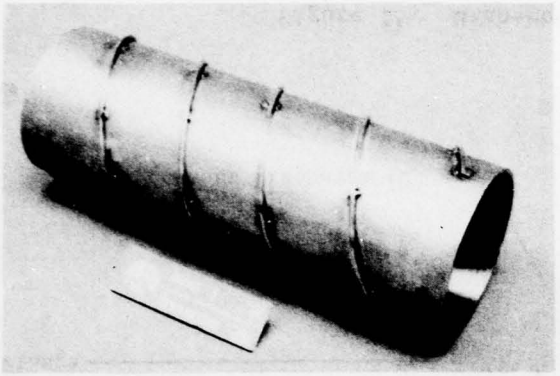

COMBUSTOR INNER TUBE

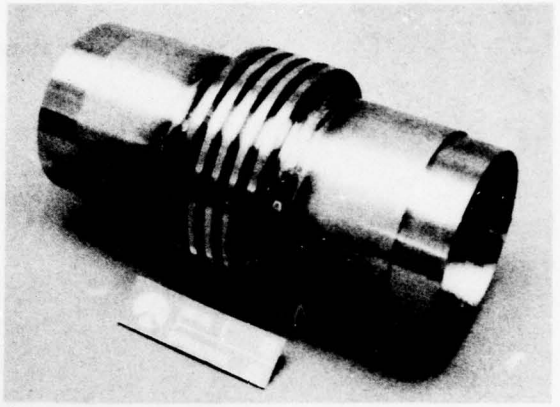

COMBUSTOR OUTER TUBE

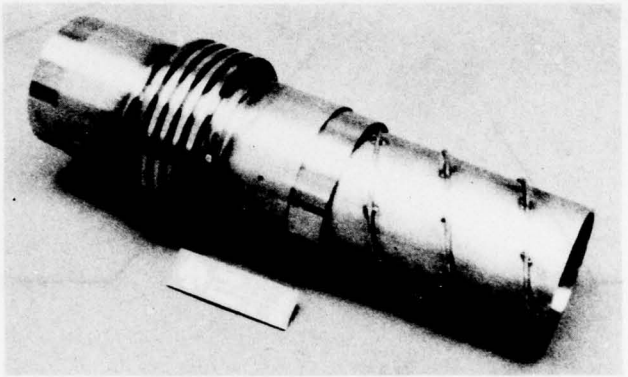

Figure 24. High-Power Gas Generator Combustor Tubes

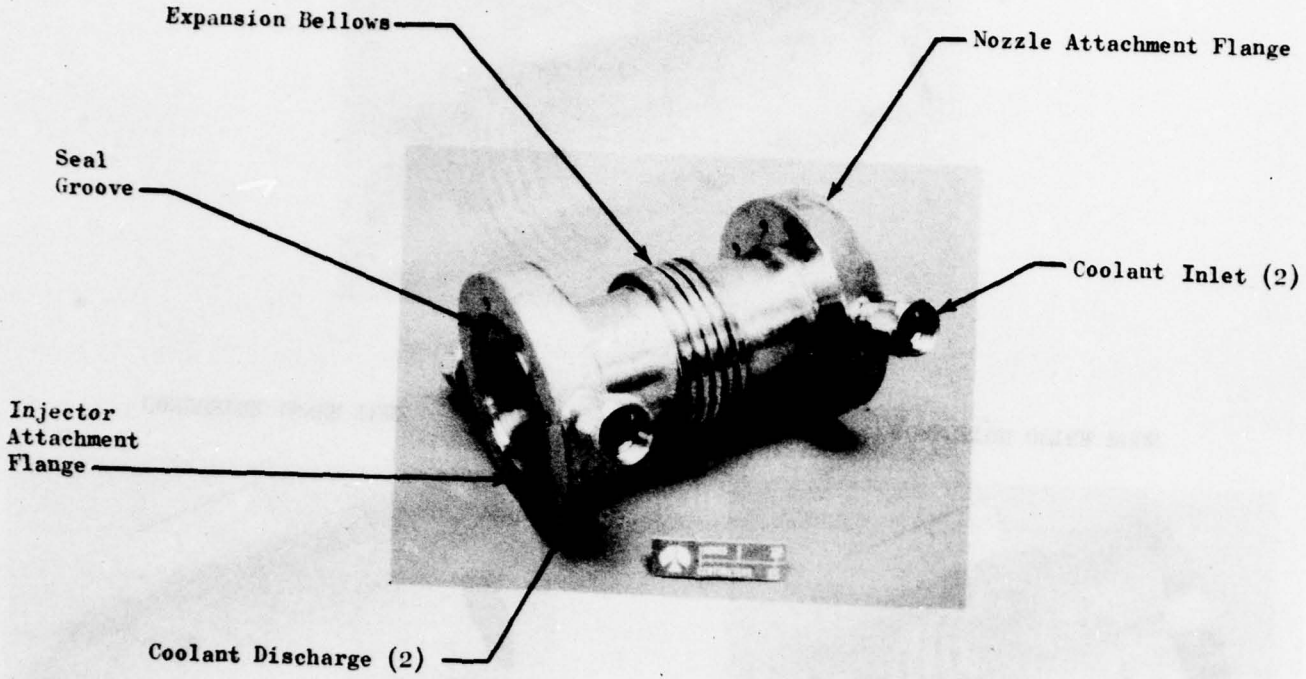

Figure 25. High-Power Gas Generator Combustor

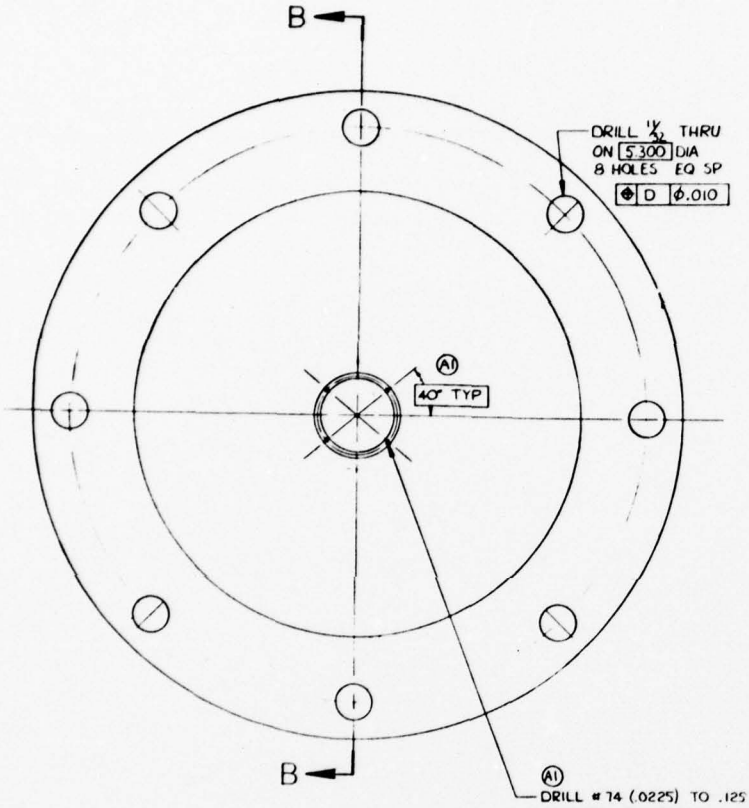

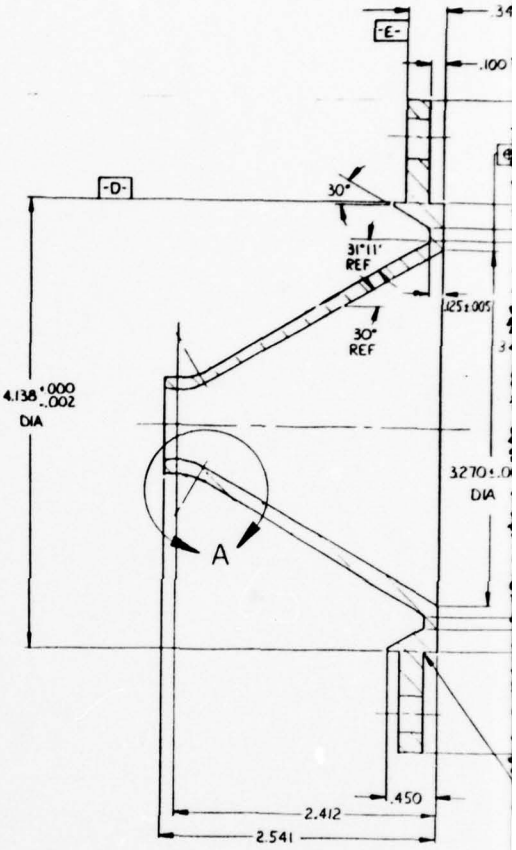

SECTION B-B

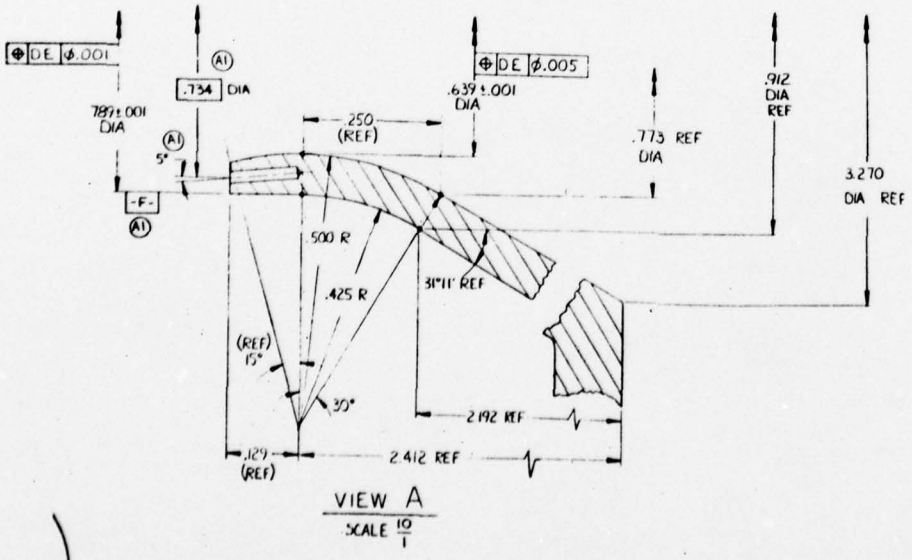

VIEW A
SCALE 10/1

DETAIL -003 LINER

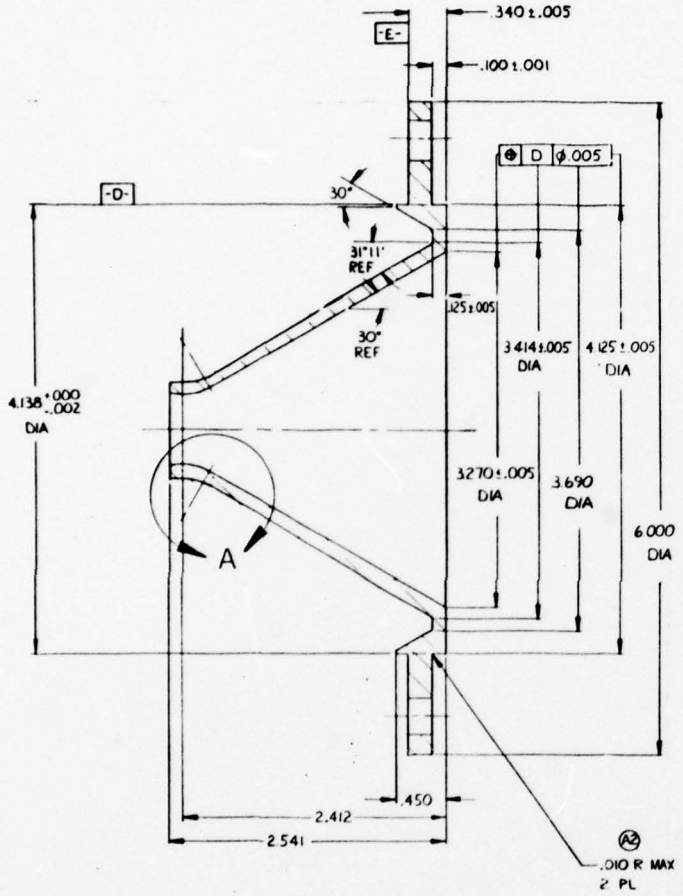

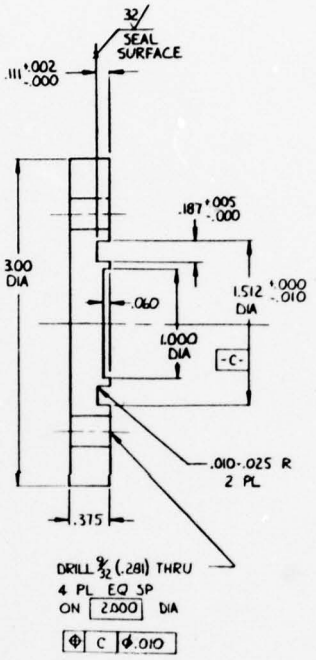

DETAIL -009 PLATE

DETAIL -003 LINER

Figure 26. High-Power Gas Generator Nozzle Hot Wall (sheet 1 of 2)

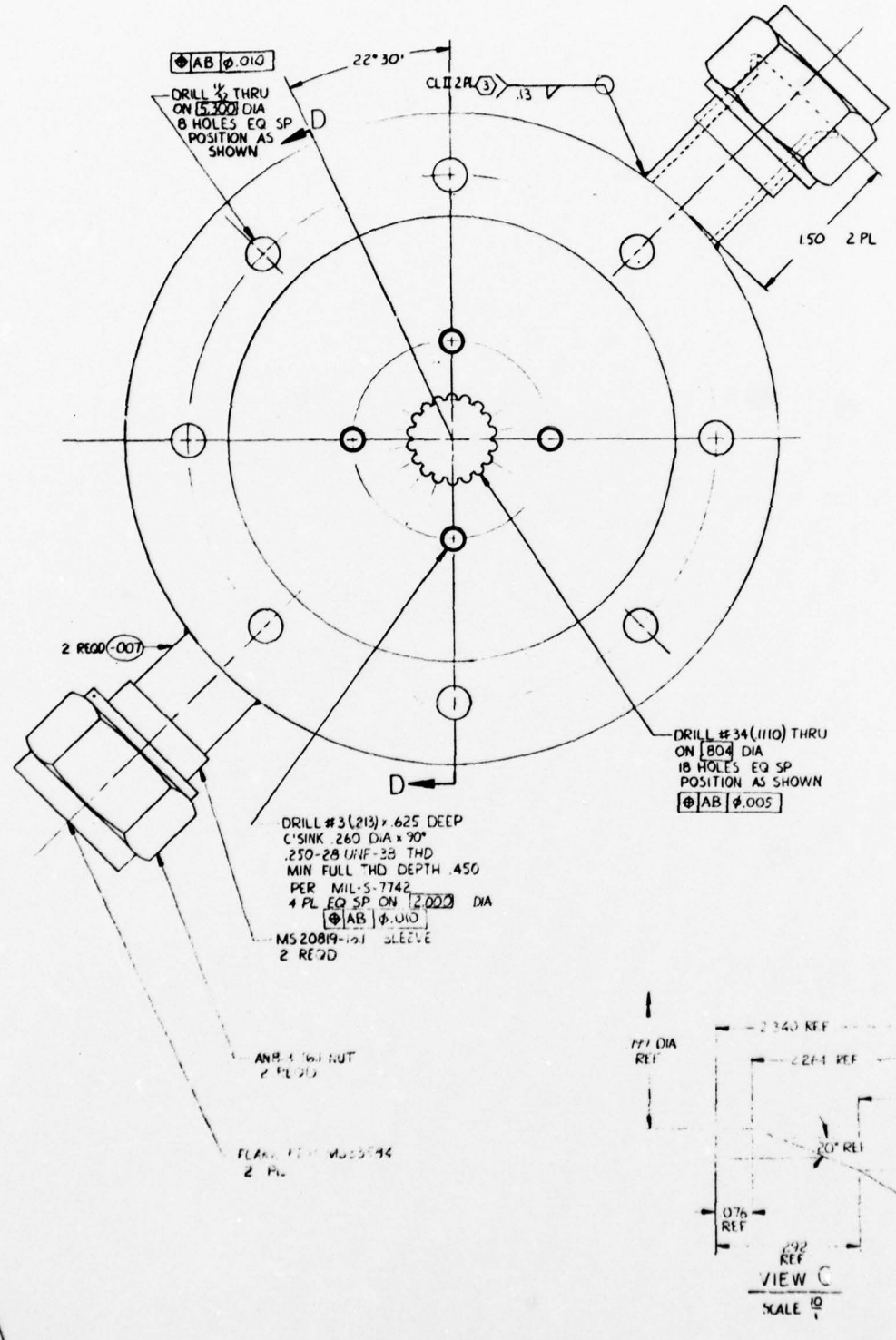
⊕ AB ϕ.010
22° 30'
DRILL ½ THRU
ON 5.300 DIA
8 HOLES EQ SP
POSITION AS
SHOWN
D
CL II 2 PL (3) .13
1.50 2 PL
2 REQD (-007)
DRILL #34 (.1110) THRU
ON .804 DIA
18 HOLES EQ SP
POSITION AS SHOWN
⊕ AB ϕ.005
D
DRILL #3 (.213) x .625 DEEP
C'SINK .260 DIA x 90°
.250-28 UNF-3B THD
MIN FULL THD DEPTH .450
PER MIL-S-7742
4 PL EQ SP ON 2.000 DIA
⊕ AB ϕ.010
MS20819-131 SLEEVE
2 REQD
ANB-4 961 NUT
2 REQD
FLANGE MS33794
2 PL
DRILL ½ (.500) DIA
8 PL EQ SP
CL II 2 PL (3)
1 REQD
.799±.001
DIA
⊕ AB ϕ.001
4.500
DIA
32
SEAL
SURFACE
2.340 REF
2.248 REF
20° REF
.076
REF
.292
REF
31°11' REF
VIEW C
SCALE 10/1

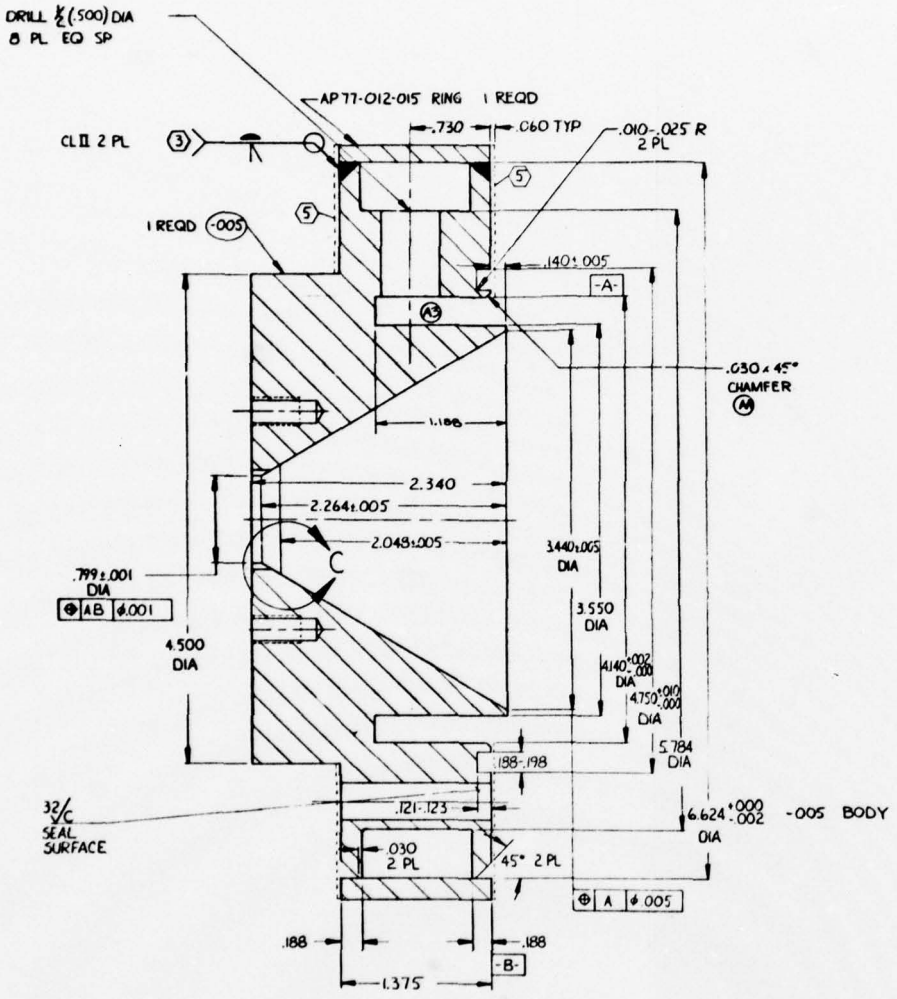

SECTION D-D

-001 BODY ASSY

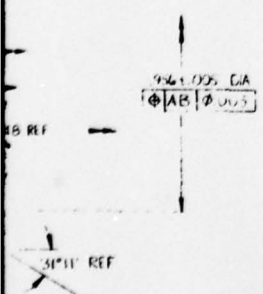

Figure 26. High-Power Gas Generator Nozzle Hot Wall (sheet 2 of 2)

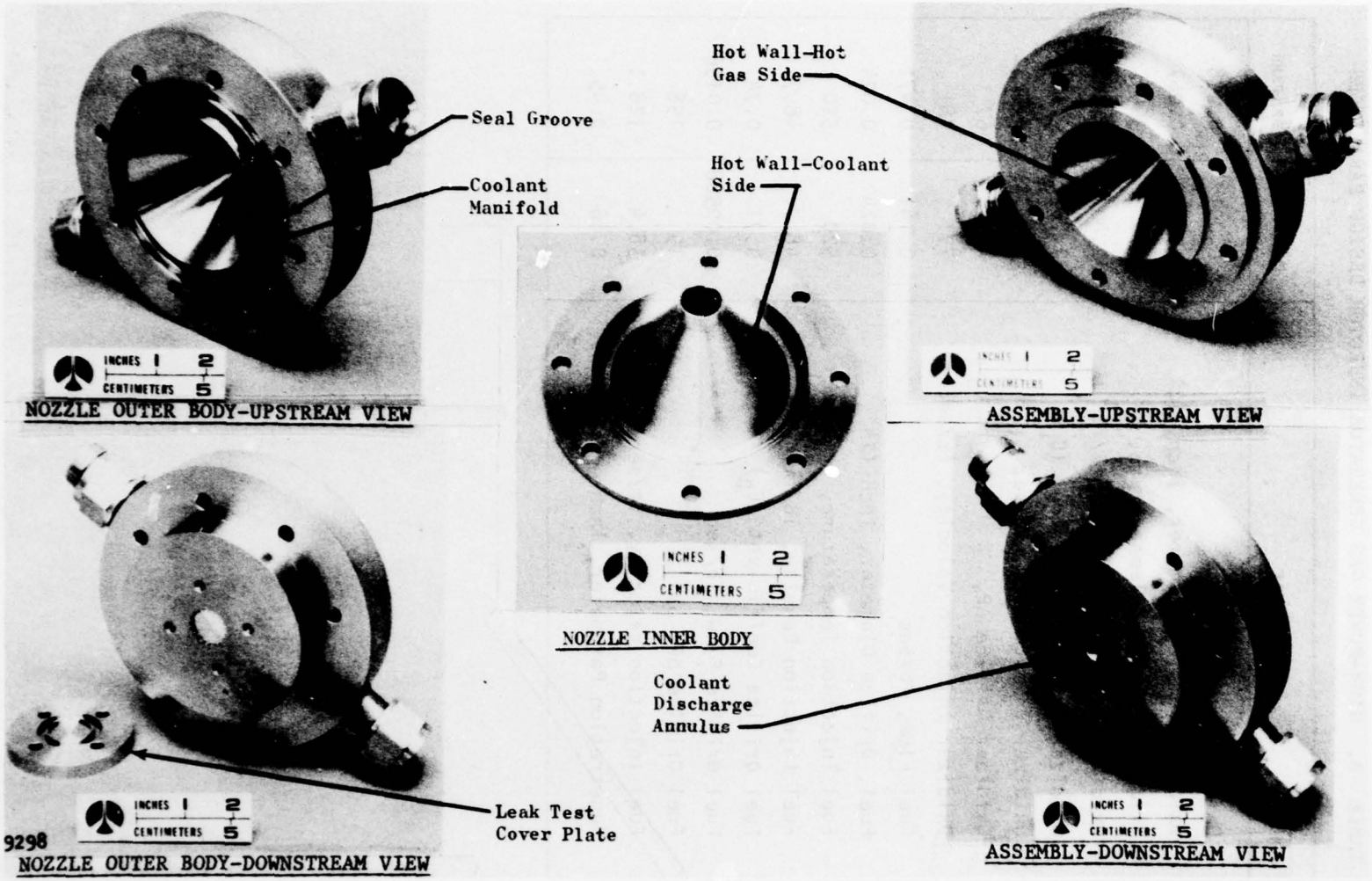

Figure 27. igh-Power Gas Generator Nozzle

TABLE 8. HIGH-POWER GAS GENERATOR INJECTOR DESIGN PARAMETERS

Parameter	Minimum	Maximum
Oxidizer Flow, lb/sec	0.091	0.278
Oxidizer Orifice Diameter, inch (12)	0.067	0.067
Oxidizer Injection Temperature, R	670	369
Oxidizer Injection Density, lb/ft^3	0.4014	2.488
Oxidizer Orifice Coefficient (C_D)	0.79	0.79
Oxidizer Orifice Flow, lb/sec	0.00758	0.0232
Oxidizer Orifice ΔP,	43	67
Oxidizer Injection Velocity, ft/sec	771	381
Fuel Flow, lb/sec	0.141	0.471
Fuel, Orifice Diameter, inch (24)	0.024	0.024
Fuel Injection Temperature, R	520	520
Fuel Injection Density, lb/ft^3	48.7	48.7
Fuel Orifice Coefficient (C_D)	0.71	0.74
Fuel Orifice Flow, lb/sec	0.00588	0.0196
Fuel Orifice ΔP, psi	15	158
Fuel Injection Velocity, ft/sec	38.4	128.1
Penetration Parameter, inch	0.16	0.45

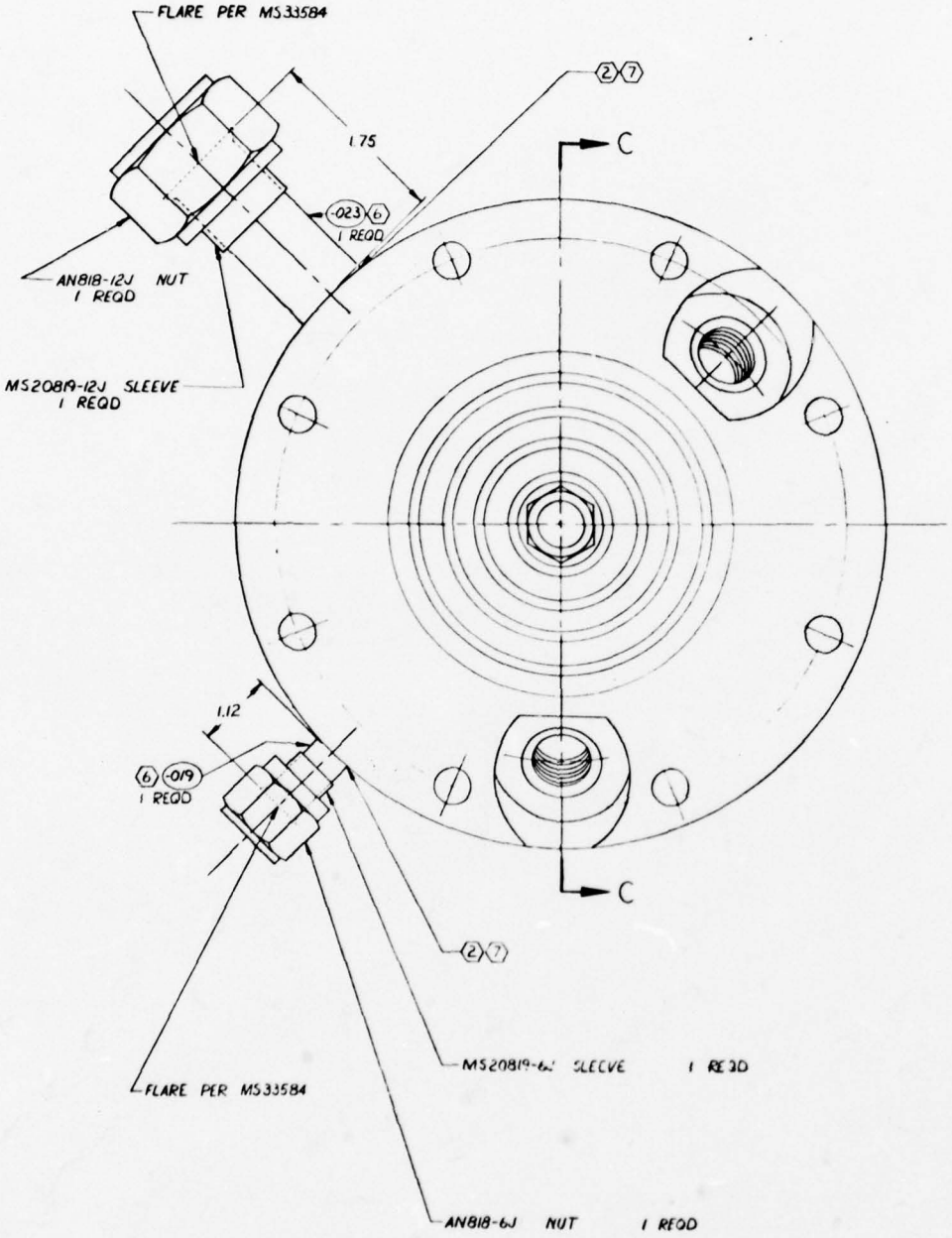

-001 ASSY

SECTIO

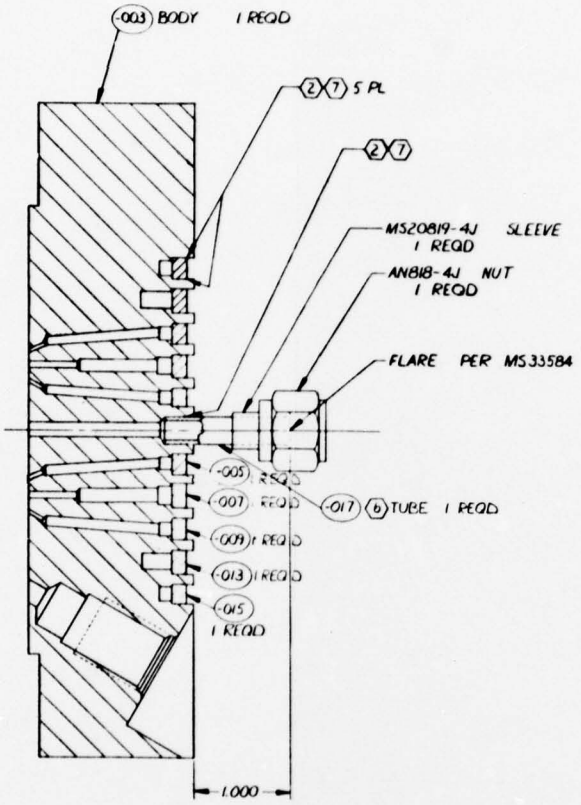

SECTION C-C

-001 ASSY

Figure 28. High-Power Gas Generator Injector (sheet 1 of 2)

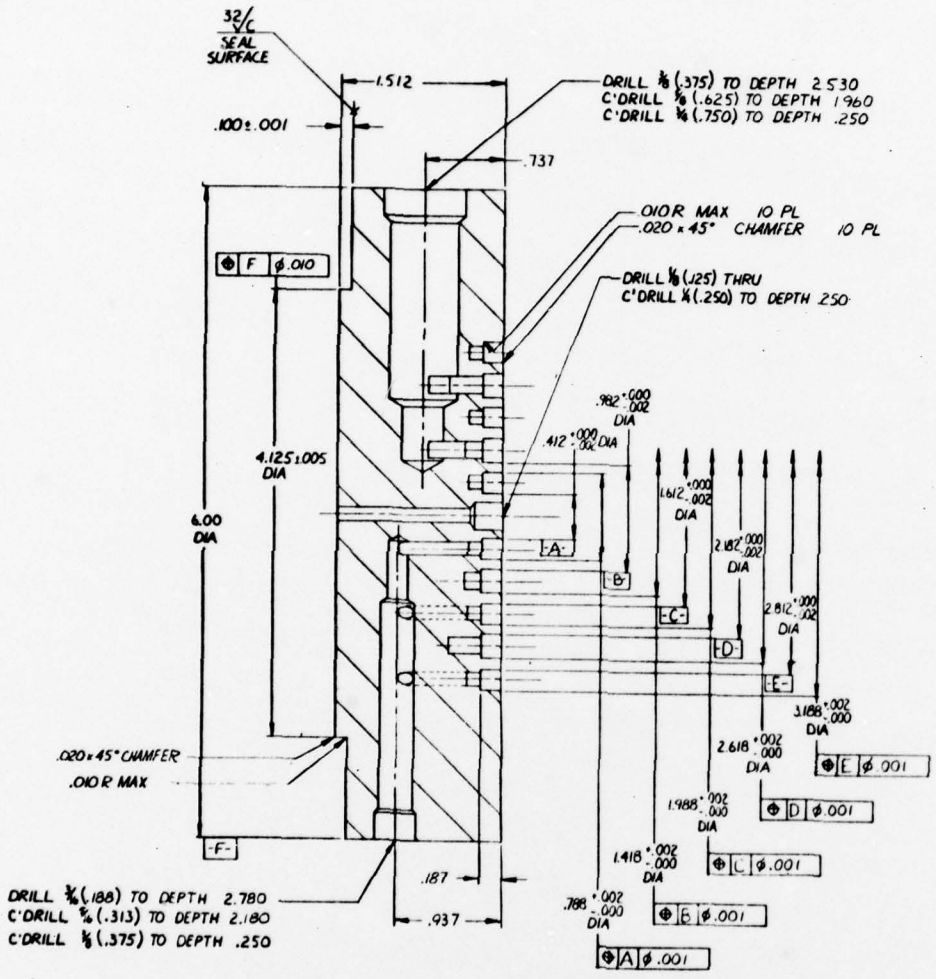

SECTION A-A

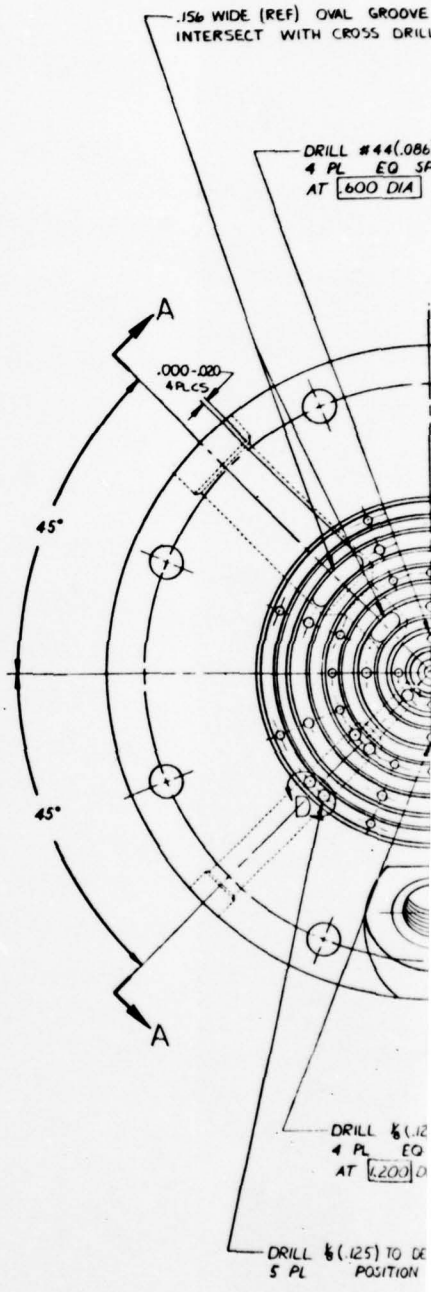

DETAI

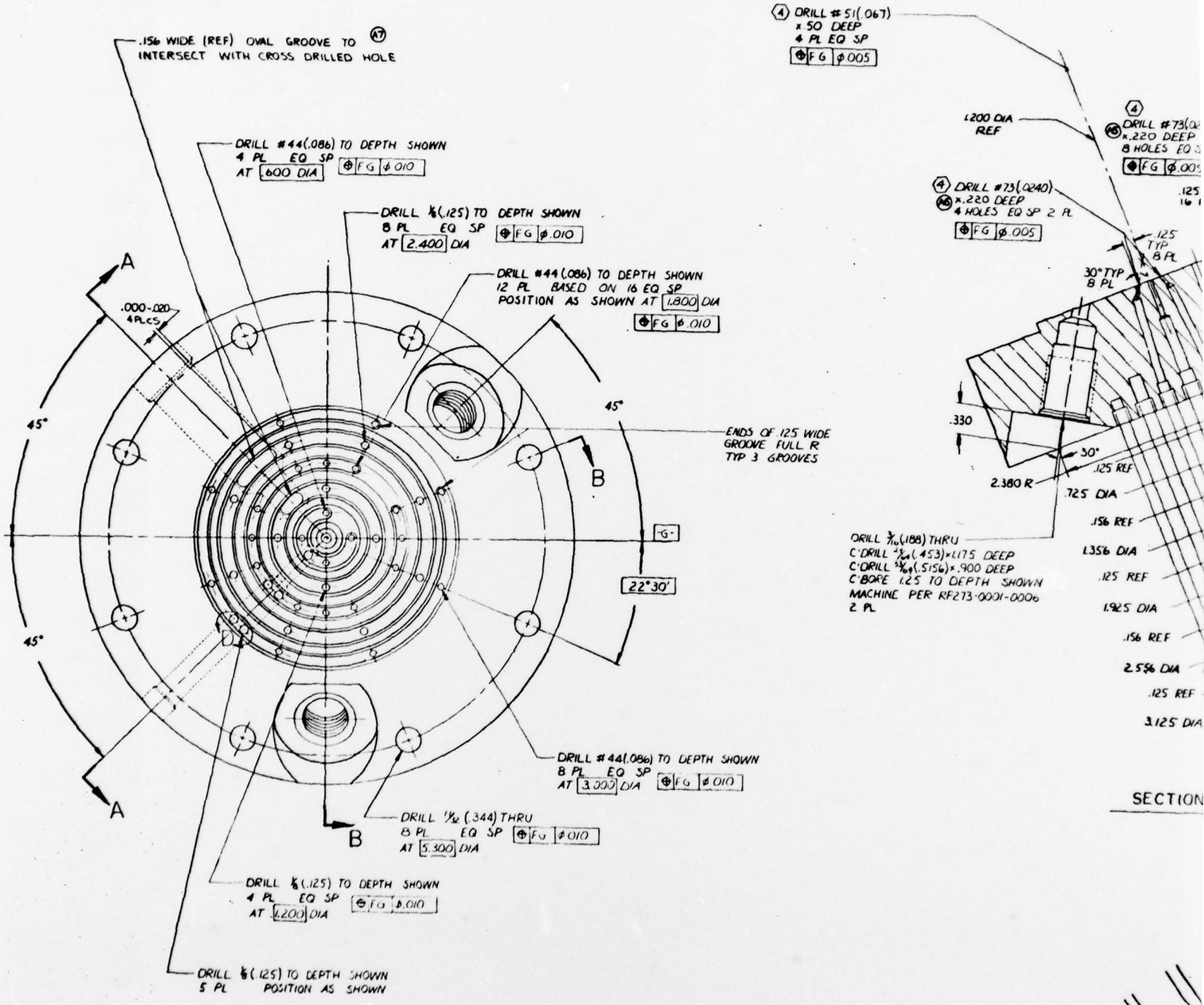

DETAIL -003 BODY

SECTION

VIE

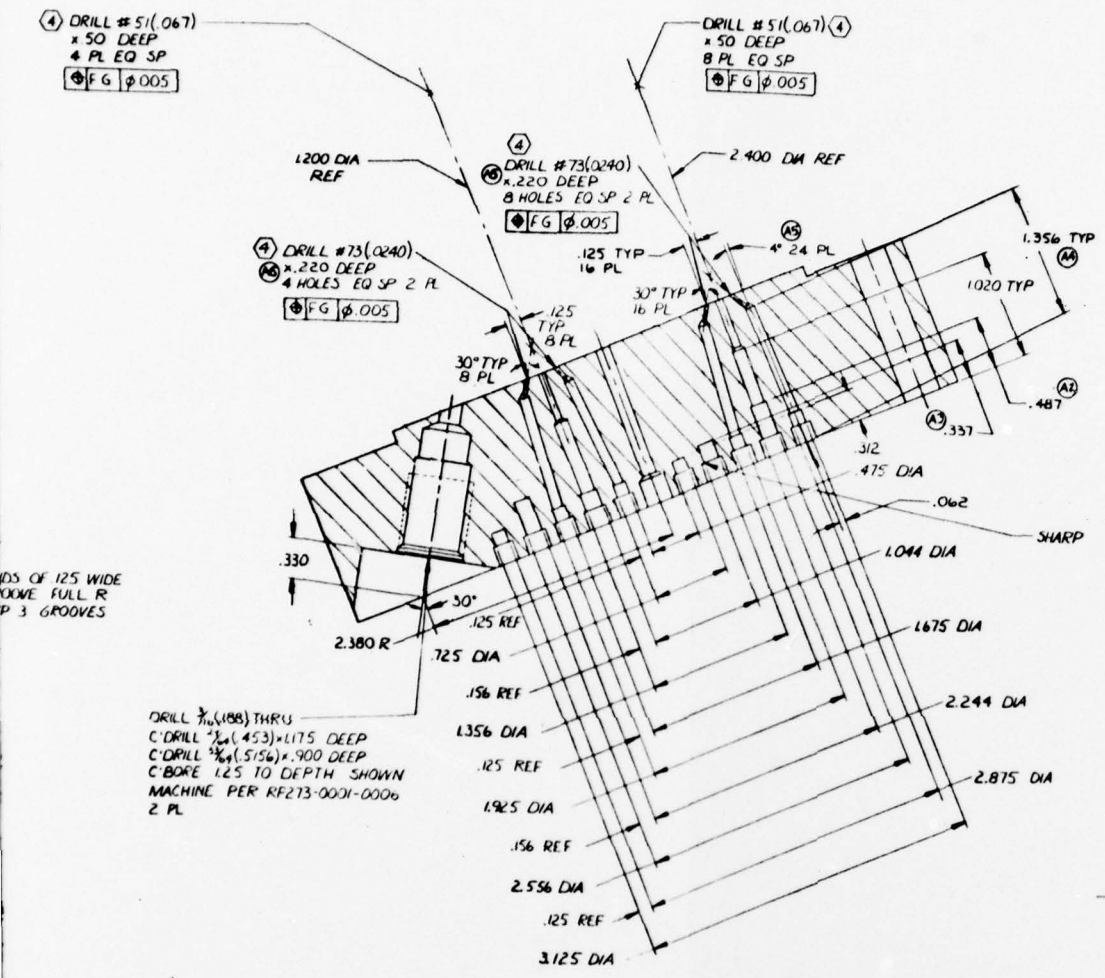

SECTION B - B

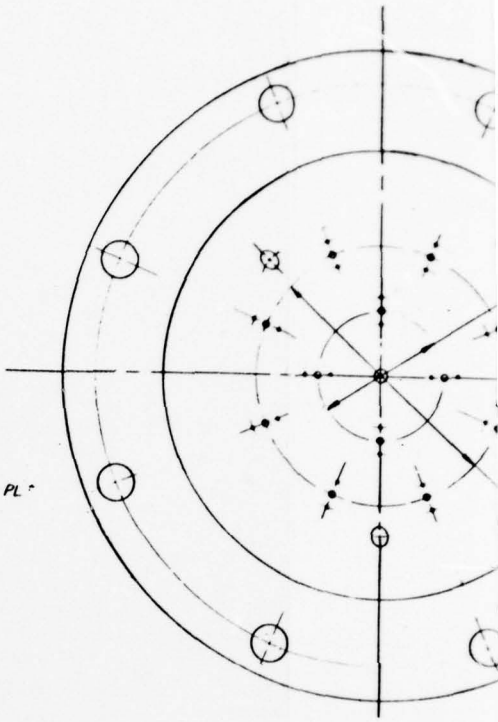

FACE VIEW

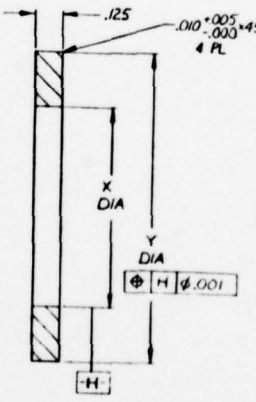

NO	X	Y	NO OF PC
-005	.417 (5)	.733 (5)	1
-007	.987 (5)	1.413 (5)	1
-009	1.617 (5)	1.983 (5)	1
-013	2.187 (5)	2.613 (5)	1
-015	2.817 (5)	3.183 (5)	1

DETAIL -005, -007, -009, -013, -015 RINGS
NO SCALE

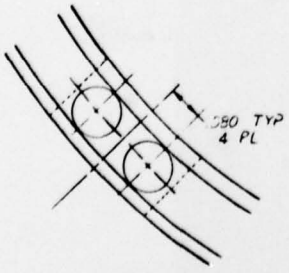

VIEW D
SCALE 8:1

Figure 28. High-Pow
Injecto

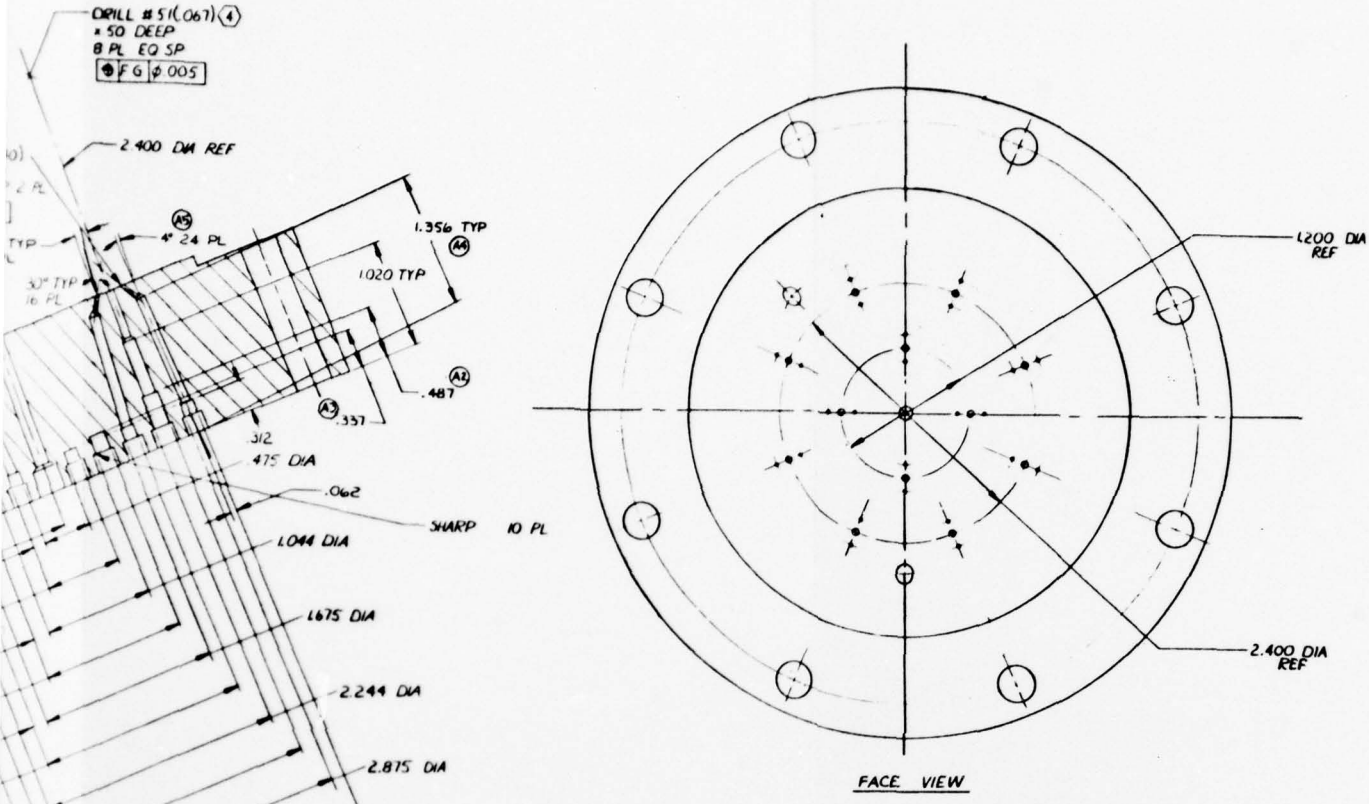

FACE VIEW

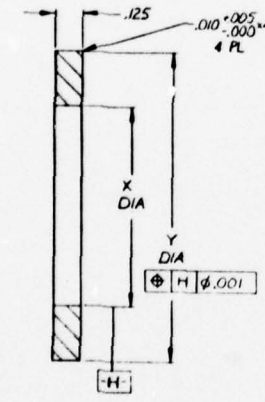

NO	X	Y	NO OF PCS
-005	.417 (5)	.783 (5)	1
-007	.987 (5)	1.413 (5)	1
-009	1.617 (5)	1.983 (5)	1
-013	2.187 (5)	2.613 (5)	1
-015	2.817 (5)	3.183 (5)	1

DETAIL -005, -007, -009, -013, -015 RINGS
NO SCALE

N B-B

.380 TYP 4 PL

IEW D
SCALE 8:1

Figure 28. High-Power Gas Generator Injector (sheet 2 of 2)

Figure 29 shows two photographs of the completed injector. The 12-triplet-element injector, both sparkplug ports, and the center chamber pressure tap can be seen. The closeouts of the propellant manifolds on the back side of the injector can also be seen.

Sparkplug Wafer Design. The design of the optional sparkplug wafer is shown in Fig. 30. The design provides two 180-degree opposed sparkplug ports in the chamber wall at a distance from the injector face approximately equal to the impingement distance for the triplet injector. The ports are positioned between injector elements since this was the position used for most of the low-power gas generator testing. An annular coolant passage is provided with a single inlet and outlet. Both water and GN_2 cooling could be used. The sparkplug wafer is constructed of stainless steel to allow operation at 800-900 F wall temperatures when GN_2 cooled to inhibit carbon formation. The completed wafer is shown in Fig. 31. The sparkplug installation port, the spark discharge port, and the coolant inlet and outlet are shown.

Gas Generator Hardware Assembly. The completely assembled high-power gas generator is shown in Fig. 32. The various components making up the assembly are identified, including the optional sparkplug wafer. The gas generator assembled without the wafer is shown for comparison in Fig. 33. Both injector-end and nozzle-end views are presented for the assemblies with and without the wafer.

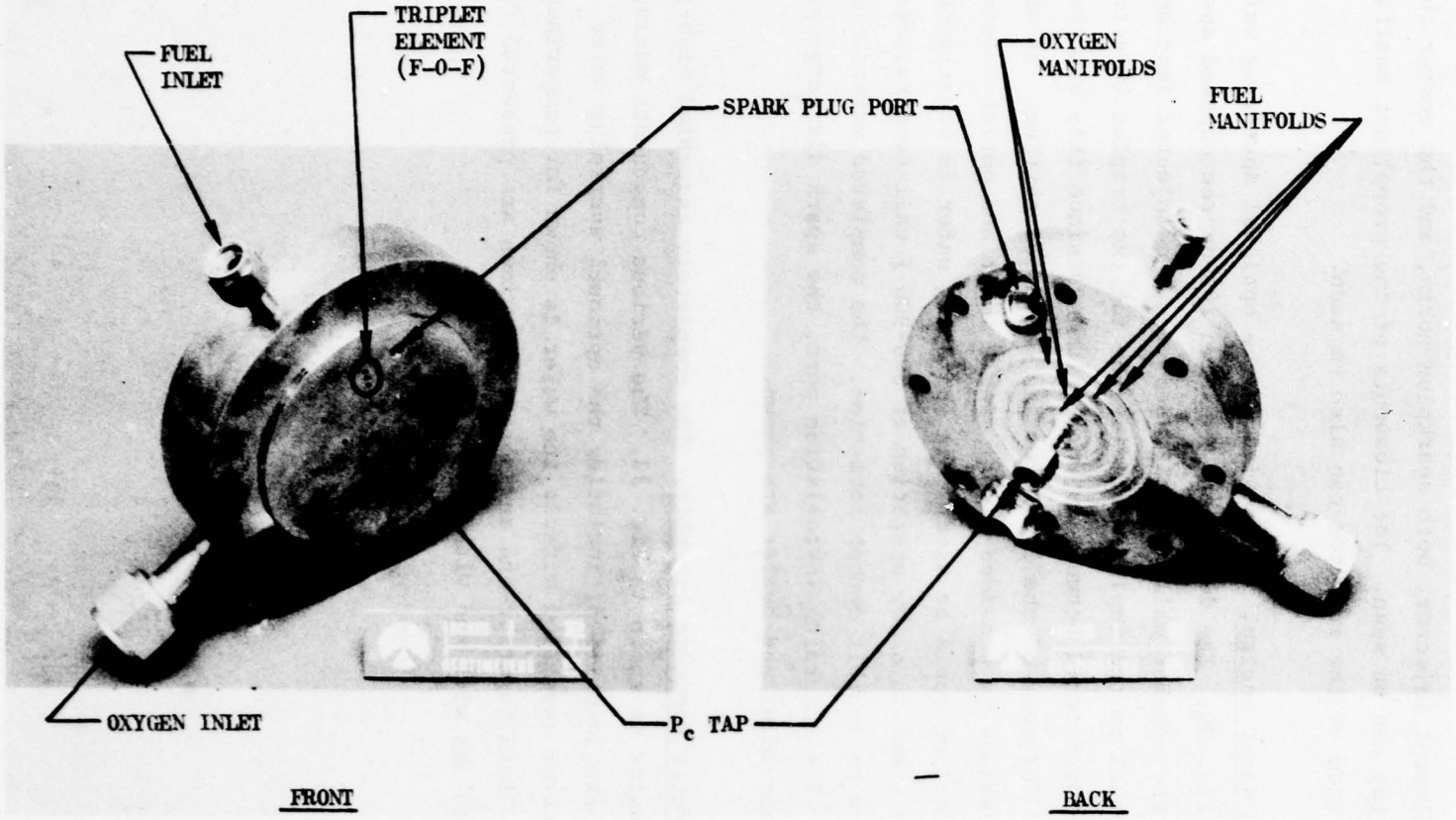

Figure 29. High-Power Gas Generator Injector

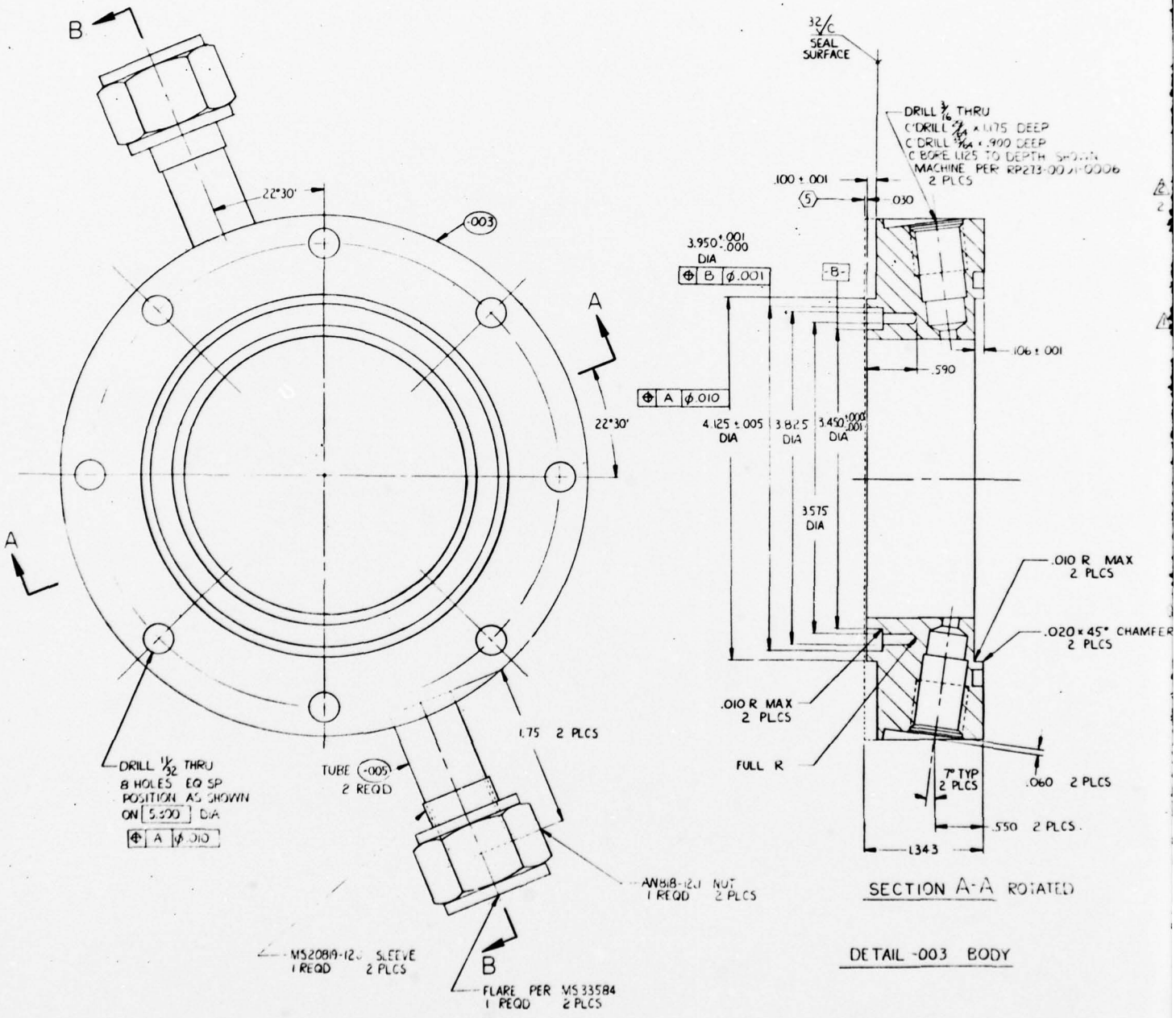
B
22°30'
-003
A
A
22°30'
DRILL 1/32 THRU
8 HOLES EQ SP
POSITION AS SHOWN
ON 5.300 DIA
⊕ A ϕ.010
TUBE -005
2 REQD
1.75 2 PLCS
AN818-12J NUT
1 REQD 2 PLCS
MS20819-12J SLEEVE
1 REQD 2 PLCS
B
FLARE PER MS33584
1 REQD 2 PLCS
32√C
SEAL
SURFACE
DRILL 3/16 THRU
C'DRILL 5/16 x 1.175 DEEP
C DRILL 5/16 x .900 DEEP
C BORE 1.125 TO DEPTH SHOWN
MACHINE PER RP273-0001-0006
2 PLCS
.100 ± .001
5
.030
3.950 +.001 -.000
DIA
⊕ B ϕ.001
-B-
.106 ± .001
.590
⊕ A ϕ.010
4.125 ± .005
DIA
3.825
DIA
3.450 +.000 -.001
DIA
3.575
DIA
.010 R MAX
2 PLCS
.020 x 45° CHAMFER
2 PLCS
.010 R MAX
2 PLCS
FULL R
7° TYP
2 PLCS
.060 2 PLCS
.550 2 PLCS
1.343
SECTION A-A ROTATED
DETAIL -003 BODY

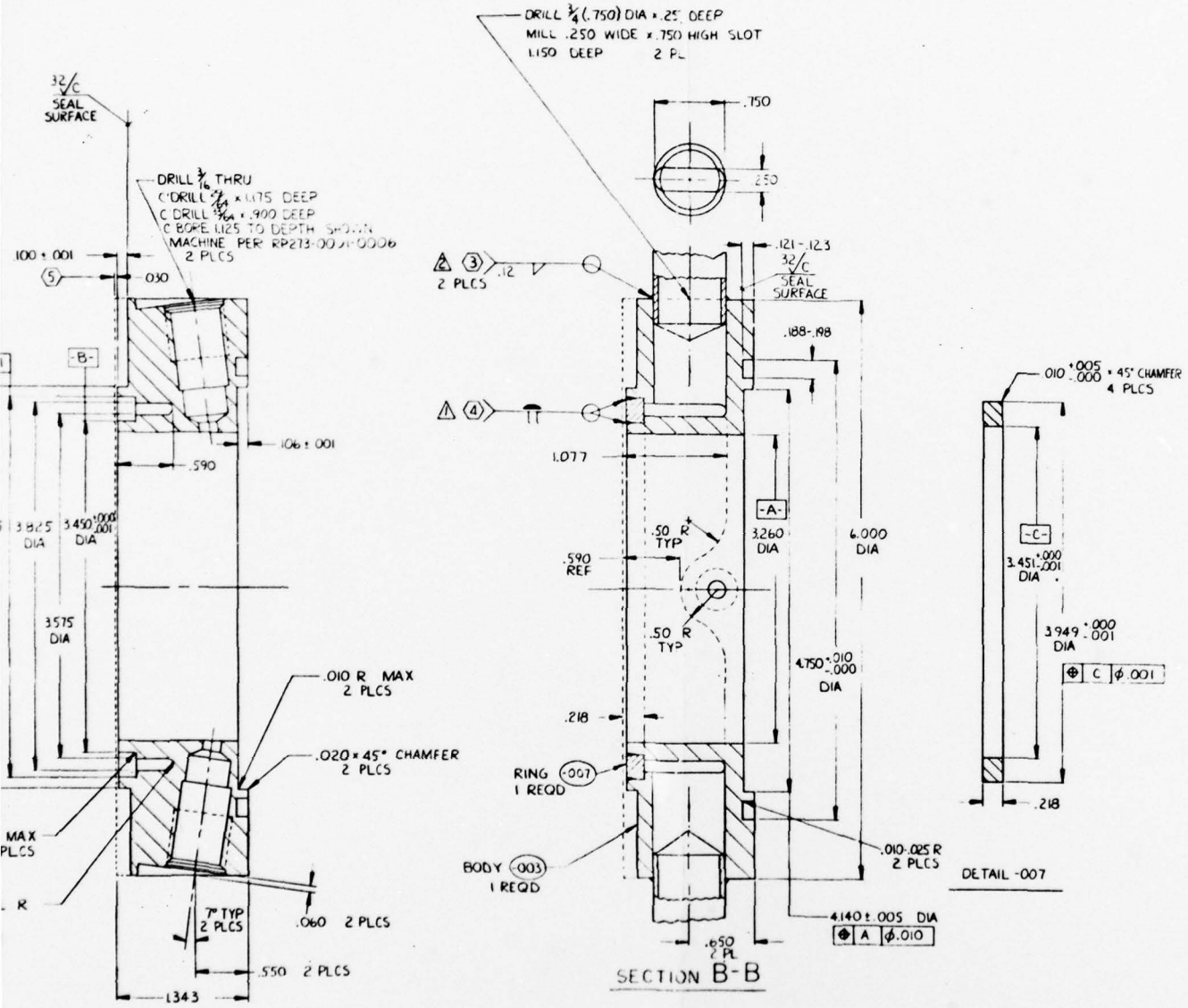

Figure 30. High-Power Gas Generator Sparkplug Wafer Assembly

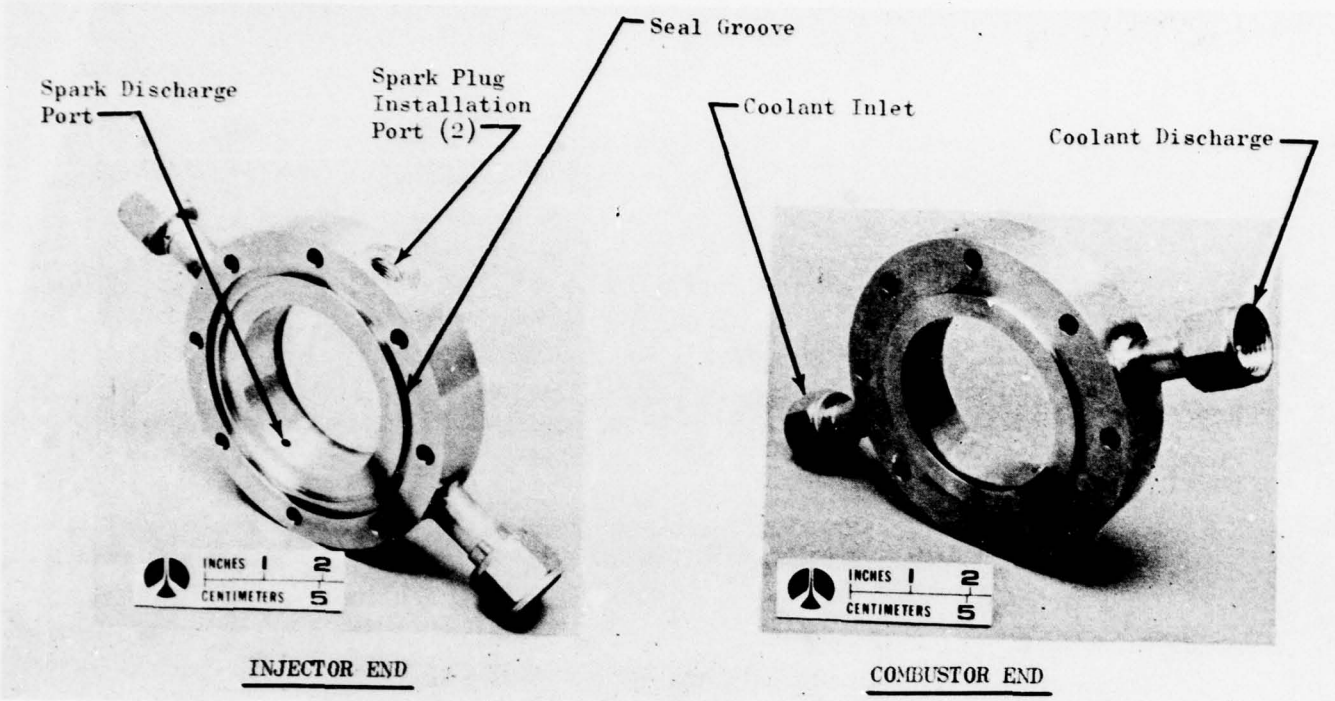

Figure 31. Sparkplug Wafer

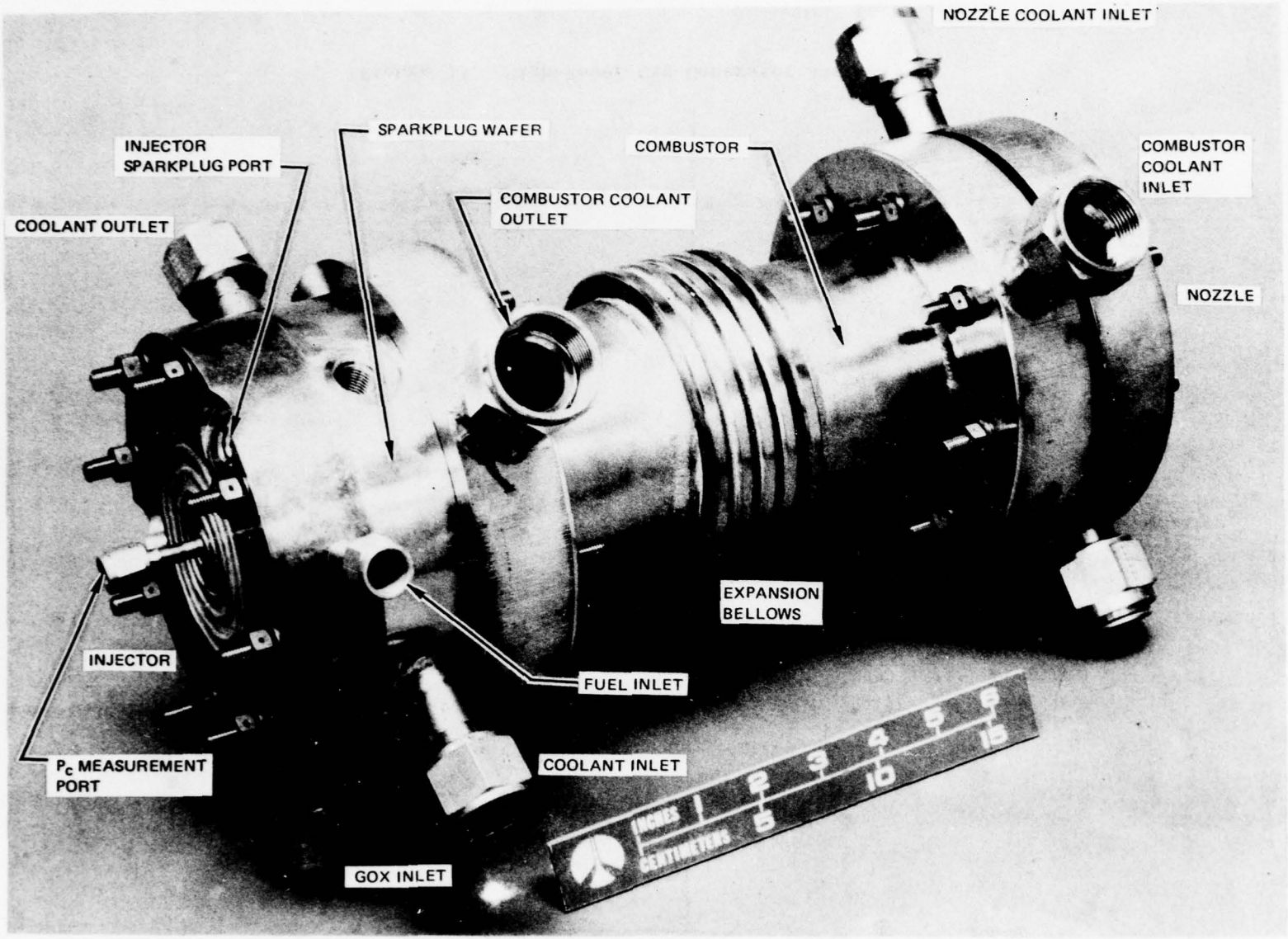

Figure 32. High-Power Gas Generator Test Hardware Assembly

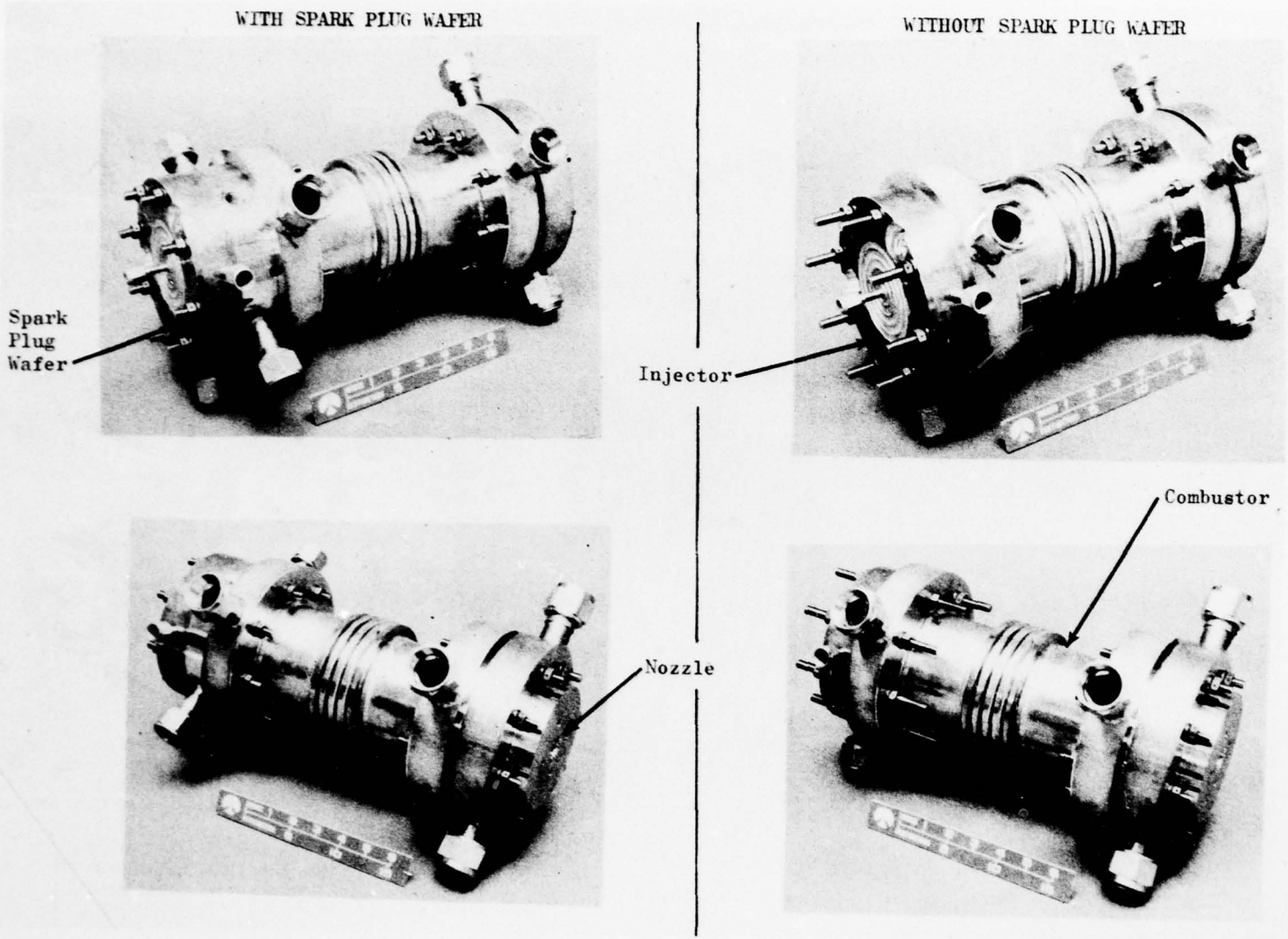

Figure 33. High-Power Gas Generator Assembly

TEST FACILITY

This section describes the test installation, instrumentation, and data acquisition systems used during the IPU gas generator test program.

Test Installation

The gas generator hot-gas tests were conducted at the Rockwell International Los Angeles Division, Thermodynamics Laboratory, located in El Segundo, CA. A schematic of the general test setup is shown in Fig. 34. Photographs of the overall basic low- and high-power gas generator installations are shown on Fig. 35 and 36, respectively. Several modifications to the basic installation were made throughout the test program as required to accomplish specific test objectives.

The primary test orientation for both the low- and high-power gas generators was in the vertical position (i.e., nozzle downward). However, the low-power gas generators were also tested in the horizontal position to demonstrate reliable gas generator ignition in either positions. Figure 37 shows the low-power gas generator horizontal test installation.

The vertical test orientation required the use of a flame deflector (Fig. 35 and 36) and a GH_2/air burner was located at the deflector exit to combust the fuel-rich gas generator exhaust gas.

An existing GH_2 ejector also was modified to mate with the low-power gas generator for altitude ignition testing, and Fig. 38 shows the test installation.

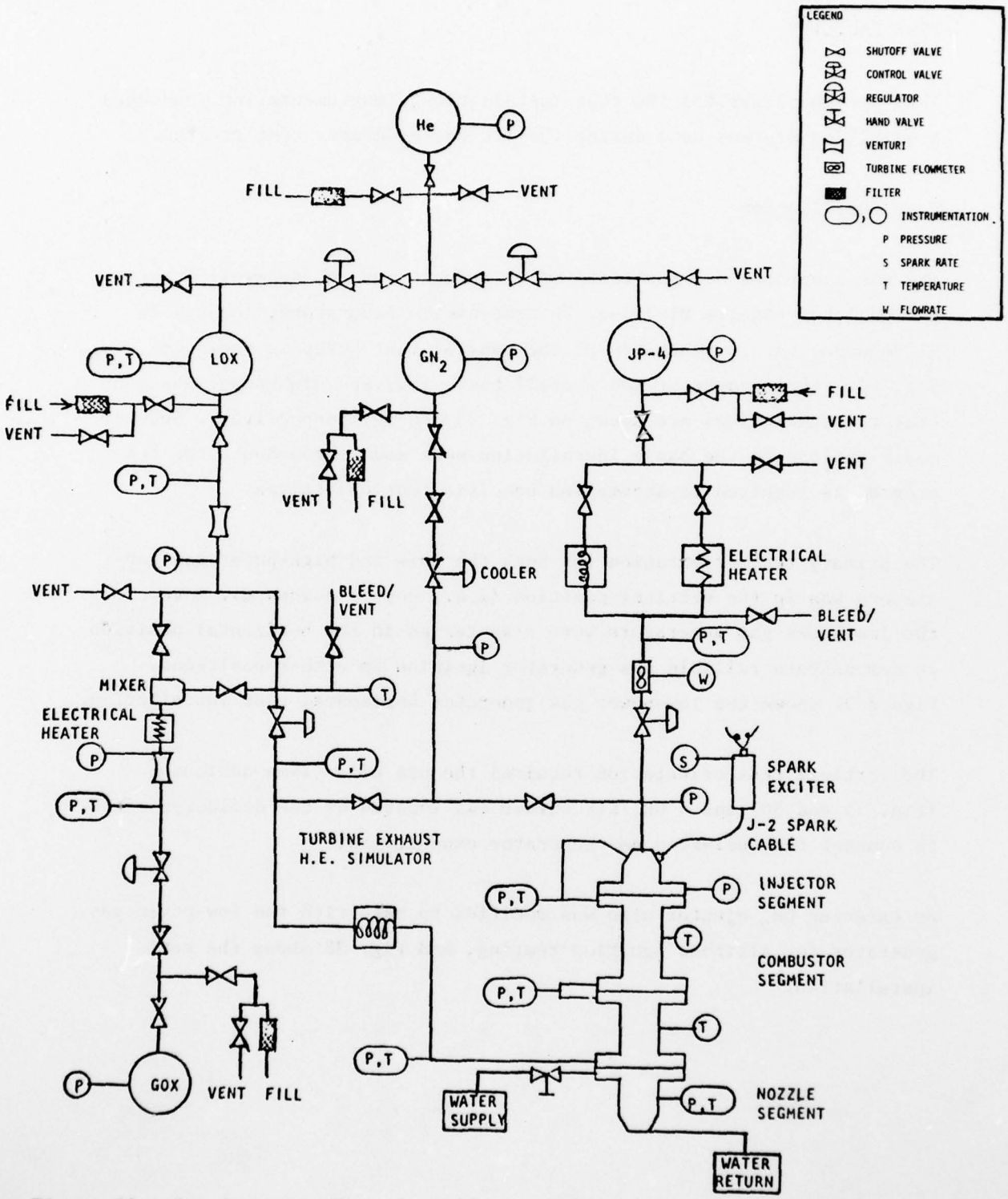

Figure 34. Gas Generator Test Installation Schematic and Instrumentation

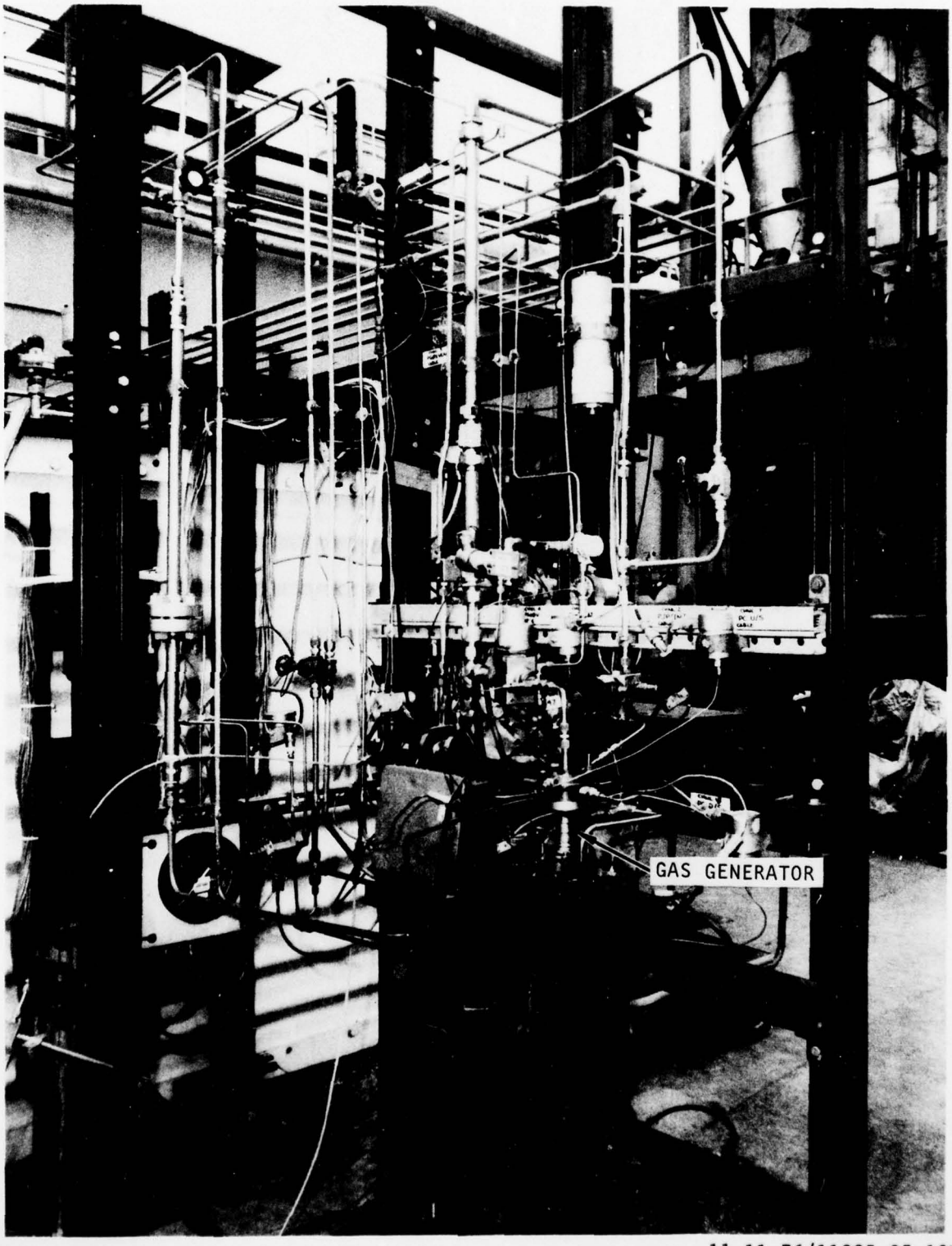

11-11-76/11305-95-10B

Figure 35. Overall Low-Power Gas Generator Test Installation

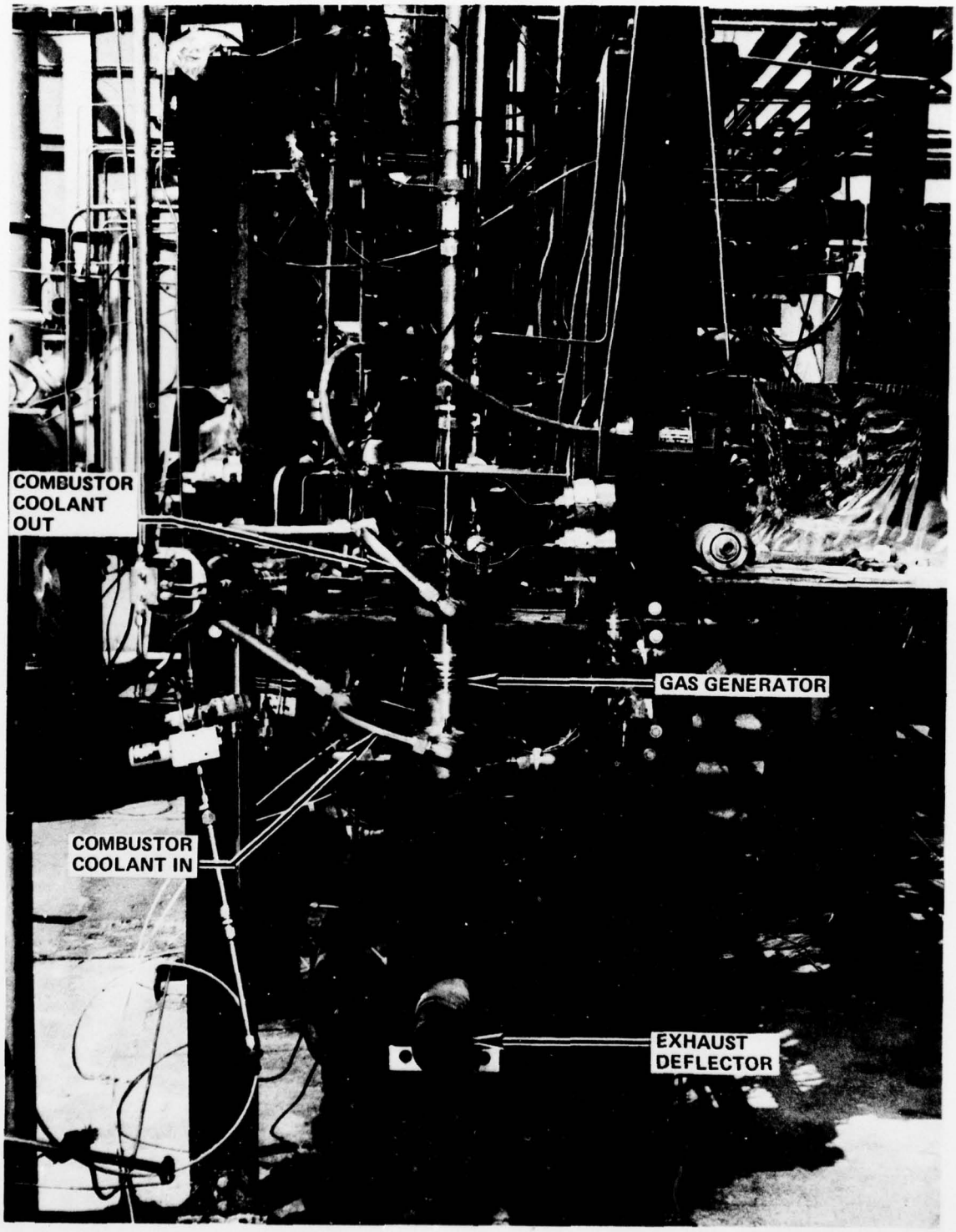

3-26-77/11305-95-22D

Figure 36. Overall High-Power Gas Generator Test Installation

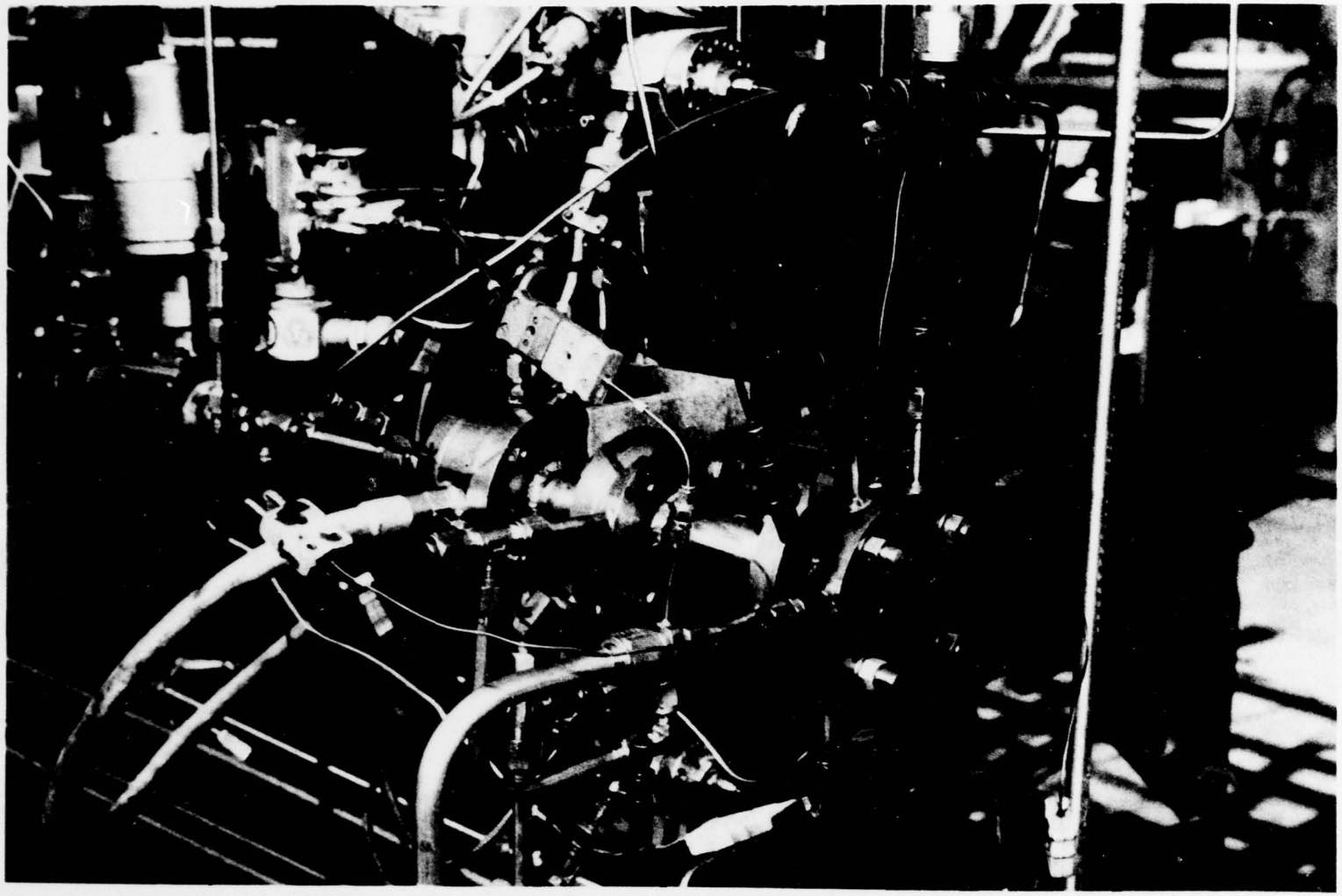

2-21-77/11305-95-17B

Figure 37. Low-Power Gas Generator Horizontal Test Installation

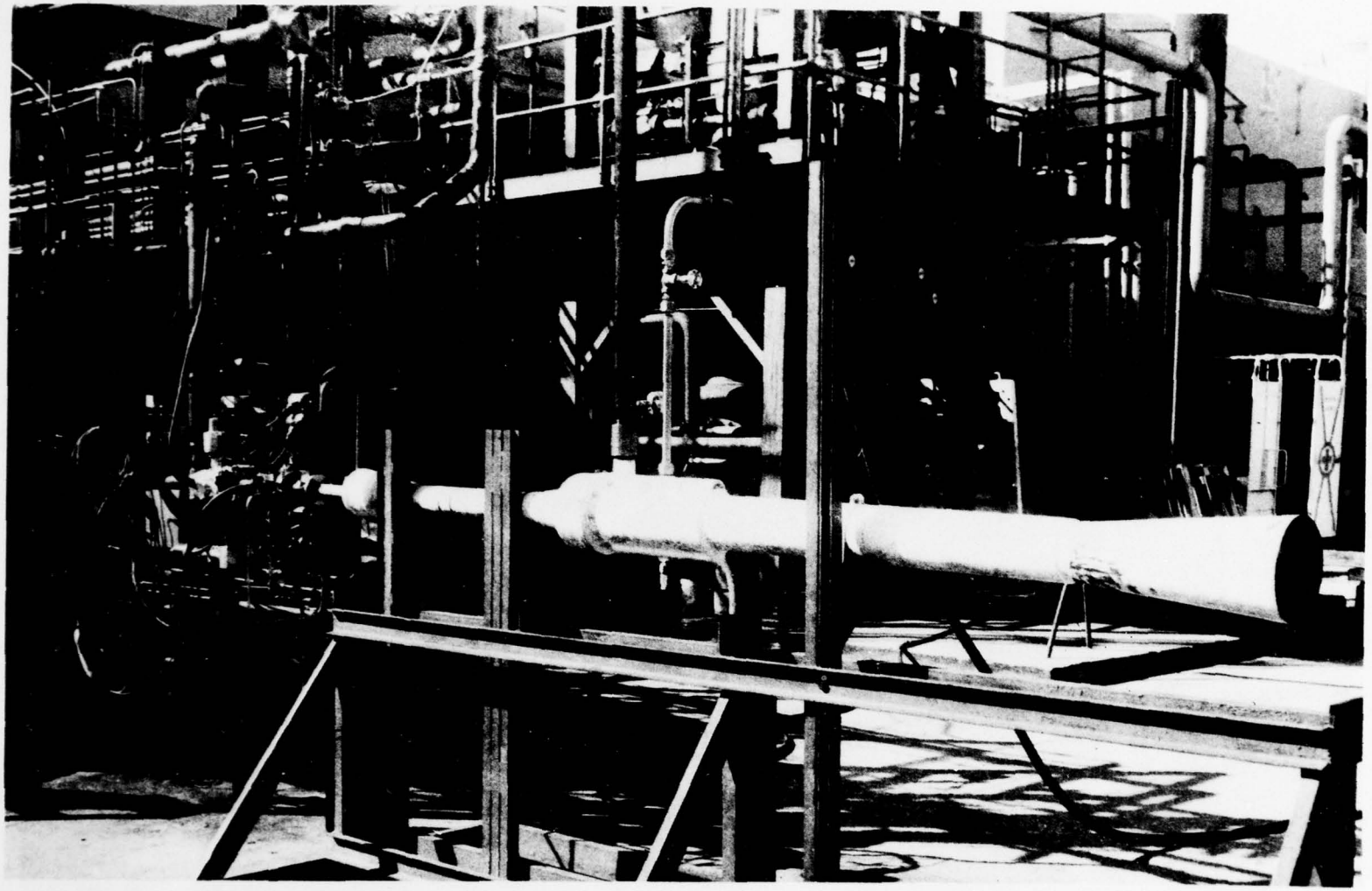

3-3-77/11305-95-20A

Figure 38. Low-Power Gas Generator High-Altitude Ignition Test Installation

Propellant conditioning to obtain both the low- and high-temperature propellants for gas generator testing was accomplished by jacketing the oxidizer and fuel feed system lines. A controllable mixture of GN_2 and LN_2 was used in the jacket to accomplish the cold propellants conditioning tests, while steam was used to condition the propellants for the hot-temperature extreme tests. The jacketing was accomplished by welding tubing around the feed system lines and insulating the jacket as required.

Instrumentation and Data Acquisition

A list of the instrumentation utilized for the LOX/JP-4 test program is shown on Table 9. Four types of data recorders were utilized:

1. Visual indicators, such as gages, were installed in the control console to set and/or monitor the prestart propellant tank, fluid supply, and purge pressure levels.
2. Brush recordings of critical parameters were made from which a quick-look, preliminary analysis could be conducted right after testing.
3. Oscillograph recordings of parameters where dynamic response was important were made from which a posttest analysis could be made of any transient condition.
4. Digital recordings of all parameters were made on FM tape and were subsequently utilized as the primary data for complete analyses.

TABLE 9. GAS GENERATOR INSTRUMENTATION LIST

System	Parameter	Range	Recorder/Display				Comments
			Visual	Brush	Oscillograph	Astrodata	
Helium	Tank Pressure	0 to 3000 psi	1	-	-	1	
Gaseous Nitrogen	Tank Pressure	0 to 3000 psi	1	-	-	1	
	Purge Pressure	0 to 500 psi	1	-	-	1	
JP-4	Tank Pressure	0 to 1000 psi	1	-	-	1	
	Conditioner Outlet Pressure	0 to 1000 psi	1	-	-	1	
	Conditioner Outlet Temperature	-65 to +165 F	-	1	-	1	
	Flowrate	0 to 1 lb/sec	-	-	-	1	
	Injection Pressure	0 to 750 psi	-	1	1	1	
Spark Exciter	Spark Rate	0 to 100 Hz	-	-	1	-	
LOX	Tank Pressure	0 to 1000 psi	1	-	-	1	
	Tank Temperature	0 to -300 F	1	-	-	1	
	Venturi Inlet Pressure	0 to 1000 psi	-	-	-	1	
	Venturi Inlet Temperature	0 to -300 F	-	-	-	1	
	Venturi Outlet Pressure	0 to 1000 psi	-	-	-	1	
	Mixer Bleed Temperature	+300 to -300 F	1	-	-	1	
	Heat Exchanger Inlet Pressure	0 to 1000 psi	-	1	-	1	
	Heat Exchanger Inlet Temperature	+300 to -300 F	-	1	-	1	

TABLE 9. (Concluded)

System	Parameter	Range	Recorder/Display				Comments
			Visual	Brush	Oscillograph	Astrodata	
GOX	Tank Pressure	0 to 300 psi	1	-	-	1	
	Venturi Inlet Pressure	0 to 1000 psi	-	1	-	1	
	Venturi Inlet Temperature	+100 to -100 F	-	-	-	1	
	Venturi Outlet Pressure	0 to 1000 psi	-	-	-	1	
Combustor	Lower Combustor Segment Inlet Pressure	0 to 500 psi	-	1	1	1	
	Lower Combustor Segment Inlet Temperature	+300 to -300 F	-	-	-	1	
	Upper Combustor Segment Inlet Pressure	0 to 500 psi	-	1	1	1	
	Upper Combustor Segment Inlet Temperature	+300 to -300 F	-	1	1	1	
	Injection Pressure	0 to 500 psi	-	1	1	1	
	Injection Temperature	+300 to -300 F	1	-	-	1	
	Combustion Pressure	0 to 500 psi	-	1	1	2	
	Upper Combustor Segment Wall Temperature	-200 to +500 F	-	-	-	8	Random Locations
	Lower Combustor Segment Wall Temperature	-200 to +500 F	-	-	-	8	Random Locations
	Combustion Temperature	0 to 2250 F	1	1	-	4	Various Insertion Depths

TEST PROGRAM

The objective of the IPU Phase I test program was to evaluate experimentally the performance of promising injector types with the low-power gas generator, and to select the best injector type for further performancee verification and development with the high-power gas generator. All IPU operating conditions and environments were simulated in these tests. The gas generator hot-fire test program was divided into three main test series as follows: low-power gas generator test series, high-power gas generator test series, and modified high-power gas generator test series. Each will be discussed separately below.

Low-Power Gas Generator Test Series

The low-power gas generator test series was the first phase of the IPU test program. Testing was initiated on 11 October 1976 and completed on 11 March 1977. Test objectives included demonstration of the combustor performance efficiency, ignition reliability, combustion stability, and hardware integrity. Additional goals included the verification of the planned IPU operational limits and run duration capability. This was accomplished by evaluating three injector concepts, three combustor lengths, and various spark igniter locations and orientation.

During the test series a total of 311 hot-fire runs was completed, accumulating a total of 7035 seconds of steady-state duration. All test objectives were met, leading to the selection of an optimum triplet injector for the high-power gas generator. The triplet injector with a 10-inch combustor, in its final configuration, accumulated a total of 72 tests and 560 seconds of testing in completing the ignition, performance, and long-duration tests. A discussion of the test series is given below.

ASI Injector. The low-power gas generator matrix testing was initiated using the ASI-type injector. All tests were conducted using the 10-inch combustor length shown in Fig. 39 and a single J-2 sparkplug and exciter.

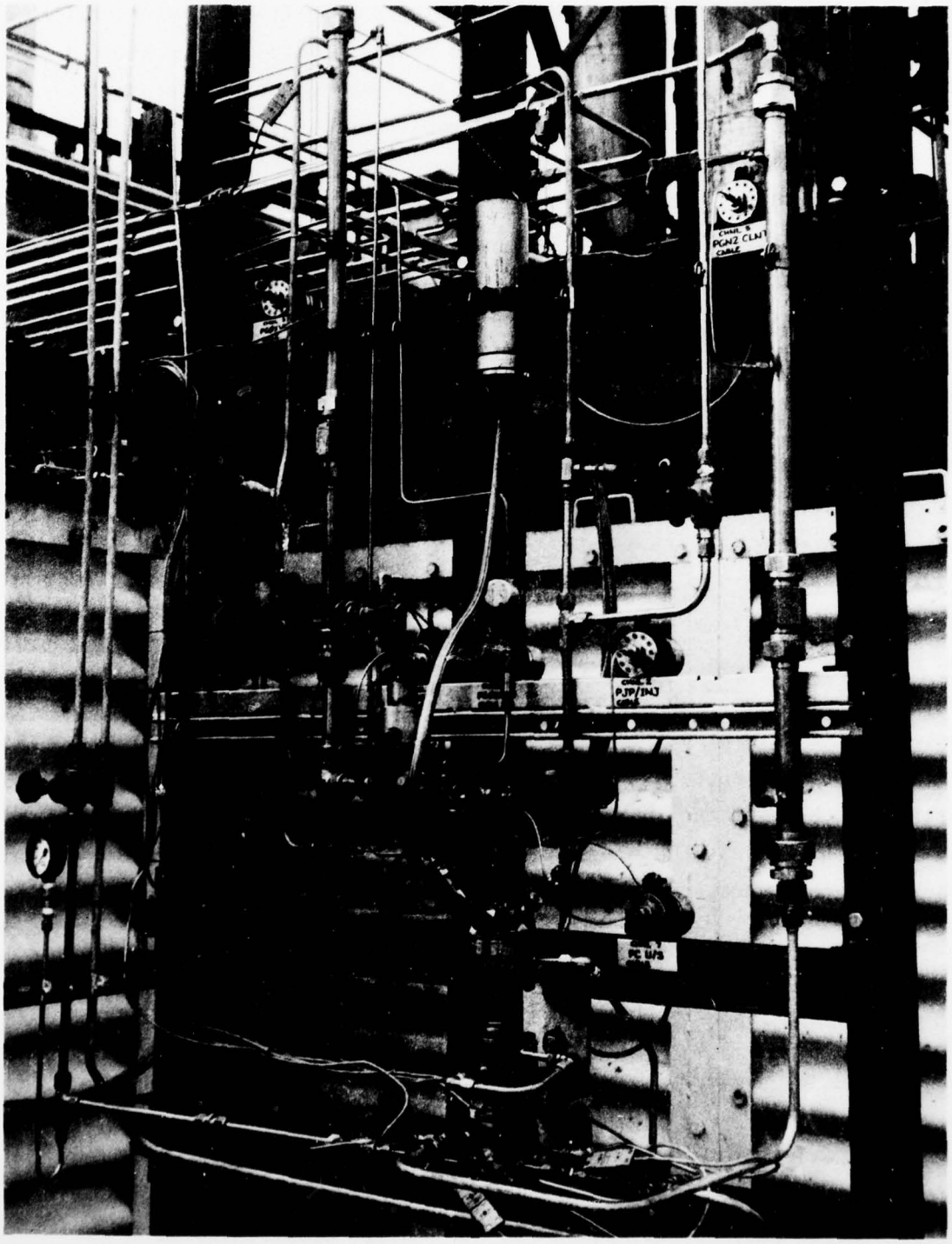

Figure 39. Low-Power Gas Generator Test Installation

Based on a review of Rocketdyne experience with this type of injector, the two GOX tubes were inserted as far as possible into the combustor, until they touched. Seven GOX and seven fuel blowdown tests were then conducted to determine the fluid system resistance, valve opening time, and fluid system priming time, as well as to flow-calibrate the flow measurement devices. The first tests were planned to check out ignition and cutoff transients and, therefore, a GOX ignition lead, a fuel cutoff lag, a high purge flowrate, and nominal test conditions (0.48 MR and 190-psia chamber pressure) were selected for evaluation. A total of 11 tests was conducted to check out the ignition and cutoff transients. During these tests, ignition delays of 400 to 1340 milliseconds were experienced. The long ignition delays were eliminated by reducing both fluid system purge flowrates and using a GOX cutoff lag to burn off all residual JP-4. The GOX lag caused a small rise in combustion temperature at cutoff (less than 50 F), which was acceptable.

The first planned test was then successfully accomplished. The second and third planned tests were then conducted, preceded by mixture ratio checkout tests. Posttest inspection (Fig. 40) revealed all surfaces were coated with a film of particulate carbon. There was an agglomerate buildup of carbon above the intersection of the two GOX tubes, and a partial blockage of the sparkplug cavity entrance hole. Also, one GOX tube had a burnout at the tip in the shape of a small "V" notch. All other injector, combustor, and nozzle surfaces were in good condition.

A modified ASI injector (Fig. 41) with a larger combustor inernal diameter at the injector face and a larger choke ring exit internal diameter was also tested. Eight starts totalling close to 400 seconds of operation, including a 5-1/2-minute test covering several chamber pressures and mixture ratios, were completed. Posttest inspection revealed that the GOX tubes remained perfect, but the choke ring was eroded (Fig. 42) in the region that would be expected to experience the highest mixture ratio. Carbon buildup was evident in the coolest areas. The location of the eroded areas suggested that four fuel inlets instead of one would correct the problem. Further iteration on the ASI design was not made.

10-11-76/11305-95-2A

Figure 40. ASI-Type Injector Posttest Condition

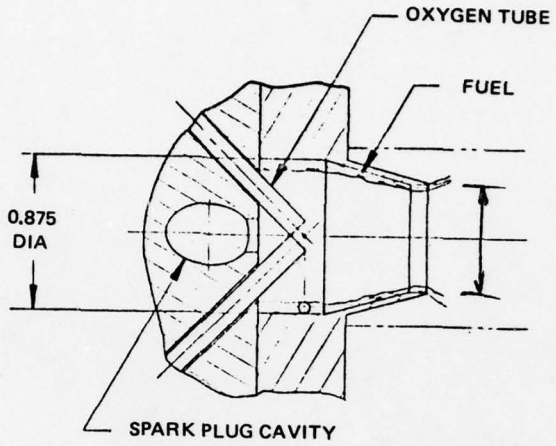

MODIFIED DESIGN

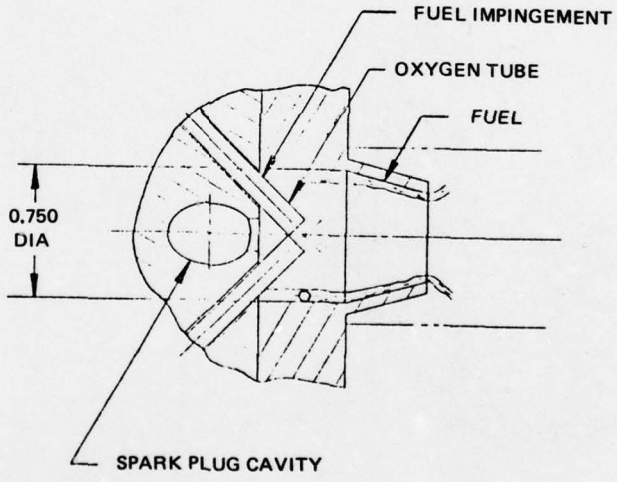

ORIGINAL DESIGN

Figure 41. ASI Injector Modifications

AD-A066 543 ROCKWELL INTERNATIONAL CANOGA PARK CALIF ROCKETDYNE DIV F/G 21/5
INTEGRATED POWER UNIT.(U)
DEC 78 G S WONG, T I YU, J J WARD F33615-76-C-2054
UNCLASSIFIED RI/RD78-237 AFAPL-TR-78-98 NL

2 OF 3
AD
A066543

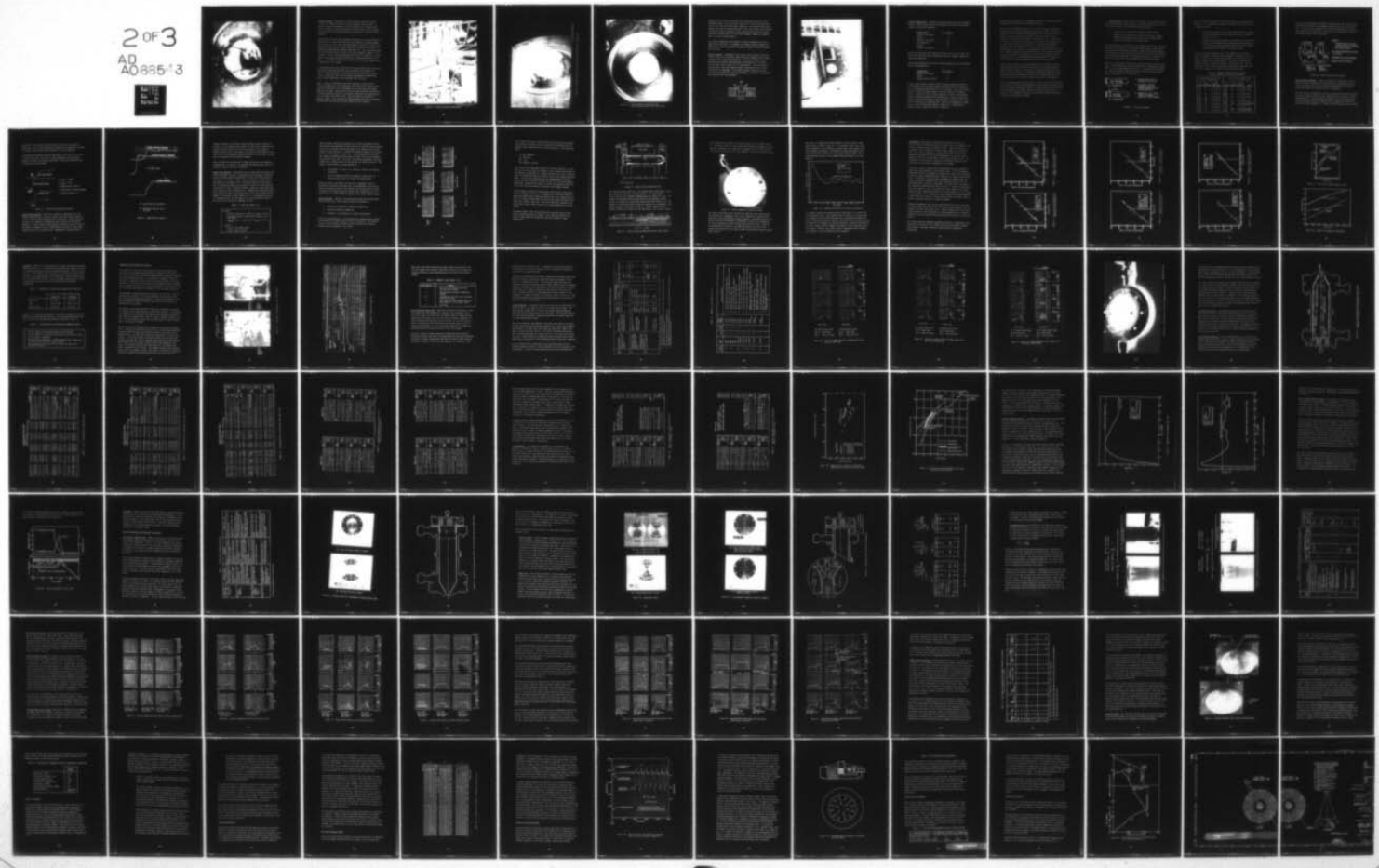

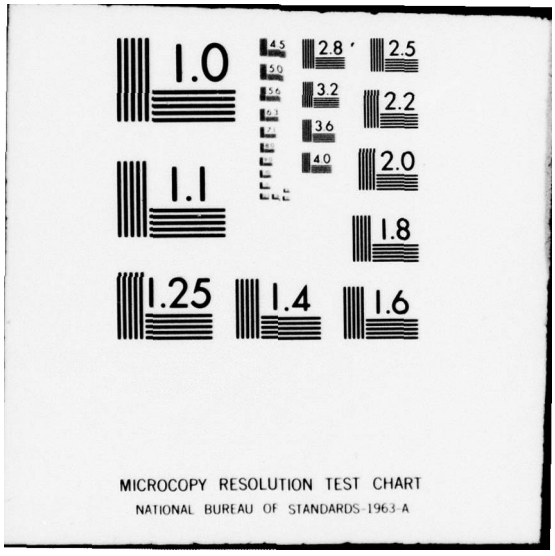
1.0
1.1
1.25
1.4
1.6
1.8
2.0
2.2
2.5
2.8
3.2
3.6
4.0
4.5
5.0
5.6
6.3
7.1
MICROCOPY RESOLUTION TEST CHART
NATIONAL BUREAU OF STANDARDS-1963-A

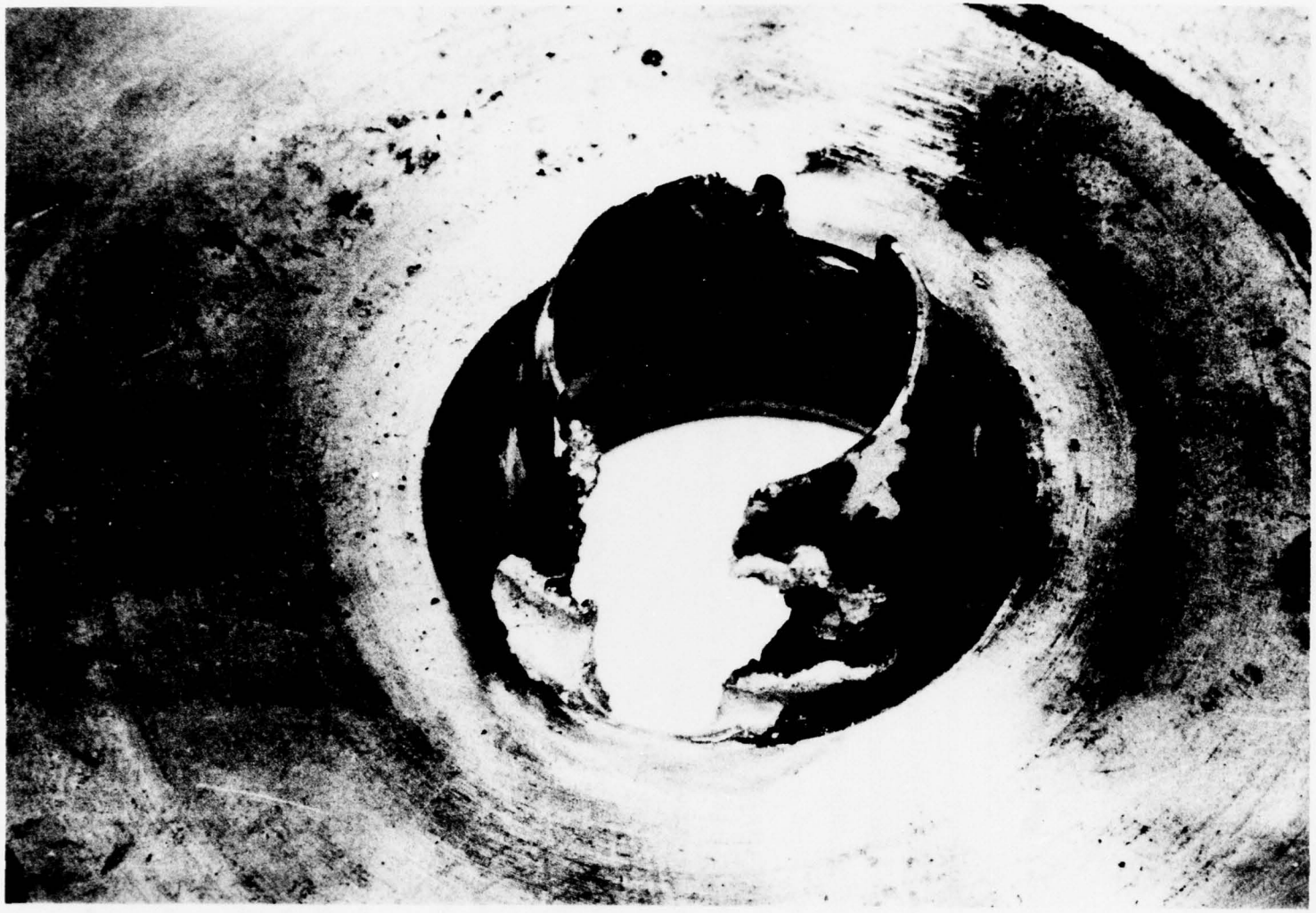

Figure 42. ASI Injector Choke Ring Damage

Triplet Injector. Subsequent to the ASI injector tests the triplet injector was installed with the 10-inch combustor (see Fig. 43). A series of five GOX blowdowns, one JP-4 blowdown, and 17 ignition and cutoff transient tests were conducted to check out the triplet injector. The major problem during this series was quenching of combustion after ignition.

Two planned tests were then completed successfully, the second after one checkout test. Inspection after each test revealed no hardware damage. The injector face was coated with approximately 1/32-inch of carbon, and around each GOX injection orifice there was a buildup in the shape of a hollow cone approximately 1/8-inch high (Fig. 44). Also, there was moderate carbon buildup (Fig. 45) only in the upper combustor segment at four locations. Each location encompassed approximately 15 degrees of circumference, each being equidistant between its corresponding orifice elements. The buildup extended down from the top of the upper combustor for a distance of 2 to 3 inches.

A long-duration test was conducted where the gas generator was started at (relatively) high flowrates and throttled down to low flowrates by reducing supply pressures. A 13-minute test was accomplished successfully, verifing that the triplet injector gas generator configuration would sustain combustion at the low-power level (90 psia).

Next, a series of five matrix tests was conducted to check out the triplet gas generator at the high-power level (290 psia). Ingition problems were experienced, and an assessment of the test setup and instrumentation was made. Three matrix tests were then completed successfully, although quenching (followed by successful reignition) was experienced at the low mixture ratio (MR = 0.38). Posttest inspection revealed no hardware damage. This completed the planned matrix tests for the triplet configuration, and the injector was removed from the combustor.

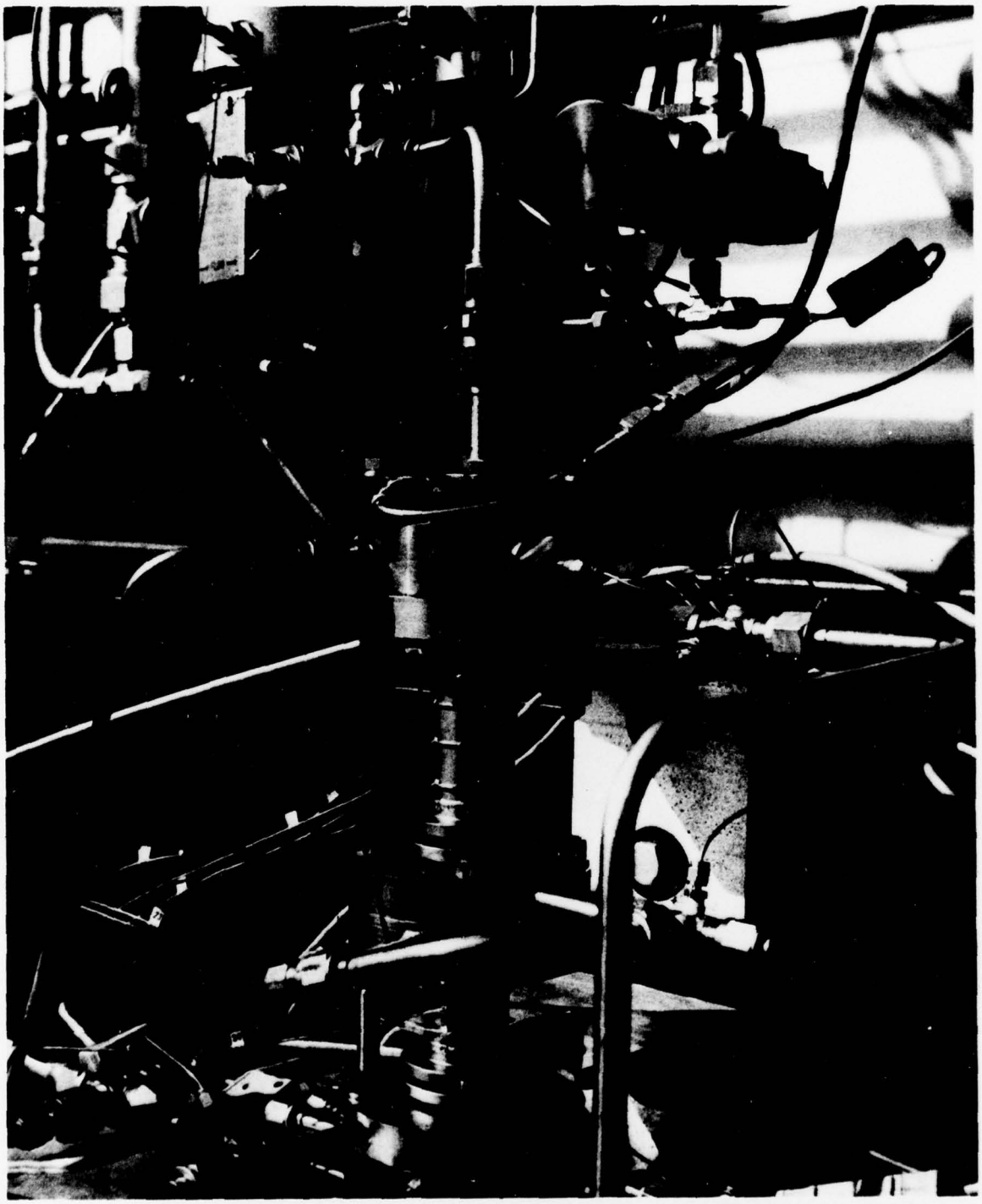

10-25-76/11305-95-7A

Figure 43. Triplet Injector Installation

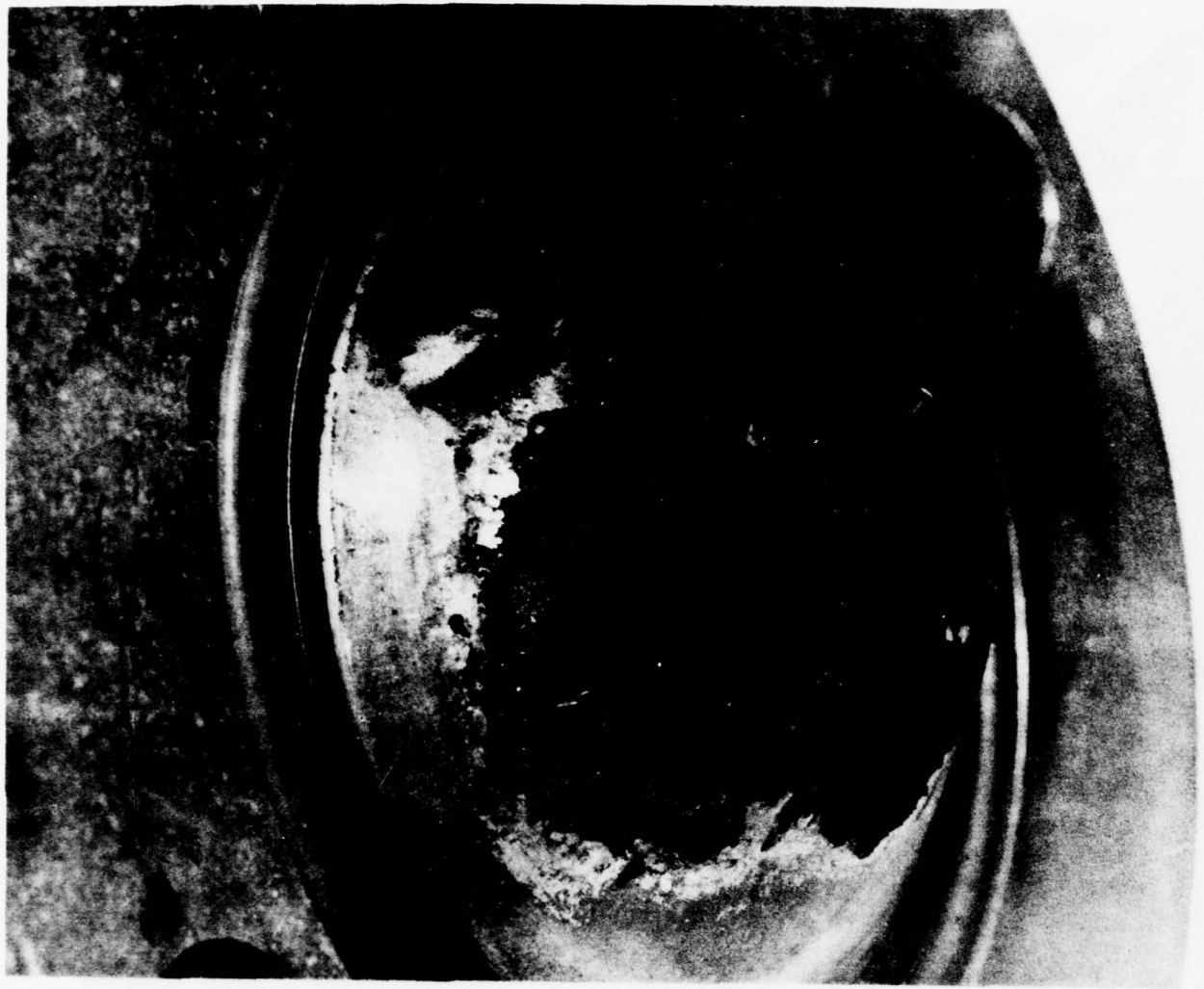

10-20-76/11505-95-5A

Figure 44. Triplet Injector Face Carbon Buildup After First Test Series

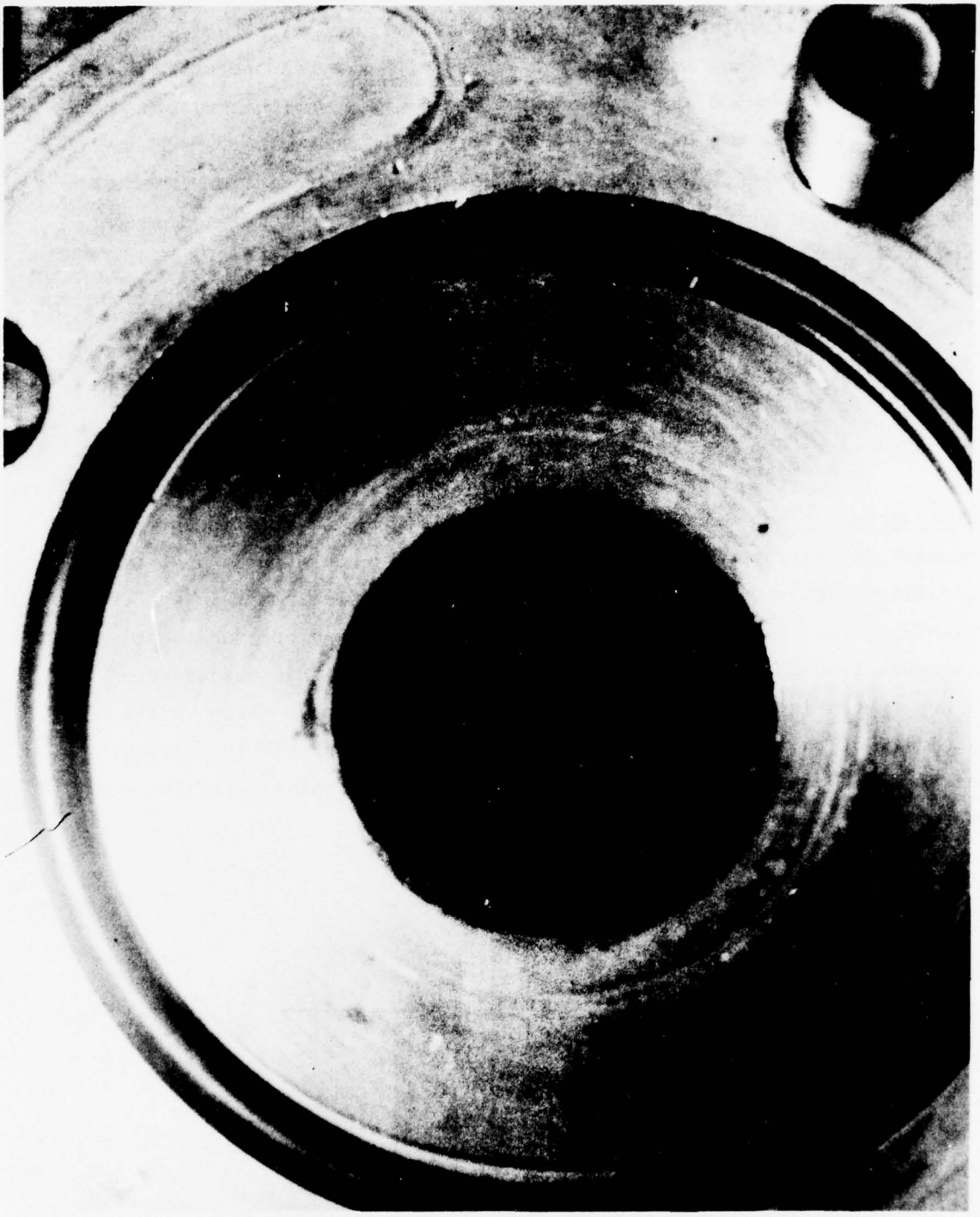

Figure 45. Carbon Buildup in Combustor Body
After Triplet Injector First Test Series

Testing of the triplet injector was then reinitiated with the 4-inch combustor length, and 17 successful starts with a total operating duration of more than 500 seconds were completed. The variable-energy spark exciter (Fig. 46) was used during part of this test series; spark energies as high as 2 joules (compared to 0.09 joules used for earlier testing) were used. (During test 31.1, the 6-inch combustor segment was damaged due to a lack of coolant water.)

The triplet configuration was unable to sustain combustion at the low-power level of 90 psia. It appeared that chamber pressure momentarily built up to a value exceeding fuel injection pressure, thereby shutting off fuel flow.

Coaxial Injector. Subsequent to the triplet injector matrix tests, the coaxial injector was installed with the 10-inch combustor, and 42 tests totalling 1200 seconds were completed. The coaxial-element injectors displayed good ignition characteristics, particularly for fuel post recesses less than or equal to 2 x D (see sketch). This was expected since oxygen in the outer annulus yields a high mixture ratio in the vicinity of the sparkplug. For larger recesses, substantial mixing occurs before propellants reach the sparkplug; the mixture is therefore more fuel-rich and less ignitable.

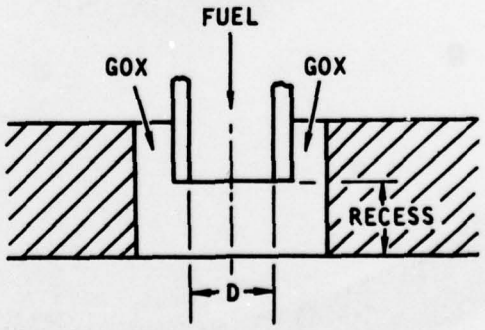

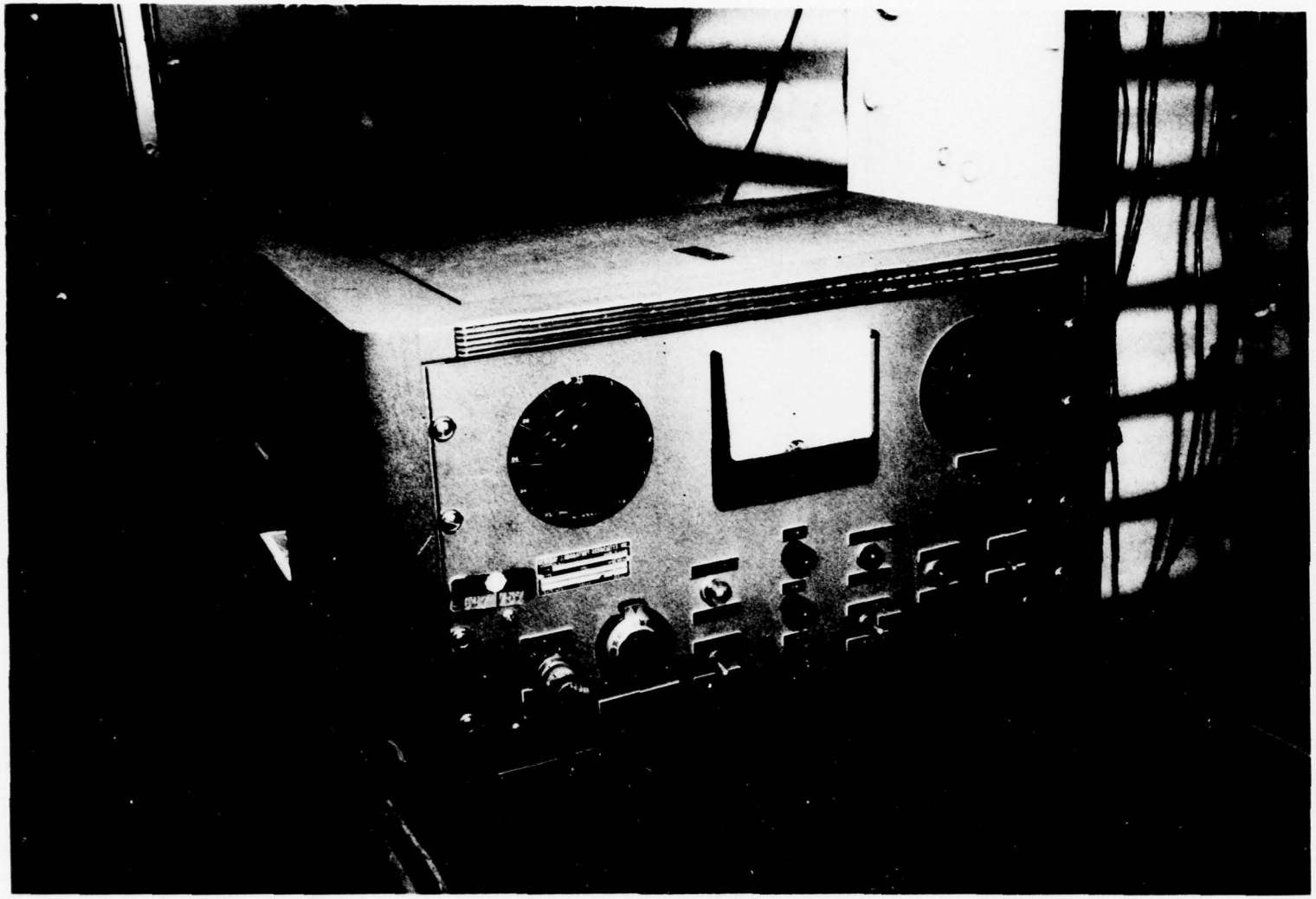

11-11-76/11305-95-10C

Figure 5. Variable Energy Spark Exciter

Combustor Length (L*). Testing was continued using the 4-inch combustor segment. The following injector configurations (in order of test) and numbers of tests were completed:

Configuration	No. of Tests
Coaxial (2-D recess)	2
Triplet	8
Coaxial (1-D recess)	6
Two-stage ASI	17
Triplet	6
Coaxial (2-D recess)	3

During test 41.03 with the coaxial 2-D recess injector, the 4-inch combustor wall suffered a small burnthrough and the combustor segment was removed and repaired.

Testing was resumed with the 6-inch combustor segment with the following injector configurations:

Configuration	No. of Tests
Coaxial (3-D recess)	6
Triplet	4
Coaxial (Zero-D recess)	12

During the last group of coaxial tests, ignition problems occurred in configurations that previously demonstrated good ignition reliability, e.g., the coaxial injector with zero or 1-D recess. In the case of zero recess, the two test series (Tests 22 and 44) differed in combustor length. In Test 22, with a 10-inch combustor, perfect or near-perfect ignition occurred during all nine planned tests. Test 44 (6-inch combustor) was precisely opposite, experiencing 8 no-ignitions and 4 long ignition delays in 12 attempted tests. Based on an assessment of these data, it was concluded that combustor length (i.e., characteristic length L*) has a significant effect on ignition.

Testing was then directed at a systematic evaluation of combustor length, together with the other factors affecting ignition.

First, the 6-inch combustor with the 1-D coaxial injector was tested to investigate the effect of various GOX and fuel lead times. Tests continued to result in ignition problems delays. The coax injector with zero recess of the fuel post was tested (Runs 46 and 47) with a 10-inch combustor to duplicate the successful results of Test 22. Of nine runs in Test 46, six yielded perfect ignition, and three (corresponding to low P_c and/or mixture ratio) had successful, though anomalous, ignitions. Increasing the spark energy from 90 to 250 millijoules upgraded the anomalous ignition to perfect. It was apparent from the results obtained that combustor length was the governing factor in the difference between the successful ignitions observed in Test 22 and the repeated failures observed in Test 44. The mechanism is deemed related to the stay-time for reactants to combust and pressurize the gas generator volume.

Based on this rationale, it was hypothesized that the triplet injector could be improved in its ignition reliability by increasing combustor length beyond 10 inches or by otherwise increasing reactant stay time. Since it was not practical to fabricate an additional combustor section, an uncooled nozzle extension was fabricated, reducing throat area from 0.100 to 0.038 $in.^2$ to increase reactant stay time in the combustor.

Prior to testing with the reduced throat, a series of runs (Tests 48 and 49) was made to duplicate the ignitions problems observed in earlier runs with low flowrates and mixture ratios. The small-throat nozzle extension was then added, and successful ignitions were achieved in each of a series of runs (Tests No. 50 and 51) representing flowrates and mixture ratios that had previously failed.

Spark Ignition. Early in the test program, after injector selection had narrowed to either the coaxial or the triplet injectors, the following conclusions were reached regarding spark ignition:

1. Ignition of the coaxial was essentially 100% reliable.
2. Ignition of the triplet was satisfactory for most targeted mixture ratios and power levels, but was less than satisfactory at low power or low mixture ratio

The apparent ignition limitation of the triplet system did not preclude the use of the triplet in an operational system since a start sequence could easily be established to provide the high flow and high mixture ratio necessary for good ignition followed by throttling to the desired steady-state operating point. Sustaining combustion at low power and mixture ratio had been clearly demonstrated in the test program.

Figure 47 provides some insight to the potential cause of ignition failures. In the preignition condition, essentially a strong gaseous oxygen "wind" occurs at approximately 80 ft/sec. If ignition were successful, the combustion chamber becomes pressurized, and the entering gaseous oxygen is slowed to 11 ft/sec (Fig. 47).

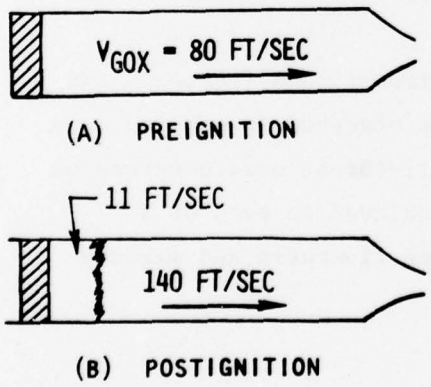

- MAXIMUM FLAME VELOCITY ESTIMATED AT 30 FT/SEC
- SUCCESSFUL IGNITION DEPENDENT UPON RAPID CHAMBER PRESSURE BUILDUP OR RECIRCULATION
- COAXIAL OK; AT 10 INCHES LENGTH AND CURRENT DIAMETER; TRIPLET MARGINAL

Figure 47. Ignition Mechanism

Since the flame propagation velocity was estimated to be approximately 30 ft/sec, it is apparent that ignition could be successful only if the following occurred:

1. Recirculation pockets exist in which GOX and JP-4 are present in suitable amounts and at suitable velocities to develop an adequate torch, or
2. High-velocity gaseous oxygen and entrained JP-4 droplets burn as they proceed downstream and generate sufficient pressure to slow down the entering gaseous oxygen before the partially combusted materials "wash out" through the nozzle

The latter mechanism suggests that a long combustor has the better chance of igniting. Table 10 presents dramatic evidence of this occurrence. In the two test sequences described, all factors other than combustor length were nearly identical. The 10-inch combustor was wholly successful; the 6-inch combustor failed every time. When the additional 4-inch combustor segment was subsequently reinstalled with the 6-inch combustor, successful ignitions were duplicated.

TABLE 10. COMBUSTOR LENGTH EFFECT ON IGNITION
(Coaxial Injector, Zero Fuel Post Recess)

Combustion Chamber Length; 10 inches Test 22: 4 November 1976				Combustion Chamber Length; 6 inches Test 44: 17 December 1976			
Run	Target Pressure Chamber	Target MR	Result	Run	Target Pressure Chamber	Target MR	Result
01	167	0.49	OK	01	173	0.47	300 ms delay
02	78	0.44	OK	02 03	78	0.44	No ignition
03	251	0.40	OK	04 05 06	251	0.40	No ignition
04	157	0.32	OK	07	157	0.32	No ignition
05	128	0.17	OK				
06	240	0.32	OK	08	240	0.32	No ignition
07	191	0.54	OK	09 10	193 191	0.54 0.54	1.8 seconds delay No ignition
08	90	0.45	OK				
09	291	0.51	OK	11 • 12	293 291	0.52 0.51	140 ms delay No ignition

A special test was made to determine if ignition with the triplet injector would be more reliable if the gaseous oxygen velocity were 30 ft/sec or less. A steel nozzle extension (Fig. 48) was fabricated and tested with the combustor, and consistently good ignition was obtained at conditions that had previously been unsuccessful.

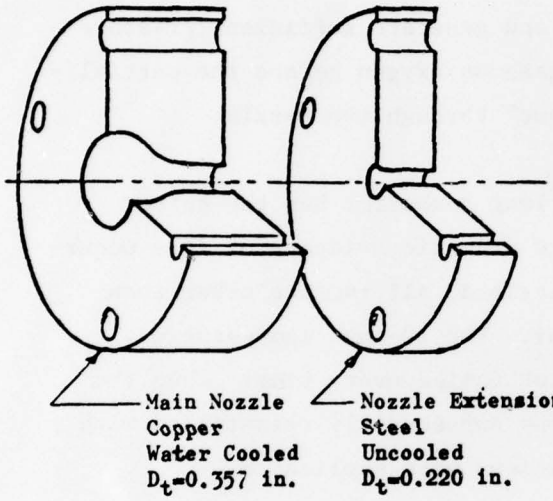

- OBJECTIVE

  TO EVALUATE BENEFIT OF HIGHER CONTRACTION RATIO ON IGNITABILITY WITH TRIPLET INJECTOR

- GOX VELOCITY REDUCED FROM 80 FT/SEC TO 30 FT/SEC
- CONSISTENT GOOD IGNITION OBTAINED
- CHUGGING DUE TO LOW FUEL ΔP

Figure 48. Small Throat Nozzle Extension

Cold Propellant Ignition. Tests were conducted to demonstrate that the 10-inch combustor length with the triplet-injector configuration could operate satisfactorily over the planned IPU environmental extremes of propellant temperature, altitude, and JP-4 volatility.

The test facility was modified to install temperature-conditioning jackets on both the oxidizer and fuel lines. Repeated tests were made to verify observed results. Cold propellant testing proved to be the most difficult since warming effects of ambient lines or purge gas increased propellant injection temperatures. Adequate prechilling with liquid nitrogen

and deletion of the purges finally allowed chilling to the targeted conditions. The 250 mJ, 50-spark/sec energy level, established as nominal in previous tests, proved clearly adequate for cold propellants.

A representative ignition transient with GOX at -240 F and JP-4 at -60 F is shown in Fig. 49. The trend is indistinguishable from successful ignitions obtained with ambient propellants. Thus, cold propellant ignition poses no special problems.

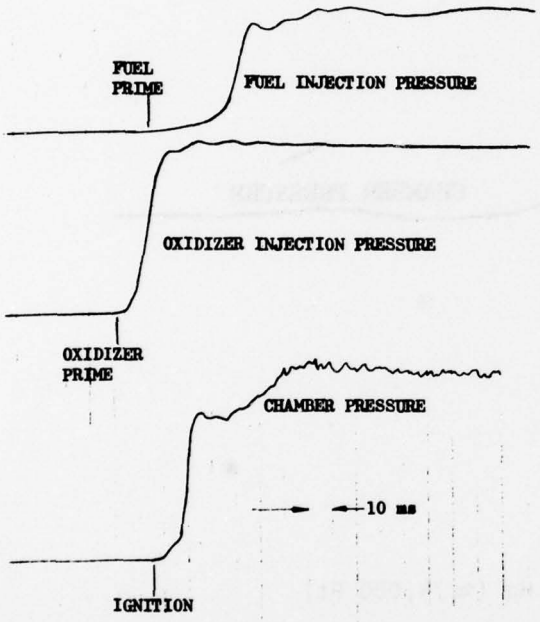

- T_{GOX} = -240 F
- T_{Fuel} = -60 F
- Spark Energy = 250 mJ
- Spark Rate = 50 Sparks/Second
- Ignition Delay ≈ 0

Figure 49. Typical Cold Propellant Ignition

High-Altitude Ignition. Tests were conducted to demonstrate that the 10-inch combustor with the triplet injector also could operate satisfactorily at high-altitude conditions up to 74,000 feet. A GN_2 ejector installed at the combustor discharge was used to obtain the low ambient pressure. A typical high-altitude ignition transient is shown in Fig. 50. The moment of ignition is easily identified as the point at which rapid chamber pressure (P_c) buildup occurs. Assessment of ignition delay is

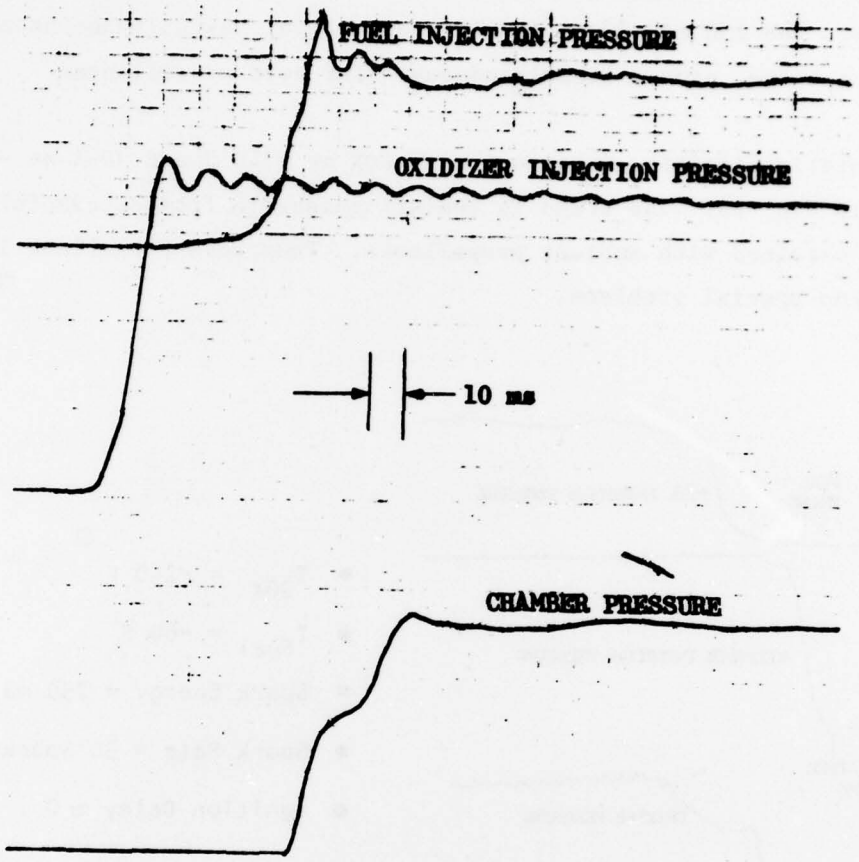

- $P_A \approx 28$ mm Hg ($\approx 74{,}000$ Ft)
- No Change From Sea Level Ignition

Figure 50. High-Altitude Ignition

somewhat obscured by the shallow ramp preceding the rapid buildup of pressure, but the observed value between 10 and 30 msec. (measured from pressure buildup in the slower injection manifold to the moment of chamber pressure rise) is the same as the ignition characteristic in sea level tests. The transducer mounting provisions are such that a $\pm$5 msec. band was estimated for the pressure readings.

Since the GOX flow is sufficient to choke the nozzle at the combustor discharge prior to ignition, the high-altitude ignition was found to be similar to that at sea level as expected.

Low-Cut Fuel Ignition. Additional tests were made with the 10-inch combustor and triplet injector to demonstrate that satisfactory operation could be obtained with low-volatility or low-cut JP-4 fuel as well as with high-cut JP-4 fuel. A minor logistic problem was encountered in obtaining low- and high-cut JP-4. The specification for JP-4 states that the minimum allowable vapor pressure (at 100 F) is 2 psia and that the maximum is 3 psia. Suppliers provide a nominal 2.4-psia blend and cannot easily provide off-nominal JP-4. Simulants were therefore formulated using RP-1 (23%), and to make low-cut JP-4 and n-hexane (19% by weight) as an additive to make high-cut JP-4. The approach and resultant formulations for low- and high-cut JP-4 are described in Table 11. Jet A-50 was also tested as a simulant for JP-8.

TABLE 11. HIGH- AND LOW-CUT JP-4

- *Approach*
  - Assume that available JP-4 is nominal cut at P_{Vapor} = 2.4 psia
  - Add sufficient hexane to increase theoretical P_{Vapor} to 3 psia for high cut
  - Add sufficient RP-1 to reduce theoretical P_{Vapor} to 2 psia for low cut

Test Fuels

- High Cut: 19% n-hexane by weight
- Low Cut: 23% RP-1 by weight

Normal reliable ignition was obtained in all tests with high-cut JP-4. Good ignition was obtained with both low-cut JP-4 and JP-8 low-volatility fuels, with or without pretest GN_2 purge, at the nominal mixture ratio ($\approx$0.68) as seen in Fig. 51. Low-cut JP-4 failed to ignite at low mixture ratio even with purge off (Fig. 51f). At low mixture ratios ($\leq$0.45), JP-8 ignited satisfactorily with purge off (Fig. 51b), and was marginal with purge on (Fig. 51a). The effect of purge was repeatable, and purge probably has a diluent effect on the GOX and fuel ignition process. The impact of these results on system design are:

1. GOX purging, if used at all, should be limited to postfiring procedures.
2. The start sequence should be arranged to ensure that the initial mixture ratio is at least the nominal value.

Neither of these requirements is difficult to implement. Much of Rocketdyne's experience indicates that a self-emptying of the gas generator precludes the need for any purging, and precise control of flow transients (by suitable design of valves, lines, manifolds, etc.) is a routine facet of rocket engine gas generator and thrust chamber design.

Carbon Formation. Review of test experience within and outside Rocketdyne indicated that carbon formation could be minimized by:

1. Operation at appropriate combustion temperatures
2. Efficient mixing and combustion
3. Avoidance of cold surfaces for carbon precipitation

From these considerations, it was decided that a minimum-carbon configuration based on a triplet injector could be formulated. The incentive to verify this possibility stemed from the favorable heat transfer characteristics displayed by the triplet.

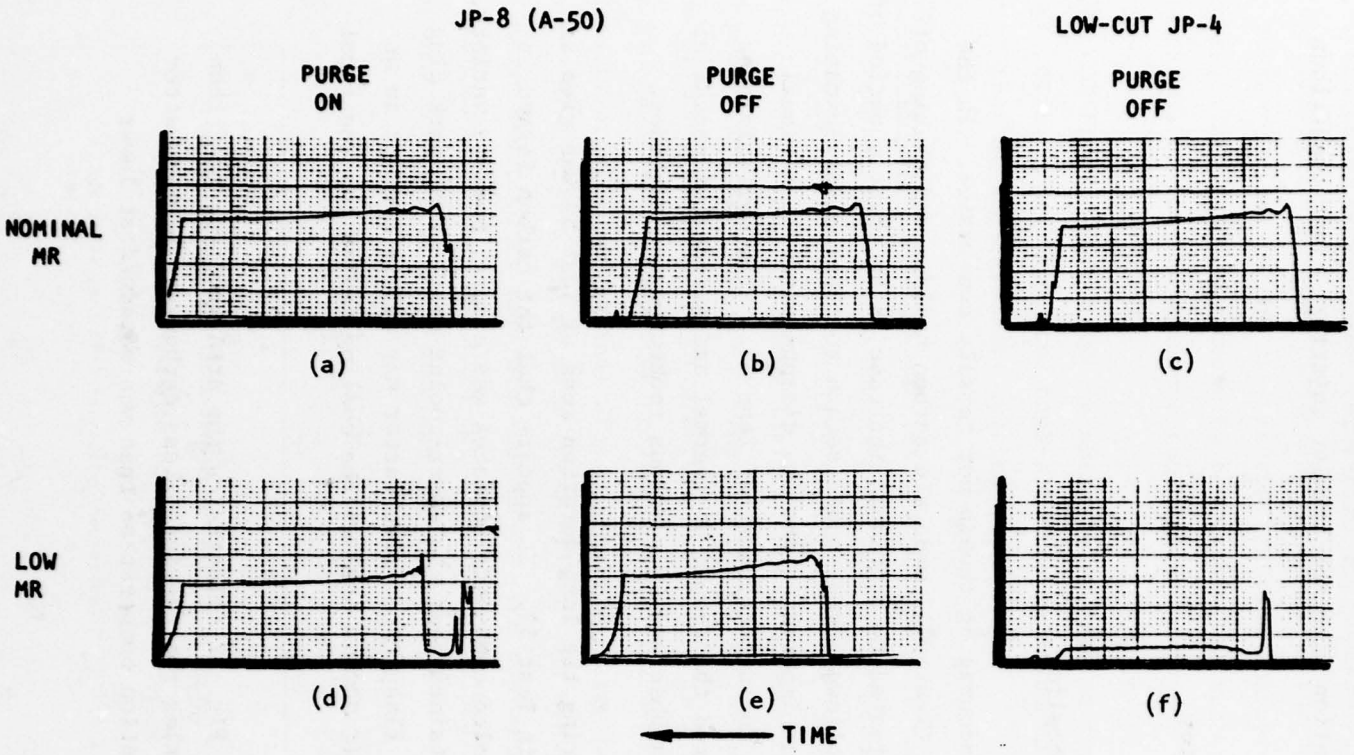

Figure 51. Low Volatility Fuel Ignition Tests

As a result, tests were conducted with the objectives of providing a short-duration checkout, then a long-duration verification test of minimum carbon formation with the triplet injector. Test conditions were:

10-inch combustor
P_c = 200 psia
MR = 0.65
GN_2 combustor cooling

Test results were encouraging though not totally conclusive. In the initial test series (Test 52), moderate carbon buildup and flaking-off were observed, manifested by a gradual increase in P_c (over a period of about 30 seconds) followed by a sudden return to the nominal operating point. Of particular importance was the disappearance of residual carbon from Test 52 during the start of Test 53. This self-cleaning phenomenon, considered the result of thermal and mechanical shocks at test start, has been observed in numerous rocket engine turbines.

Carbon formation during the long-duration runs of Test 53 was greater than that observed in Test 52. It appears that the carbon formed on gaseous-nitrogen-cooled combustor surfaces was a soft, powdery variety, while the carbon obtained near the water-cooled nozzle and spark plug wafer was a harder, flaky type. The latter may not be present in an operational system if GOX is used as the cooling medium for the total system.

The sketch shown in Fig. 52 illustrates the area and type of carbon buildup observed during the testing. Less carbon was present after tests at high combustion temperature than was obtained at lower temperatures.

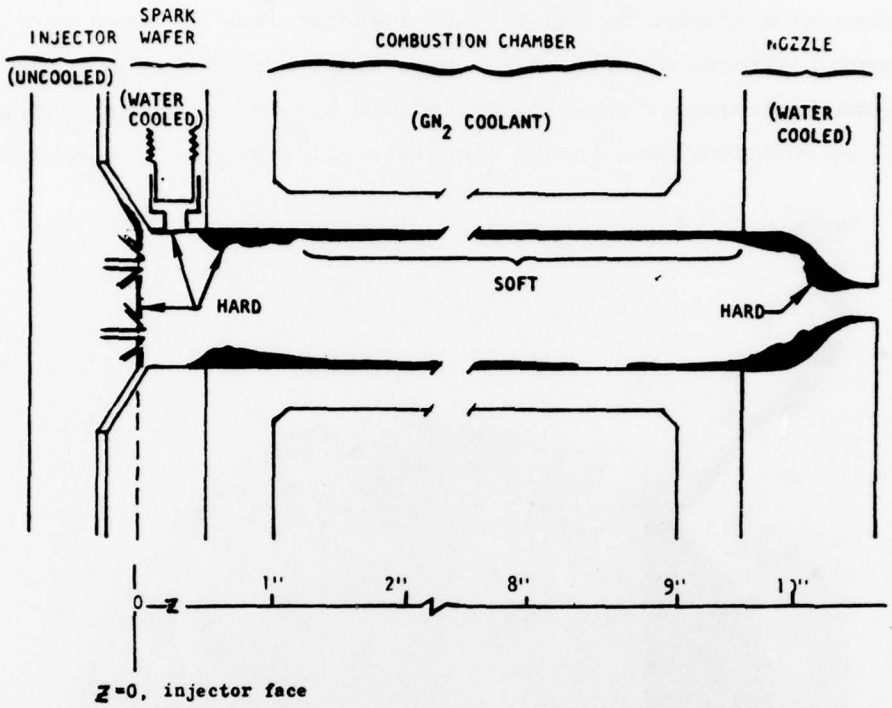

Figure 52. Typical Carbon Buildup in IPU

The carbon on hotter walls (i.e., the combustor walls when gaseous nitrogen coolant was used) was a powdery variety. All carbon except on the injector face frequently disappeared at the start of a test. The thermal and mechanical shocks associated with gas generator startup appears to dislodge the carbon that formed during the previous test. The tendency of carbon particles to flake off during a run is apparent in the chamber pressure record shown in Fig. 53. Gradual chamber pressure buildup followed by a sudden drop and repetition of the cycle is evident.

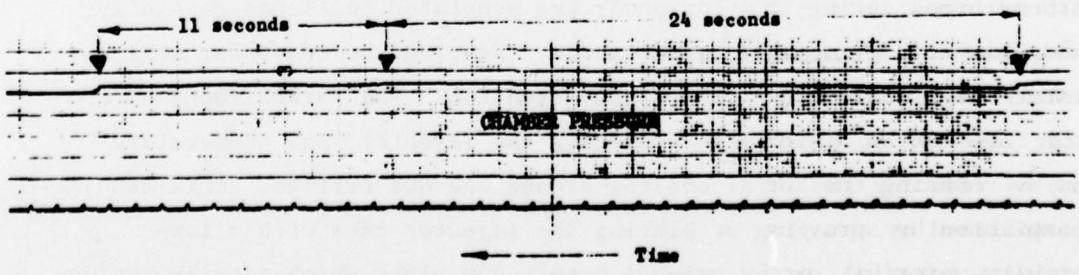

Figure 53. Typical Carbon Accumulation Effects (Test 53.03)

The accumulation of carbon on the triplet injector face is shown in Fig. 54. No harmful effects of this carbon were manifested throughout the test program. Avoiding carbon formation is impeded by the fact that injected fuel cools the injector face in the immediate vicinity of the fuel orifices.

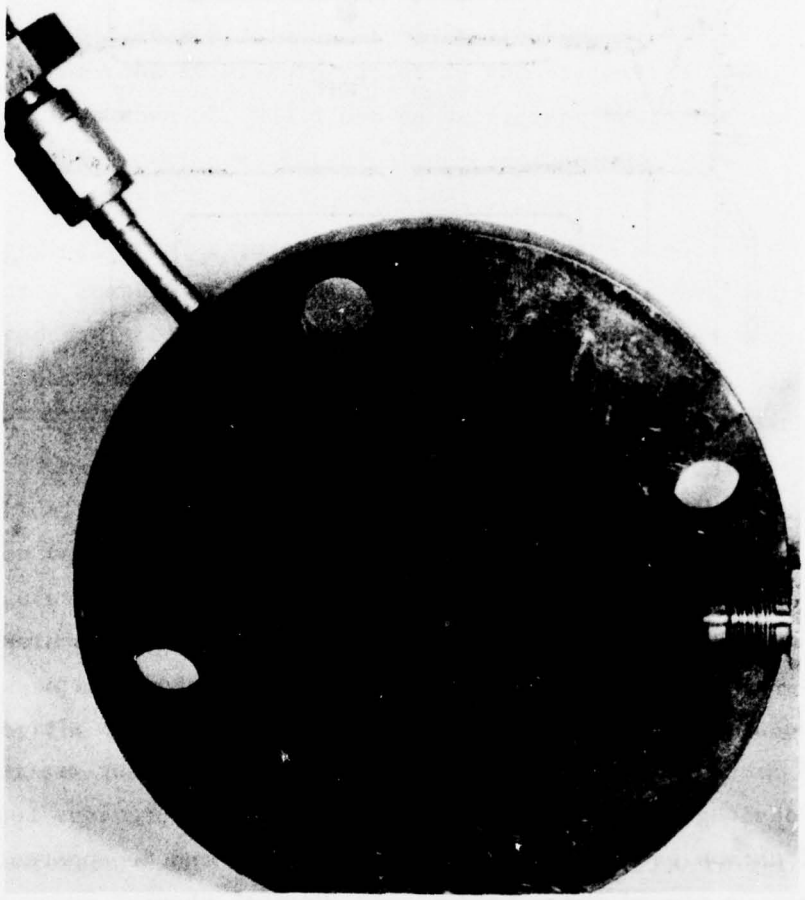

10-20-76/11305-95-5C

Figure 54. Carbon Formation on Injector Triplet

The carbon formed during the low-power gas generator tests was generally soft and does not accumulate after tests. Keeping the combustor wall temperature high would minimize carbon formation. The carbon found on the injector face can be minimized by keeping the injector face temperature hot and by reducing the local cooling around the GOX orifice. This can be accomplished by spraying or plating the injector face with a low-conductivity material, or by using a premix-cup plate which totally avoids local cooling.

Heat input to the gaseous nitrogen combustor coolant during a long-duration test is shown in Fig. 55. It is apparent that a thin carbon layer comparable to that observed in rocket engine gas generators and thrust chamber was present. The heating rate was approximately one-fourth the value that would occur on a clean combustor wall. The no-carbon heating rate was in fact observed during testing of the coax injector.

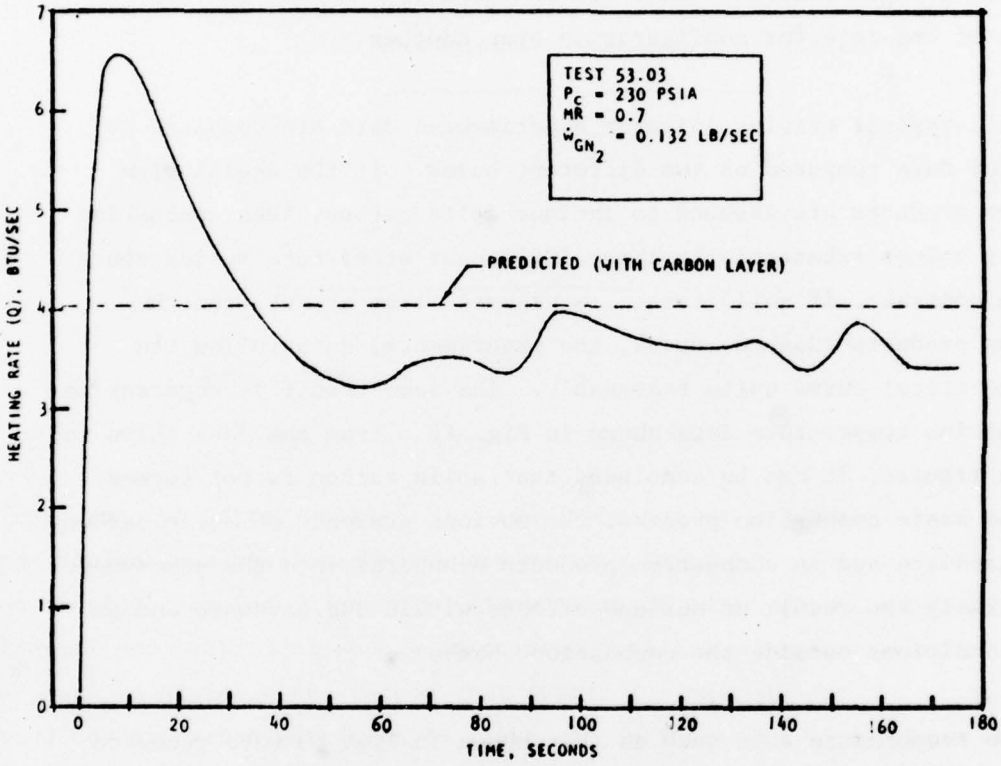

Figure 55. Combustor Heat Load in Low-power Gas Generator

The coaxial injector was characterized by the absence of a carbon layer on the combustor wall. This condition did not result in a problem when the combustor was overcooled with water but, when gaseous nitrogen was used as coolant, difficulties occurred. As in the case of the ASI injector, this need not be regarded as a serious deficiency. Several variations on the basic coaxial injector element could reduce the wall heating but was not pursued. However, the triplet injector encountered fewer problems, and solutions to these problems were more apparent.

Performance. Representative combustion performance data for the ASI, triplet, and coaxial injectors are shown in Fig. 56 through 61, and indicate trends and basic performance levels. Small differences in performance exist between the ASI and triplet injectors, and between the 6- and 10-inch combustors. The main discernible characteristic apparent in the data is the slight advantage for the ASI and triplet injectors over the coax at mixture ratios in the vicinity of 0.6. The difference, of less than 5%, would not be sufficient basis for clear selection of one injector configuration over another.

In Fig. 62, typical triplet injector experimental data are compared to theoretical data computed on two different bases. If the equilibrium combustion products are assumed to include solid carbon, then combustion efficiency values substantially above 100% occur at mixture ratios above 0.63. In contrast, if solid carbon is assumed to be absent from the combustion products (dashed curve), the experimental data follow the quasi-theoretical curve quite reasonably. The same result is apparent in the combustion temperature data shown in Fig. 63. From the data shown in these two figures, it can be concluded that solid carbon is not formed during the basic combustion process; the obvious presence of solid carbon on test hardware and in combustion products exhausted into the atmosphere is most likely the result of surface effects within the hardware and on ambient conditions outside the combustion chamber.

Combustion temperature data such as that shown in Fig. 63 were recorded by thermocouples inserted 1/8, 1/4, 3/8, and 1/2 inch (midpoint) into the chamber just before the nozzle inlet. Carbon accumulation on the thermocouples tended to limit the amount of valid temperature data obtainable. Generally, only data obtained during the first few seconds of a test were useful.

The triplet injector displayed reasonable uniformity of temperature. Differences on the order of 150 F between the lowest and highest readings were typical. The other injectors displayed greater temperature diffferences.

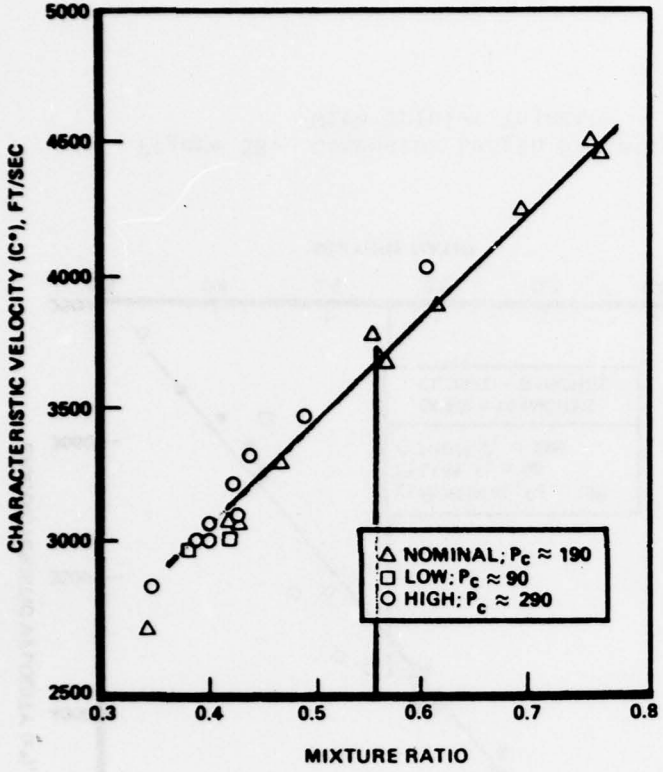

Figure 56. ASI Injector Evaluation Test Summary, 10-Inch Combustor

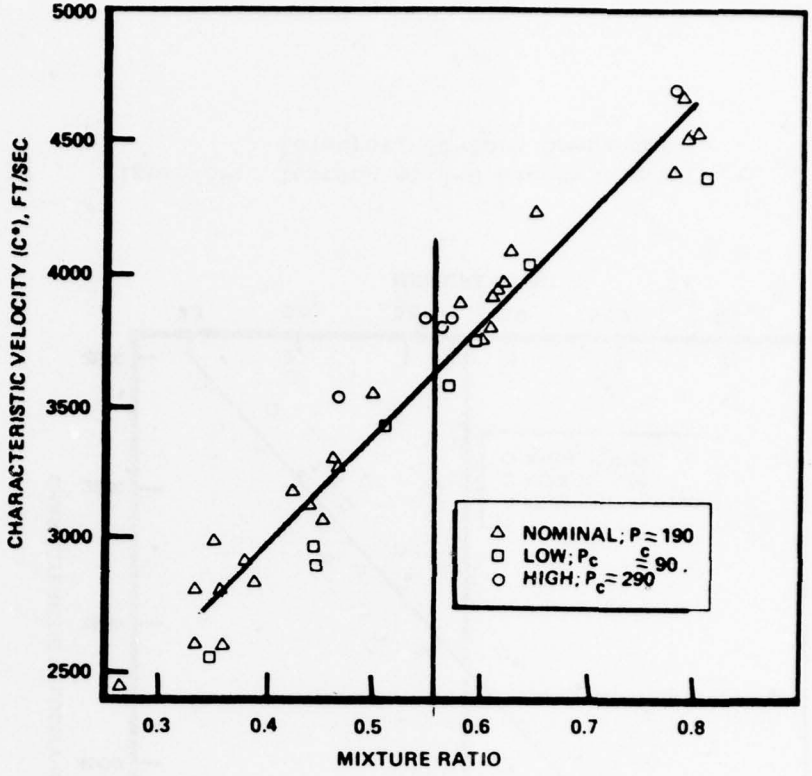

Figure 57. Triplet Injector Evaluation Test Summary, 10-Inch Combustor

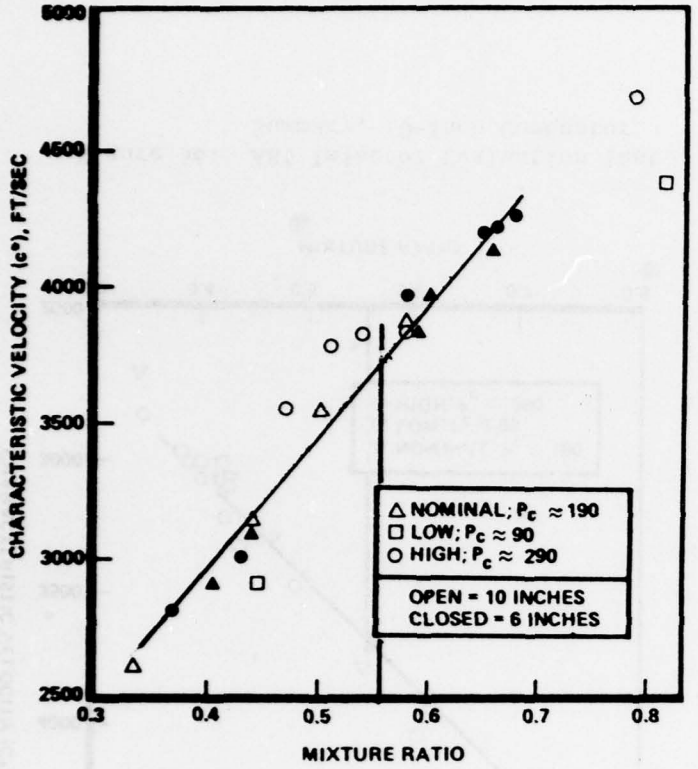

Figure 58. Combustor Length Variation With Triplet Injector

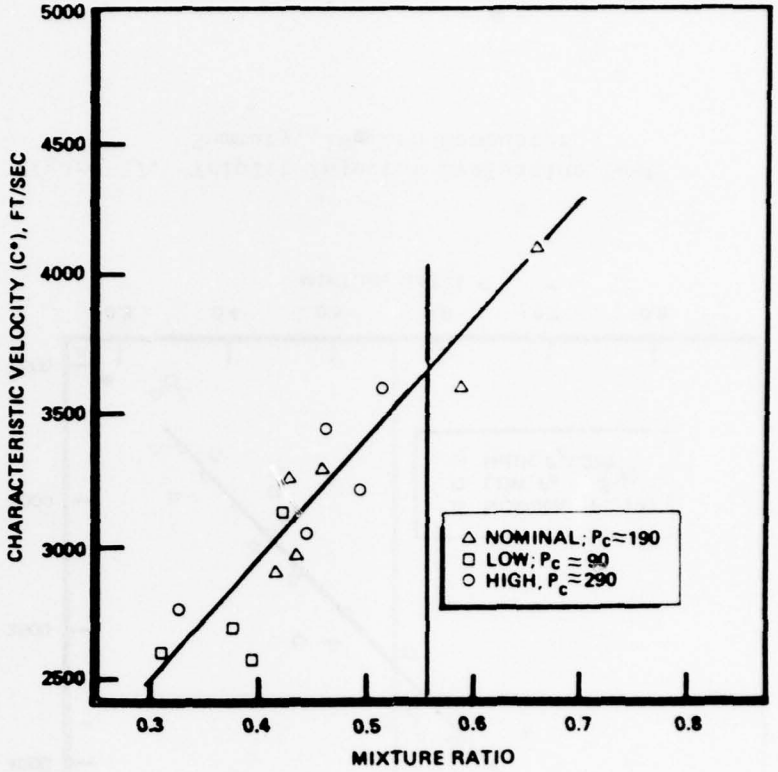

Figure 59. Testing of 1-D Recess Coaxial Injector, 10-Inch Combustor

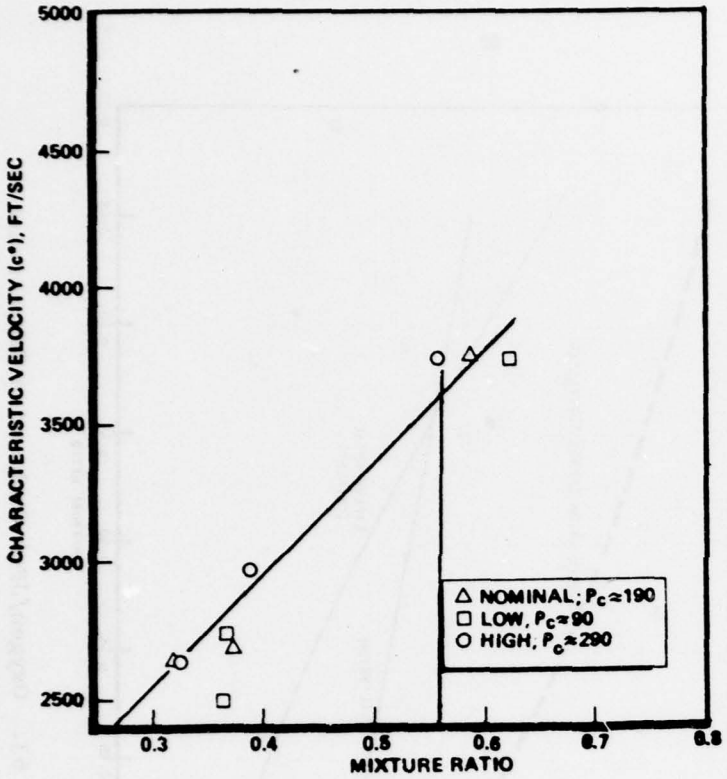

Figure 60. Testing of 2-D Recess Coaxial Injector, 10-Inch Combustor

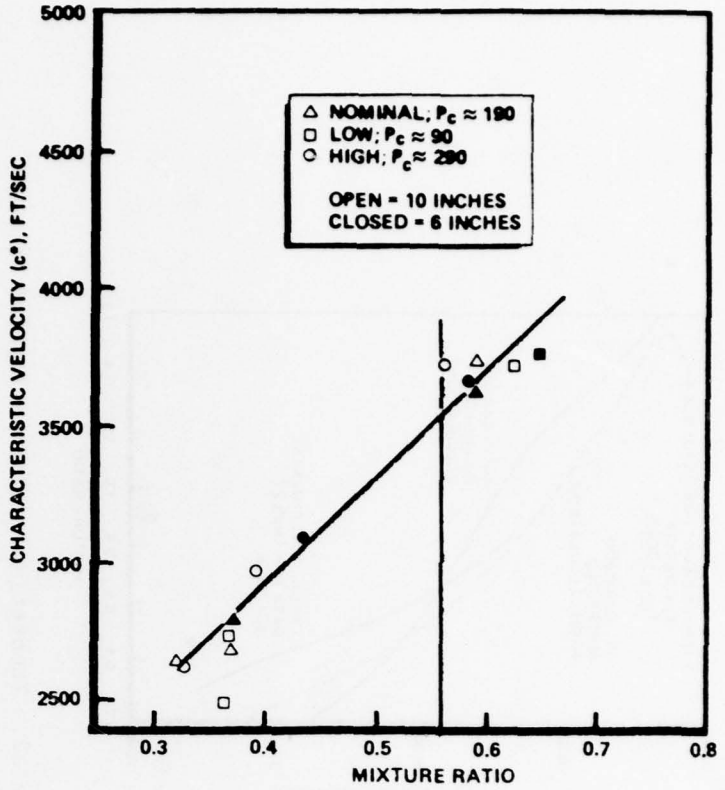

Figure 61. Combustor Length Variation With 2-D Recess Coaxial Injector

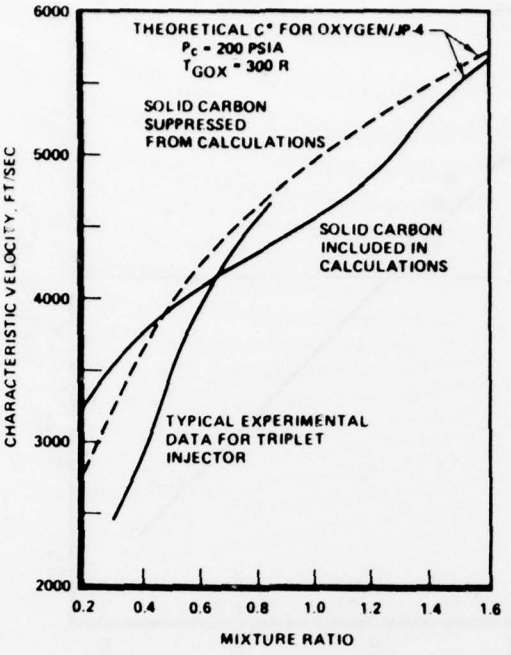

Figure 62. Theoretical and Experimental Trends

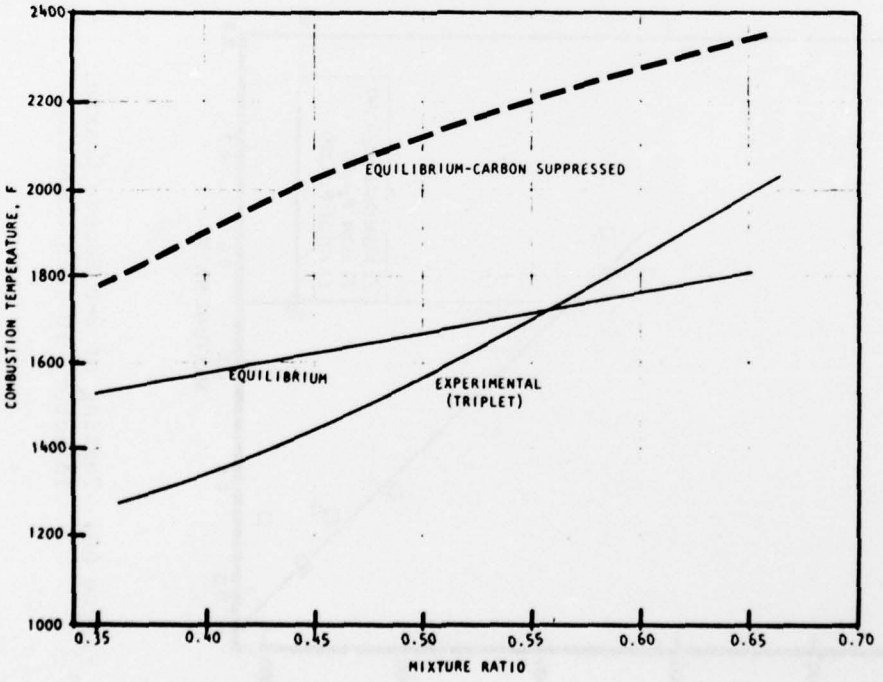

Figure 63. Oxygen/JP-4 Combustion Temperature

Assessment. Based on the experimental test results obtained and analyses presented herein, it is concluded that the planned test objectives of the lower-power gas generator task were basically achieved. First, as shown in Table 12, the planned limits testing of P_c and MR were exceeded while the power-level range was short at the high end--a condition which poses the least development problem. Also, the planned extreme limits testing of temperature, altitude, and fuel volatility were successfully demonstrated.

TABLE 12. COMPARISON OF PLANNED AND ACHIEVED TEST OBJECTIVES

	Objective	Achieved
P_c, psia	91 TO 290	75 TO 350
MR	0.38 TO 0.60	0.23 TO 1.26
Power Level, %	50 TO 150	50 TO 130

Secondly, the low-power gas generator test results provided the basis for design of the high-power gas generator. The basic guidelines which were used to design the high-power gas generator are shown in Table 13.

TABLE 13. IMPLICATIONS FOR HIGH-POWER GAS GENERATOR DESIGN

- Triplet element provides good mixing, uniform heating
- Select diameter for preignition GOX velocity less than 30 ft/sec
- 10-inch length is adequate
- High combustion temperature (~2000 F) and high wall temperature (~1000 F) should minimize carbon formation
- 250 mJ spark at 50 SPS can provide ignition for worst-case (coldest) conditions

High-Power Gas Generator Test Series

The objective of this test series was to verify the performance and operation of the high-power gas generator. During the test series a total of 112 tests were completed, accumulating 2663 seconds of operation. The high-power gas generator, in its modified, successful, final configuration, completed a total of 81 tests and 1440 seconds in both gas generator tests (59 tests, 1047 seconds) and subsequent Phase II engine starter demonstrator tests (22 tests, 393 seconds). A description of the test activities and analyses is presented in the following discussion.

The high-power IPU gas generator tests began on 26 July 1977. The gas generator was installed in the test stand (Fig. 64) previously used for testing the low-power gas generator. The test stand required only minor modification, mainly sizing the main valves and rerouting the plumbing near the injector.

The combustor cooling was provided by GN_2 with a provision for varying the flowrate over a wide range about the oxidizer flowrate. This approach also permitted safe cooling of the combustor and isolating the injector flow (GOX) from combustor heat load for accurate combustor thermal analysis. The nozzle/throat section was air cooled using a flowrate comparable to the oxidizer flowrate.

Hot-fire testing was initiated after completion of a series of blowdown tests. Ignition was satisfactory in each test but, during mainstage, low-frequency chamber pressure oscillations occurred in the initial tests. Modifications to the fuel feed system were incorporated to correct this problem. A 0.070-inch-diameter cavitating venturi was installed downstream of the main fuel valve to maintain fuel flowrates between maximum and slightly less than nominal, thereby eliminating chugging in this range. The testing indicated some improvement but, with higher flowrates, chugging was still present. The chugging operation was characterized by an 11 cps chamber pressure oscillation; it appeared that ignition followed by complete flame extinction occurred each cycle (Fig. 65).

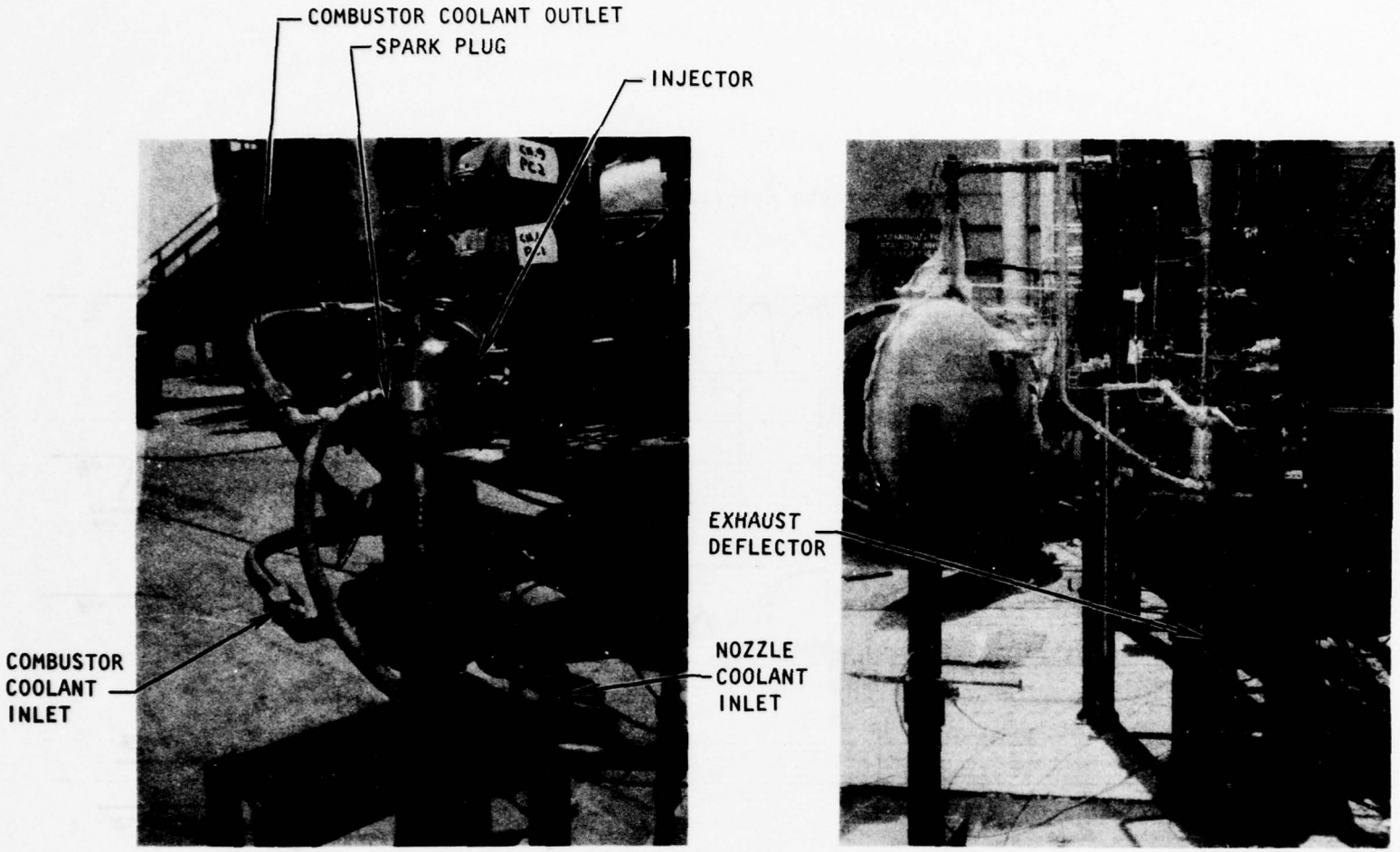

Figure 64. High-Power Gas Generator Test Installation

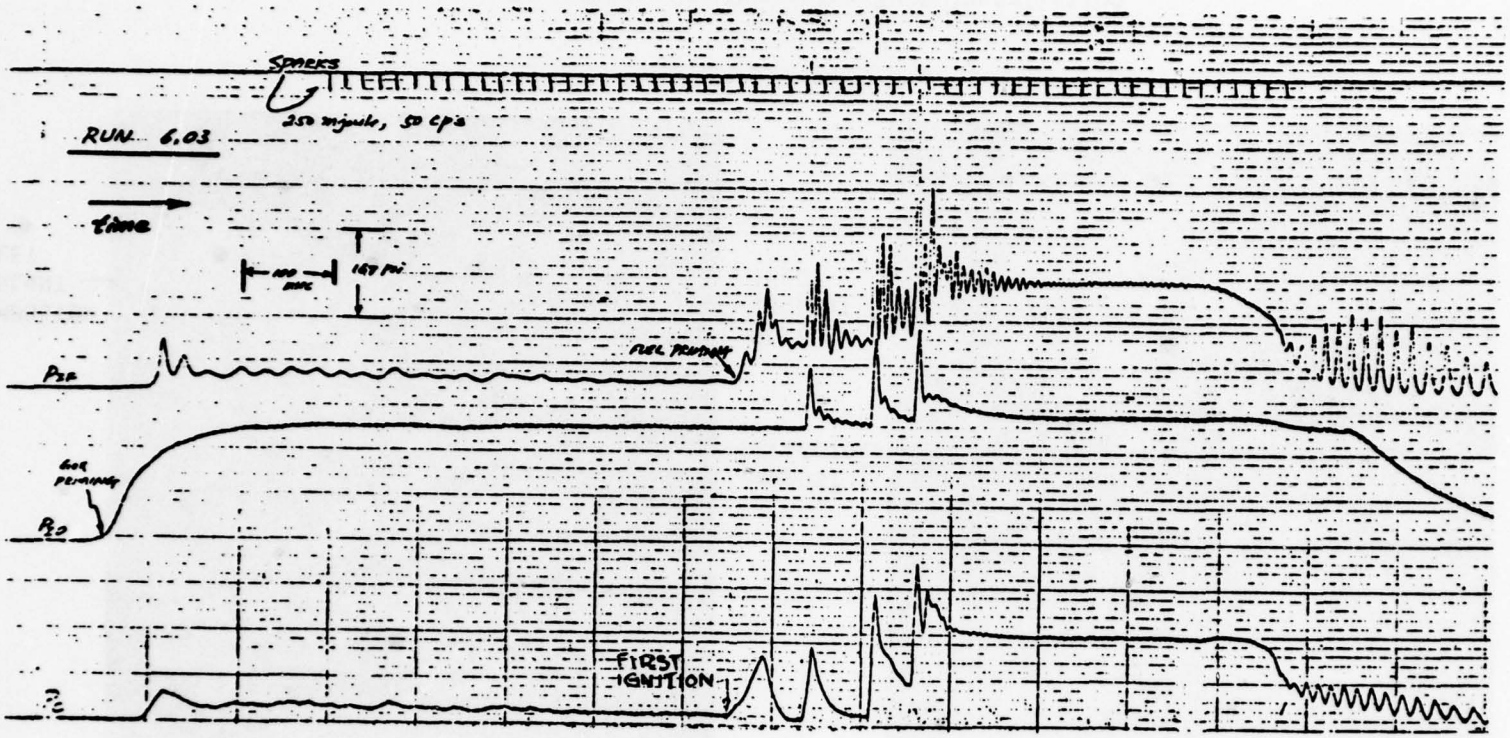

Figure 65. Partially Stable Test

Additional feed system modifications made include stiffening the fuel line and ramping fuel flowrates (described in Table 14) to correct the chugging problem, but these modifications did not produce the desired results.

TABLE 14. SUMMARY OF TEST SERIES 2 TO 7

Test Series	Remarks
2	Fuel line stiffening (0.125-inch orifice) near injector
3	Fuel cavitating venturi (0.070-inch throat)
4, 5	100-300 msec fuel flow ramp with close-coupled fuel valve
6	Fuel ramp with close-coupled GOX sonic downstream of main oxidizer valve
7	Fuel lead

Helium Purge and Choke Ring. Additional procedural and hardware corrective changes were then implemented. Because of the possibility that excessively rapid JP-4 entry into the chamber might be triggering mild detonations that tend to shut off fuel flow and thereby extinguish the flame, mixing helium purge gas with the initial JP-4 flow was used as a means of limiting the fuel flow buildup rate during start as well as promoting good mixing. It is for this same reason that the ramped fuel priming was used to restrict the rate of fuel flow buildup.

The other corrective change consisted of minimizing recirculation of combustion products that could be extinguishing the flame and preventing the onset of stable, steady-state operation. An annular choke ring was fabricated to extend 0.5 inch into the combustor at a position 1 inch

downstream of the injector face. In addition, the spark plug opening was increased to 0.375 inch from 0.125 inch to improve the exposure of reactants to the ignition source.

Following these modifications, stable combustion was achieved during Test Series 8 through 15 using either gaseous helium purge mixing or choke ring, or a combination of both. The purge gas applications was only limited to the start transient, and was either checked off by the priming propellant pressure or was interlocked to the MFV open signal for cutoff. During these test series, consisting of more than 30 test runs, all of Case I and most of Case II of the planned test matrix (Table 15) were completed. A summary of general test results is shown in Table 16. Some typical combustion data obtained during the exploratory test series are presented in Fig. 66 through 68.

Carbon Formation. A purge gas lead also was used for the 180-second test duration runs in Test Series 14 and 15, to study carbon buildup. The purge gas was checked off by the fuel flow itself during priming, and spark ignition was turned off after 1.50 seconds. Five of eight planned test runs were successfully completed; these were for nominal power and 1.3 times nominal power levels.

Hard carbon deposits, approximately 1 mm thick, were found on the injector face after the first 180-second duration run. Softer carbon deposits approximately 5 mm thick were found along the combustion chamber walls, about 2 inches below the injector. The nozzle converging wall had the most carbon buildup (Fig. 69) varying from 2 to 5 mm. The nozzle throat was clean. This condition of equilibrium carbon buildup did not change significantly after each of five 180-second duration tests were completed.

Three low-power-level, long-duration tests were made which ran into unstable combustion similar to that encountered in the early phase of the test program. A series of short-duration runs was then conducted with

TABLE 15. HIGH-POWER GAS GENERATOR TEST MATRIX

CASE	TEST OBJECTIVES	TEST CONDITIONS	OPERATION PARAMETERS					TEST POINTS
			POWER LEVEL	MR	COOLING*	SPARK @ 50 cps	TEST TIME	
I	Initial check-out and diagnosis of spark ignition	Ambient temperature propellants, normal power, 150 percent coolant flow	Normal	.62	0.3 lb/sec	500 mj 250 mj 100 mj	1 sec each	1 **
						250 mj	2 sec	1 **
							5 sec	1 **
II	Evaluation of carbon build-up and coking characteristics under varied test conditions Inspection of injector and chamber after each test run	Ambient temperature propellants Varied power level, mixture ratio, and coolant flowrate	Low	.64	0.20, 0.10		180 ▼	1 each
			Normal	.62	0.30, 0.20			
			High	.59	0.45, 0.30			
			Low	.50	0.10			
			Normal	.50	0.20			
			High	.50	0.30			
III	Ignition diagnostics	(1) Cold propellants	Low	.64	0.15		~2 sec or maximum possible	2 each
			Normal	.62	0.25			2 each
								2 each
		(2) Low-cut JP-4	Normal	.62	0.25		1 sec+	4 each
		(3) JP-8(or JET-A)	Normal	.62	0.25		1 sec+	4 each

* For both chamber and nozzle, independently

** First set of test points with spark source at injector face. Should poor ignitions result, repeat with spark wafer installed

▼ All long duration runs with over-temperature cut

\+ Test duration revised from the originally scheduled 5 sec; 1 sec test duration is sufficient to yield steady-state characteristics.

TABLE 16. SUMMARY OF TEST SERIES 8 TO 15

Test Series	Spark-plug	GHe	Choke Ring	Spark Energy, joules	General Test Results
8	Wafer	X	X	0.070	• Stable combustion ≈ 1.0 second smooth start
	Wafer	-	X	1,0.07	• Initial oscillation, then stable combustion ≈ 1.0 second
9	Wafer	X	X	0.250	• Stable combustion, smooth start
	Wafer	-	X	0.250	• Initial oscillation, then stable combustion
	Wafer	X	-	0.250	• Smooth ignition, stable combustion
10	Injector	X	X	0.250	• Smooth ignition; stable combustion ≈ 1.0 second
	Injector	-	X	0.250	Initial oscillation, then stable combustion
11	Injector	X	-	0.250	• Initial oscillation, then stable combustion ≈ 1.0 second
12	Injector	X	-	0.250	• Initial oscillation, then stable combustion ≈ 2.0 seconds
13	Injector	X	-	0.250 (1.5 sec)	• Duration runs 10, 30, 60 seconds, stable combustion; carbon buildup 1/2 to 3 mm in spots
14	Injector	X	-	0.250 (1.5 sec)	• Two 180-second-duration runs • Carbon buildup: injector face 1 mm; walls 5 mm; nozzle walls ≈ 10 mm; nozzle throat clean
15	Injector	X	-	0.250 (1.5 sec)	• Three 180-second-duration runs, stable combustion • Carbon buildup same as above • Nozzle high-temperature erosion observed after 1.3 nominal power run

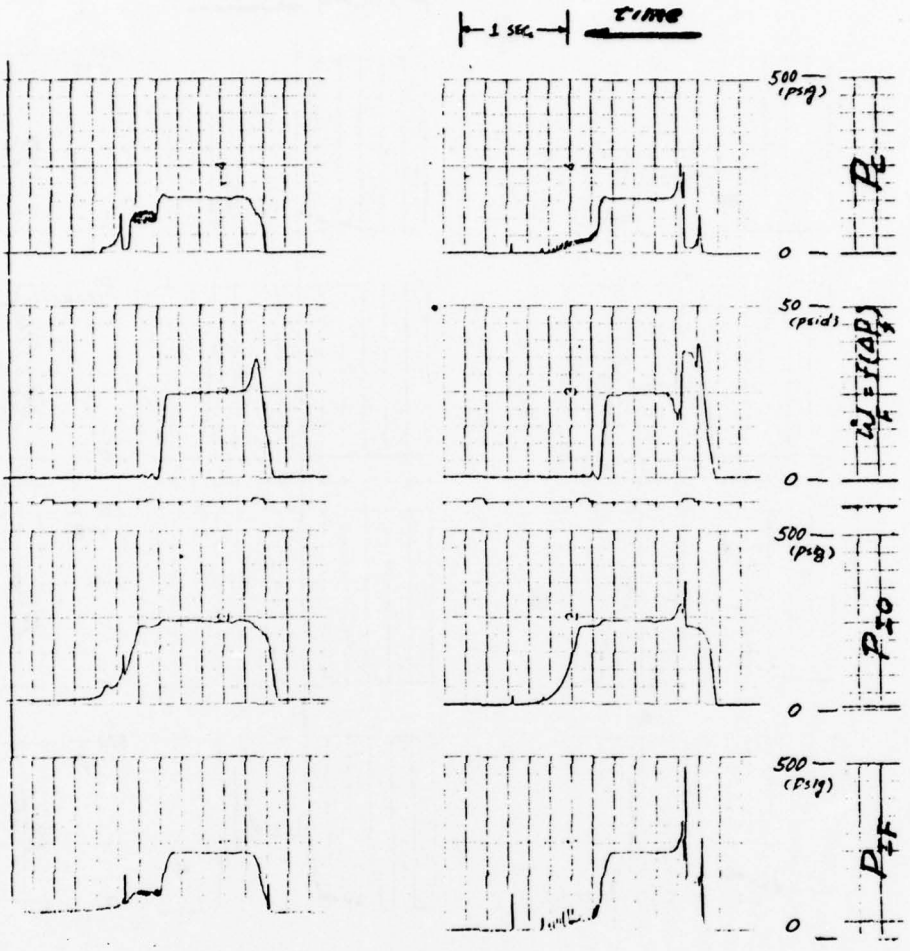

Run 10.01

- Normal Power Level
- w/ Choke Ring
- w/ Purge Gas Lead

Run 10.02

- Normal Power Level
- w/ Choke Ring
- w/ Purge Gas Lead

Figure 66. Effect of Purge Gas Lead at Normal Power Level and With Choke Ring

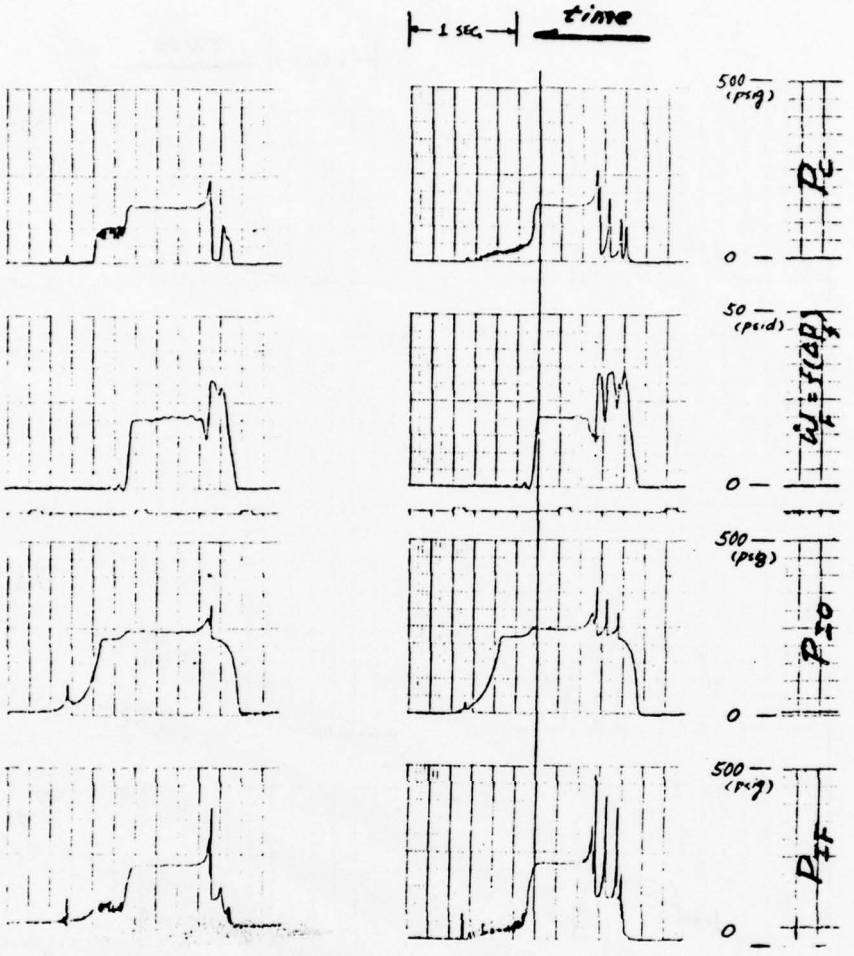

Run 11.05

- Normal Power Level
- w/o Choke Ring
- w/ Purge Gas Lead

Run 11.06

- Normal Power Level
- w/o Choke Ring
- w/ Purge Gas Lead

Figure 67. Effect of Purge Gas Lead at Normal Power Level and Without Choke Ring

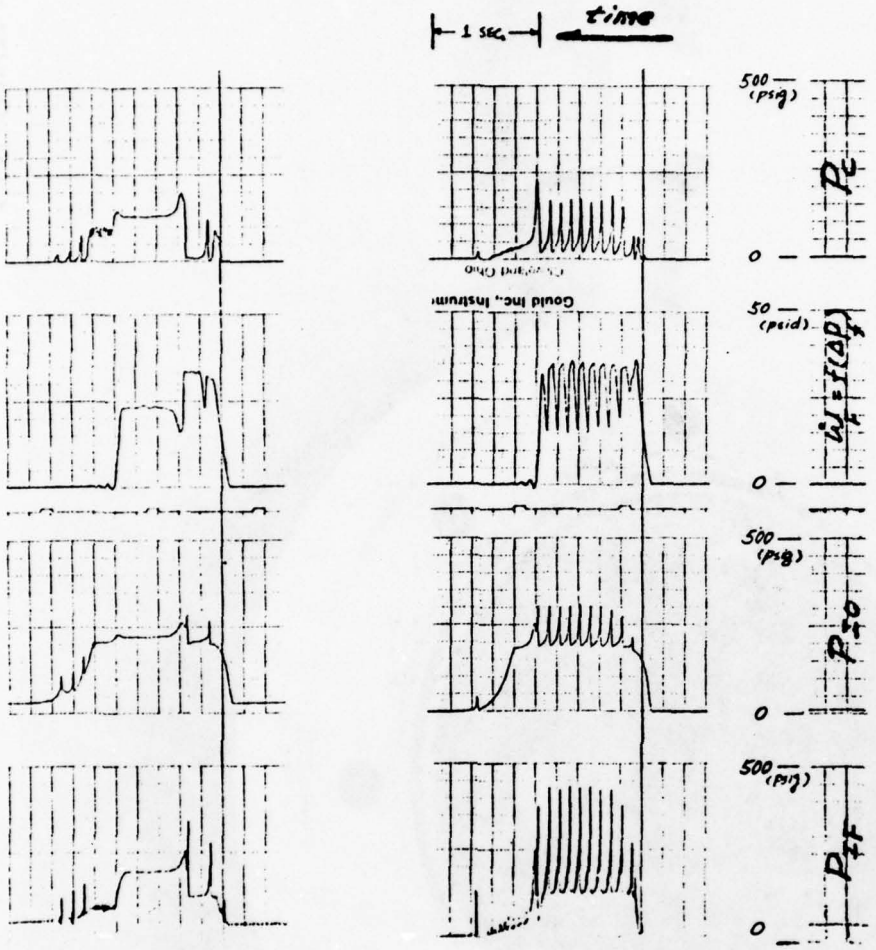

Run 11.08

- .75 Normal Power Level
- w/o Choke Ring
- w/ Purge Gas Lead

Run 11.10

- .75 Normal Power Level
- w/o Choke Ring
- w/ Purge Gas Lead

Figure 68. Effect of Purge Gas Lead at Lower Power Level and Without Choke Ring

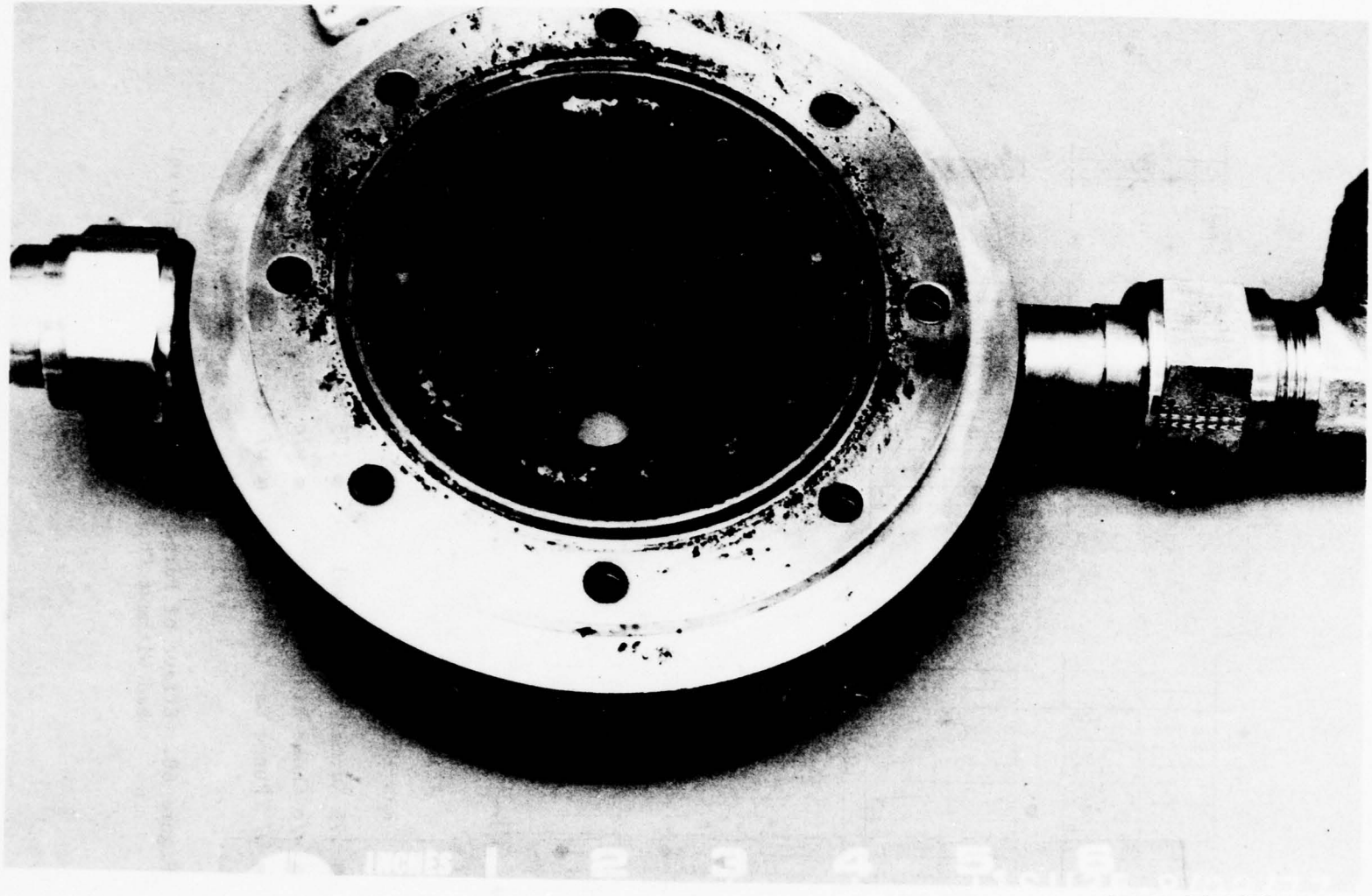

1SU35-8/23/77-C1B

Figure 69. Carbon Buildup in Nozzle Following Test Series 15

the throttle valve reinstalled, which revealed that stable combustion was reproducible at normal power level, but only marginally at 75% of normal power level. Subsequently, the test activity proceeded to a long-duration test at 130% power level, which was concluded successfully with a full 180-second duration and with a 200 msec fuel lag in the shutdown transient.

The fresh carbon built up during the foregoing long-duration run appeared to be about half of the equilibrium thickness. This was consistent with the result observed previously. Figure 70 describes the distribution of the equilibrium carbon buildup that was reached after 1000 seconds of long-duration test runs (180 sec). Typical traces of the 180-second-duration test are shown in Fig. 71 through 73. After the last duration test (run 15.01) at 1.3 times nominal power level, some high-temperature erosion was observed at the exit of the nozzle throat. The nozzle hardware was in satisfactory condition to complete the remaining tests (Cases II and III) in the planned test matrix.

Low-Cut Fuel Ignition. The ignition diagnostic runs of Test Case III were conducted with the propellant flowrates generally set for normal power level operation. The low-cut JP-4 was simulated by a mixture of RP-1 (23 wt. %) and JP-4. Both low-cut JP-4 and JP-8 test series were conducted with the same feed system configuration used in the prior testing with ~150 msec of GOX lead at the start. The ignition transients observed in both series showed little significant difference when compared to those obtained with neat JP-4. Typical ignition transients are shown in Fig. 74 and 75.

Cold Propellant Ignition. The cold propellants test series were performed after some facility rework for added jacketing of the feed system and for replacement of the main fuel valve (throttle type) with the direct-acting valve used earlier. The valve replacement for the cold propellants test series was necessary due to the larger mass of the throttle valve and the increased difficulty of prechilling it.

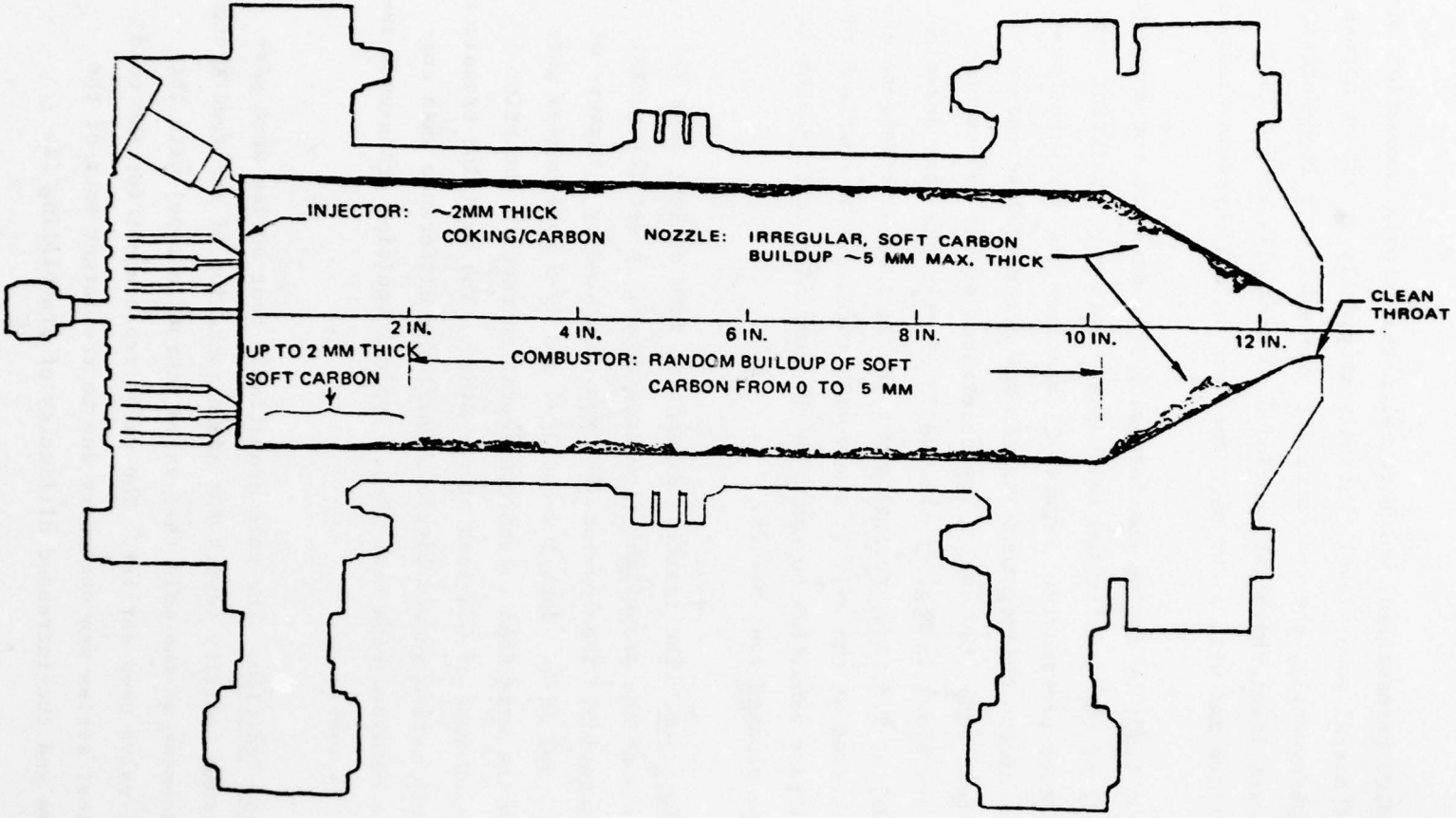

Figure 70. Typical Carbon Buildup Characteristics After ~1000 Seconds of Long Duration (180 Seconds) Test Run

NORMAL(100%) POWER LEVEL
MR(O/F) = 0.5
COMB. CLNT.(GN_2)= 150% of $\dot{W}_{GOX}$

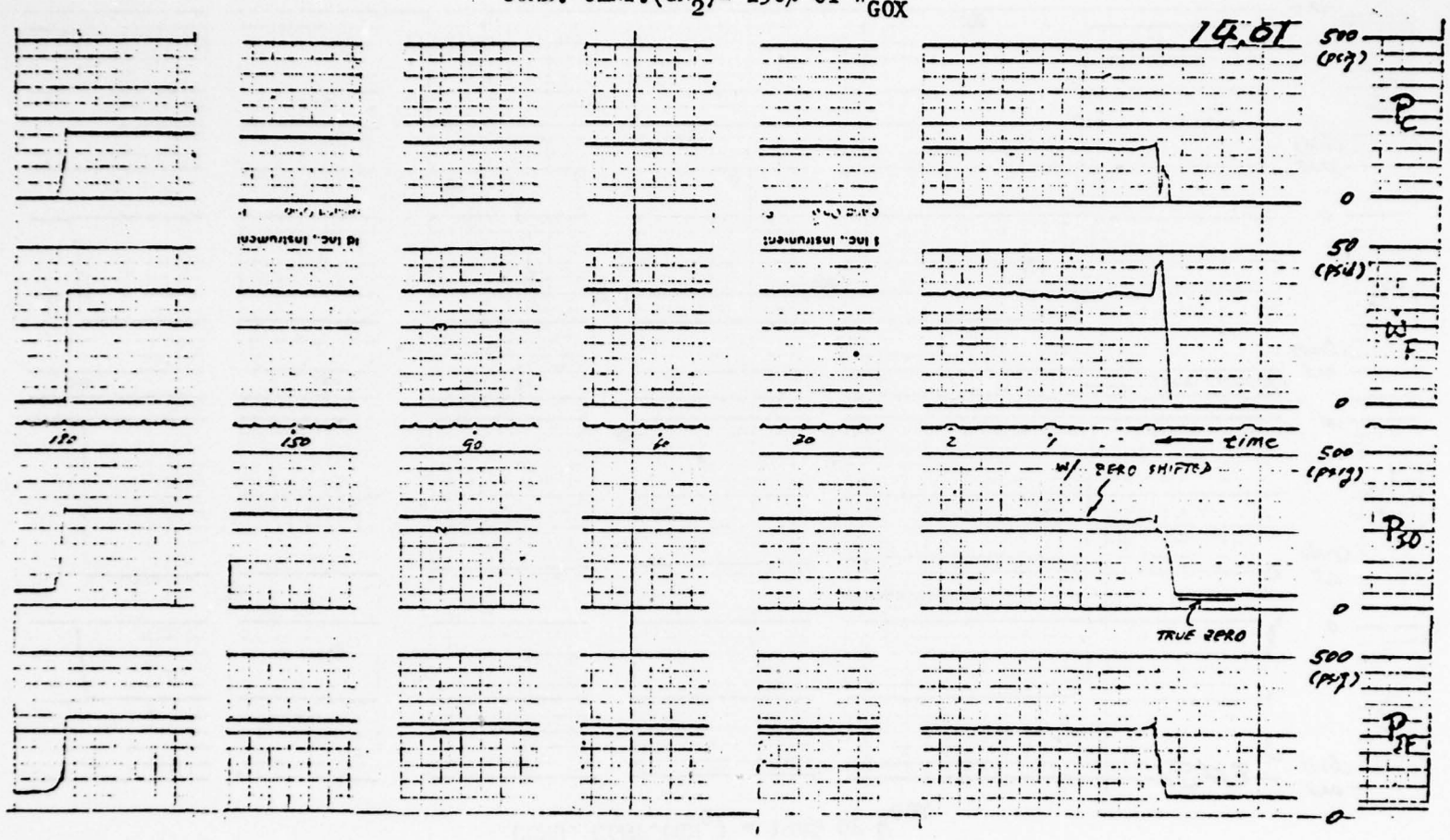

Figure 71. Lon Duration Test at 100% Power Level

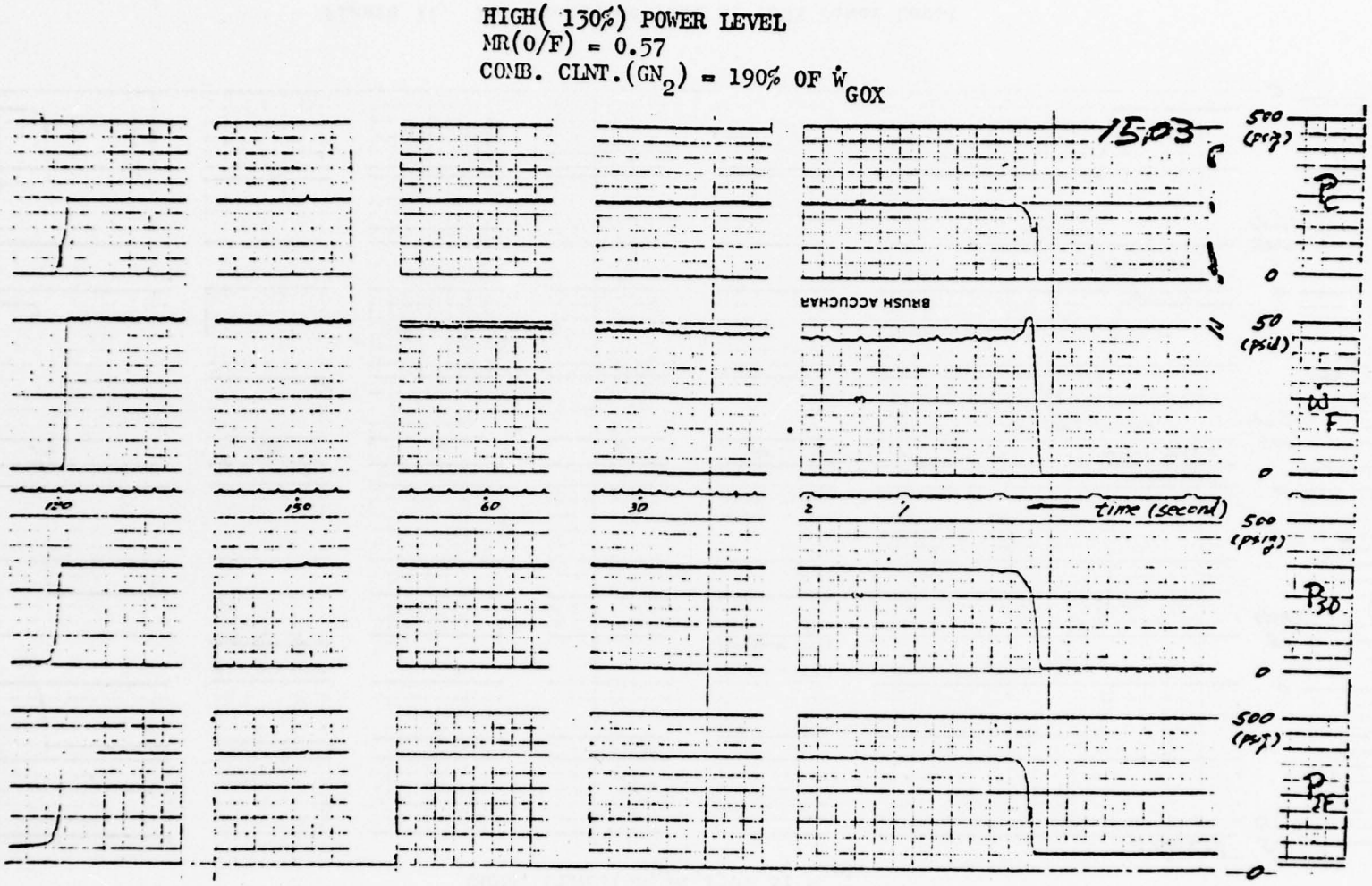

Figure 72. Long Duration Test at 130% Power Level (MR = 0.57)

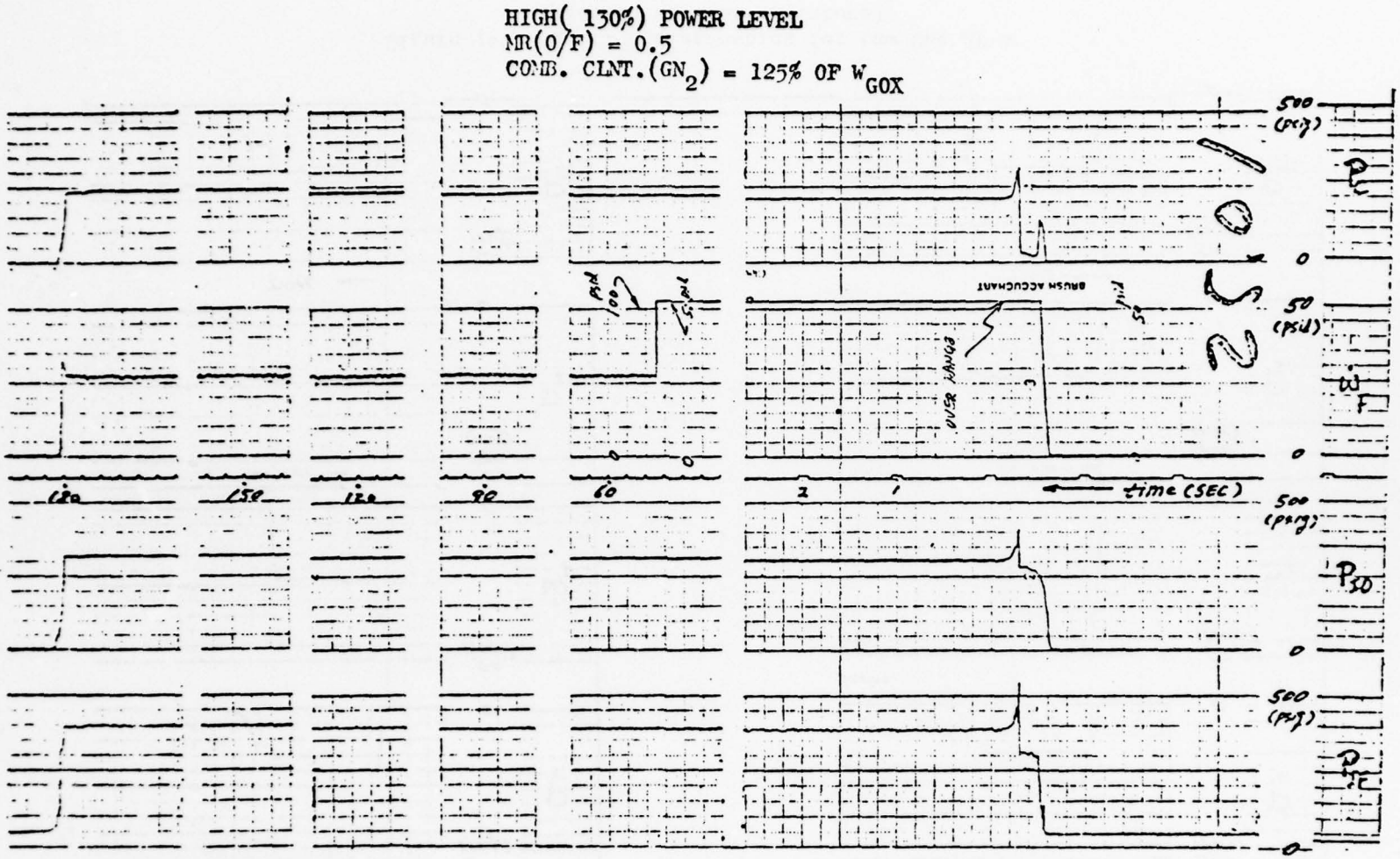

Figure 73. Long Duration Test at 130% Power Level (MR = 0.50)

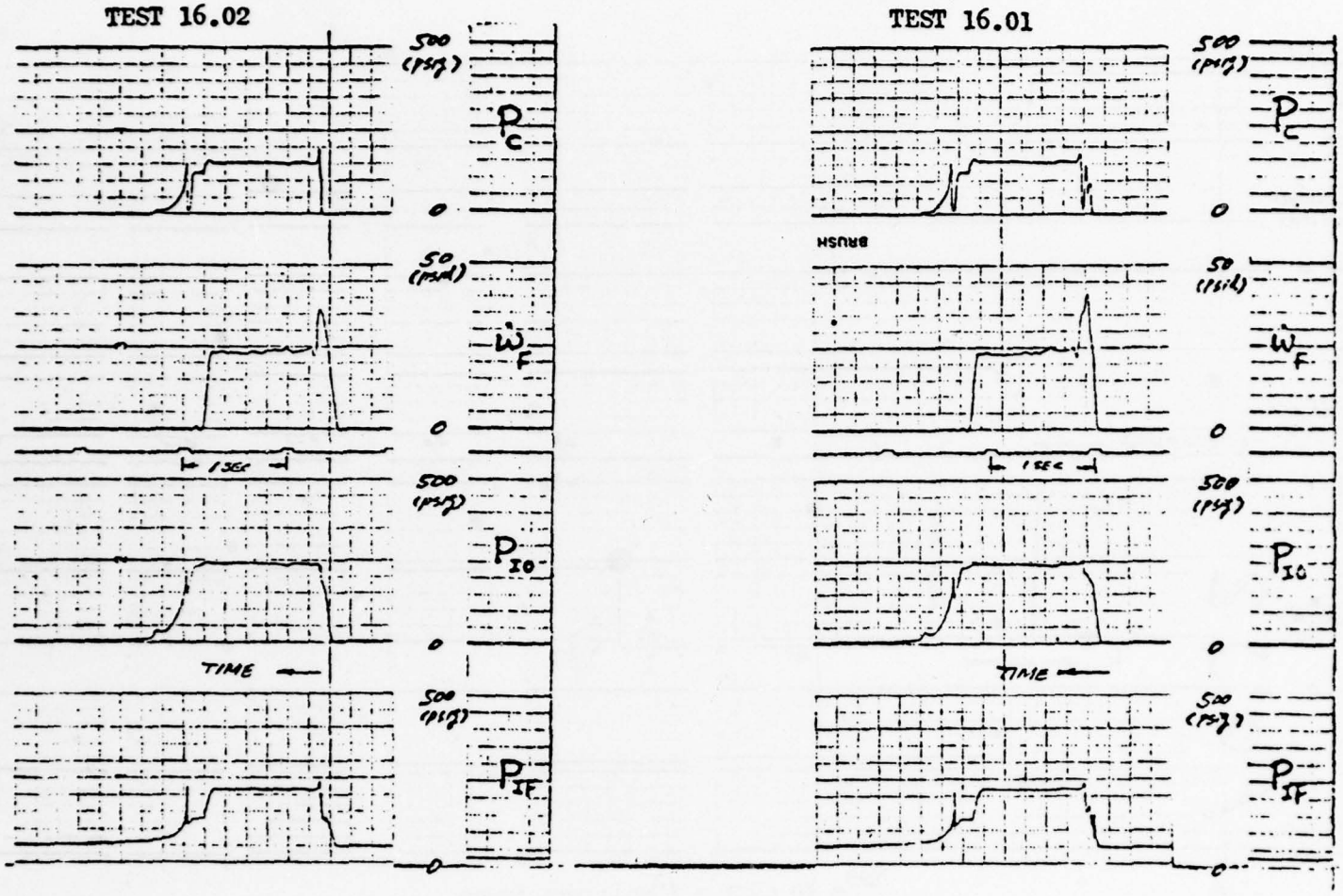

Figure 74. Ignition Diagnostics for Low Cut JP-4
(With 23 wt.% RP-1 Mixture)

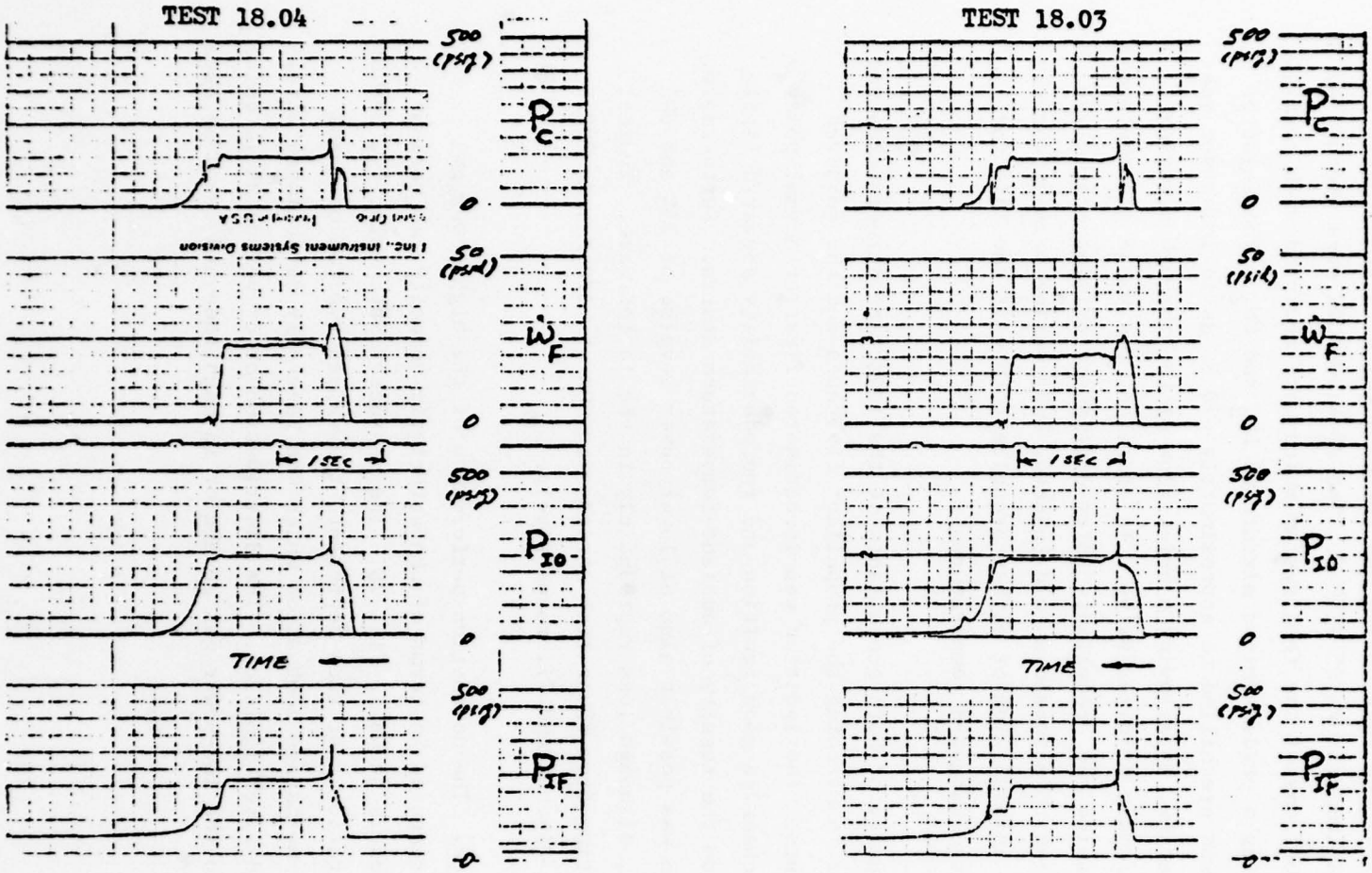

Figure 75. Ignition Diagnostics for JP-8 Fuel
(With Jet-A Fuel)

The cold propellants test series was targeted for JP-4 temperature of -65 F and GOX temperature of -150 F. The JP-4 and GOX were prechilled in downstream portions of the feed system which were equipped with coaxial jackets flowing a predetermined mixture of LN_2 and GN_2. The injector body itself was prechilled to approximately -70 F, as in low-power gas generator testing, by allowing a brief flow of LN_2 through a region downstream of main oxidizer valve. In addition, the purge gas (helium), which accompanied the propellants entry during the priming stage, was also prechilled to maintain a cold injector body during priming, thereby enabling the initial slug of either propellant to exit the injector orifices at the targeted temperatures.

Increased density of both propellants at the injection temperatures was accounted for in matching the propellant flowrates and the required supply pressure. The ignition was investigated first at normal power level. The observed good ignition and reproducibility appeared little different from the results of ambient-temperature starts. Furthermore, good ignition was possible also at lower power levels, of 75% and 60% power levels, although less reproducibly in the latter case. Typical traces resulting from these test series with GOX at -170 F and -200 F are shown in Fig. 76 and 77, respectively.

c* Performance. The combustion performance of the high-power gas generator, presented in terms of characteristic velocity, at various mixture ratios is shown in Fig. 78. The characteristic velocity, c*, of the short-duration test runs represents the values typical of quasi steady-state mainstage combustion which was generally established within a half second after ignition. The distribution of c* versus MR is quite comparable to the low-power gas generator in magnitude and trend as seen in Fig. 79.

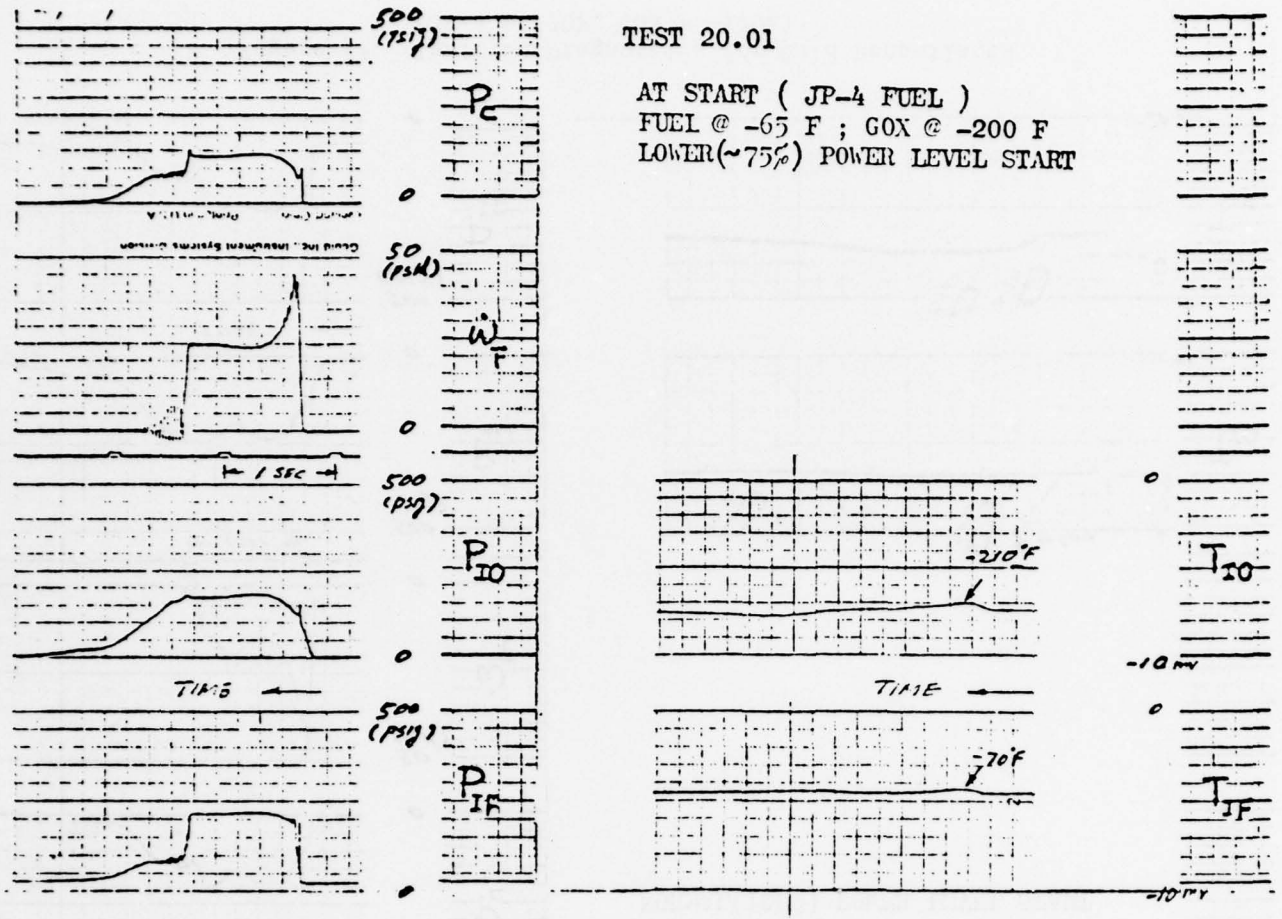

Figure 76. Ignition Diagnostics for Cold Propellants
(JP-4 = -65F, GOX = -200F)

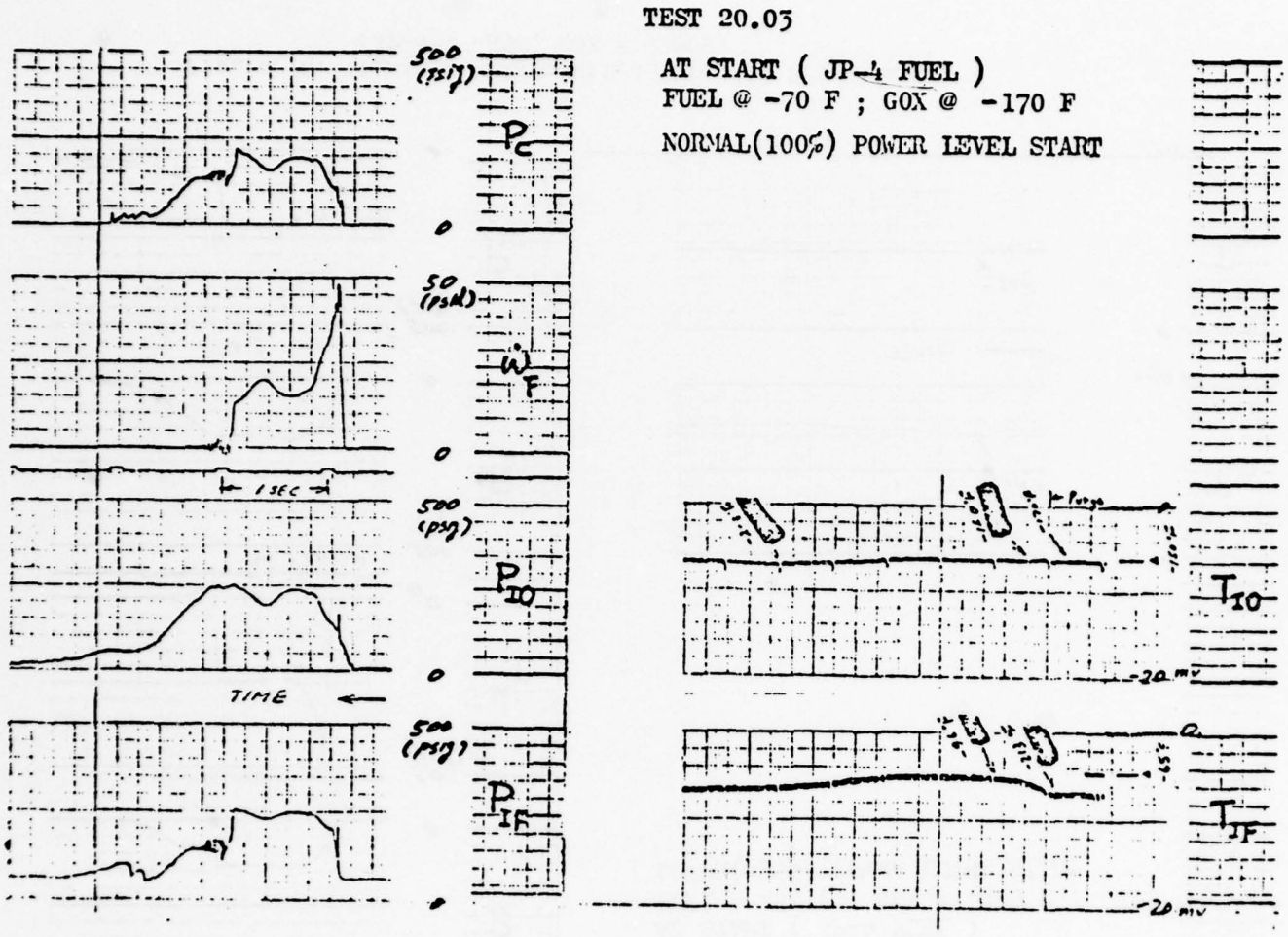

Figure 77. Ignition Diagnostics for Cold Propellants
(JP-4 = -70F, GOX = -170F)

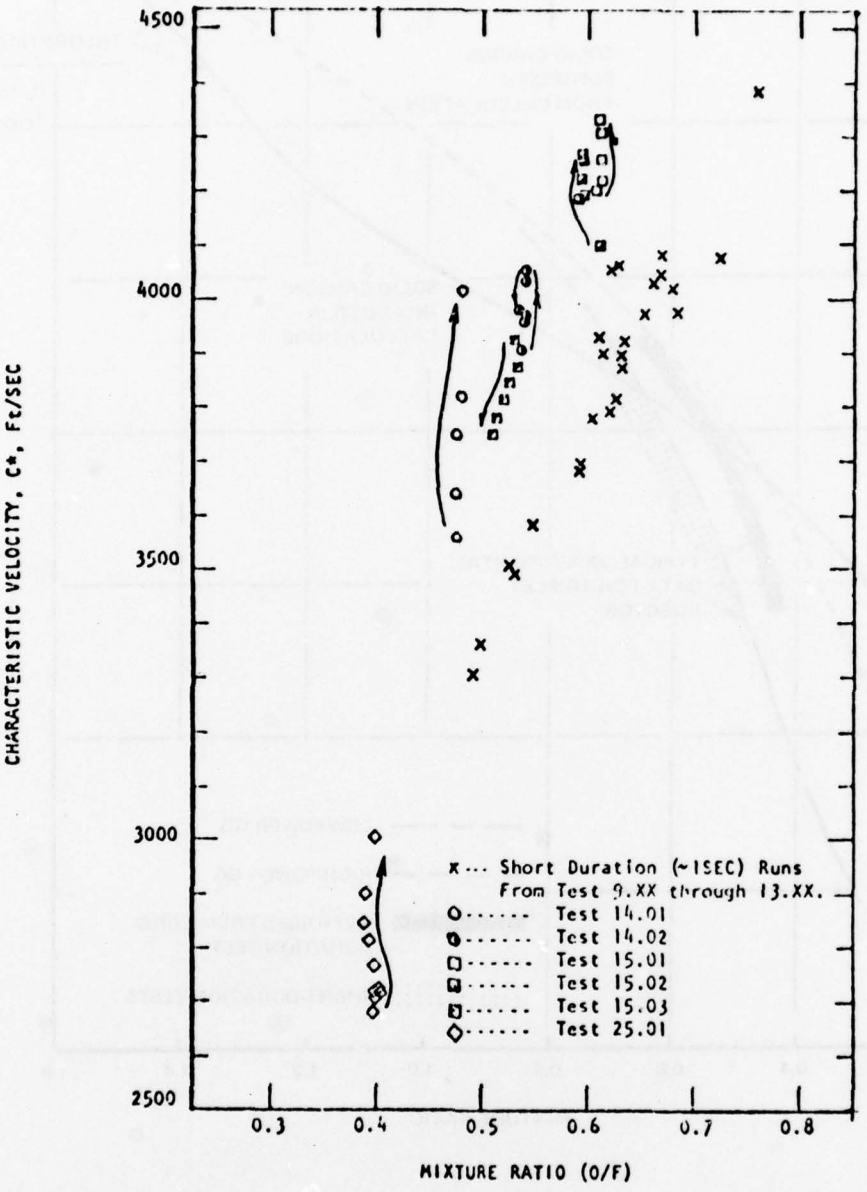

Figure 78. High-Power Gas Generator Test Results, Characteristic Velocity vs Mixture Ratio

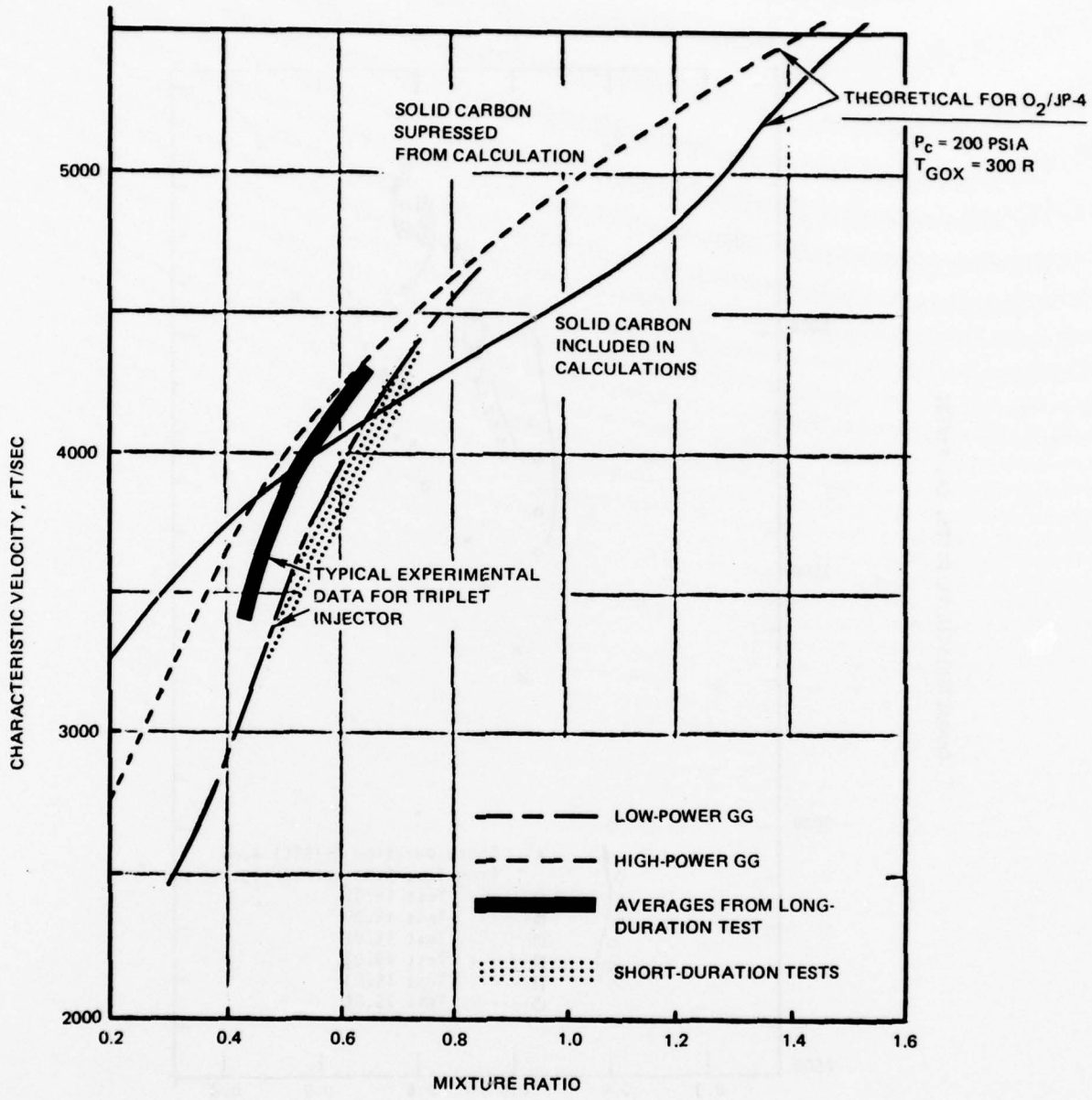

Figure 79. Theoretical and Experimental Data Trends of Characteristic Velocity

The characteristic velocity of the long-duration tests showed marked change, with time (generally an increase) as indicated in Fig. 78 by the plot of mean c* values, each averaged over 20- to 30-second intervals. The result of Run 15.02 shows reversal of the increasing trend in the middle of the run, which persisted through the subsequent run (Run 15.03). This was determined to be the result of throat erosion due to disturbance created by nozzle carbon deposits. In general, however, the characteristic velocity of the long-duration tests were significantly higher than those of the short-duration tests, and closer to the theoretical values.

Combustor Thermal Analysis. The primary combustor thermal data obtained from the high-power gas generator testing was total heat load as determined from measured GN_2 coolant flowrate and temperature rise. The combustor heat load as a function of time for nominal P_c (190 psia) operation is shown in Fig. 80. There was about a 30% overshoot in heat load as compared to the final equilibrium value. The equilibrium heat load is seen to be less than that predicted based on assumed carbon layer formation. This indicates that carbon formation did occur on the combustor walls, a fact verified by posttest inspection.

For comparison purposes, the heat load results from an earlier low-power gas generator test is shown in Fig. 81. Two items are to be noted: (1) the heat load overshoot is about 86% above the steady-state value as compared to approximately 30% for the high-power gas generator as a result of a clean wall at start, and (2) the measured heat load for the low-power gas generator agrees more favorably with the predicted value based on assumed carbon formation. This latter observation implies that the carbon layer formation was somewhat greater for the high-power design in spite of the higher design wall temperatures utilized. It is believed that the very high combustor contraction ratio ($\simeq$28:1) employed in the high-power gas generator design to improve ignition, resulted in an extremely low gas shear levels and an increase in wall carbon formation.

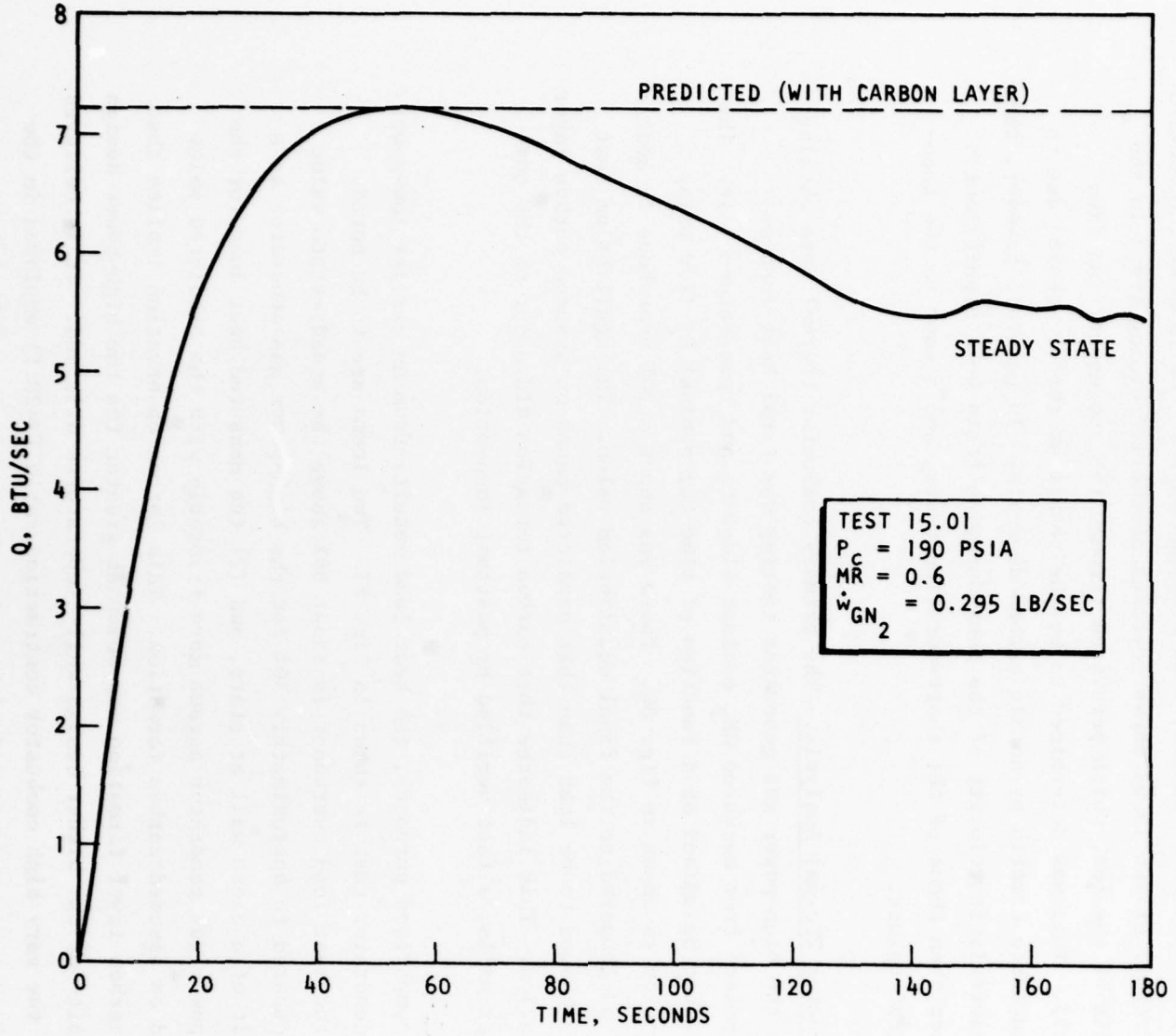

Figure 80. High-Power IPU Combustor Heat Load

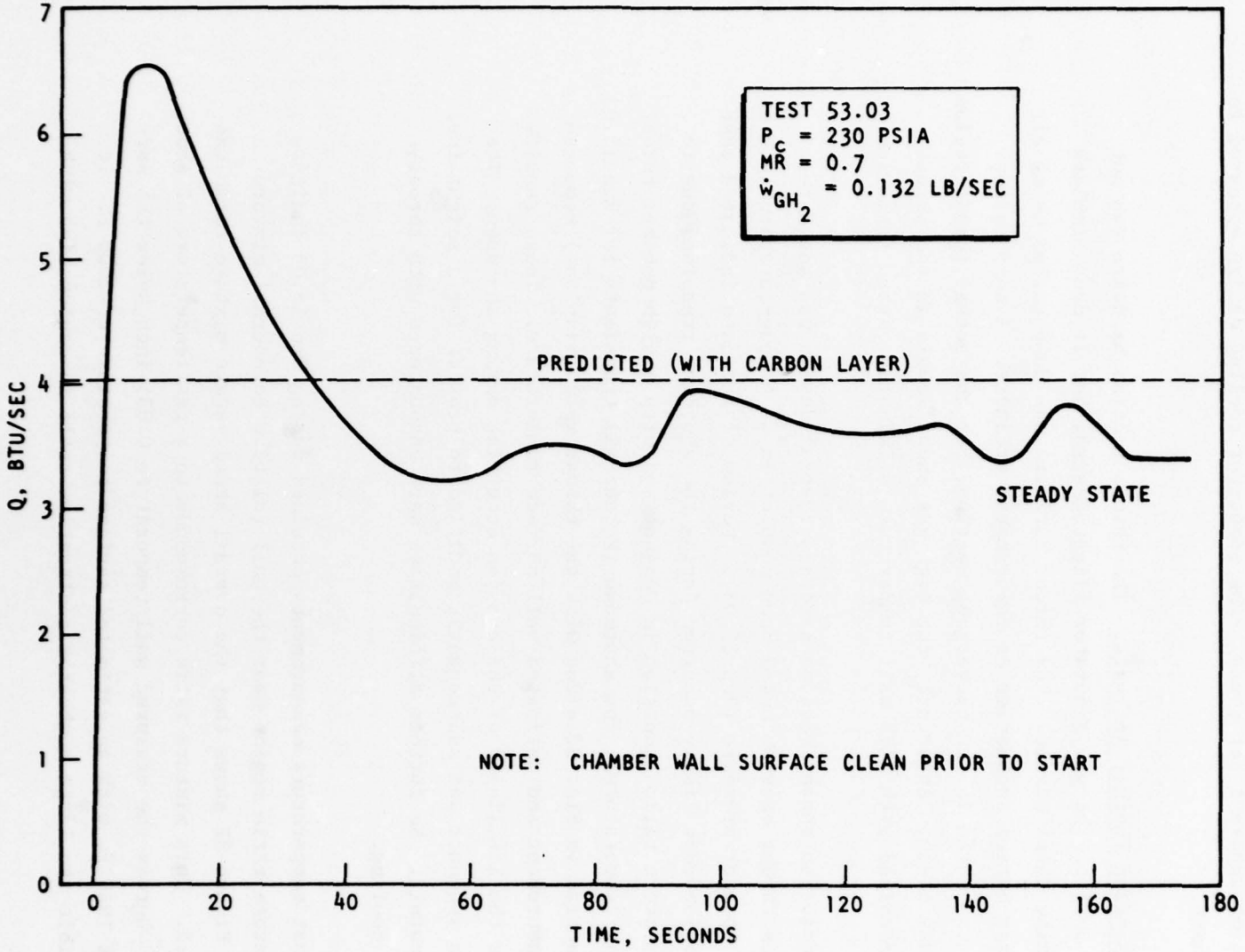

Figure 81. Low-Power IPU Combustor Heat Load

Inspection of the combustor upon completion of the testing indicated no erosion, or apparent hot spots. The combustor cooling design appeared to be adequate.

Throat Section Thermal Analysis. The throat section hardware was not a basic part of the gas generator flight design, but it does simulate the turbine inlet nozzle. The throat hardware was dump cooled using air to provide better combustion of the exhaust products. A soft carbon buildup was noted in the converging section, but the actual throat region itself was clean. Apparently the high gas shear levels in the throat region combined with high wall temperature eliminated carbon formation.

In general, the throat section hardware thermal design was adequate. There was throat erosion noted upon completion of a long-duration test at maximum chamber pressure (Run 15.03). Review of the data indicated that this erosion most likely occurred during the shutdown transient due to a high mixture ratio excursion in conjunction with a high nominal throat operating temperature. The shutdown (P_c and MR) transients for Run 15.03 are presented in Fig. 82 along with the throat wall (midplane) temperature measurement and estimated wall surface temperature. These results indicate the likelihood of the erosion occurring during shutdown. The shutdown sequence was subsequently modified to provide for a slight fuel lag at cutoff. No further difficulties were encountered with throat section cooling.

The throat temperature measurements obtained during Run 15.03 indicate a high mixture ratio region near the wall relative to overall mixture ratio. Figure 82 shows that the overall steady-state mixture ratio was about 0.5. This mixture ratio corresponds to a gas temperature of about 1600 F, whereas the measured wall temperature 0.035 inch below the surface was 1940 F, with an estimated surface temperature of 2000 F. It is possible the large combustor contraction ratio in conjunction with

the injector element placement relative to the combustor wall resulted in a higher wall region mixture ratio due to more rapid expansion of the gaseous oxygen as compared to the liquid fuel.

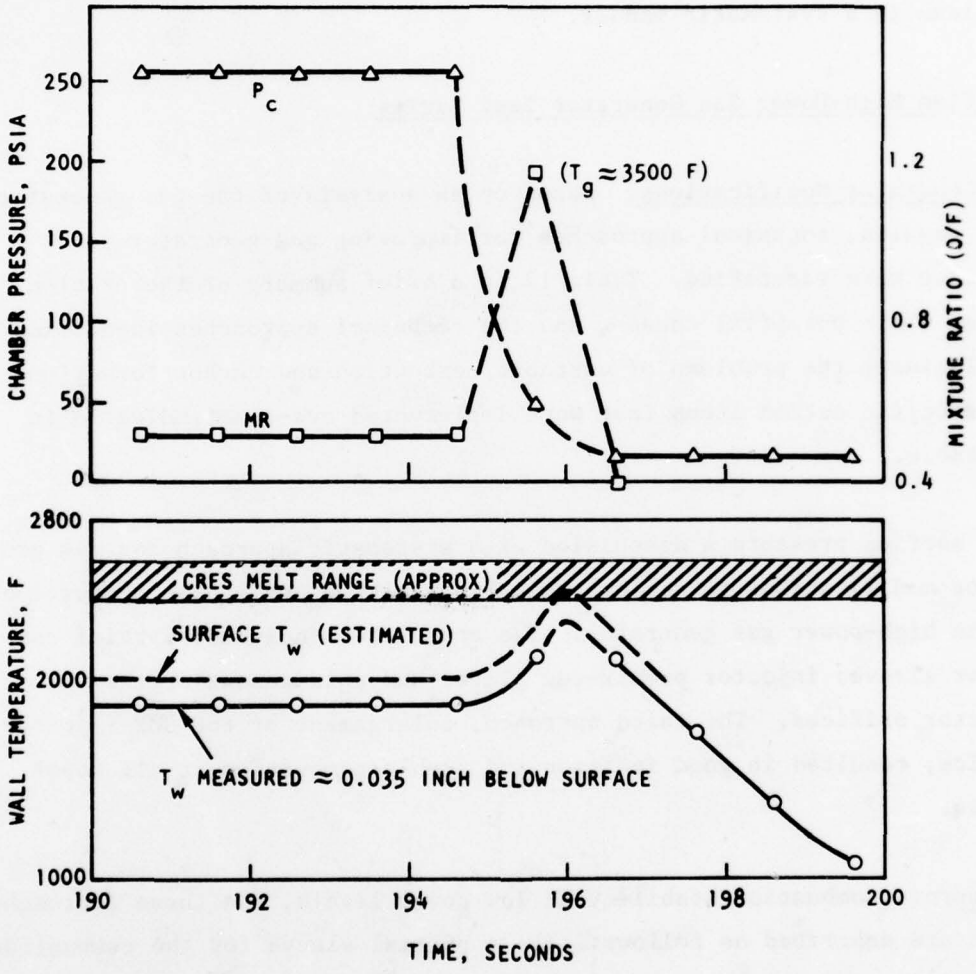

Figure 82. Cutoff Transients for Test 15.03

Assessment. Based on the test results and analyses, several unresolved problem areas still existed with the high-power gas generator, and an upgraded test series was formulated and conducted to eliminate (1) unstable combustion at low power levels, and (2) hard carbon formation in the small areas around the GOX orifices. Therefore, design and test modifications to the gas generator were made to solve the remaining problems in a systematic manner.

Modified High-Power Gas Generator Test Series

Gas Generator Modifications. Based on an analysis of the gas generator test results, technical approaches for improving gas generator performance were identified. Table 17 is a brief summary of the problem areas, their potential causes, and the technical approaches identified to eliminate the problems of unstable combustion and carbon formation. The specific action items that were implemented are also indicated in the table.

This section presents a discussion of a systematic approach for gas generator modifications to achieve reliable ignition and stable combustion in the high-power gas generator. The approaches included: partial combustor sleeve; injector premix-cup plate; and enlargement of the GOX injector orifices. The third approach, enlargement of the GOX injector orifice, resulted in good ignition and stable combustion at all power levels.

To improve combustion stability at low power levels, the three approaches taken are described as follows: (1) a partial sleeve for the combustion wall at the injector face was fabricated. The sleeve reduces the combustor diameter at the injector and reduces recirculation of combustion gases back toward the injector face. Photographs of the partial sleeve are shown in Fig. 83, and the assembly is shown schematically in Fig. 84; (2) two premix-cup plates were fabricated, which increased premixing of GOX and JP-4 prior to combustion. The two premix-cup plates, with different

TABLE 17. DEFINITION OF PROBLEM AND ACTION

PROBLEM AREA	POTENTIAL CAUSES	APPROACHES	ACTION ITEMS (*)
(A) Brief Flame-out of First Ignition	●Excessive MR (O/F) drop due to fuel flow overshoot during start transient ●Recirculation of combustion product gas toward injector	●Suppress initial P_{IF} surge using ramped rise of P_{IF} and/or added flow resistance near injector ●Minimize annular space devoid of injector elements adjacent to combustor wall	●Cavitating venturi close-coupled to injector @ d/s of MFV ●Install MFV with linear flow valve plug ●Fill-up sleeve near injector
(B) Cyclic, Unstable Combustion	●Insufficient fuel feed system resistance ●Excessive combustor volume akin to pulse jet with blow-down frequency of ~11 Hz ●Fuel-into-GOX penetration weakened at lower power level operation	●Increase/concentrate feed system Δp near injector ●Reduce physical volume of combustor, or reduce GOX injection velocity to render the effect of increasing characteristic frequency of combustor blow-down ●Reduce momentum flux of GOX injection jet	●Cavitating venturi and/or stiffener orifice close coupled to injector ●Fill-up sleeve extending full length of combustor ●Resizing/enlarging of GOX injector orifice outlets so as to obtain M=0.5 instead of M=0.7 (present)
(C) Volcanic Shell (coking) Around GOX Orifice Outlets	●Cold injector face near GOX orifices (T=20F, estimated)	●Keep pyrolysis product from recirculating/impinging on cold surface ●Keep injector face hotter	●Premixing cup for each triplet element ●Extension tubes on GOX orifice outlets ●Refractory coating on injector face
(D) Carbon Build-Up	●Insufficient temperature maintained at wall ●Excessive reaction time allowing pyrolysis to form carbon	●Keep the cooled wall hotter ●Promote fuel-GOX mixing by slow-down of GOX and fuel-GOX mixture	●Reduce cooling of combustor wall ●Premixing cups with enlarged GOX orifice outlets

(*) Note the redundancy of action items

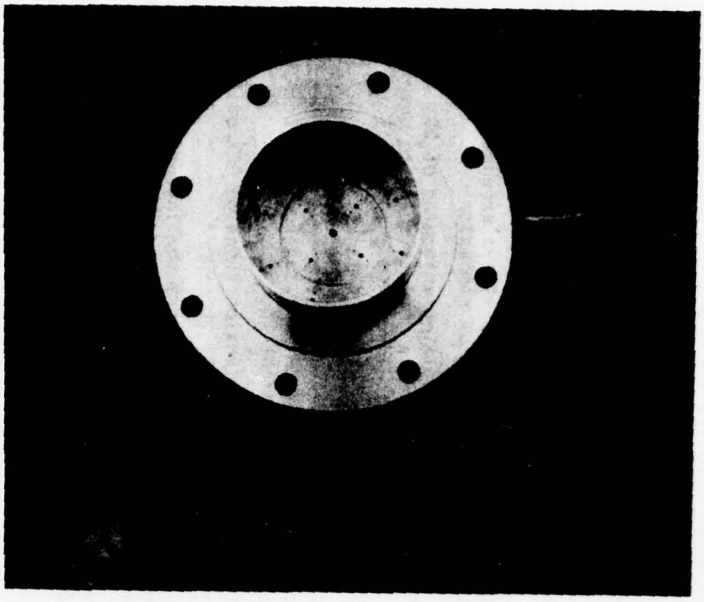

(a) Partial Sleeve Placed on Injector

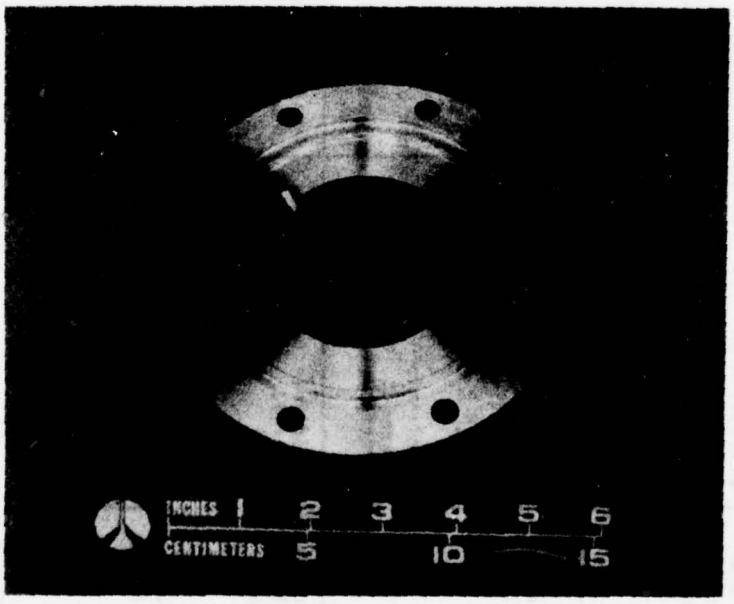

(b) Top View of Partial Sleeve

Figure 83. Partial Sleeve for Suppression of Recirculation Zone

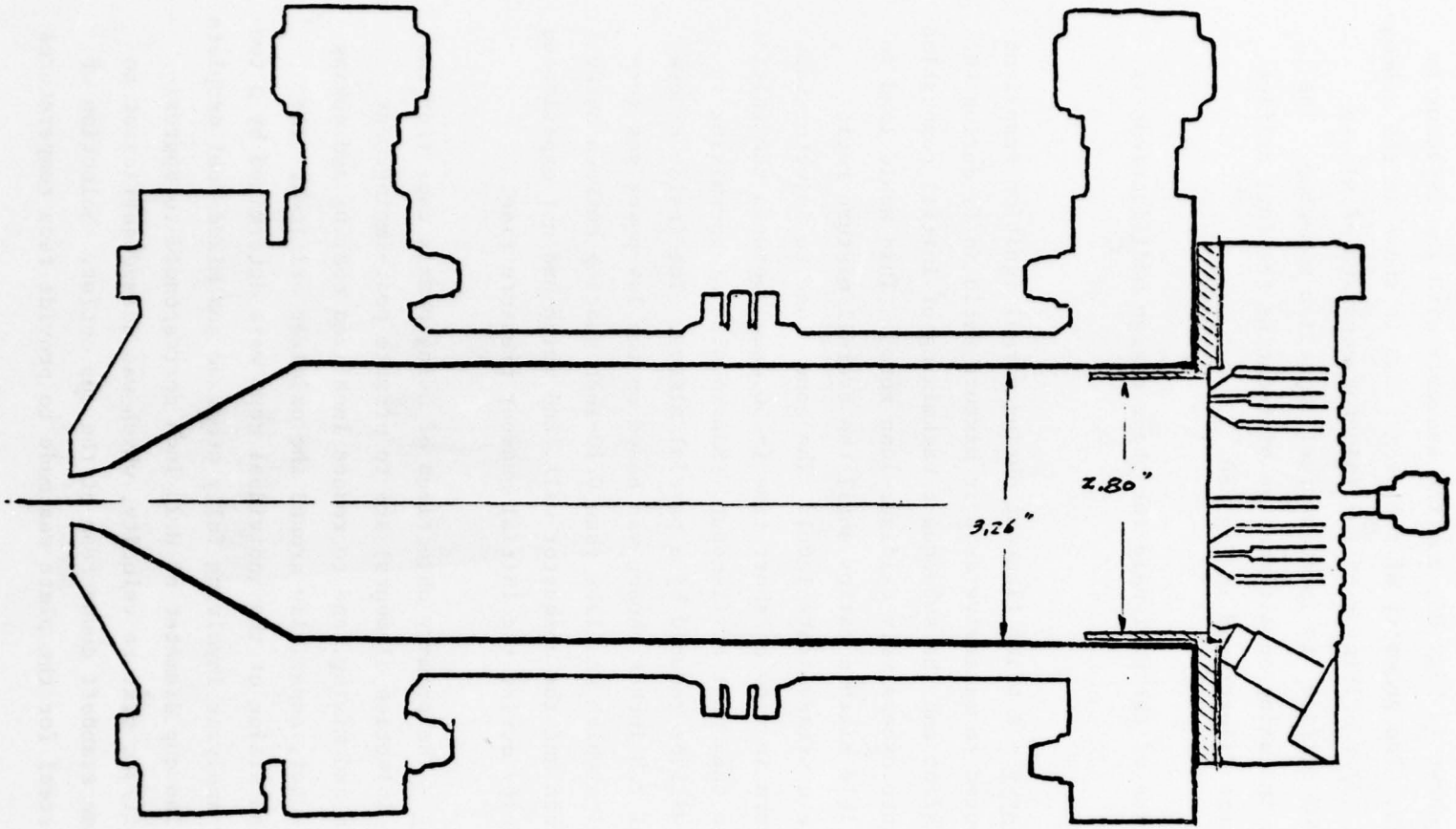

Figure 84. Partial Sleeve Near Injector Face (~25% Area Reduction Near Chamber Wall)

L/D ratios are shown in Fig. 85, and the assembly with the injector is shown in Fig. 86. The geometry of the premix cup is shown in the schematic of Fig. 87; (3) reorificing of the injector consists of simply enlarging the GOX orifice to increase fuel injection momentum. The orifice rework, including an alternative of reducing the fuel orifice with a sleeve, are illustrated in Fig. 88.

A brief discussion of the rationale for these design modifications is presented below:

Partial Sleeve - A brief flameout during normal ignition transient was attributed to excessive drop in mixture ratio (o/f) during the start transient and the subsequent backmixing of initial combustion products into excessively oxidizer-lean zones. This would lead to noncombustible mixture ratios until the overall mixture ratio returned to a steady-state level. The zone close to injector face was a concern in view of short time ($\sim$ 30 msec) between the initial ignition to the onset of flameout. Suppression of backmixing in this zone will be reduced by a partial sleeve. The inside sleeve diameter of 2.8 inches chosen was based on the low-power gas generator design which has less than 0.10-inch spacing between outer fuel orifices and the combustor wall, and which had not experienced any difficulty during the initial chamber pressure rise.

Premix Cups - The primary objectives of using premix cups (for the individual injection elements) are to promote post-impingement atomization and mixing, and to reduce localized cooling and coking on the injector, especially around the oxidizer orifices. The geometry and sizing of the individual cups were determined by a two-phase flow analysis involving fully atomized and mixed fuel droplets and GOX. The cup diameter of 0.20 inch corresponded to approximately 70-ft/sec mixture velocity, which was deemed sufficient to ensure flame standoff downstream of the cup outlet. Selection of stainless steel for the plate was made to provide face temperatures

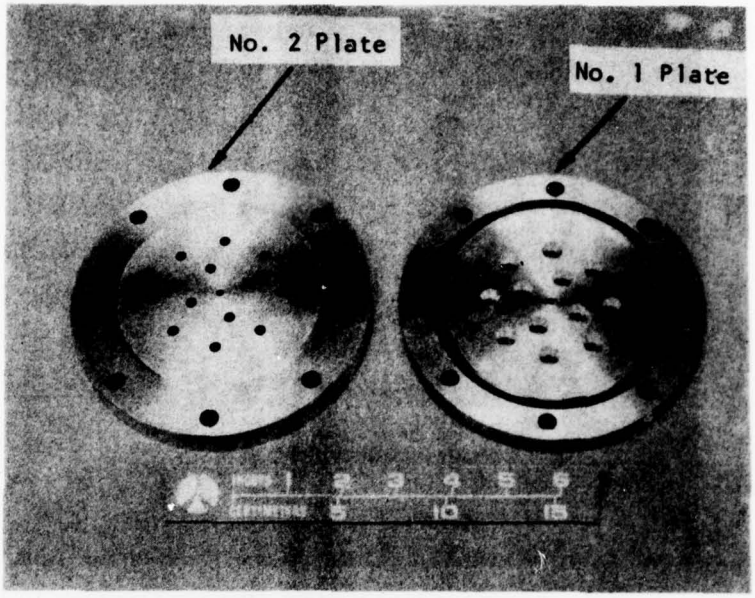

(a) No. 1 Plate with L/D = 2.5
No. 2 Plate with L/D = 3.8

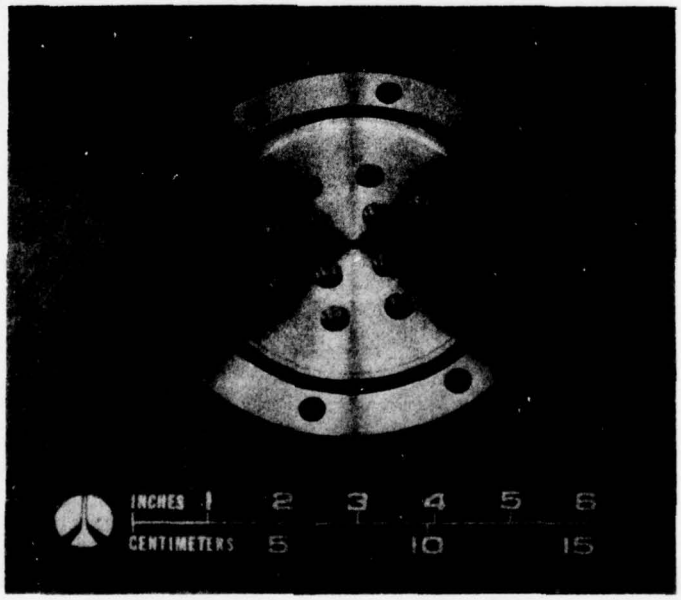

(b) Closeup View of No. 2 Plate

Figure 85. Premix-Cut Plates

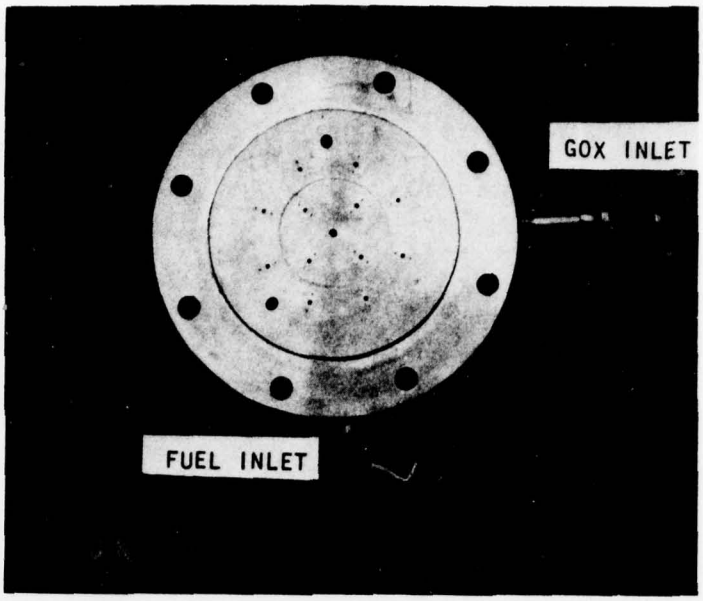

(a) Bare Injector Face (Note slight rework of face of gap-free mating with premix-cup plate)

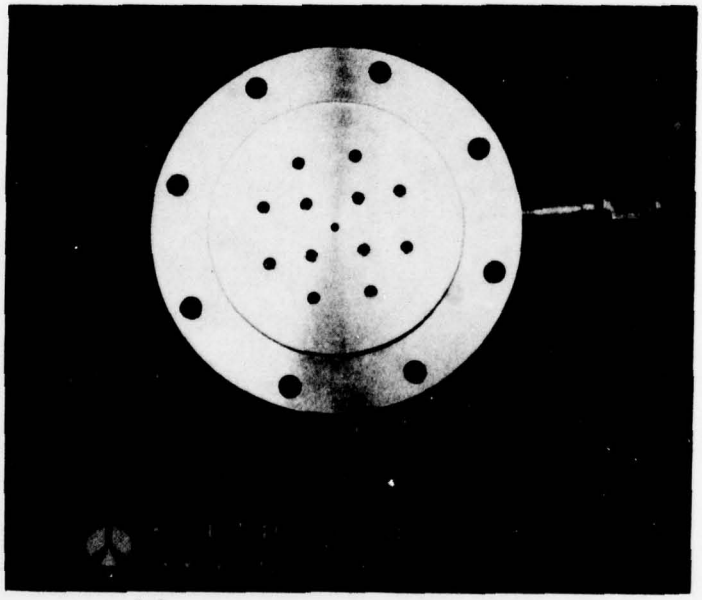

(b) Injector covered with No. 1 Premix-cup plate

Figure 86. Gas Generator Premix-Cup Injector Assembly

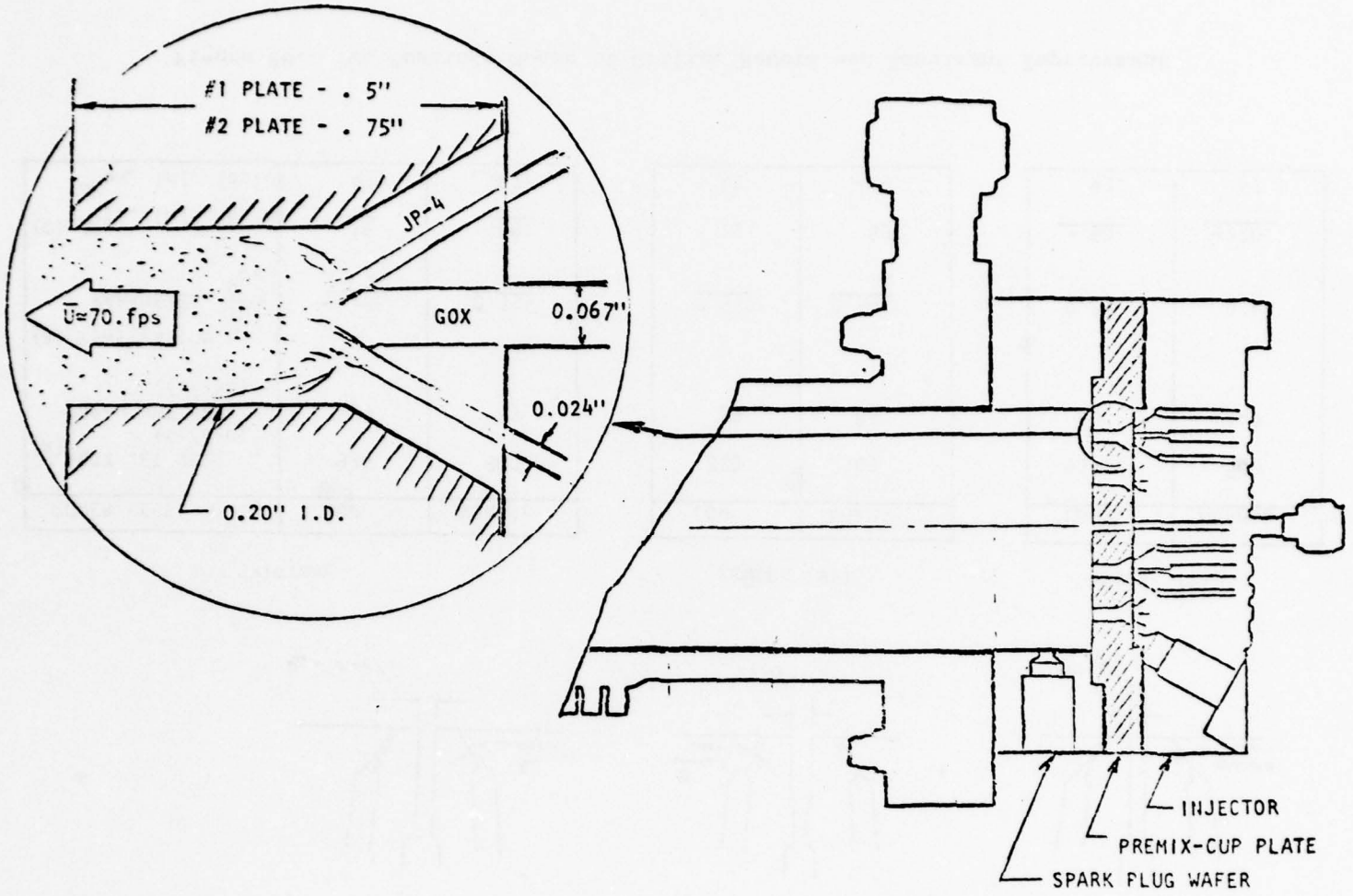

Figure 87. Premix-Cup Plate Location and Dimension

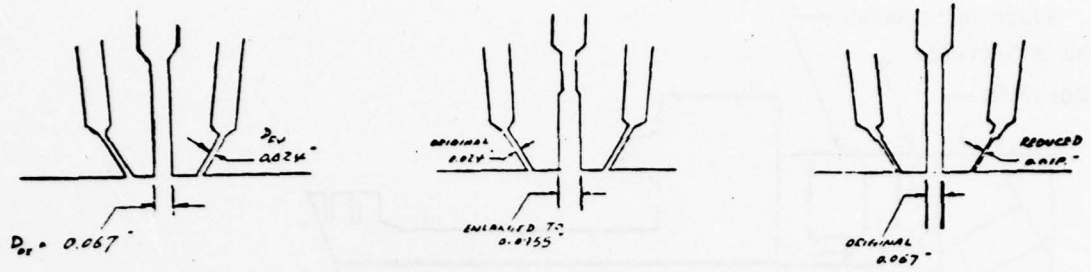

	ORIGINAL		REWORK (#1)		REWORK (#2)	
POWER LEVEL	LOW	NORMAL	LOW	NORMAL	LOW	NORMAL
(A) GOX JET VEL. (ft/sec)	934	800	320.	309	934.	800
(A) JP-4 JET VEL. (ft/sec)	39	83	39	83	69	147
(B) PENETRATION - PARAMETER, $\frac{X_D}{D_{ox}}$	0.186	0.334	0.330	0.535	0.25	0.44
(C) $\Delta P_{fu.\ inj}$ (psid)	15.	69.	15	69.	~50	~220.
$\Delta P_{ox.\ inj}$ (psid)	43.	67.	~45	~70	43.	67

Figure 88. Two Possible Modes of Orifice Rework and Resultant Improvement

higher than the bare copper injector and reduce the chance of coking on the injector face. Two plates with L/D of 2.5 and 3.8 were fabricated. A series of cold-flow tests, shown in Fig. 89 and 90 were conducted to check out the design.

Reworked GOX Orifice - The objective of the GOX orifice rework is to increase the penetration of fuel jets into GOX jets for better mixing by altering the momenta of the jets. Also, the fuel-side injector pressure drop was further steepened to attain $\Delta P/P_c \geq 35\%$ even at the lower power levels, a minimum criterion set for feed system-coupled instability modes, given by

$$\frac{\Delta P}{P_c} \geq \frac{0.5}{1 + MR}$$

Testing of the modified high-power gas generator was initiated on 16 November 1977 and completed on 10 February 1978. During the test series, 99 tests were conducted for a total accumulated steady-state duration of 1101 seconds. The planned test matrix for the modified high-power gas generator is presented in Table 18. The test facility and the instrumentation were basically identical to that used for the initial high-power gas generator test series.

During this test series, a single J-2 sparkplug was used at 0.250 Joule (nominal) and 50-cps spark frequency. The sparkplug was mounted in the injector for the partial sleeve tests and in the wafer for the premix-cup plate tests. The combustor and nozzle sections were again cooled by gaseous nitrogen and air, respectively, at 0.20 lbm/sec, which was comparable to the oxidizer flowrate for normal power level operation. Purge gas (helium), operated manually, was used primarily to keep the feed system lines clear by applying it only before and after each test run.

FUEL SIMULANT: WATER @ 0.032 LBM/SEC

OXIDIZER SIMULANT: GN_2 @ 0.023 LBM/SEC

PENETRATION PARAMETER, $\frac{X_p}{D_{ox}} \simeq 0.1$

(NOTE: FLOWRATES AND $\frac{X_p}{D_{ox}}$ DO NOT REPRESENT REAL OPERATING RANGE)

NOTE SOME OVERSIZED DROPLETS DUE TO FILM FLOW ON CUP WALL

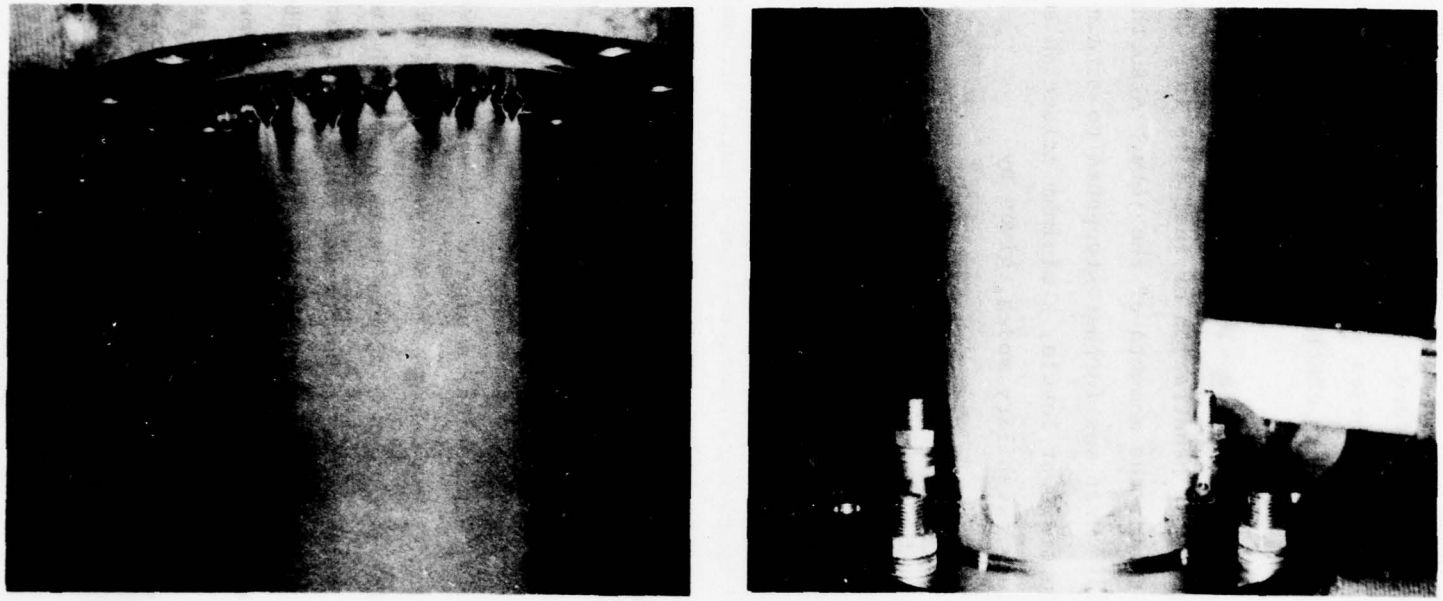

Figure 89. Comparison of Fan Characteristics Without and With Premix-Cup (No. 1)

FUEL SIMULANT: WATER @ 0.096 LBM/SEC

OXIDIZER SIMULANT: GN_2 @ 0.024 LBM/SEC

PENTRATION PARAMETERS, $\frac{X_p}{D_{ox}} \simeq 0.26$

(NOTE: FLOWRATES ARE FAR LOWER THAN REAL OPERATING RANGE)

NOTE SOME OVERSIZED DROPLETS DUE TO FILM FLOW ON CUP WALL

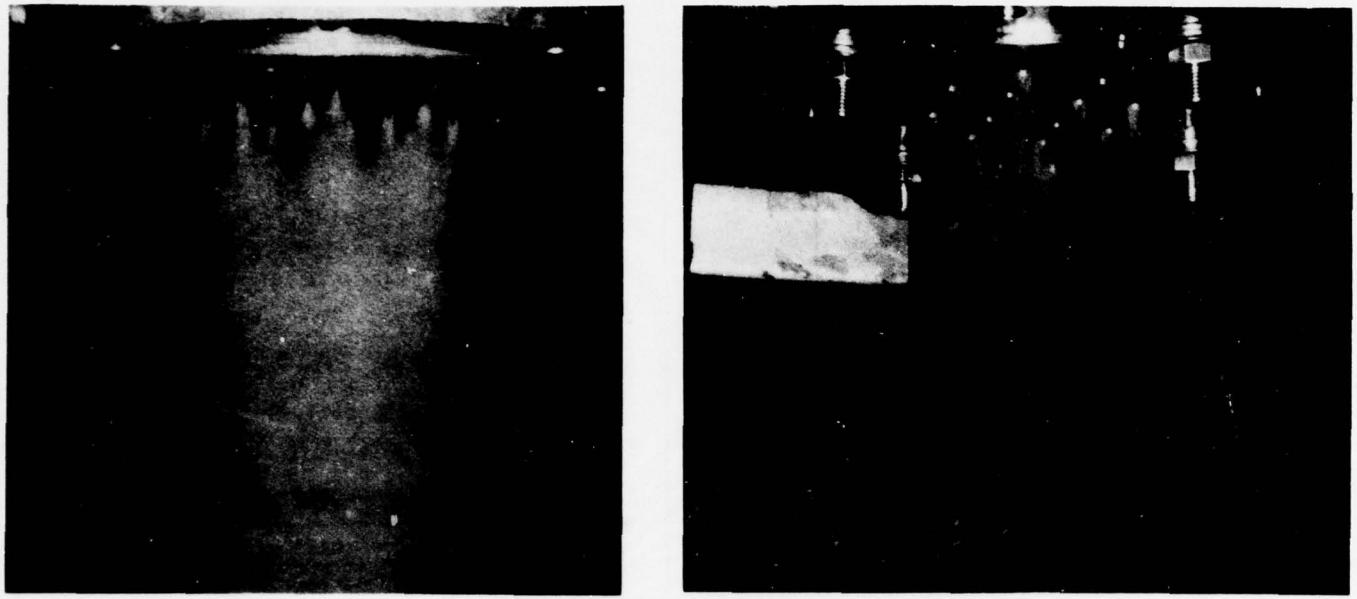

Figure 90. Comparison of Fan Characteristics Without and With Premix-Cup (No. 1)

TABLE 18. TEST MATRIX, MODIFIED HIGH-POWER GAS GENERATOR TESTS

Test Case	Test Objective	Hardware Configuration				Test Condition	
		Premixer Plate	Chamber Sleeve	Fuel Line Rework	Elements Rework	Power Level	Mixture Ratio
I	• To suppress fuel flow overshoot • Reduction of recirculation zone • To suppress initial chugging		✓ (Partial)	✓		Low Normal	0.55
II	• Ramp fuel priming • Uniform mixture • Stable combustion at low-power level start • Prevent coking at orifices	✓		✓		Low Normal	
III	• Low-power level start • Reduced box injection velocity for better mixing	✓		✓	✓	Low Normal	
IV	• High wall temperature for reduced carbon buildup	✓	✓ (Full)	✓	✓	Low Normal	
V	• Suppress low-frequency blow-down-type chugging • High-wall temperature for reduced carbon buildup	✓	✓ (1/2 volume plug)	✓	✓	Low Normal	

Partial Sleeve Testing. Three tests were made at normal power level and two tests at 75% of normal power level. Each duration was kept short, at approximately 1 second, to minimize shock loading in the gas generator that might have occurred as a result of prolonged unstable combustion. Except for the first test (26.04) when purge gas was left on, ignition was followed by a series of flameouts and reignitions, and mainstage combustion was never obtained. Typical data traces for these tests are shown in Fig. 91.

Premix-Cup Plate Testing. The premix-cup test series were made to evaluate the effect of added mixing of fuel and oxidizer in the cups and the potential improvement at low-power level operation. Three tests at normal power level and two tests at 75% of normal power level were conducted (with the thin premix-cup plate). Repeat tests were made to verify reproducibility of the results. The premix-cup plate was found to produce good ignition and stable mainstage combustion at normal power level operation. At 75% of normal power level, unstable ignition transients were encountered, but stable mainstage combustion was achieved and shown by the two typical data traces in Fig. 92. The thin plate displayed threshold start capability at ~75% power level operation while showing the tendency of better ignition transient at higher mixture ratios. Hence, the test cases were expanded to investigate the effect of mixture ratio involving both premix-cup plate configurations.

At normal power level operation, the combustion characteristics at ignition were found almost identical with either premix-cup plates, while the test results at 75% power level operation showed improvement with the thick premix-cup plate as shown in Fig. 93 and 94. However, neither premix-cup plate provided stable mainstage combustion at 50% power level.

Reworked GOX-Orifice Testing. The injector GOX-orifice was remachined to enlarge the orifice diameter from0.067 to 0.0955 inch (see Rework No. 1, Fig. 88). As a result of the larger flow area, the GOX injection velocity was reduced by almost a factor of three, from a Mach

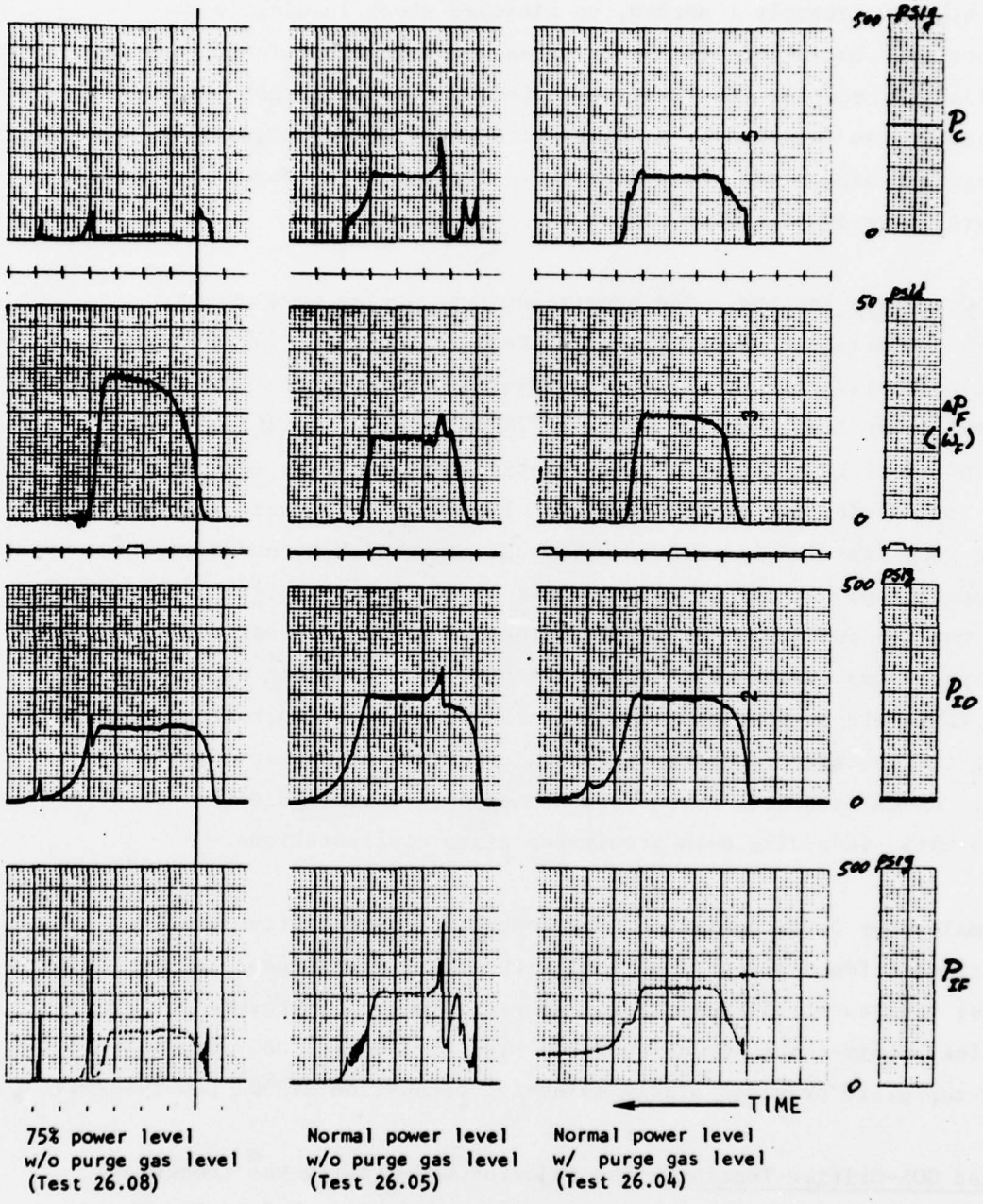

Figure 91. Ignition Diagnostics With Partial Sleeve Configuration

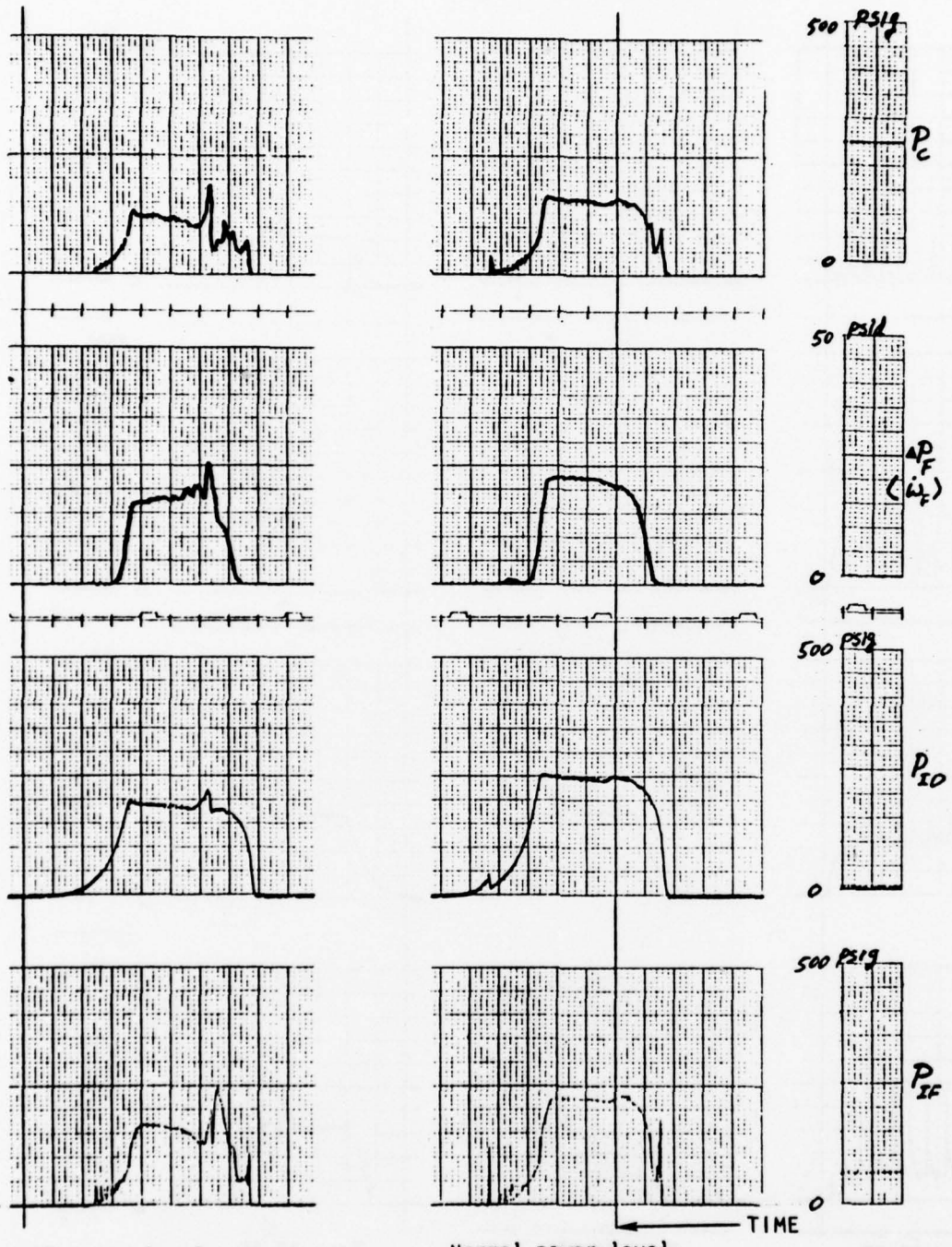

75% power level
w/o purge gas level
(Test 27.04)

Normal power level
w/o purge gas level
(Test 27.03)

Figure 92. Ignition Diagnostics With Thin Premix-Cup Plate

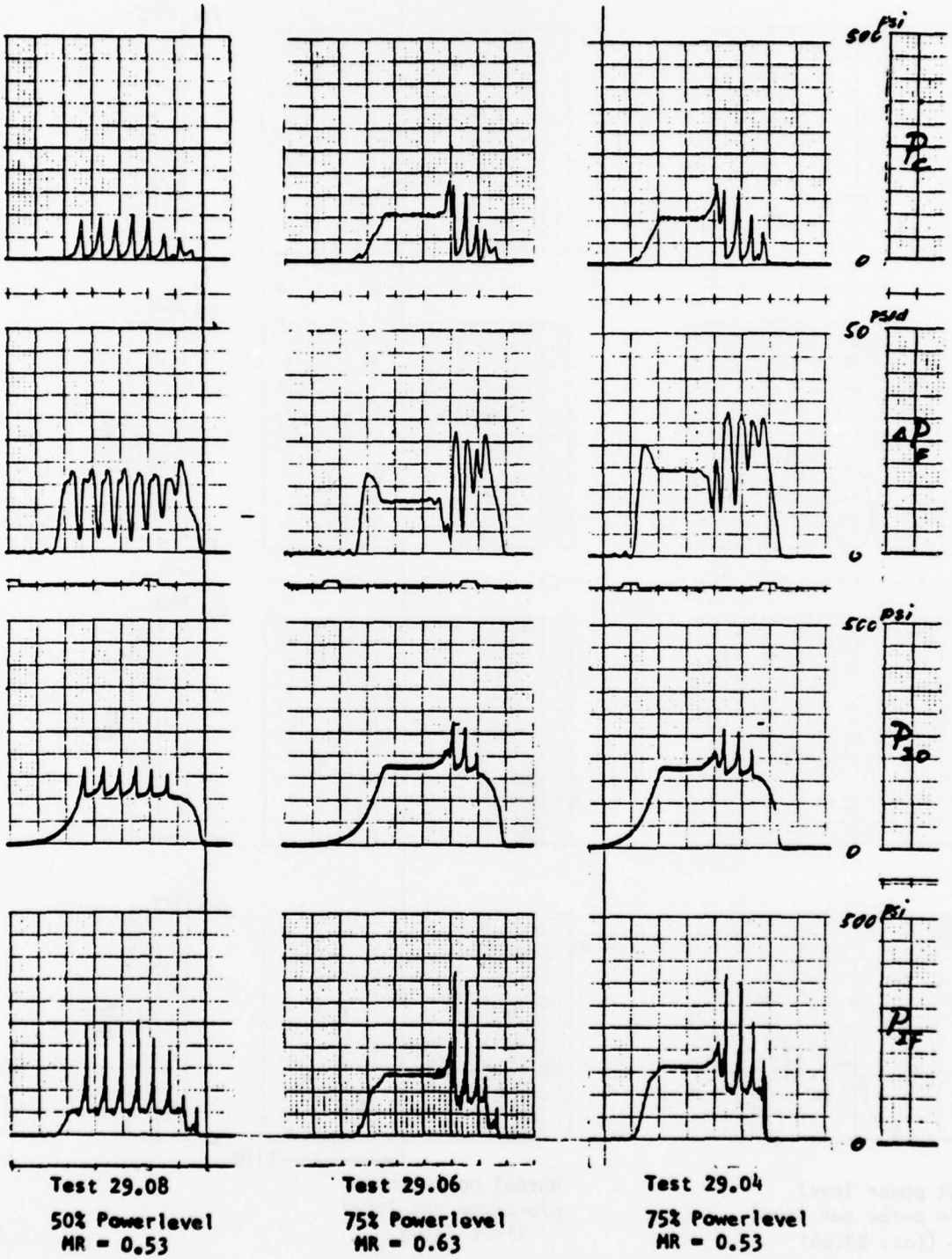

Figure 93. Typical Test Results of Thin Premix-Cup Plate

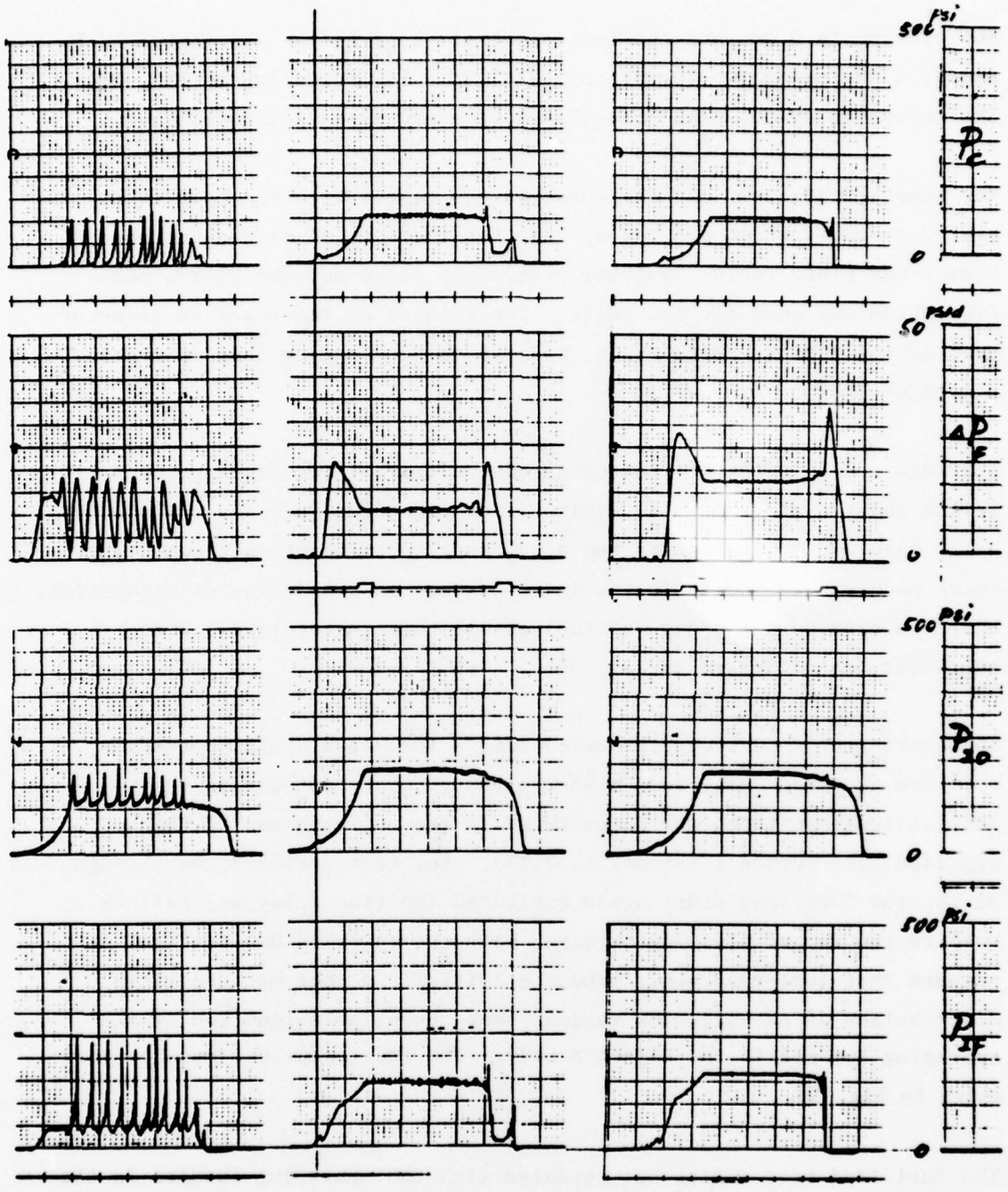

Figure 94. Typical Test Results of Thick Premix-Cup Plate

No. of 0.80 to 0.30, and the fuel penetration parameter was increased by almost a factor of two (0.186 to 0.330) at a low power level (Fig. 88). The injection ΔP for both propellants remained essentially unchanged.

The reworked GOX-orifice configuration was tested with the same test procedure and test conditions as that for the partial sleeve and the premix-cup plate tests. Neither premix-cup plate nor the sleeve configuration was used for the tests. The results of the reworked injector test series are discussed below, and typical combustion characteristics are shown in Fig. 95 through 97.

The reworked injector was tested extensively examining three power levels and two mixture ratio limits. The first test series consisted of a 150 msec GOX-lead at start and a 100 msec fuel lag at shutdown. The spark plug was installed in the injector body as a baseline configuration. The resulting performances obtained at all three power levels were excellent, as indicated in Fig. 95.

The above test series were repeated with a fuel-lead start to examine both the ignition delay and chamber pressure overshoot during the initial ignition transient encountered in the early phases of the upgraded test series (test series 7.XX). For test series 31.01 through 31.14, the fuel-lead start again exhibited ignition delay and failure. Despite the improved mixing obtained with the reworked GOX orifice, it appears that fuel-lead start produced initially a poor mixture ratio distribution at the injector region, hence unreliable ignition by the sparkplug located in the injector body. The fuel-lead test results are shown in Fig. 96.

The fuel-lead test series was repeated with the sparkplug located in the wafer, which essentially consisted of a spark source firing from the combustor wall 1 inch downstream from the injector face. As seen in Fig. 97, successful ignition and stable combustion were obtained at the two lower power levels of 50 and 75%. Some ignition delay was encountered

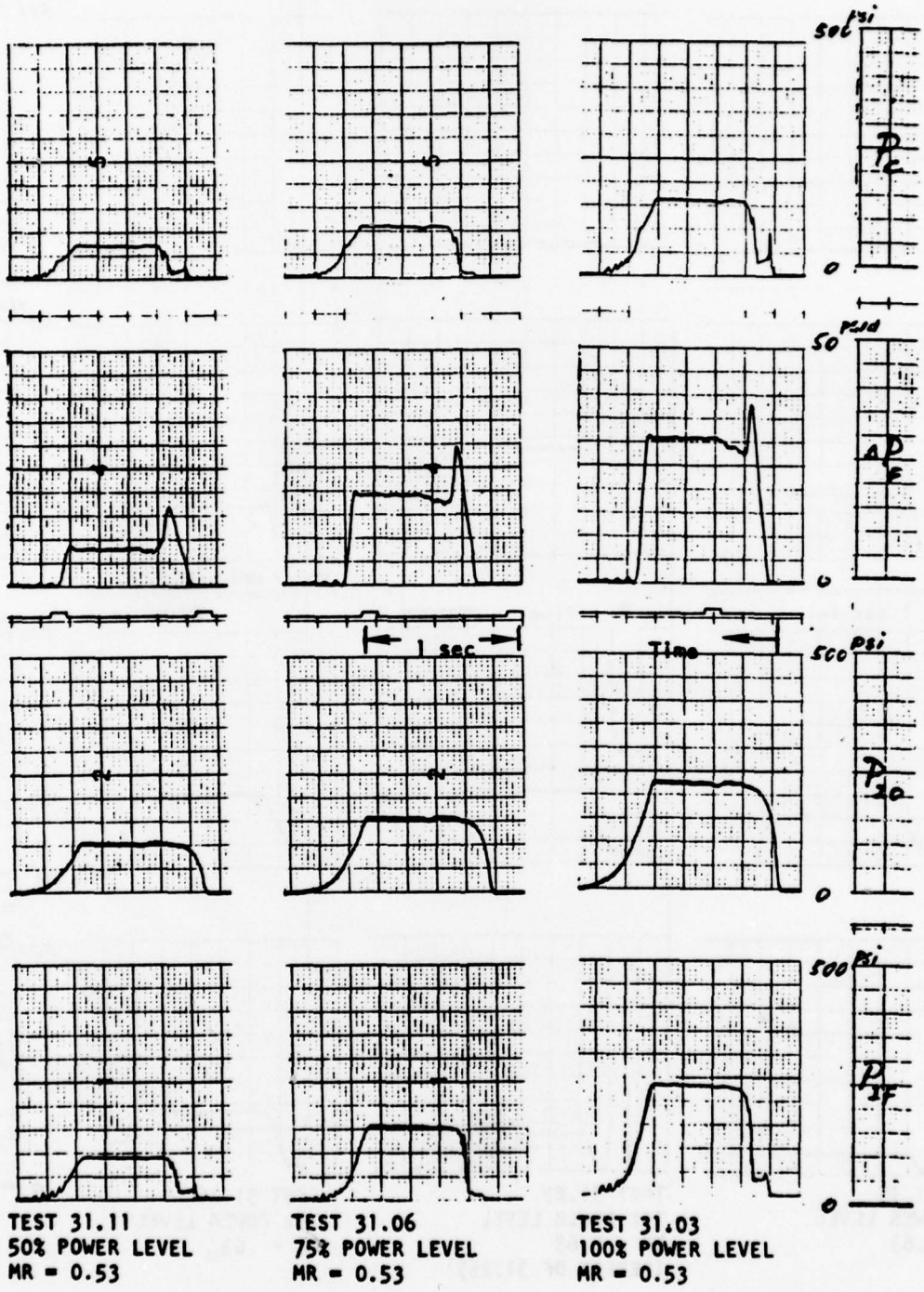

Figure 95. Reworked GOX Orifice Tests With GOX-Lead Start (Spark Plug at Injector)

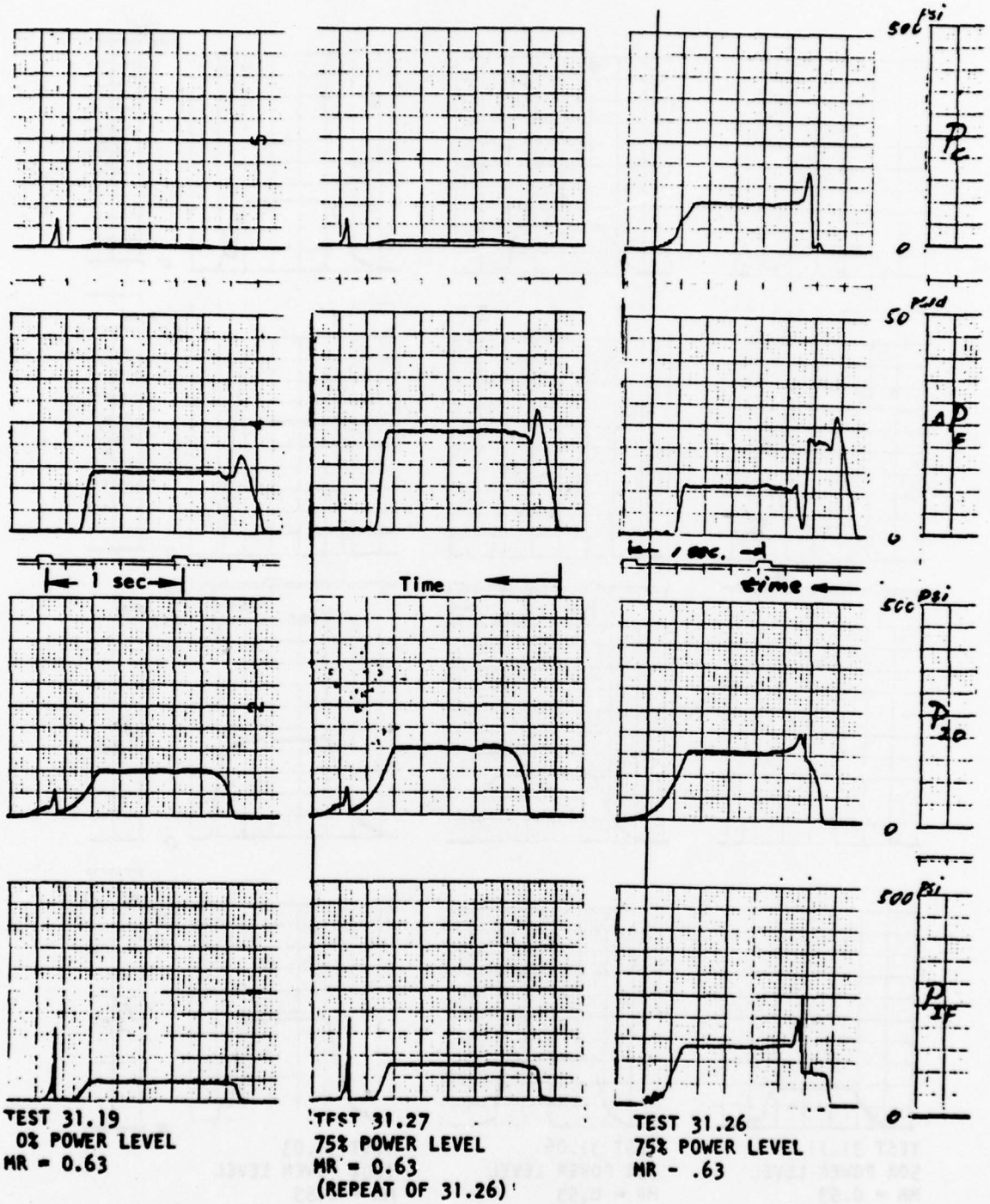

Figure 96. Reworked GOX Orifice With Fuel-Lead Start (Spark Plug at Injector)

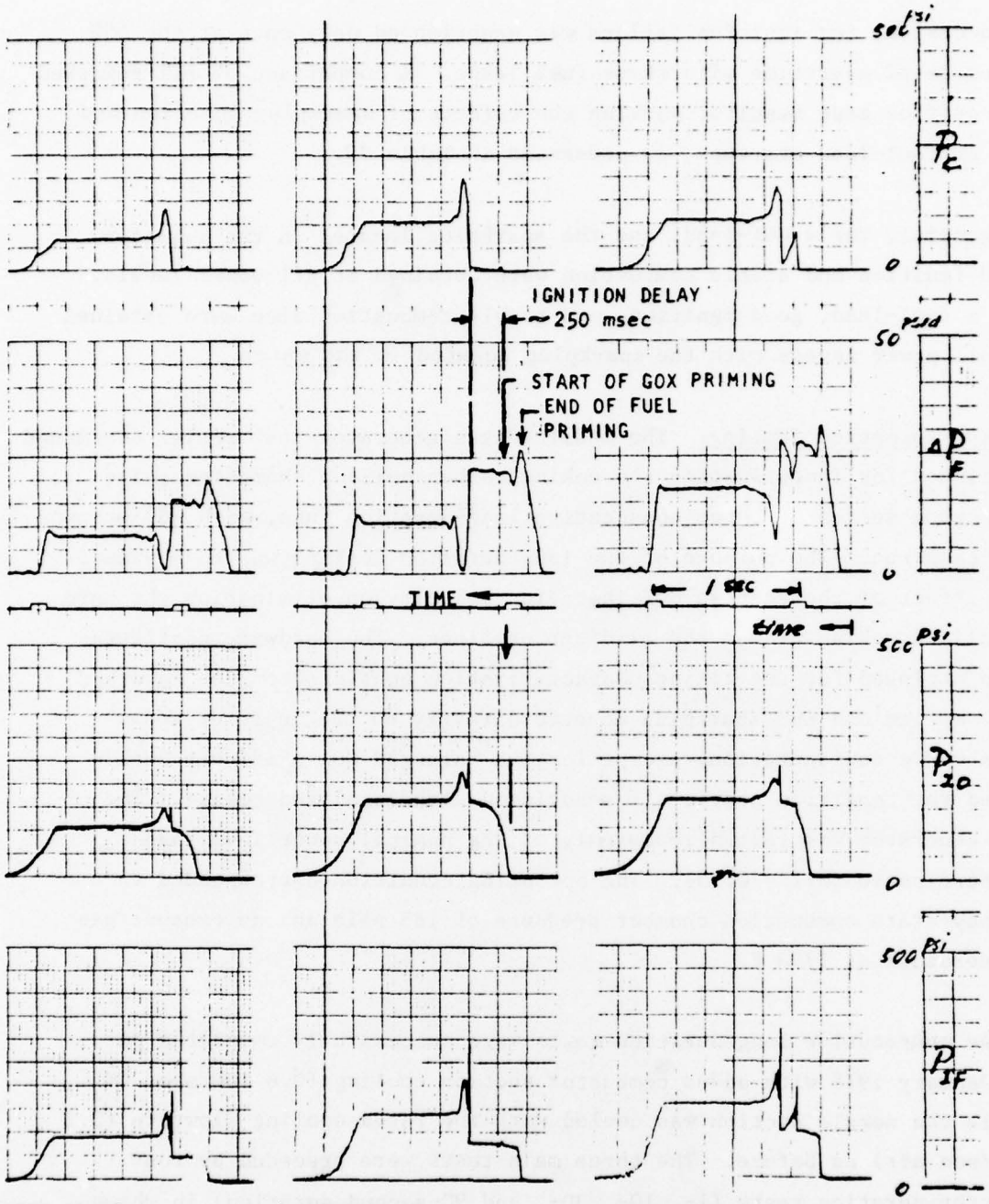

TEST 32.06
50% POWER LEVEL
MR = 0.53

TEST 32.03
75% POWER LEVEL
MR = 0.63

TEST 32.01
75% POWER LEVEL
MR = 0.53

Figure 97. Reworked GOX Orifice Tests With Fuel-Lead Start (Spark Plug at Wafer)

on occasion, and ignition failure was experienced only once at the 50% power level operation with these fuel leads. A comparison of all reworked GOX orifice test results, showing the effects of sparkplug location and GOX or fuel-lead startups, is presented in Table 19.

In general, for a GOX-lead, and the sparkplug located in the injector, good ignition and stable combustion were obtained at all power levels. For a fuel-lead, good ignition and stable combustion also were obtained at all power levels with the sparkplug located in the wafer.

Carbon Formation Testing. The modified gas generator test series continued continued for investigating the coking/carbon buildup characteristics through a series of three consecutive long-duration runs, with 180 seconds for each run. The purpose of the long-duration testing was to evaluate the effect of the reduced GOX injection velocity on eliminating the hard localized coking around the oxidizer orifices. The hardware configuration employed for the coking characterization consisted of the reworked GOX orifice and the sparkplug mounted directly on the injector body. This basic configuration, except for the enlarged GOX orifices, duplicated the condition previously associated with localized coking. The gas generator was tested repeatedly at the nominal power level and mixture ratio (o/f = 0.55). The operating condition corresponded to a steady-state combustion chamber pressure of 185 psia and an exhaust gas temperature of 1700 F.

Three consecutive long-duration tests were successfully completed on 24 January 1978 with added combustor section cooling (0.6 lbm/sec, GN_2), while the nozzle section was cooled with the rated cooling flowrate (0.2 lbm/sec air) as before. The three main tests were preceded by four shorter-duration tests (1-, 10-, 30-, and 90-second duration) in which the combustor wall hot spots were found to be established after the 30-second run. The carbon buildup at the injector face was not disturbed through the three main tests. The combustor carbon buildup was partially removed after the first 180-second run to examine the wall surface, but

TABLE 19. HIGH-POWER GAS GENERATOR TEST SUMMARY REWORKED GOX ORIFICE
(Test Series 31.00 to 33.00)

Power Level %	No. Test	GOX Lead (150 msec)	Fuel Lead (100 msec)	Spark Plug		Results		
				Injector	Wafer	Ignition Delay	Good Ignition	Stable Combustion
100	4	X	-	X	-	-	X	X
75	5	X	-	X	-	-	X	X
50	4	X	-	X	-	-	X	X
100	4	-	X	X	-	-	X	X
75	5	-	X	X	-	X	X*	X*
50	5	-	X	X	-	X	X**	X**
100	1	-	X		X	X	X	X
75	4	-	X		X	X	X	X
50	7	-	X		X	X	X***	X***

* One test at high mixture ratio (MR≅0.63) resulted in stable combustion.

** Two tests at high mixture ratios (MR~0.63) resulted in good ignition and stable combustion.

*** One test resulted in ignition failure.

left undisturbed in the two consecutive runs. Significant results were that (1) GOX injector orifices no longer showed hard coking, and (2) carbon buildup at the injector and chamber wall was soft, readily crumbled at fingertip touch, and reached a steady-state thickness similar to the long-duration test. The carbon was removed for posttest inspection, and no evidence of progressive damage to the combustor wall was observed (Fig. 98).

The gas generator sustained minor damage in two separate incidents, but was repaired and returned to service after each incident to complete the scheduled three long-duration tests. The first incident occurred as the result of fuel-depletion at the facility fuel tank during the first of the three scheduled runs, and inadvertent lean fuel condition existed for 5 seconds prior to the cutoff. The second incident occurred near the end of the first 180-second run resulting in one localized burnthrough of the combustor wall. The burnthrough was found to be 1 inch from the injector face, about halfway between the two outboard injector elements adjacent to the injector GOX inlet.

The combustor wall also revealed five additional hot spots or stains that were found within 2 inches from injector and situated again halfway between the elements. These spots, including the eroded spot, were found at four places forming four corners equidistant apart. The cause was attributed to the formation of four strong oxidizer fans resulting from the four injector inner ring fans merging with and reinforcing the adjacent outer ring oxidizer fans. It was concluded that the GN_2 coolant flowrate of 0.2 lbm/sec, equivalent to oxidizer flowrate at the normal power level operation, was marginal to prevent localized heating. A water-flow test of the injector showed no blockage of the orifices near the burnthrough area.

Extended Testing. The high-power gas generator test series was extended to evaluate the premix cup plate with the modified injector to further reduce carbon formation and eliminate the localized combustor

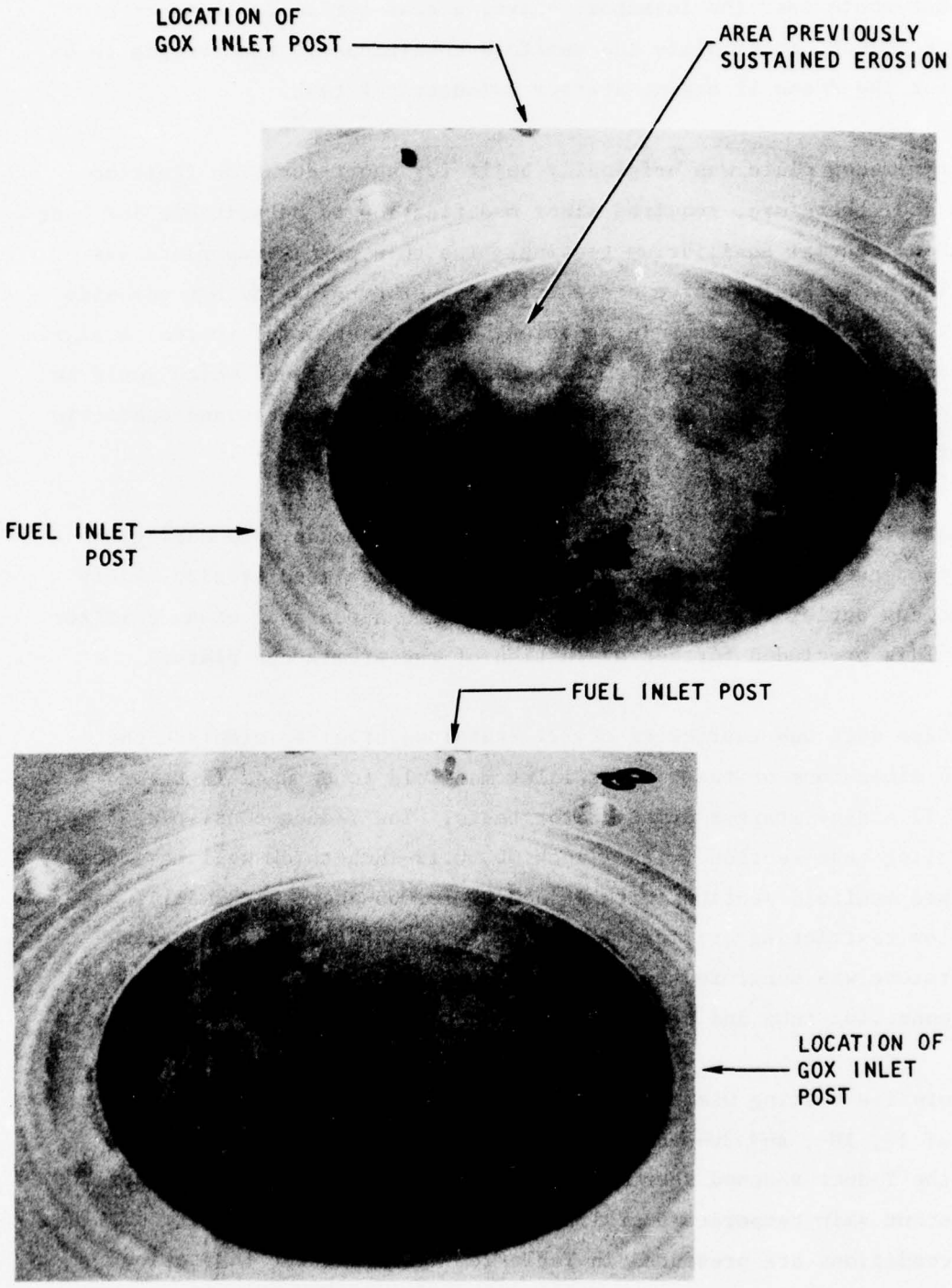

Figure 98. Posttest Combustor Wall Condition-Carbon Removed

wall hot spots near the injector. Also, a test series was conducted using a Y-duct, to simulate the manifold conditions of the turbine to be used for the Phase II engine starter demonstrator task.

The premix-cup plate was originally built for short-duration ignition tests and, therefore, required minor modification to be suitable for long-duration, thermal equilibrium testing. The thin premix-cup plate was modified by machining three concentric ring grooves on the hot-gas-side face to prevent buckling. In addition, a two-dimensional thermal analysis was conducted to determine the plate temperature response which would be monitored by a thermocouple positioned at the midthickness and geometric center of three cups.

Two hot-fire tests were conducted for 2 and 10 seconds, and during the 10-second run, the premix-cup plate sustained localized erosion mainly at the cup outlet region. The erosion had the appearance of an oxidizer fan. This precluded further evaluation of the premix-cup plate.

A Y-shape duct was fabricated of 321 stainless steel to simulate the design dimensions of the turbine inlet manifold to be used in the Phase II engine starter demonstrator tests. The Y-duct consisted of a connecting tube section (with 1-inch OD, 0.12-inch-thick wall thickness), U-shaped manifold section (with 1-inch OD, 0.065-inch-thick wall), and two flow restricting orifices in place of turbine nozzles. The skin temperature was monitored by a thermocouple located at the junction of the connecting tube and U-duct.

The hot-fire testing was then performed at normal power level in three runs of 1-, 10-, and 30-second duration. The 30-second test showed that the Y-duct reached thermal equilibrium in 10 seconds and maintained a constant skin temperature of 1750 F through the remaining period. The test conditions are presented in Table 20. The posttest inspection revealed no visible hardware discrepancies except the color change at the duct skin. Inspection of the gas generator hardware interior showed

little carbon buildup and a nearly bare surface appearance at the uncooled Y-duct nozzles. The carbon buildup elsewhere appeared comparable to the observations made in other earlier tests.

TABLE 20. HIGH-POWER GAS GENERATOR TESTED AT DEMONSTRATOR CONDITIONS

	Tested 2/10/78
Flowrate, lb/sec	0.54
Combustor Pressure, psia	215
Mixture Ratio (o/f)	0.56
Combustion Temperature, F	1750
Duration, seconds	30
GN_2 Coolant Flowrate, lb/sec	0.6
Discharge Duct	Simulated Manifold

PHASE I ASSESSMENT

The IPU gas generators have been tested over a range of mixture ratio and throttle limits. Both the low- and high-power gas generators demonstrated a high combustion performance with all c* efficiencies greater than 90%, and with the measured combustion temperatures correlating very well with the predicted equilibrium values. These combustion performance parameters were found to differ very little for the three types of injectors tested with the low-power gas generator. This was due primarily to the large flow residence time in the low-power gas generator combustion chamber. The selection of the triplet-element injector for the high-power gas generator, therefore, was based on overall merits such as best hardware integrity and unifrom carbon buildup characteritistics demonstrated through a number of long-duration tests.

The start transient, i.e., transition from ignition to stable mainstage combustion, was found to be the area needing greatest development in the operation of both gas generators. Mainstage combustion generally showed excellent stability. Much of the test effort was directed to the ignition diagnostics with extensive variation of the operating parameters such as spark energy level, sparkplug position, combustion chamber length, power level, mixture ratio, etc. The major findings related to the ignition performance are:

1. Effect of combustor length was most apparent with the coaxial-element injector, with reliable ignition requiring an appropriate longer chamber length.

2. The triplet-element injector was relatively insensitive to the chamber length, but initially encountered ignition problems at low-power-level operation of the high-power gas generator. The cause was traced to excessive oxidizer injection velocity and a mismatch of fuel and oxidizer jet momentum at the throttled conditions. The problem was resolved by enlargement of the oxidizer orifices, which reduced the oxidizer injection velocity as well as the post-impingement fuel/oxidizer mixture.

3. Spark operation, with energy levels varied from 250 milijoules up to 2 joules and pulse frequencies up to 50 cps, had no significant influence on ignition. However, some improvement was possible with the use of higher spark energies for test conditions which otherwise would have resulted in ignition failure. In general, the spark energy level of 250 milijoules and spark frequency of 50 cps were found to be sufficient for good ignition over the entire range from ambient to cold propellant temperatures considered. However, lower energy levels, 70 to 90 milijoules, were adequate for ambient-temperature propellants.

4. The order of propellant priming was found to result in marked differences in ignition transients. With all other test conditions being equal, the oxidizer-lead priming displayed consistently better ignition. The fuel-lead priming involved finite ignition delays (100 to ~240 msec) and chamber pressure overshoots at ignition. The ignition for the fuel-lead priming was also sensitive to the sparkplug position, being better at the side-wall mount position than the injector mount position. The oxidizer-lead priming resulted in rapid ignition regardless of the sparkplug location.

The carbon buildup at the combustor wall and the injector face displayed a replenishing behavior, generally growing to 3 to 5 mm in thickness as a steady-state limit, but with some localized heavier buildup. The heavier accumulation of carbon at the nozzle converging section, found during tests with the original triplet-element injector, moved closer to the injector after the oxidizer orifice rework. Furthermore, the carbon buildup on the downstream surfaces appeared thin and uniform.

The combustor heat fluxes determined from the coolant temperature rise under the influence of steady-state carbon buildup at the hot-gas side wall indicated that the low-power gas generator could serve as a heat exchanger for LOX gasification, whereas the high-power gas generator would require augmentation from a separate heat exchanger of approximately the same size as the gas generator.

Purge-Free Operation

During the low-power and high-power gas generator testing, a helium gas purge of the injector manifold was used before and after hot firing. This is a standard test procedure used in gas generator development testing to keep the feed system downstream of the main control valves free of residual fuel or combustible gaseous mixture. The purge valve control was sequenced and interlocked with the main valve control sequencing.

In the modified high-power, gas generator test series, a high-level, helium gas purge was used in an exploratory study to improve ignition by better atomization of fuel and early mixing with the gaseous oxygen already in the chamber. As part of the start transient, the purge control valve was opened by the oxidizer valve open command signal 100 msec prior to fuel valve opening, and the purge gas flow was checked off by the fuel injection pressure rise as the injector manifold became primed.

Since purge-free operation is a feature of the IPU system, this mode of operation was demonstrated in a rapid, pulse-mode firing of the low-power gas generator under an IR&D program. For this test, the facility feed system was modified to obtain maximum close coupling between the injector and main control valves. A flight-type system would have a significantly closer coupling than could be achieved with facility hardware. As a facility precaution, purge was used only as a pretest and posttest checkout where purge gas injection was controlled by a check valve in both the fuel side and oxidizer side, which were opened and checked off by propellant pressures. Backup control valves also were installed and interlocked with the main valve control sequence to preclude accidental backflow of propellants into the feed system in the event of a leaking check valve.

The pulse-mode test firing of the low-power gas generator was conducted in a series of nominal 4-second-on duration followed by a 1-second-off duration. A total of five consecutive pulses were made without using a purge between pulses during the "off" period. As shown in Fig. 99, each hot-firing pulse attained rapid, stable mainstage operation reliably, and reproducibility of the pulse, without between-pulse purge, was excellent.

Cold Gas Generator Startup

Prior to hot gas generator operation, the only heat source for gasifying the liquid oxygen to obtain GOX at the injector is the residual heat

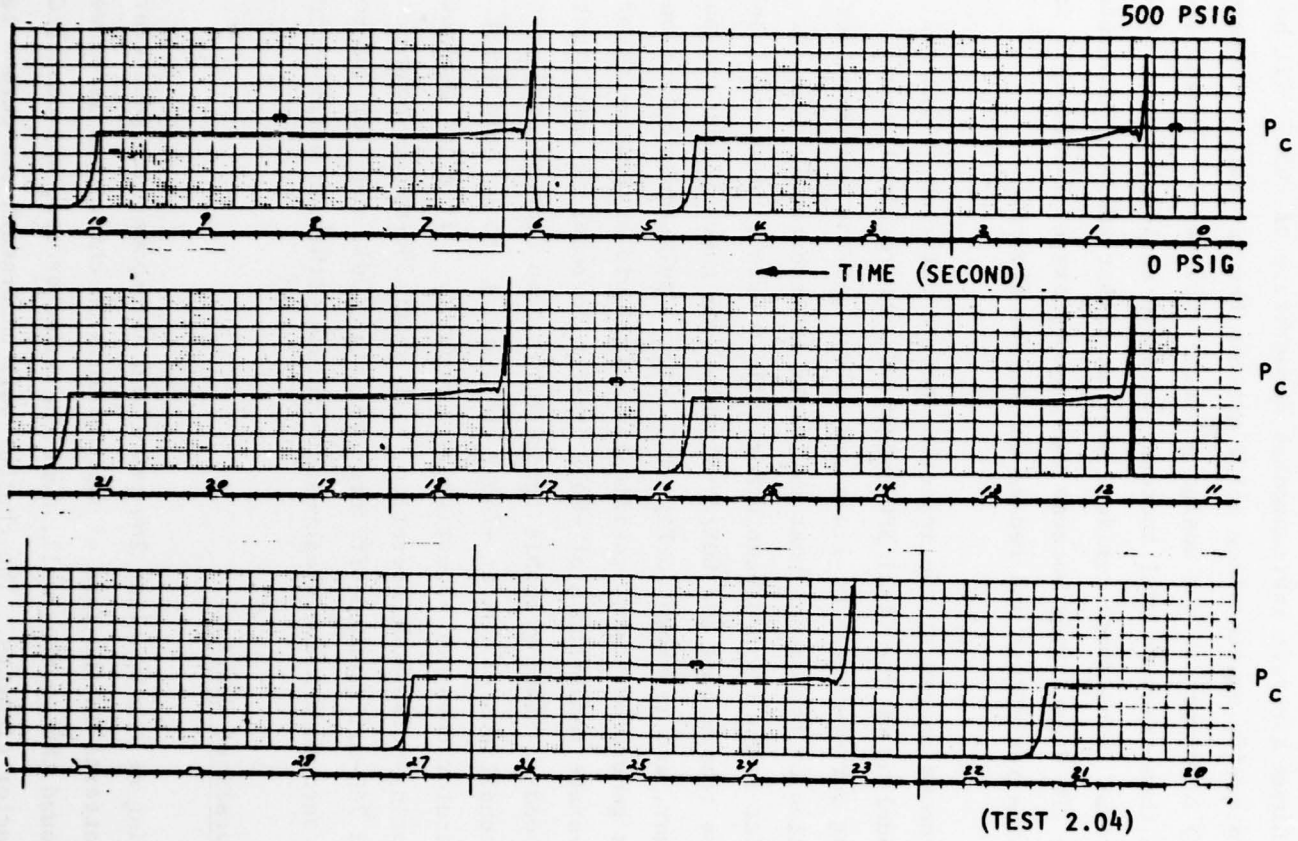

Figure 99. P_c Purge-Free, Pulse-Mode, Low-Power Gas Generator Test

contained in the IPU hardware, such as oxidizer line, valves, and heat exchanger. Preliminary analyses indicate that residual heat in the IPU system at minimum aircraft environmental temperature of -65 F will be sufficient to gasify oxygen since -65 F exceeds the saturation temperature (-210 F) of oxygen at the design pressure (290 psia). Longer line lengths than those assumed will increase hardware residual heat. However an increase in hardware residual heat at higher ambient temperatures may increase IPU start times because the gaseous oxygen formed will increase the line resistance and reduce the oxygen flowrate.

To ensure gaseous oxygen at the injector face, a detailed analytical transient modeling of the final IPU system will be required, where corresponding surface areas of lines and valves and the heat transfer characteristics of the oxygen heat exchanger are accurately modeled. A system similar to the IPU has been dynamically modeled, using -65 F initial hardware temperature and GOX/JP-4 combustion gases in the oxygen heat exchanger, and is shown in Fig. 100. for a pulse-mode operation. Prior to gas generator start, gasification of liquid oxygen to GOX at near steady-state temperature of -80 F is seen to occur in approximately 200 milliseconds. Since reliable ignition has been demonstrated at cold propellant conditions of GOX at -240 F and fuel at -65 F, cold start of the gas generator does not appear to be a problem. After gas generator start and during pulse-mode operation, with short 250-millisecond-on duration and 250-millisecond-off duration (Fig. 100), injector GOX temperature is seen to achieve steady-state values within 80 milliseconds.

Combustor Localized Heating

During testing of the baseline low-power and high-power gas generators, injection patterns in the form of fan imprints on the carbon layer were observed around the chamber wall, near the injector end, and centered between injector elements. The chamber wall underneath the carbon layer showed little sign of distress and posed no problem to the long-term hardware integrity at the nominal chamber coolant (GN_2) flowrate.

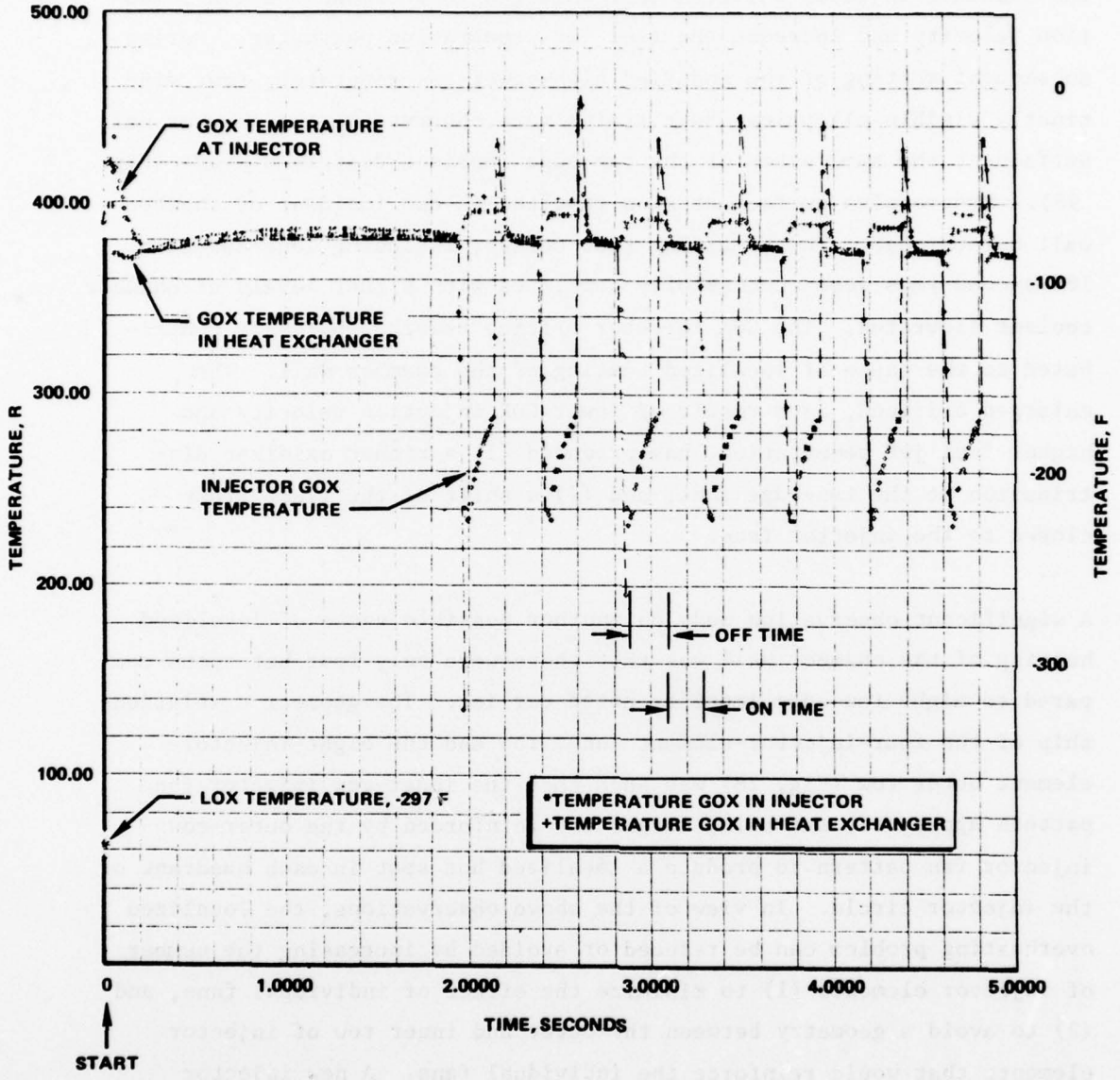

Figure 100. Typical Injector GOX Temperature Response With -65F Initial Hardware Temperature

To improve low-power-level performance of the high-power gas generator, the oxidizer injector orifices were enlarged to decrease the GOX injection velocity and increase the fuel jet penetration parameter. During subsequent testing of the modified high-power gas generator, four distinctly visible elliptical heat stains were observed on the chamber wall surface at the same sites of the fan-edge imprints described above (Fig. 98). Progressive surface erosion resulted in one incident of chamber wall burnthrough. The remaining test series, including long-duration, 180-second runs were successfully completed with higher levels of chamber coolant flowrates. The GOX injector orifice rework apparently contributed to the cause of localized heating of the chamber wall. The enlarged orificed, as a result of lower GOX injection velocity and higher fuel jet penetration, has produced (1) a richer oxidizer distribution at the fan-edge zone, and (2) a shift of the flame front closer to the injector face.

A significant observation made on another possible cause of localized heating of the chamber wall was that there were only four hot spots compared to eight fan-edge imprints noted earlier. The geometric relationship of the four-injector-element inner row and the eight-injector-element outer row (Fig. 28) was such that the inner-row injector fan pattern apparently was being merged and reinforced by the outer-row injector fan pattern to produce a localized hot spot in each quadrant of the injector circle. In view of the above observations, the localized overheating problem can be reduced or avoided by increasing the number of injector elements (1) to minimize the effect of individual fans, and (2) to avoid a geometry between the outer and inner row of injector elements that would reinforce the individual fans. A new injector design with 18 triplet elements distributed in two concentric rows, with 6 elements in the inner row and 12 elements in the outer row is shown in Fig. 101. Despite a reduction of element size by approximately 40%, the injector pressure drop still has sufficient margin to avoid feed-system-coupled combustion instability, and adequate penetration parameter for atomizing the fuel stream and uniform mixing with the oxidizer.

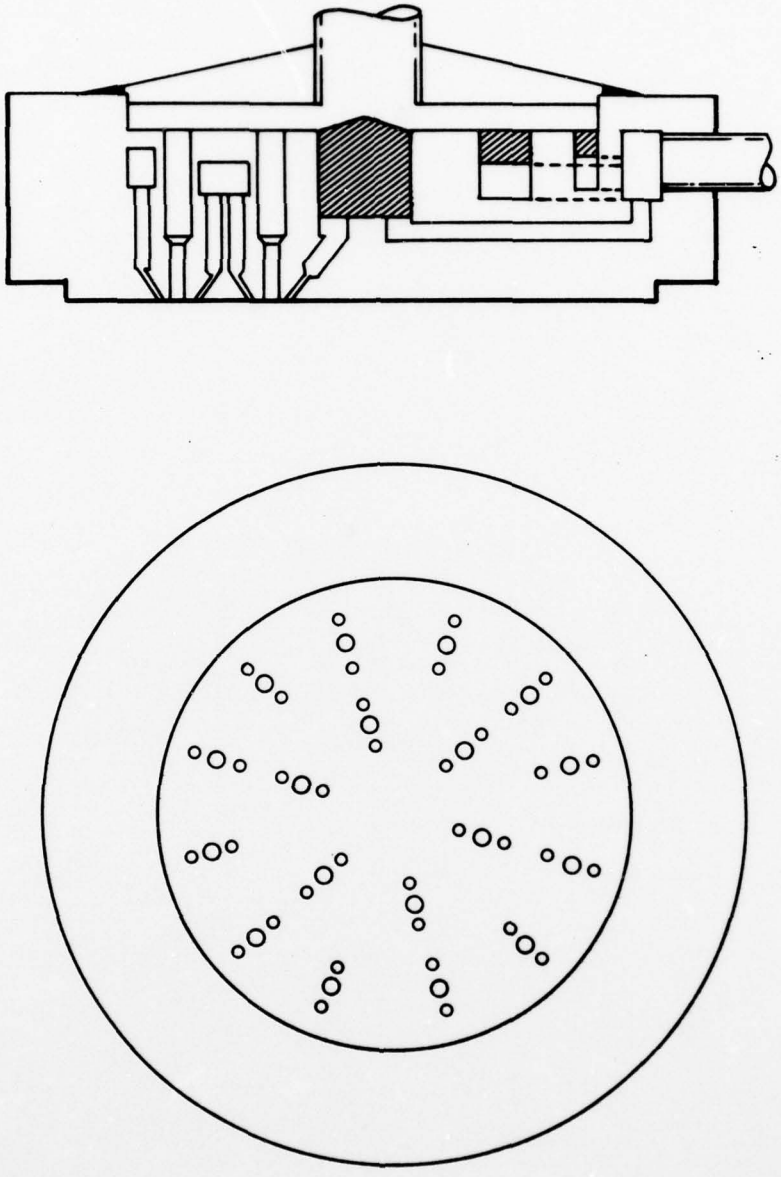

Figure 101. New High-Power Gas Generator 18-Element Injector Design

PHASE II IPU ENGINE STARTER DEMONSTRATOR

The objectives of Phase II are (1) to identify critical component tests required to demonstrate the feasibility of operating an IPU as a complete system, and (2) to fabricate a breadboard ground demonstrator system and perform systems tests to demonstrate IPU operation. The test resutls and hardware in Phase I are used to accomplish these objectives.

The most appropriate IPU system is an aircraft-type engine starter which can be simulated by a demonstrator built by using the high-power gas generator and existing power turbine and gearbox. The aircraft engine is simulated by an existing flywheel system. This section describes the design, fabrication, and test of the IPU engine starter demonstrator system. Facility propellant feed system and controls were used with the demonstrator.

ENGINE START REQUIREMENTS

Three current aircraft engines were evaluated for simulation, and these are: JT8D-209, TF33-P-7, and CFM56-28. Basic characteristics of these engines are given in Table 21. The stored energy in the engine is the kinetic energy of the engine rotating assembly at the speed at which the starter cuts out. This is a rough indication of the relative starter power requirements. A better indication, however, is the starter power delivered at the cutout speed. This represents the size of a starter required to accelerate the engine, with its inertia and drag torque, to the engine idle speed in 36 seconds. The starter cuts out at a speed slightly below the engine idle speed.

TABLE 21. IPU/STARTER REQUIREMENTS KC-135 RE-ENGINE PROGRAM

Engine Designation	JT8D-209	TF33-P-7	CFM56-2B
Engine Stored Energy at Starter Cutoff, lb-ft	1.294×10^6	1.777×10^6	3.210×10^6
Starter Power at Cutout, hp	107	104	194

The start power requirement of the CFM56-2B matched the capability of the high-power gas generator most closely and was therefore selected for simulation with the starter demonstrator. The predicted start characteristics of this engine with an IPU starter is shown in Fig. 102. The starter is sized for starting this engine at -40 F since this represents the worst drag torque/condition on the engine. The engine is seen to reach idle speed in just under 36 seconds. At higher ambient temperatures, the engine would reach idle speed in less than 36 seconds.

A starter demonstrator to match the CFM56-2B, therefore, must have a delivered shaft power at starter cutout at approximately 200 hp. The stored energy in the inertial flywheel simulator at that cutout speed must be at least equal to that stored by the engine at starter cutout. These were the basic requirements for the design of the demonstrator design.

DEMONSTRATOR ASSEMBLY

The design of the IPU engine starter demonstrator makes use of existing hardware for all major components like the gas generator, turbine, gearbox, and a flywheel load simulator, integrated into a simple skid-mounted test assembly.

The gas generator for the engine starter is the final configuration of the high-power gas generator tested during the end of Phase I. The turbine was assembled from major parts of an existing Rocketdyne Mark 44F turbopump. A gearbox was obtained from Alturdyne, Inc., of San Diego, California. An existing Rocketdyne flywheel assembly was modified to duplicate the inertial load of the CFM5-2B engine. These existing components were used to comprise a breadboard system and, therefore, do not reflect an optimized system.

Figure 103 shows the design layout for the demonstrator showing cross sections of all the major components and their installation in a

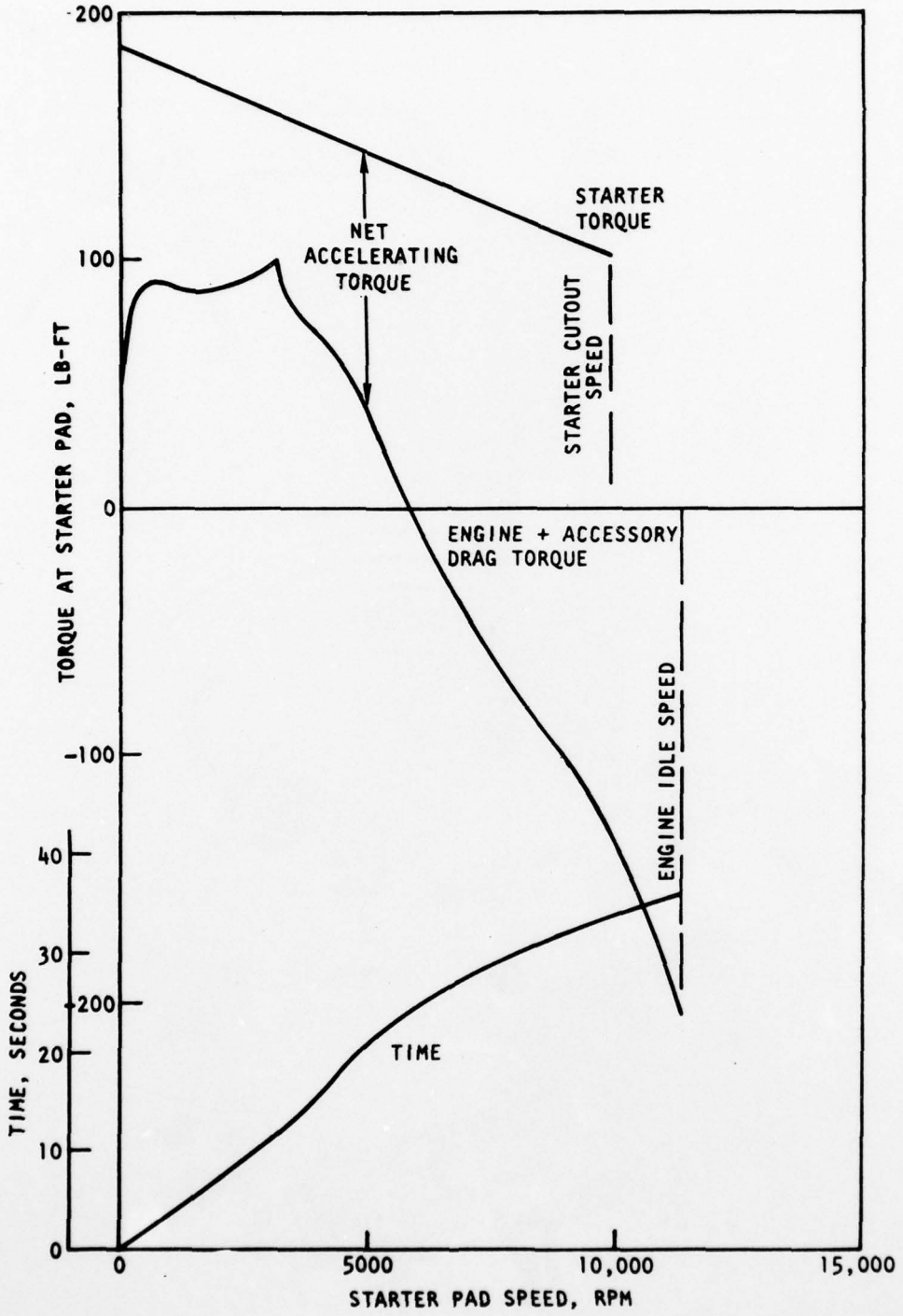

Figure 102. Start Characteristics of CFM56-2B Engine at -40 F With IPU Starter

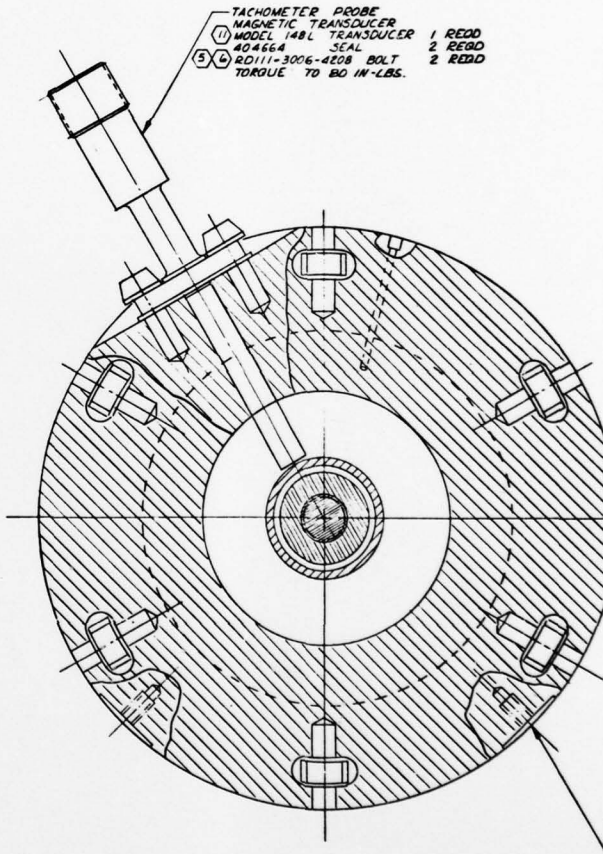

SECT D-D
SCALE: 2 X 1

(17) CAUTION: INSTALL TURBINE BEARINGS PROPERLY TO TAKE THRUST LOAD IN DIRECTION OF TURBINE WHEEL.
(16) BALANCE ROTOR ASSEMBLY TO WITHIN .002 GRAM-INCHES. MATCH MARK ALL ROTOR ASSEMBLY COMPONENTS PER RADIO4-008 BY CHEM-ETCH. CODED PARTS ARE COMPONENTS OF THE ROTOR ASSEMBLY.
15. ASSEMBLE PER ENGINEERING INSTRUCTIONS.
14. PRIOR TO ASSEMBLY CLEAN PER RADIIO-004.
(13) LUBRICATE PER RADII2-002. MOLYKOTE TYPE L SUPPLIER: DOW CORNING, MIDLAND, MICH.
(12) APPLY PER RADIO6-010.
(11) ROSEMOUNT ENGINEERING CO., MINNEAPOLIS, MINN.
(10) MACHINE SPACER THICKNESS PER DETAIL DWG. TO OBTAIN .050 ± .005 DIM. FROM NOZZLE TO WHEEL BLADE.
(9) INSTALL FITTING AND TUBE ASSEMBLIES PER RADI02-005.
(8) IDENTIFY PER RADI04-008.
7. INSTALL PROTECTIVE COVERS OVER ALL EXPOSED FLANGES, TUBE FITTINGS AND PORTS.
(6) LOCKWIRE PER RADI01-002.
(5) INSTALL THREADED FASTENERS PER RADI01-002.
4. SCRIBE LINE ON ALL WHEELS TO FACILITATE PROPER ALIGNMENT (PRIOR TO BALANCE).
(3) LUBE THREAD WITH FELPRO C5 OR EQUIV.
(2) DYNAMICALLY BALANCE FLYWHEEL FOR 5.3 SLUG-FT² MASS
(1) PAINT SURFACES ROCKWELL BLUE FOR CORROSION PROTECTION.

GENERAL NOTES

TACHOMETER PROBE
(11) MAGNETIC TRANSDUCER
MODEL 14BL TRANSDUCER 1 REQD
404664 SEAL 2 REQD
(5)(4) RD111-3006-4208 BOLT 2 REQD
TORQUE TO 80 IN-LBS.

3"-150° WNRF FLANGE (REF)

YEOR941464D4-011 COVER 1 REQD

YEOR941464D4-009 COVER 1 REQD

MS33649-4 BOSS (REF)
BRG OIL LUBE

NAS-2649I-1A BEARING 2 REQD

YEOR941464D2-007 NUT 1 REQD
YEOR941464D2-009 LOCK 1 REQD
TORQUE TO 80 FT-LBS (5)(2)

AN173-15A BOLT 1 REQD
TORQUE TO 12 FT. LBS (5)

AP77-229 SLUG SPACER 1 REQD (2)

G/M GASKET
.060 THK 1 REQD

2-471 RUBBER O-RING 1 REQD

AN178-32A BOLT 4 REQD
AN178-22A BOLT 20 REQD
1/2 SAE STD FLAT IRON WASHER
1/2 DOSI-LOCK NUTS 24 REQD
TORQUE TO 12 FT-LBS (5)

YEOR941464D4-013
BRACKET 2 REQD

AP78-012 SKID 1 REQD (1)

SECT D-D
SCALE: 2 X 1

ACCELEROMETER 2 PLCS
BOTH ENDS

SECTION C-C
ROTATED 32°

AN815-4J UNION 4 REQD
RD662-3005-0004 GASKET 4 REQD (8)(7)

Rocketdyne Division

CODE IDENT 07603	PHASE 1	
AP78-008	-	1

AD-A066 543 ROCKWELL INTERNATIONAL CANOGA PARK CALIF ROCKETDYNE DIV F/G 21/5
INTEGRATED POWER UNIT.(U)
DEC 78 G S WONG, T I YU, J J WARD F33615-76-C-2054
UNCLASSIFIED RI/RD78-237 AFAPL-TR-78-98 NL

3 OF 3
AD
A066543

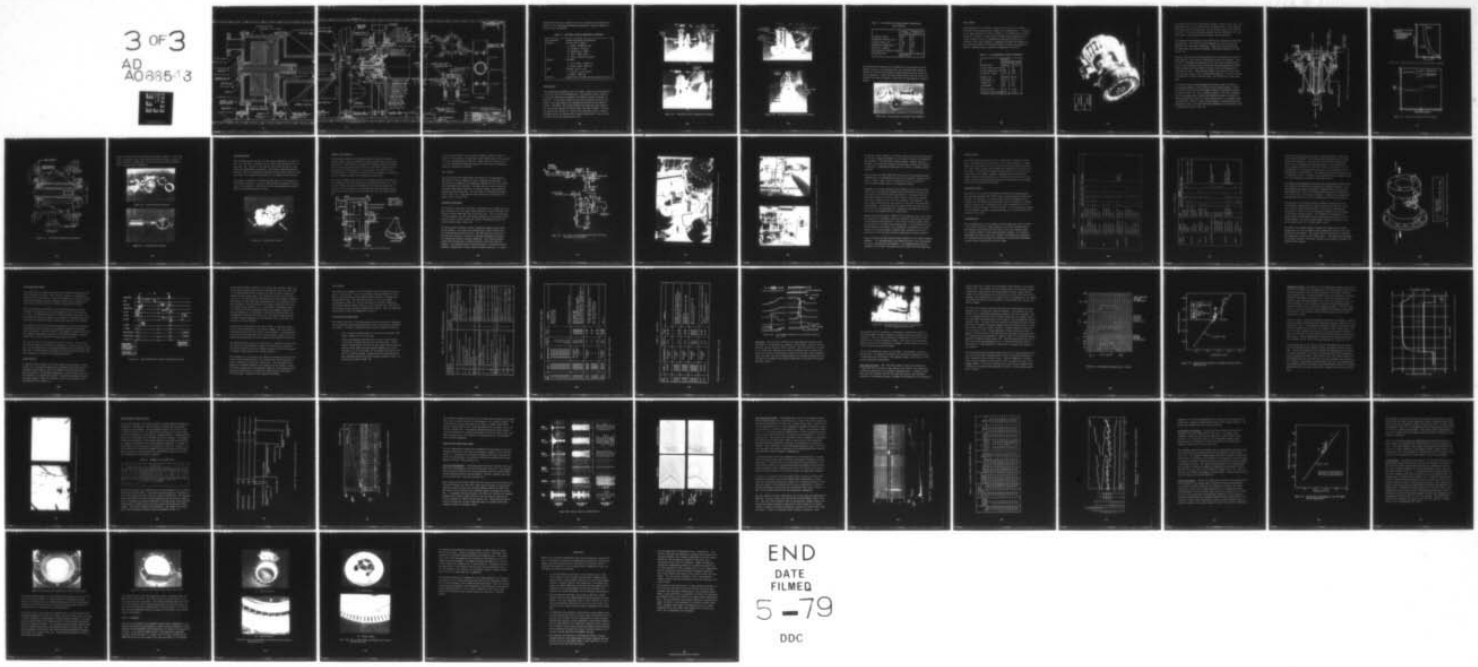

END
DATE
FILMED
5-79
DDC

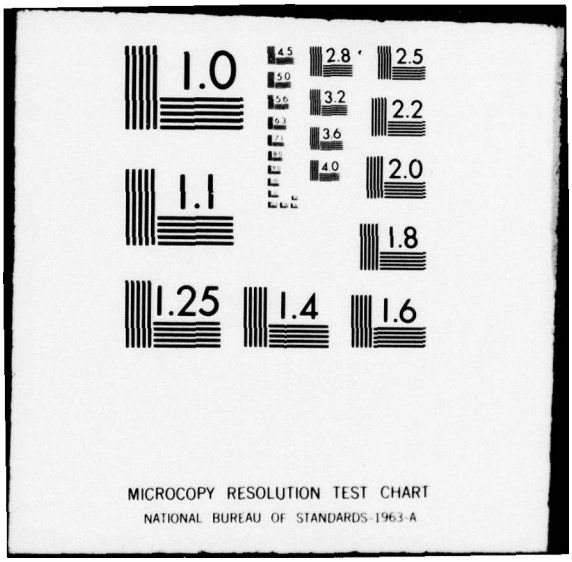
1.0
1.1
1.25
1.4
1.6
1.8
2.0
2.2
2.5
2.8
3.2
3.6
4.0
4.5
5.0
5.6
MICROCOPY RESOLUTION TEST CHART
NATIONAL BUREAU OF STANDARDS-1963-A

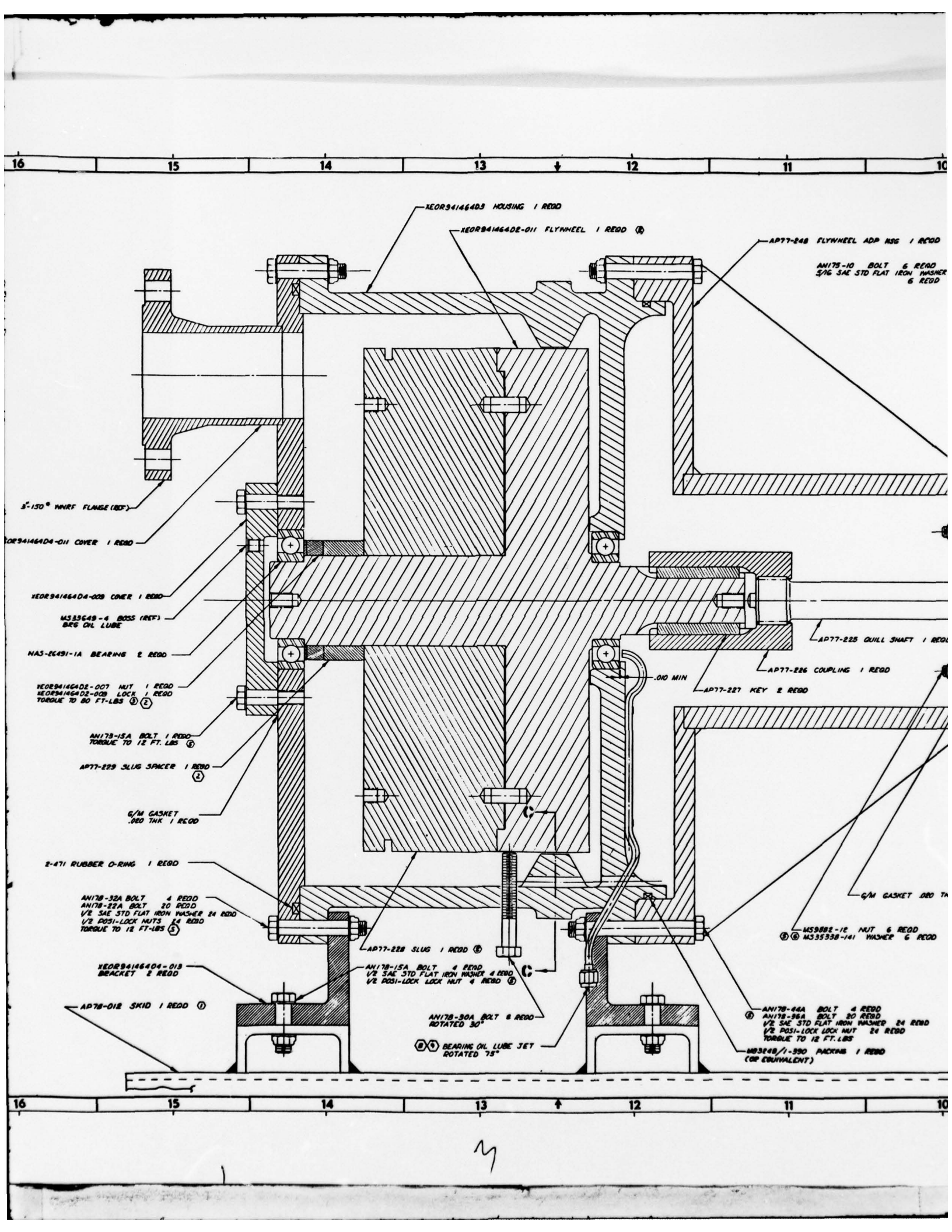
16
15
14
13
12
11
10
XEOR941464D3 HOUSING 1 REQD
XEOR941464D2-011 FLYWHEEL 1 REQD (1)
AP77-248 FLYWHEEL ADP HSG 1 REQD
AN175-10 BOLT 6 REQD
5/16 SAE STD FLAT IRON WASHER 6 REQD
3"-150# WNRF FLANGE (REF)
XEOR941464D4-011 COVER 1 REQD
XEOR941464D4-009 COVER 1 REQD
MS35649-4 BOSS (REF) BRG OIL LUBE
NAS-6491-1A BEARING 2 REQD
XEOR941464D2-007 NUT 1 REQD
XEOR941464A02-008 LOCK 1 REQD
TORQUE TO 80 FT-LBS (3) (2)
AN179-15A BOLT 1 REQD
TORQUE TO 12 FT. LBS (5)
AP77-229 SLUG SPACER 1 REQD (2)
G/M GASKET .080 THK 1 REQD
2-471 RUBBER O-RING 1 REQD
AN178-32A BOLT 4 REQD
AN178-22A BOLT 20 REQD
1/2 SAE STD FLAT IRON WASHER 24 REQD
1/2 POSI-LOCK NUTS 24 REQD
TORQUE TO 12 FT-LBS (5)
XEOR941464D4-013 BRACKET 2 REQD
AP78-012 SKID 1 REQD (1)
AP77-228 SLUG 1 REQD (1)
AN178-15A BOLT 4 REQD
1/2 SAE STD FLAT IRON WASHER 4 REQD
1/2 POSI-LOCK LOCK NUT 4 REQD (5)
AN178-30A BOLT 2 REQD ROTATED 30°
(3) (5) BEARING OIL LUBE JET ROTATED 75°
AP77-225 QUILL SHAFT 1 REQD
AP77-226 COUPLING 1 REQD
.010 MIN
AP77-227 KEY 2 REQD
G/M GASKET .080 THK
MS9882-12 NUT 6 REQD
(2) (6) MS35338-141 WASHER 6 REQD
(4) AN178-44A BOLT 4 REQD
AN178-96A BOLT 20 REQD
1/2 SAE STD FLAT IRON WASHER 24 REQD
1/2 POSI-LOCK LOCK NUT 24 REQD
TORQUE TO 12 FT. LBS
MS9240/1-390 PACKING 1 REQD
(OR EQUIVALENT)

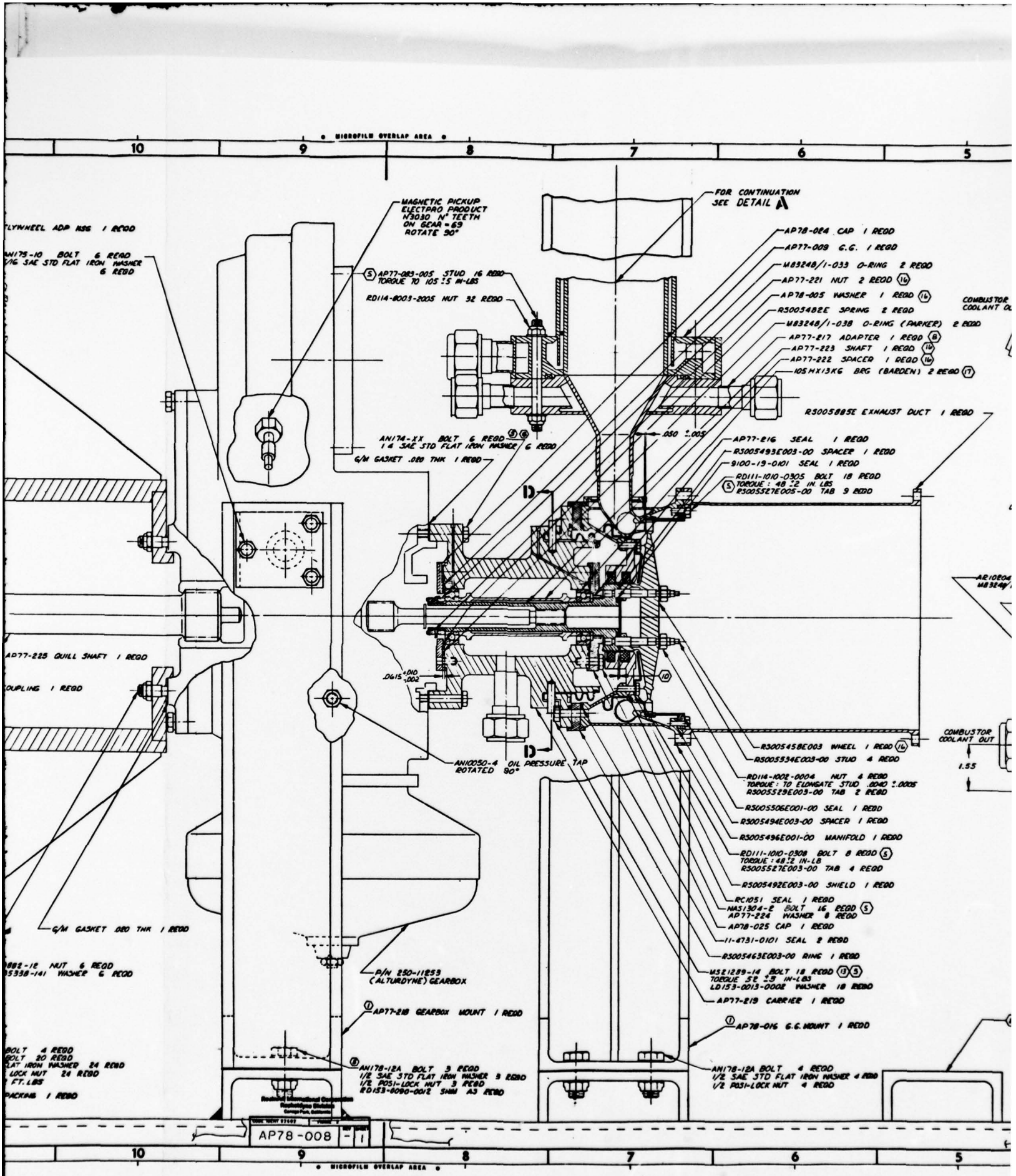
MICROFILM OVERLAP AREA
10
9
8
7
6
5
FOR CONTINUATION SEE DETAIL A
MAGNETIC PICKUP ELECTPRO PRODUCT N3030 N° TEETH ON GEAR = 69 ROTATE 90°
FLYWHEEL ADP RING 1 REQD
AN175-10 BOLT 6 REQD
W/G SAE STD FLAT IRON WASHER 6 REQD
AP77-089-005 STUD 16 REQD TORQUE TO 105 ±5 IN-LBS
RD114-0003-2005 NUT 32 REQD
AP78-024 CAP 1 REQD
AP77-009 G.C. 1 REQD
MS3248/1-033 O-RING 2 REQD
AP77-221 NUT 2 REQD (16)
AP78-005 WASHER 1 REQD (14)
R3005482E SPRING 2 REQD
MS3248/1-038 O-RING (PARKER) 2 REQD
AP77-217 ADAPTER 1 REQD (18)
AP77-223 SHAFT 1 REQD (16)
AP77-222 SPACER 1 REQD (16)
105MX13KG BRG (BARDEN) 2 REQD (17)
COMBUSTOR COOLANT OUT
R3005885E EXHAUST DUCT 1 REQD
AN174-XX BOLT 6 REQD (15)(6)
1/4 SAE STD FLAT IRON WASHER 6 REQD
G/M GASKET .080 THK 1 REQD
.050 ±.005
AP77-216 SEAL 1 REQD
R3005493E003-00 SPACER 1 REQD
9100-19-0101 SEAL 1 REQD
RD111-1010-0305 BOLT 18 REQD (5)
TORQUE: 48 ±2 IN LBS
R3005527E005-00 TAB 9 REQD
D
AP77-225 QUILL SHAFT 1 REQD
COUPLING 1 REQD
.0615 +.002 -.000
3
10
AN10050-4 OIL PRESSURE TAP ROTATED 90°
R3005458E003 WHEEL 1 REQD (14)
R3005534E003-00 STUD 4 REQD
RD114-1002-0004 NUT 4 REQD
TORQUE: TO ELONGATE STUD .0040 ±.0005
R3005529E003-00 TAB 2 REQD
R3005506E001-00 SEAL 1 REQD
R3005494E003-00 SPACER 1 REQD
R3005496E001-00 MANIFOLD 1 REQD
RD111-1010-0308 BOLT 8 REQD (5)
TORQUE: 48 ±2 IN-LB
R3005527E003-00 TAB 4 REQD
R3005492E003-00 SHIELD 1 REQD
RC1051 SEAL 1 REQD
NAS1304-2 BOLT 16 REQD (5)
AP77-224 WASHER 8 REQD
AP78-025 CAP 1 REQD
11-6731-0101 SEAL 2 REQD
R3005463E003-00 RING 1 REQD
MS21289-14 BOLT 18 REQD (13)(5)
TORQUE 52 ±3 IN-LBS
LD153-0013-0002 WASHER 18 REQD
AP77-219 CARRIER 1 REQD
COMBUSTOR COOLANT OUT
1.55
G/M GASKET .080 THK 1 REQD
P/N 250-11259 (ALTURDYNE) GEARBOX
(1) AP77-218 GEARBOX MOUNT 1 REQD
(1) AP78-016 G.C. MOUNT 1 REQD
(4) AN178-12A BOLT 3 REQD
1/2 SAE STD FLAT IRON WASHER 3 REQD
1/2 POSI-LOCK NUT 3 REQD
RD153-0090-0012 SHIM AS REQD
AN178-12A BOLT 4 REQD
1/2 SAE STD FLAT IRON WASHER 4 REQD
1/2 POSI-LOCK NUT 4 REQD
AP78-008 - 1
MICROFILM OVERLAP AREA

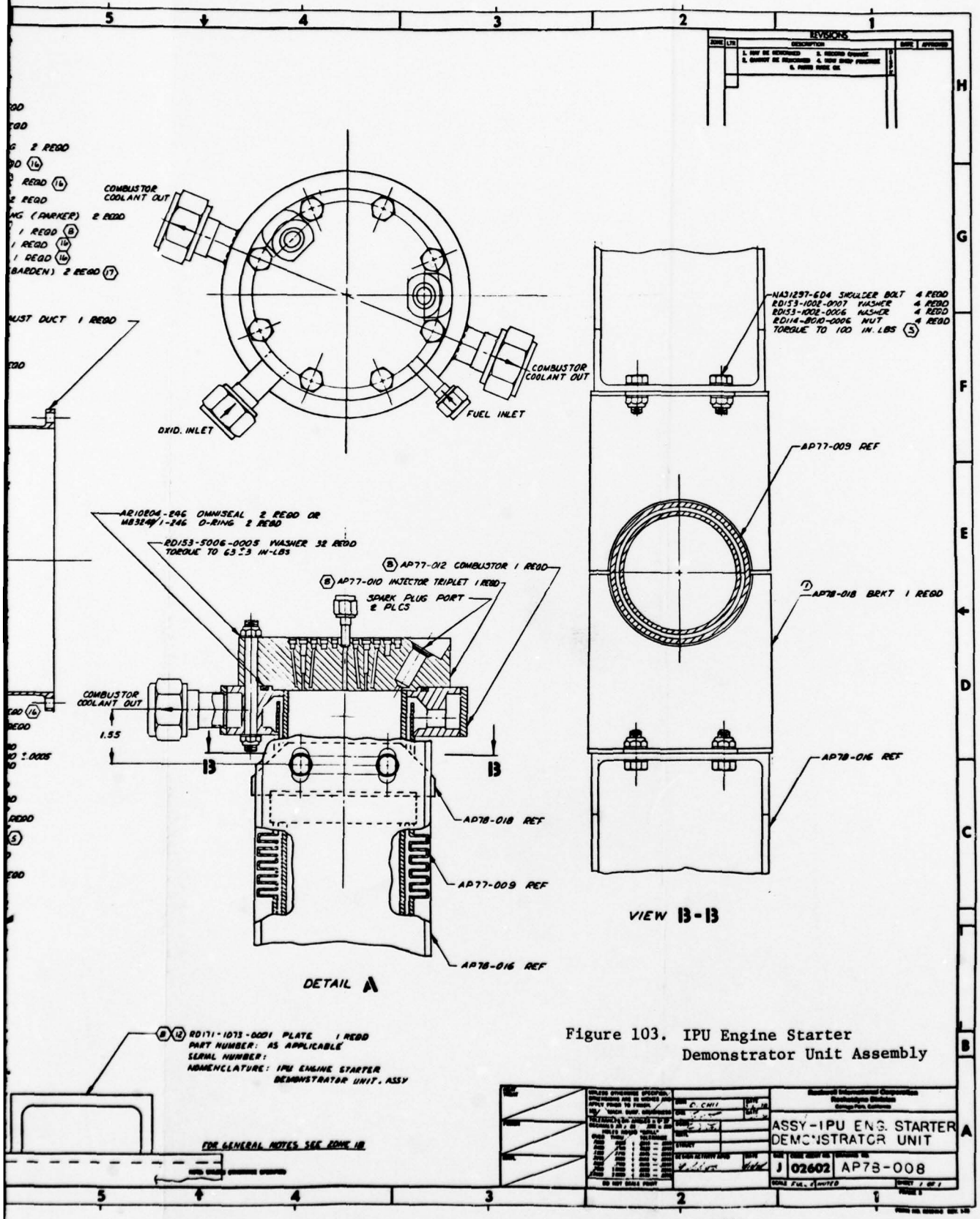

Figure 103. IPU Engine Starter Demonstrator Unit Assembly

skid-mounted test bed. Design data for the components are summarized in Table 22. The completed skid-mounted demonstrator hardware assembly is shown in Fig. 104 and 105.

TABLE 22. IPU ENGINE STARTER DEMONSTRATOR COMPONENTS

Gas Generator	Present High-Power Gas Generator
Turbine	MK 44 F (first stage) • Speed: 60,000 rpm max • Pressure: 215 psia • Temperature: 1650 F • Flow: 0.650 lb/sec • Power: 228 hp (at cutout)
Gearbox	Alturdyne • Input Speed: 60,000 rpm • Output Speed: 8000 rpm
Load	Flywheel Inertial Load • Inertia: 5.34 slug-ft^2 • Speed: 8000 rpm
Controls	Speed Cutout at 60,000 rpm Overtemperature Cutout

Gas Generator

The high-power gas generator with the triplet injector, and reworked GOX orifice was used for the demonstrator. The required starter operation of this gas generator is compared to the Phase I tested conditions in Table 23. In all cases, except for the total propellant flowrate, the Phase I test conditions met or exceeded the severity of the required starter conditions. The tested flowrate was lower than that required for the starter because the nozzle throat area used in Phase I testing was smaller than the MK 44 F turbine inlet manifold nozzles. Gaseous nitrogen used as the gas generator coolant during Phase I test was also used for the starter demonstration tests.

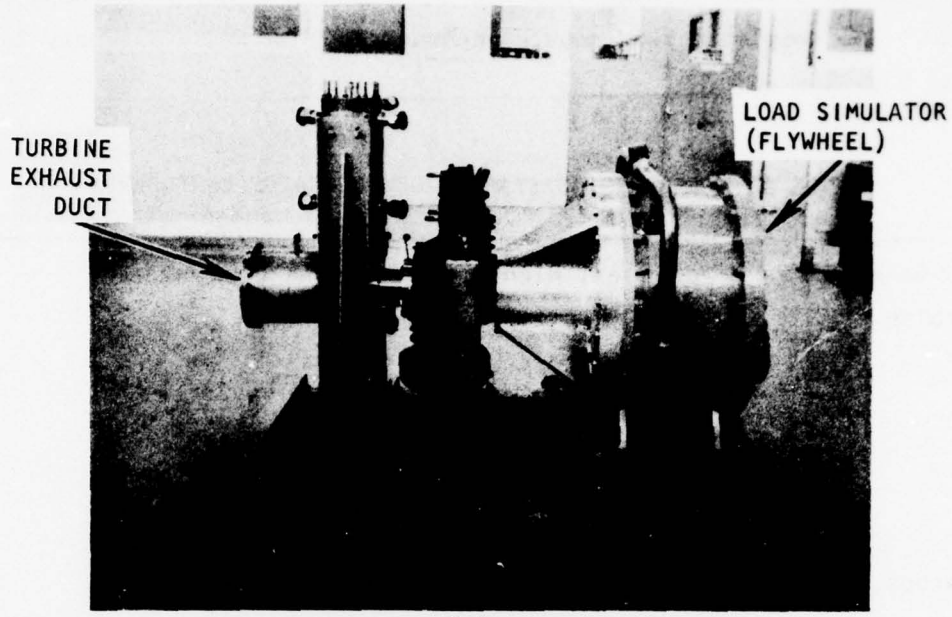

(a)

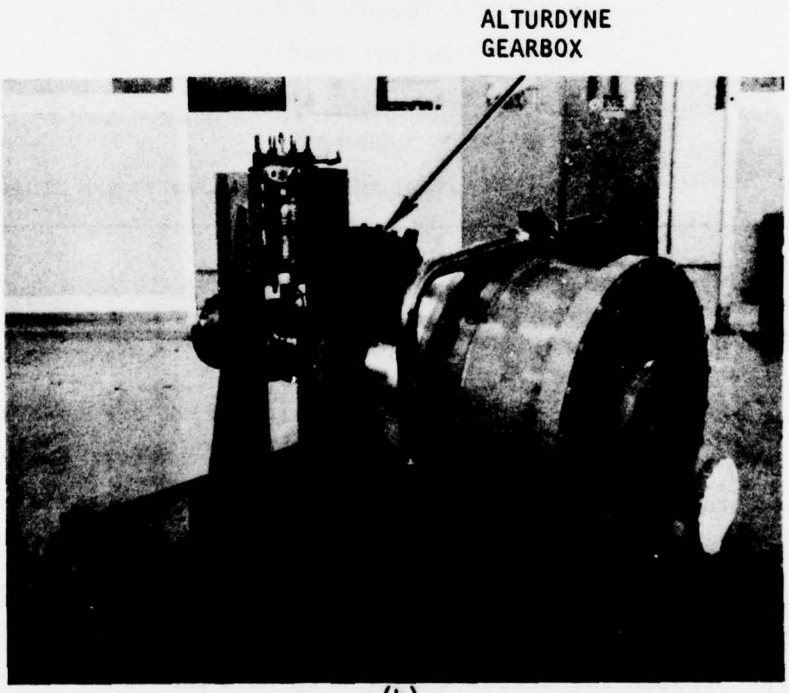

(b)

Figure 104. IPU Engine Starter Demonstrator Assembly

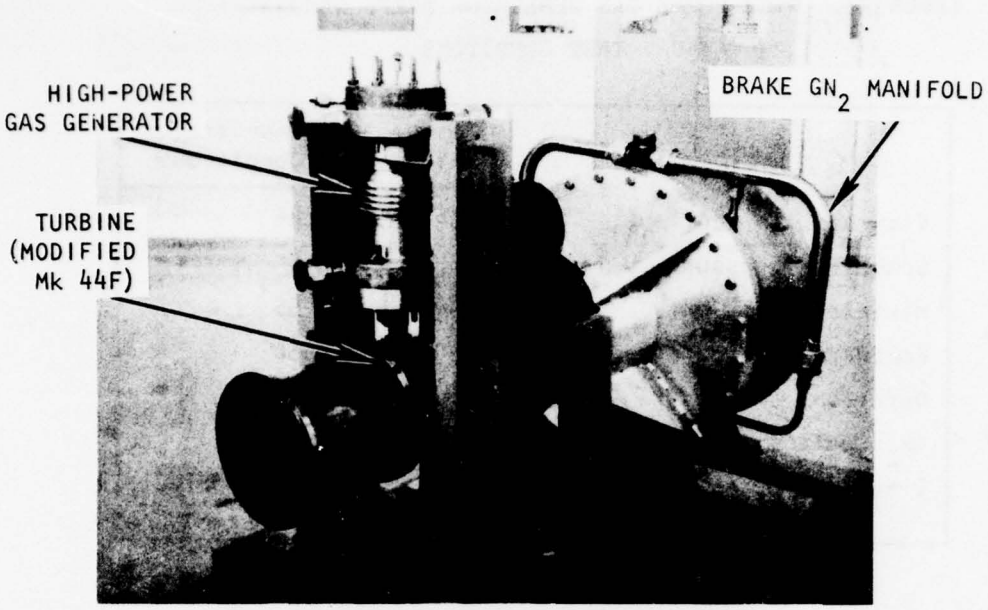

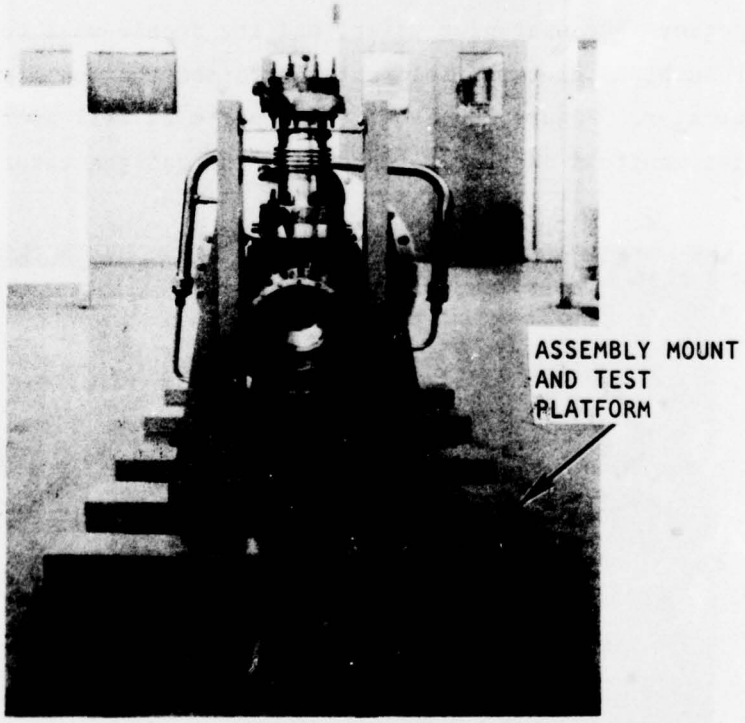

Figure 105. IPU Engine Starter Demonstrator Assembly

TABLE 23. HIGH-POWER GAS GENERATOR MEETS DEMONSTRATOR TEST CONDITONS

	Tested 2-10-78	Demonstrator Conditions
Flowrate, lb/sec	0.54	0.65
Combustor Pressure, psia	215	215
Mixture Ratio, o/f	0.56	0.55
Combustion Temperature, F	1750	1650
Duration, seconds	30	23
GN_2 Coolant Flowrate, lb/sec	0.6	0.6
Discharge Duct	Simulated Manifold	Mk 44 Manifold

The high-power gas generator was assembled with the modified triplet-element injector, the sparkplug wafer, and the double-wall combustor. The MK 44 F turbine inlet manifold nozzles formed the sonic throat for the gas generator. Figure 106 shows these parts as well as the MK 44 F turbine inlet manifold adapter to mate with the gas generator combustor flange.

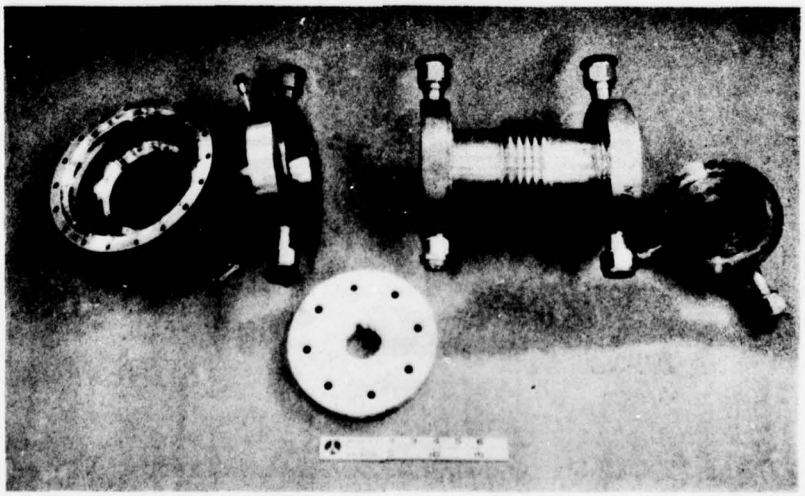

Figure 106. Gas Generator and Turbine Inlet Manifold

Power Turbine

The Rocketdyne MK 44 F turbine is shown in Fig. 107, and its design conditions closely matched those needed for the demonstrator. A comparison of these conditions is shown in Table 24. The demonstrator required the MK 44 F turbine to operate above its design inlet temperature and overall pressure ratio, but demanded far less power extraction and required a lower inlet pressure. Although the turbine was designed for O_2/H_2 combustion gases, the turbine delivers the power and speed with GOX/JP-4 combustion gases required for demonstrator operation.

TABLE 24. IPU DEMONSTRATOR TURBINE PERFORMANCE

	Mk 44F Design	Demonstrator
Propellants	GOX/H_2	GOX/JP-4
Inlet Pressure, psia	270	215
Inlet Temperature, F	1550	1650
Flowrate, lb/sec	0.60	0.65
Speed, rpm	60,000	60,000
Efficiency, %	60.3	64.3
Admission, %	100	100
Horsepower	814	228
Pressure Ratio	7.72	12.65
Velocity Ratio (U/CO)	0.172	0.357

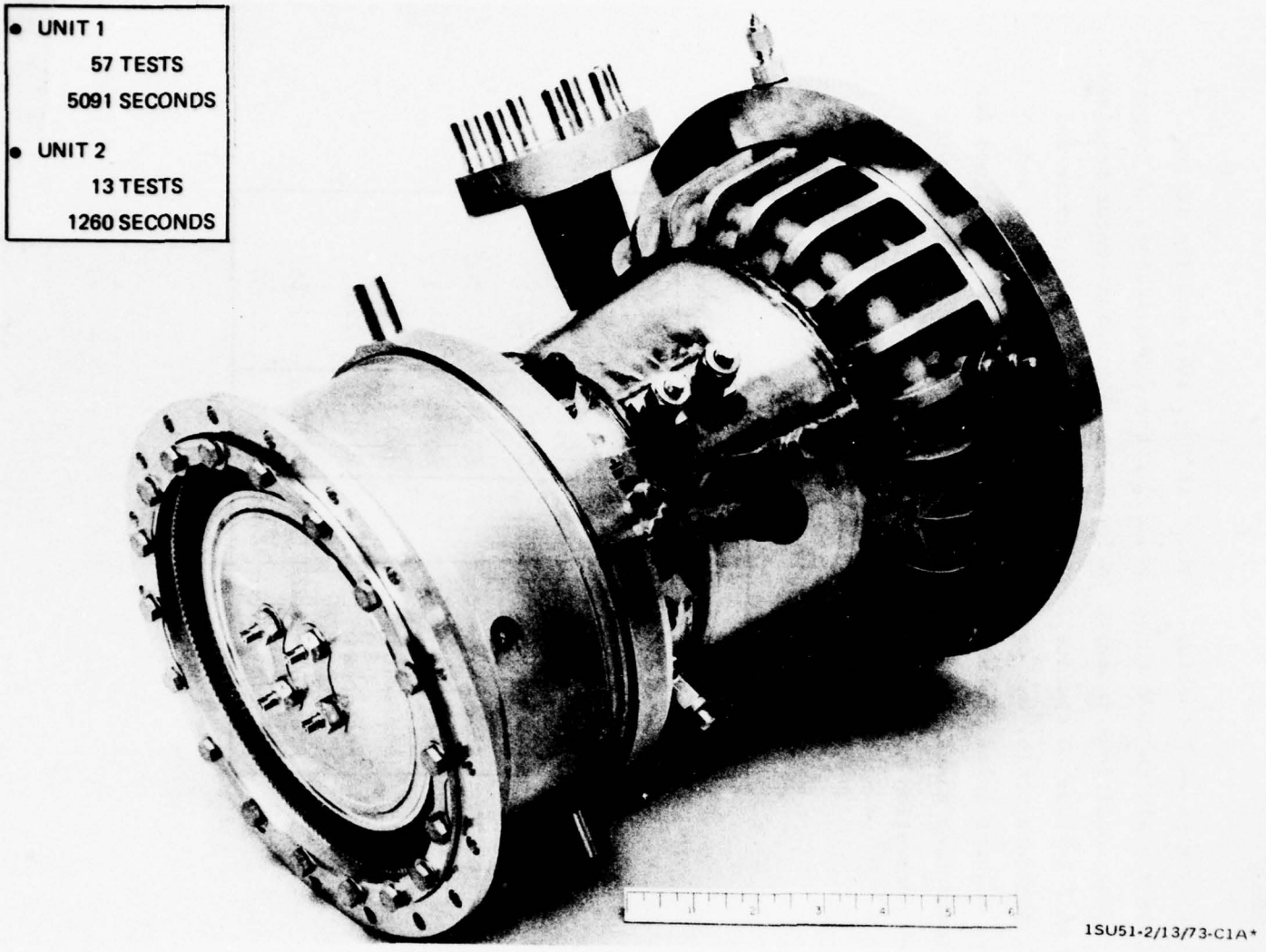

Figure 107. Mark 44 F Fuel Turbopump

The design layout for the demonstrator turbine is shown in Fig. 108. The design made use of the following MK 44 F turbine parts: inlet manifold, stator housing, first-stage wheel, and the exhaust housing (not shown in Fig. 108). To drive the Alturdyne gearbox required fabrication of a new rotor shaft, a new bearing carrier housing, and new bearings.

The turbine inlet manifold was also modified for attaching the high-power gas generator. The existing inlet flange and duct were cut from the manifold, and a new inlet containing a flange with cooling provisions was fabricated and attached by welding. The modified manifold is shown in Fig. 106.

Analysis indicated that turbine operation at the conditions of Table 24 would impose an axial thrust of 800 pounds on the rotor assembly. Since the MK 44 F bearings were designed for far less axial loading in addition to being hydrogen cooled, new bearings were designed and purchased. These bearings were pitch-diameter-riding, 25 mm ball bearings with thin metallic cages. The predicted fatigue life curves for these bearings are shown in Fig. 109 for 30,000 and 60,000 rpm. A life of 4 hours, or capability of greater than 600 starts, was predicted for these bearings.

The bearing carrier housing design also provides support stiffness to the bearings needed to avoid turbine critical speed problems. The predicted first and second critical speed curves for the modified turbine are shown in Fig. 110. For a bearing stiffness of 10^6 lb/in. designed into the bearing carrier housing, the modified turbine is predicted to operate between the first two critical speeds when at its maximum speed of 60,000 rpm. Thus, the first critical speed is traversed during each demonstrator test. Oil lubrication was designed into the bearing carrier and housing as shown in Fig. 111.

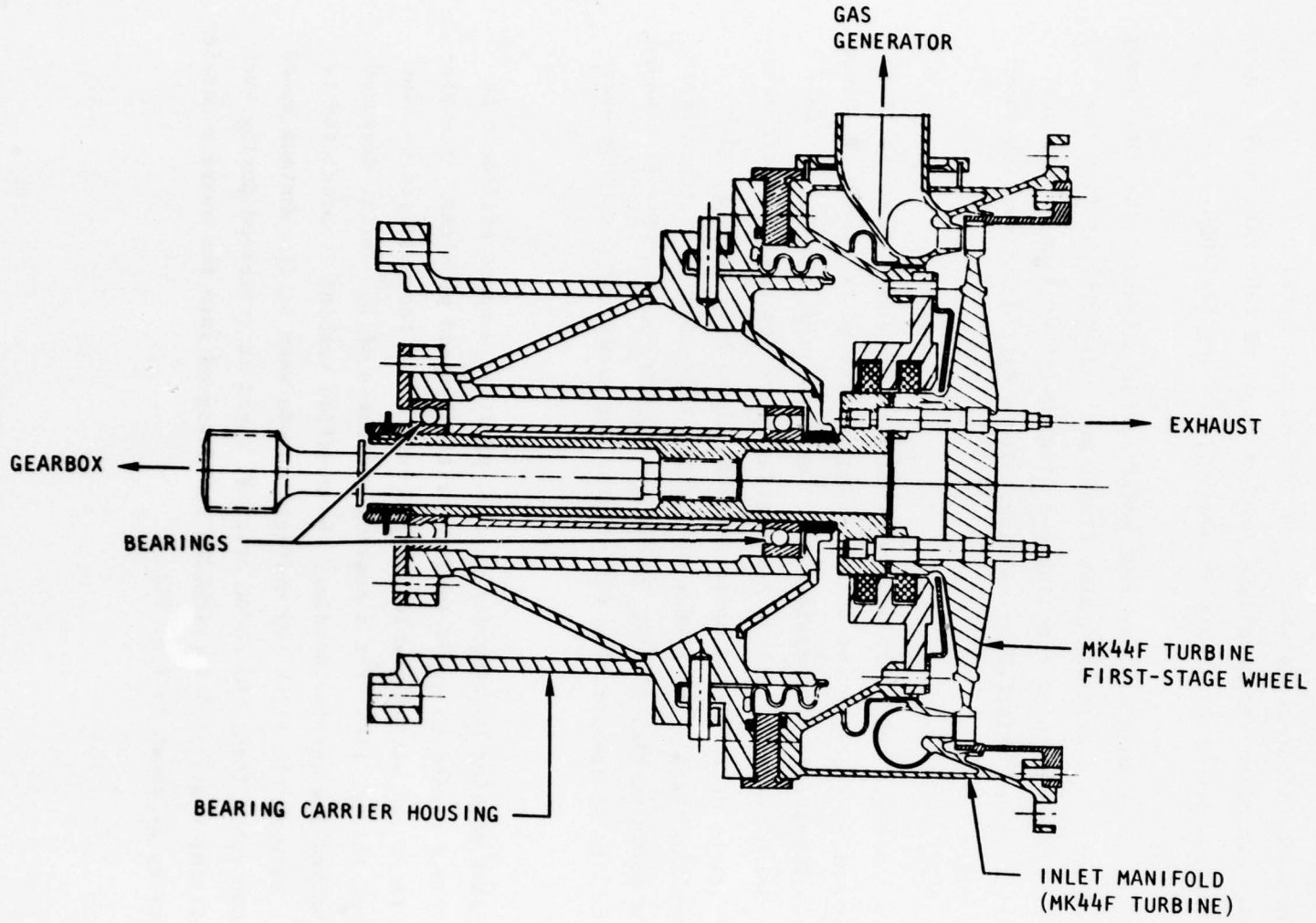

Figure 108. IPU Demonstrator Turbine (modified MK 44 F)

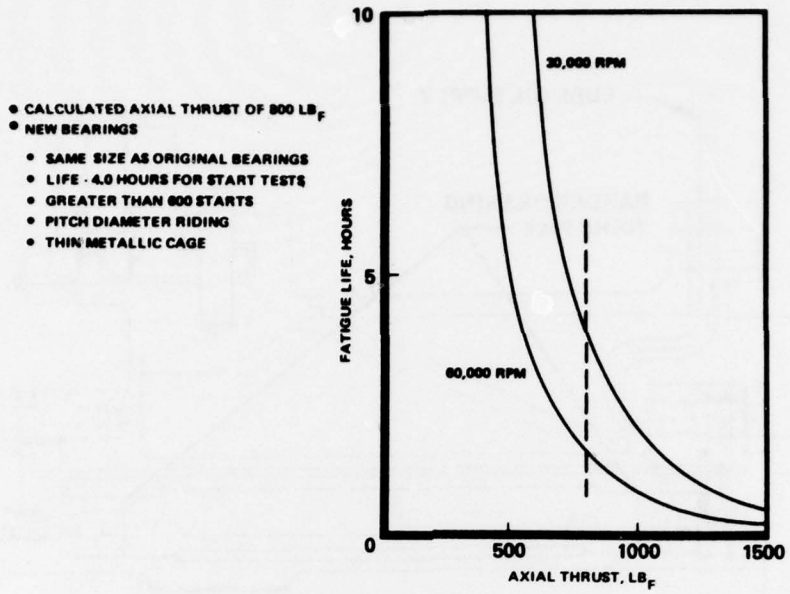

Figure 109. Fatigue Life Curves for Borden Bearing 105HX13K6

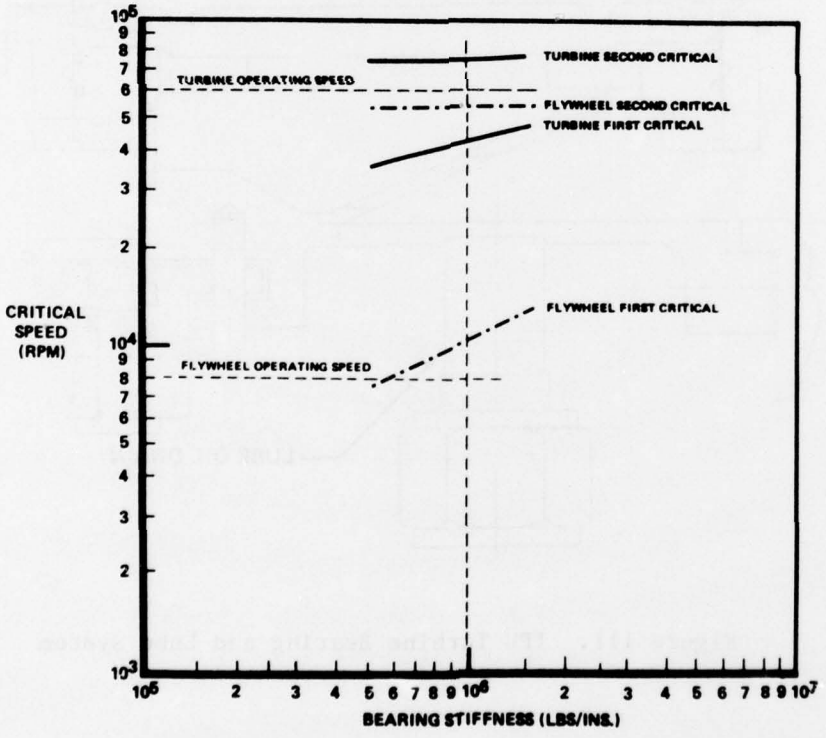

Figure 110. IPU Turbine Bearing and Lube System

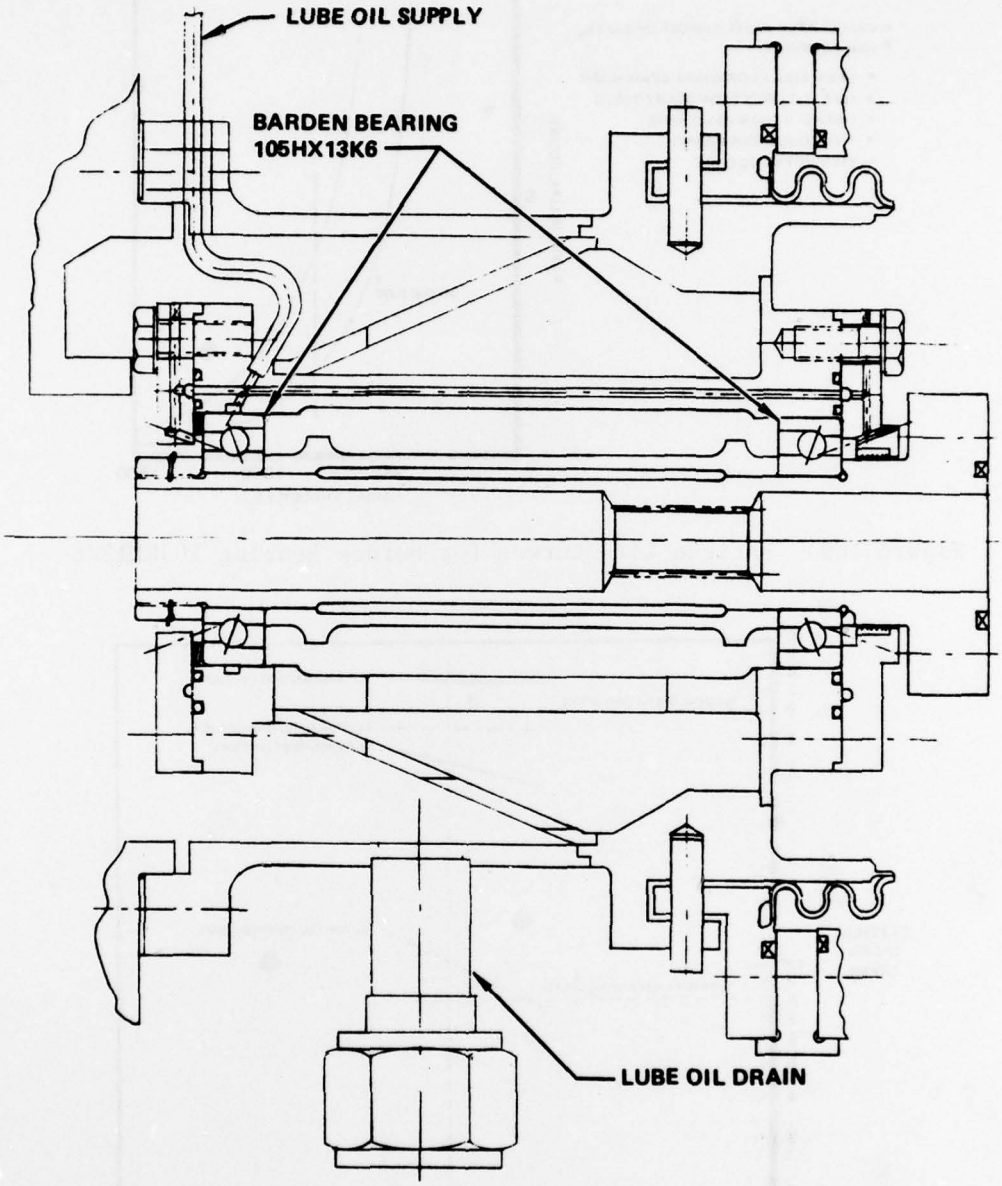

Figure 111. IPU Turbine Bearing and Lube System

Figure 112 shows the following completed turbine components: inlet manifold, its assembly pieces, and the bearing carrier housing. Figure 113 shows the MK 44 F turbine wheel, the new rotor shaft, and the hardware used to assemble these components.

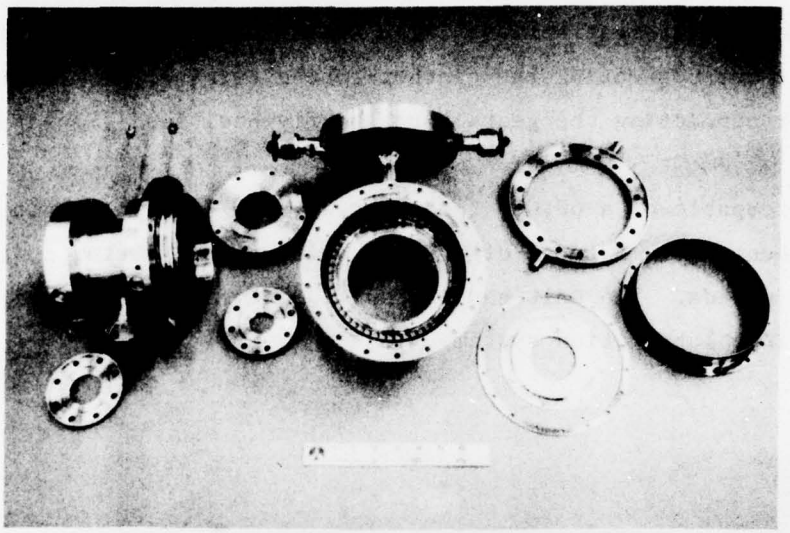

Figure 112. Turbine Housing Components

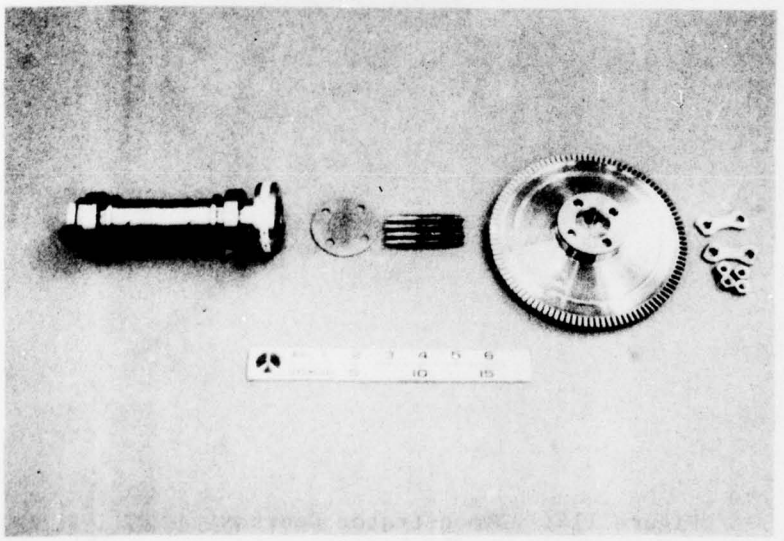

Figure 113. Turbine Rotor and Shaft

Alturdyne Gearbox

The Alturdyne gearbox selected for the starter demonstrator is shown in Fig. 114. The view is looking from the turbine side and shows the turbine mount pad. The pad to the right of the turbine pad was not used during the demonstrator test series. Also shown in the photograph are the quill shaft for connecting the gearbox to the turbine, and the larger quill shaft for connecting the gearbox to the flywheel load simulator.

The gearbox is capable of a 60,000 rpm input with a 7777 rpm output at the flywheel mount pad. A total of 300 hp could be transmitted continuously at these speeds. The unit has its own speed-measuring transducer and self-contained lubrication system.

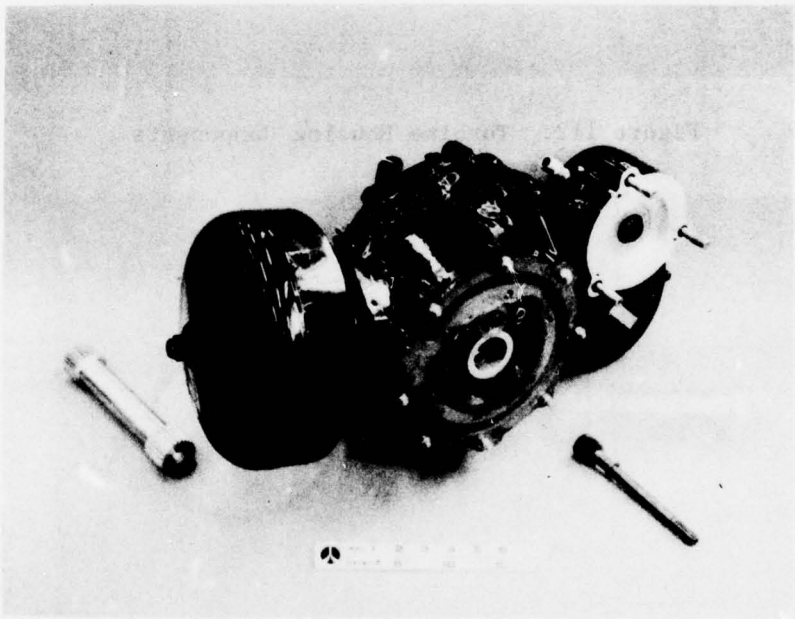

Figure 114. Demonstrator Gearbox

Flywheel Load Simulator

The Rocketdyne flywheel load simulator used in a previous fast-start turbine program (Contract F33615-74-C-2013) was modified for the starter demonstrator. Modifications consisted of an adapter section for mating with the Alturdyne gearbox (Fig. 103) and a new inertia wheel slug for increasing the flywheel inertia to the desired 5.34 slug-ft^2 of the CFM56-2B engine. In addition, a quill shaft and coupling for connection with the Alturdyne gearbox were designed and fabricated.

The flywheel assembly has provision for braking using GN_2 directed onto the periphery of the main rotor disk as illustrated in Fig. 115. Acceleration to 8000 rpm had been demonstrated with this unit during the FastStart Turbine Program so the bearings and their lubrication system were satisfactory even with the increased loads from the added inertial slug.

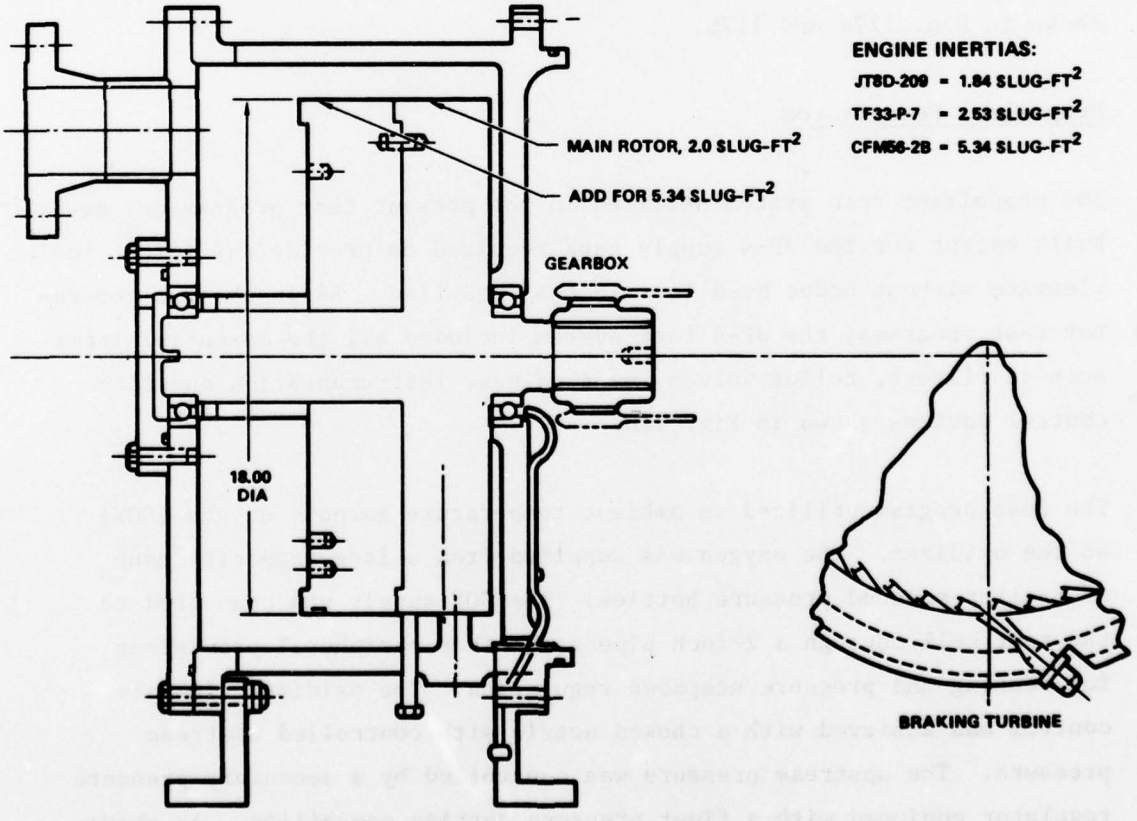

Figure 115. Flywheel Inertia Load Simulator

Critical speed analysis of the modified flywheel assembly showed the first critical speed to be 10,000 rpm (output shaft speed), with a second critical at approximately 55,000 rpm. These values are shown in Fig. 111. The approximately 8000 rpm required for the starter demonstrator, therefore, presented no problems.

TEST FACILITY

The IPU engine starter demonstrator was tested at the Thermodynamics Laboratory at the Los Angeles Division of Rockwell International. The test facility provided all the subsystems required for the test setup of the skid-mounted test hardware. The major facility items included the propellant feed system, lubricant circulation system, instrumentation, and data acquisition systems. The test setup is illustrated schematically in Fig. 116. Three general views of the test installation are shown in Fig. 117a and 117b.

Propellant Feed System

The propellant feed system utilized in the present test program was newly built except for the JP-4 supply tank required to provide sufficient fuel flowrate without undue head loss in the feed line. As in the gas generator test programs, the JP-4 feed system included all the essential items such as filters, relief valves, vent valves, instrumentation and flow control devices shown in Fig. 116.

The test program utilized an ambient temperature gaseous oxygen (GOX) as the oxidizer. The oxygen was supplied from a large capacity bank of trailer-mounted pressure bottles. The GOX supply was connected to the test cell through a 2-inch pipe with other peripheral provisions for venting and pressure stepdown regulation. The oxidizer flowrate control was achieved with a choked nozzle with controlled upstream pressure. The upstream pressure was controlled by a secondary pressure regulator equipped with a finer pressure setting capability. As shown

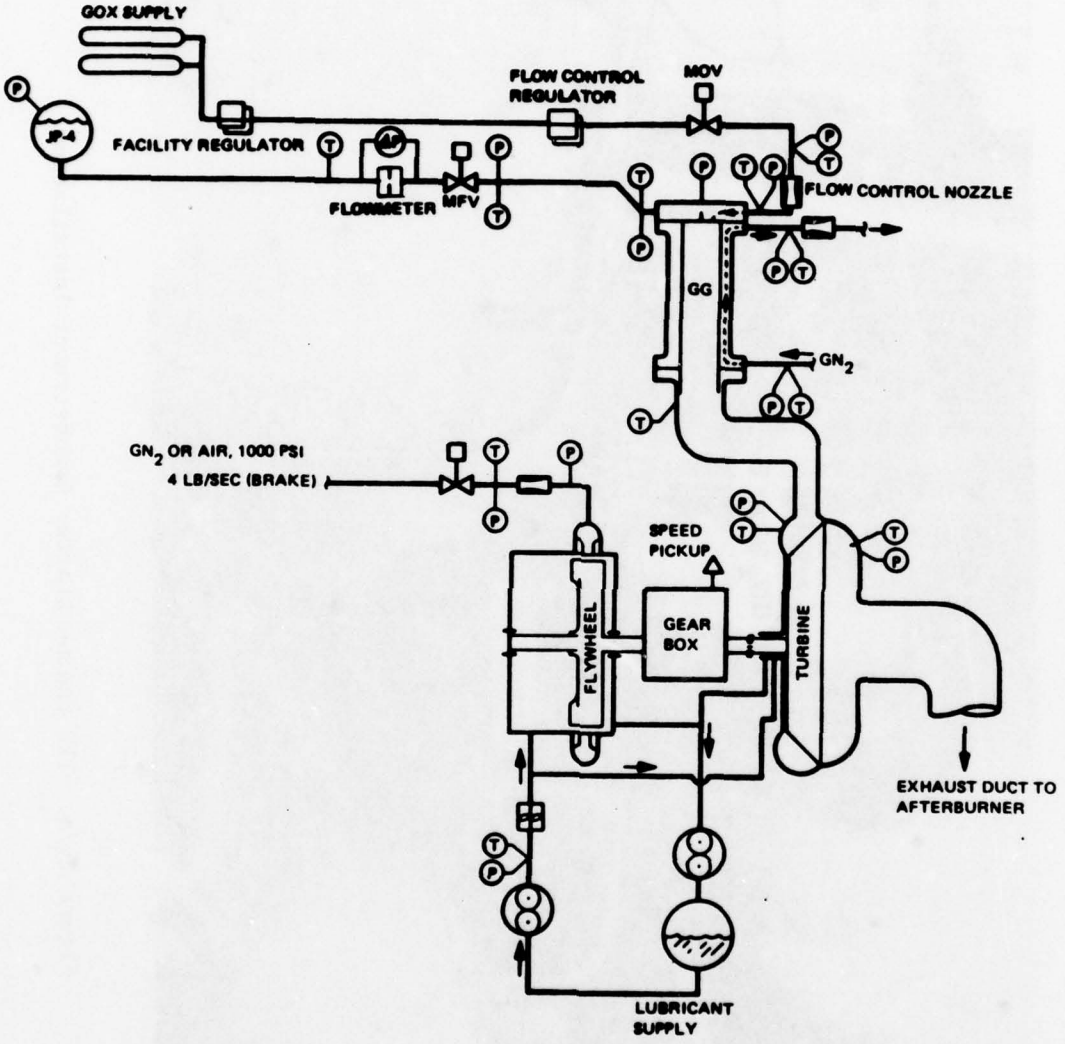

Figure 116. IPU Engine Starter Demonstrator Test Setup and Instrumentation Schematic

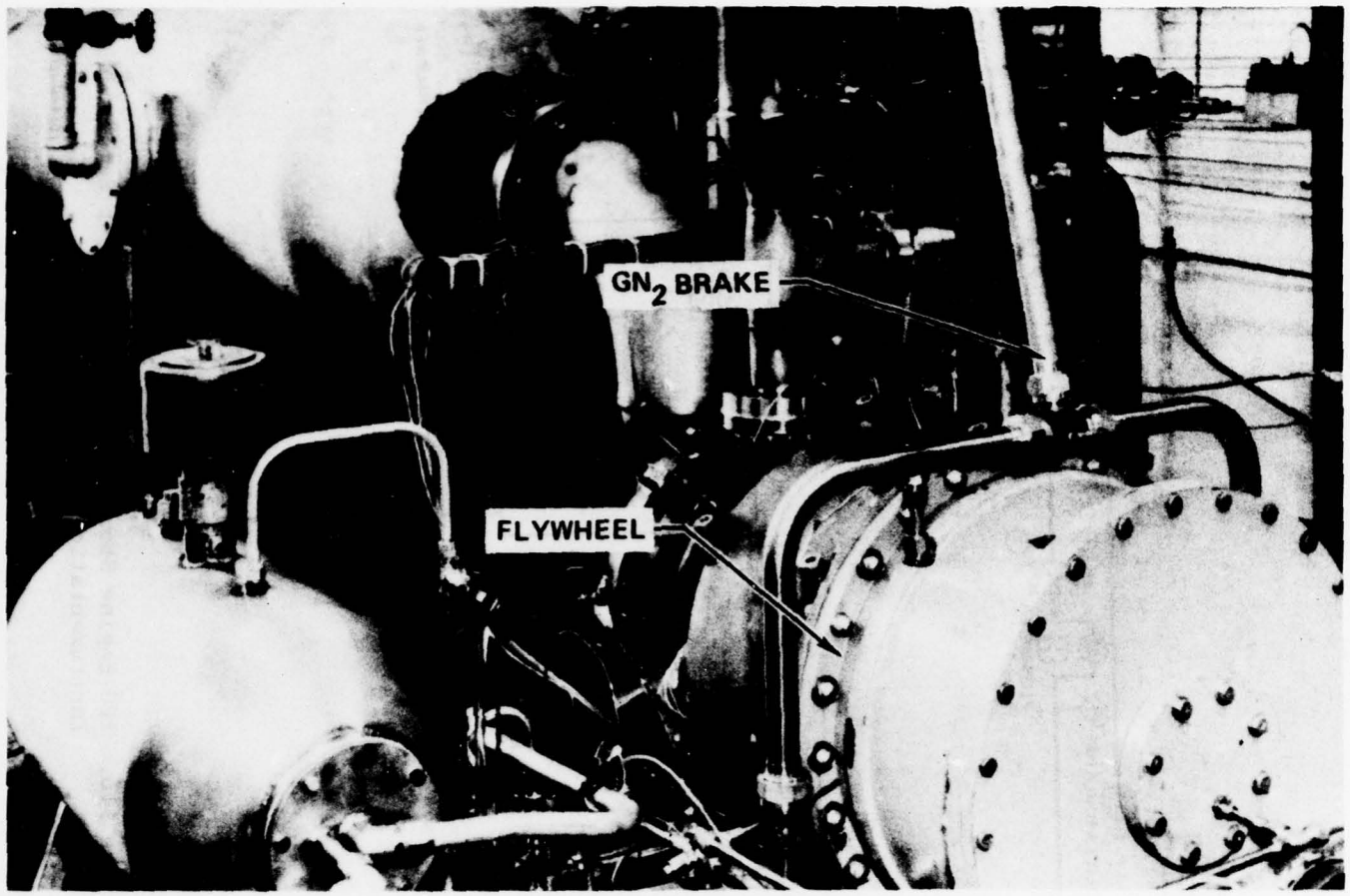

Figure 117a. IPU Engine Starter Demonstrator Installation

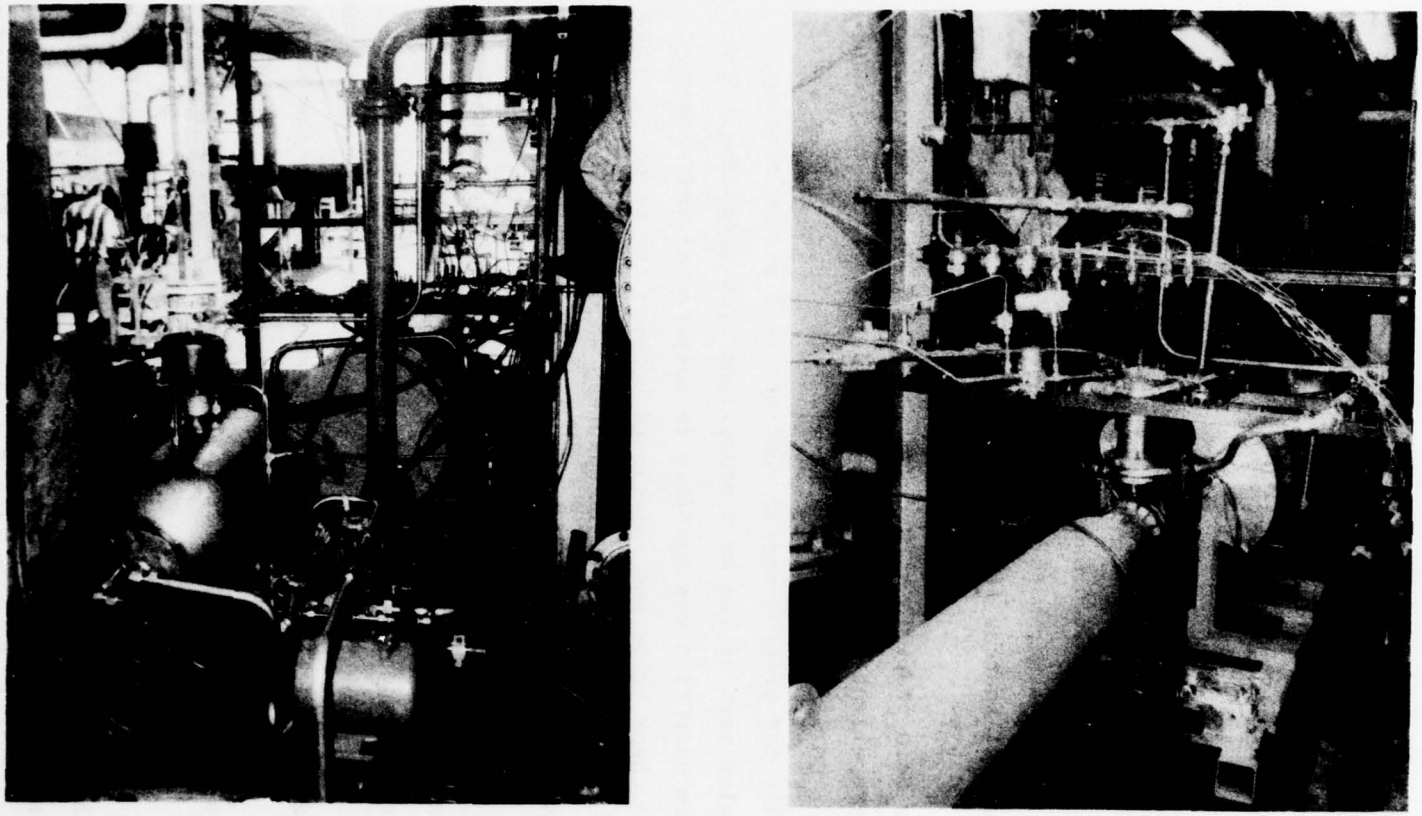

Figure 117b. IPU Engine Starter Demonstrator Installation

in the test setup schematic, the choked nozzle was positioned downstream of the main oxygen valve (MOV) as in the earlier tests of the high-power gas generator. This provided a smooth, gradual, oxidizer injection pressure rise during the oxidizer priming stage, allowing the flowrate to approach a predetermined mainstage level without a chamber pressure overshoot.

Both the main fuel valve (MFV) and the MOV were activiated/deactivated independently in a predetermined manner by an automatic sequencer located in a control room. Also, both main valves were interlocked to various redline signal sources for emergency shutdown.

Peripheral to the main propellant feed system is the GN_2 purge system "teed" into the propellant transport lines downstream of the main control valves of the GOX and JP-4, respectively. The purge system was installed primarily for pretest and/or posttest feed system cleanup, and not as a regular part of the main propellant flow seqencing. However, purge system operation was possible in both manual and sequenced control modes. A check valve was positioned between the purge gas control valve and the propellant line, immediately adjoining the tee connector for the oxidizer and fuel, respectively.

Gaseous nitrogen was used to "dump-cool" the combustor body, with a nominal flowrate of 0.6 lbm/sec, which was consistent with previous testing of the high-power gas generator. The outlet of the GN_2 coolant jacket was connected to an exhaust gas discharge pipe 2 feet downstream of the turbine exhaust duct flange. This arrangement contributed to the safe operation of the long exhaust discharge pipe, especially at start of each hot-fire test, by both cooling and diluting the exhaust products.

Gaseous hydrogen was used during cold-gas checkout of the turbine-flywheel assembly. The hydrogen supply was plumbed directly to the turbine manifold inlet bypassing the gas generator. The hydrogen feed system was provided with necessary instrumentation for pressure and flow regulation.

Flywheel System

The flywheel braking was effected by a large-capacity gaseous nitrogen flow. The brake gas and the combustor coolant were plumbed to a common supply and feed system in the test cell, with the latter being regulated by a flow control orifice placed immediately upstream of the coolant control valve. The brake gas flowrate was controlled by four nozzles contained within the flywheel assembly. Opening the brake gas control valve is usually achieved within a few seconds after the end of the flywheel acceleration and allows practically full diversion of the nitrogen supply into the brake gas feed system.

Lubrication System

Lubrication of the turbine and flywheel bearings was accomplished with the required lubricant, MIL-L-7808, using a supply pressure setting above 50 psig. The lubricant is collected from the outlets underneath the flywheel and the bearing carrier housings, and is returned by a scavenge pump for recycled use. The gearbox has a self-contained lube oil circulation system with about a 3-quart capacity. Oil cooling was not needed for the flywheel, turbine or gearbox bearings due to the relatively short duration of the tests.

Instrumentation

The instrumentation for the complete starter demonstrator tests is shown in the list of Table 25. Some elements of the listed instrumentation were employed only during the early parts of the test program, mainly for cold-gas checkout of the turbine-flywheel assembly. All pressure measuremens were made using Taber, bonded, strain-gage-type transducers. The transducers were selected and installed to provide good measurement accuracy within the expected full scale range.

TABLE 25. IPU ENGINE STARTER DEMONSTRATOR INSTRUMENTATION

SYSTEM	PARAMETER	RANGE	BR	OSC	DIGT	GAGE	TAPE	COMMENTS
JP-4	Tank Pr	0-1000 psig			X	X		
	Orifice Meter ΔP	0-100 psid	X	X	X			
	Turbine Flowmeter	0-1 lb/sec			X			
	Valve U/S Pr	0-1000 psig	X	X	X			
	Injection Pr	0-1000 psig	X	X	X			
	F/M T	0-150 F			X			
	Injection T	0-150 F			X			
GO_2	Valve U/S Pr	0-1000 psig	X		X	X		
	Venturi U/S Pr	0-1000 psig			X			
	Injection Pr	0-1000 psig	X	X	X			
	Venturi U/S T	0-150 F			X			
	Injection T	0-150 F			X			
Combustor	Chamber Pressure	0-500 psig	X	X	X			Redline
	Combustion T #1	0-2000 F	X		X			Redline
	Combustion T #2	0-2000 F			X			
GN_2 Coolant	Venturi U/S Pr	0-1000 psig			X	X		
	Inlet Pr	0-500 psig			X			
	Outlet Pr	0-500 psig			X			
	Venturi U/S T	0-150 F			X			
	Venturi Inlet T	0-150 F			X			
	Venturi Outlet T	0-500 F			X			

TABLE 25. (Concluded)

SYSTEM	PARAMETER	RANGE	RECORDER					COMMENTS
			BR	OSC	DIGT	GAGE	TAPE	
Turbine	Exhaust Pr	0-50 psig			X			
	Exhaust T	0-2000 F			X		X	
	Speed	0-75,000 rpm	X	X	X		X	Redline, 60,000 rpm = 4000 Hz
Gearbox	Speed	0-75,000 rpm	X	X	X			Redline, 60,000 rpm = 5365.8 Hz
	Lub. Oil Pr	0-100 psig			X			
	Lub. Oil T	0-500 F			X			
Brake	Valve U/S Pr	0-2000 psig			X	X		
	Valve D/S Pr	0-2000 psig	X		X			
Lub. Oil	Inlet Pr	0-100 psig	X		X			
	Inlet T	0-500 F			X			
Accelerometer	Turbine Radial #1	50g pp					X	VSC, 10g pp, 100 ms delay, 2K Hz filter
	Turbine Radial #2	50g pp					X	
	Carrier Radial	50g pp					X	
	Carrier Axial	50g pp					X	
	Flywheel Radial	50g pp					X	
GH_2 Drive	Valve U/S Pr	0-1000 psig			X	X		GH_2 drive only
	Venturi U/S Pr	0-1000 psig	X	X	X			Delete JP-4, GO_2, and GN_2 coolant parameters
	Venturi D/S Pr	0-1000 psig	X	X	X			
	Venturi U/S T	0-150 F			X			
Signals	Fuel Valve	--		X	X		X	
	Oxidizer Valve	--		X	X			
	Spark	--		X				

The fuel flowrate was measured using a standard ASME-type, sharp-edge orifice plate flowmeter. The flowrates were determined from the inlet pressure and temperature, and the orifice differential presusre data and by using a standard data reduction program. A good correlation of the flowrate data had been verified in the earlier phase of the IPU gas generator test program, and the accuracy of the demonstrator test data appeared to be consistent. The oxidizer flowrate was measured using a choked sonic nozzle. Flowrates were determined from the measured pressures and temperatures upstream of the nozzle throat.

The temperature measurements were made with chromel/alumel thermocouples with closed and stainless-steel sheaths with grounded junctions. The thermocouples were generally mounted by compression-fit connections on each welded boss. Size of the thermocouple wires was kept uniform and fine, either 1/32 or 1/16 inch in diameter. Combustion gas temperature was measured later with 1/10-inch thermocouples for better durability.

The vibration of the turbine-flywheel assembly was monitored by six accelerometers mounted firmly at various positions as depicted in Fig. 118. Both the radial and axial modes of the turbine vibration were monitored by a total of five accelerometers mounted on the end flanges of the turbine bearing carrier. The flywheel was instrumented for radial vibration monitoring by one accelerometer placed at top of the housing shroud. One of the turbine radial vibration pickups was used as the signal source for a redline safety cutoff.

The speed of the turbine-flywheel assembly was measured by two speed pickups--one for direct readout of the turbine shaft speed and the other reading from the gearbox. The signals from both pickups were calibrated and converted to yield a turbine shaft speed. Both speeds were displayed on the Brush recorder, and further relayed to the automatic sequencer for redline cutoff purposes.

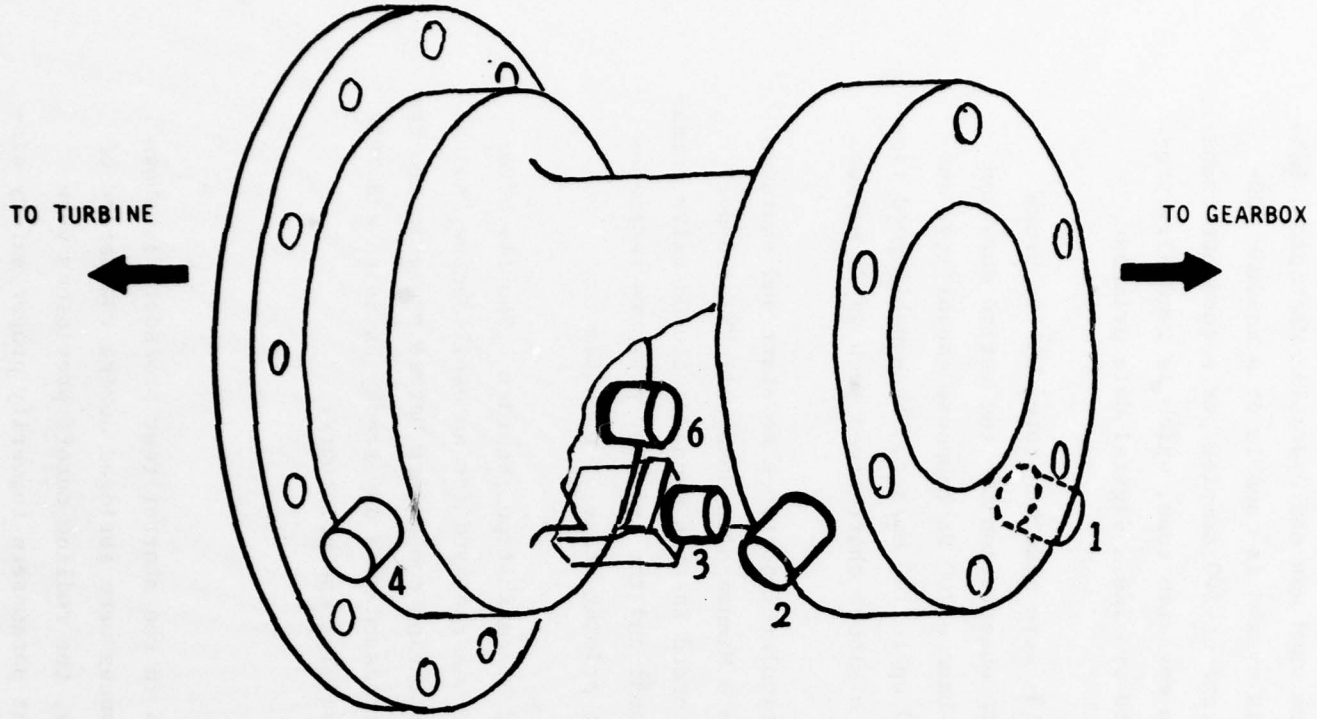

1, 2, 4	RADIAL PICKUP
3, 6	AXIAL PICKUP
5	FLYWHEEL RADIAL PICKUP (NOT SHOWN)

Figure 118. Accelerometer Positions Around Bearing Carrier

Data Acquisition System

The primary data recording system used was the Hydraulic-Mechanical Laboratory Digital Data System. This system is capable of a maximum 200-channel record, recording at a rate of 100 samples per second per channel. The actual recording was made on magnetic tape, which is generally processed shortly after each test to provide a digital data printout.

The major parameters (totaling 14) were also monitored by two Brush recorders for continuous, *in situ* observation for the entire duration of a test. The Brush recorders have a 200 Hz response capability, and were capable of fast chart speed up to 100 mm/sec. Reasonably good time resolution is possible by using a slower chart speed such as 25 mm/sec.

The parameters that were of particular importance to start and shutdown transients were also recorded on a Minneapolis Honeywell "Visicorder" type oscillograph. The data recorded in this manner included valve actuation signals, spark igniter pulses, and the injector pressure responses during the the actual propellant priming stage of each test.

The vibration data were recorded by an FM tape recorder. Shortly after each test operation, the FM tape was replayed for an oscilloscope "quick-look" at the vibrations of the rotating components before proceding to the next test. The FM tapes were processed on a day-to-day basis to add IRIG count signals and to generate oscillograph printouts.

System Controls

A complete control sequence used in the starter test procedure is shown in Fig. 119. Although the sequences were abridged during the period of individual system checkout tests, the redline cutoff provisions were always retained for the pertinent parameters to verify proper safety circuit function if a malfunction occurred. The redline parameters, either for manual pretest, and/or for automatic cutoff, are indicated in the instrumentation list (Table 25).

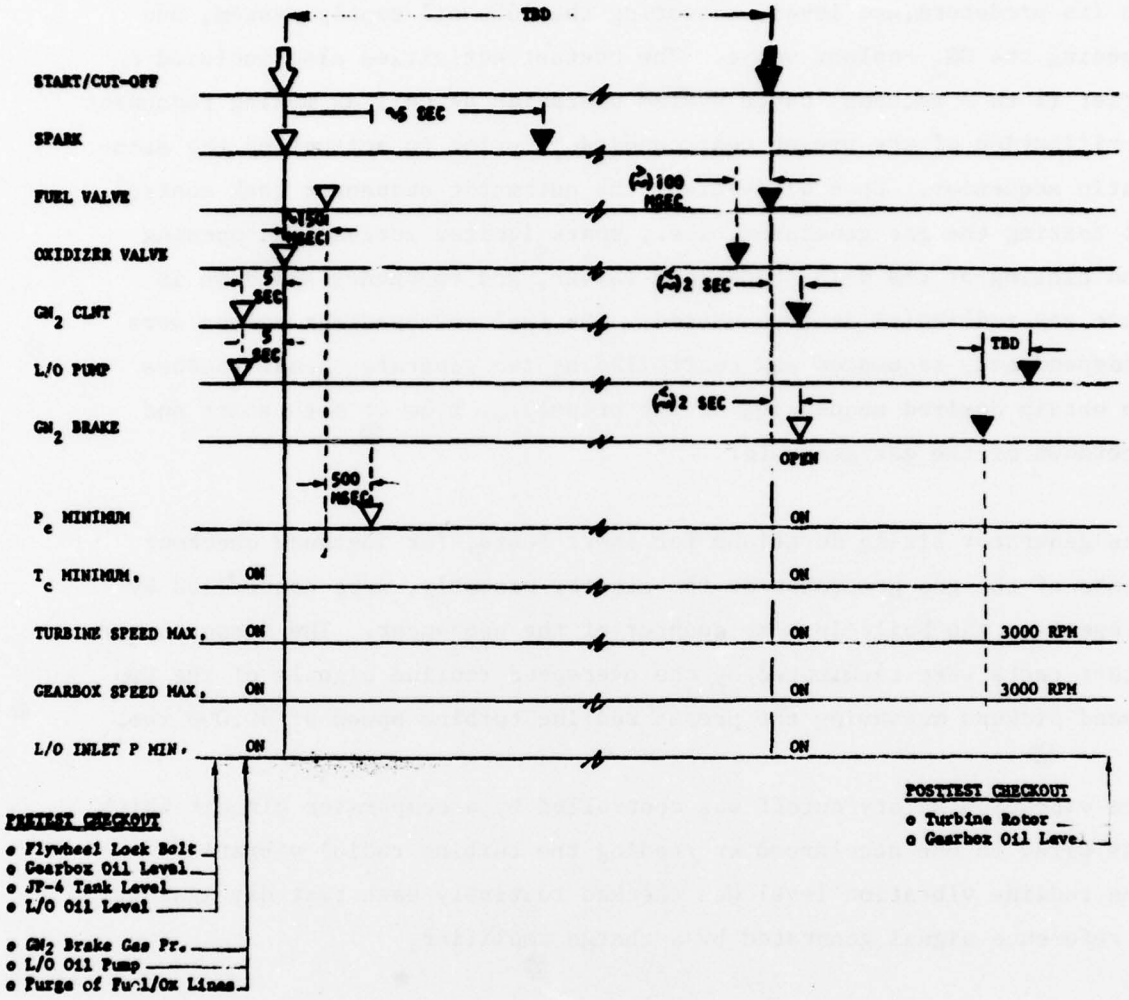

Figure 119. Test Sequencing for Starter Demonstration Tests

Under normal operating conditions, the starter test operation began with activating the support systems such as pressurizing the fuel supply tank to its predetermined level, actuating the lube-oil supply system, and opening the GN_2 coolant valve. The pretest activities also included a brief (2 to 5 seconds) purge system operation as well as making redundant verification of the preset test conditions prior to activating the automatic sequencer. Upon activation, the automatic sequencer took control of testing the gas generator, i.e., spark igniter activation, opening and closing of the main propellant valves, and emergency shutdown in case any redline(s) is encountered. The fuel and oxidizer valves were independently sequenced and controlled by two separate signal sources to obtain desired sequencing of the propellant flow at both start and shutdown of the gas generator.

Gas generator firing durations for short tests, for instance checkout tests of the gas generator or the starter assembly, were controlled by presetting the built-in time counter of the sequencer. The demonstrator start tests were terminated by the overspeed redline signals of the two speed pickups measuring the preset redline turbine speed of 60,000 rpm.

The vibration safety cutoff was controlled by a comparator circuit which was wired to one accelerometer reading the turbine radial vibration. The redline vibration level was checked routinely each test day against a reference signal generated by a charge amplifier.

The termination of each starter test began with energizing the brake gas control valve, normally within a few seconds after the gas generator cutoff, followed by closing the coolant valve. The brake gas flow remained on to rapidly decelerate the flywheel, and was turned off after the turbine slowed down to approximately 6000 rpm. The lubrication system was the last item to be turned off, normally after verification of a near static condition of the flywheel and turbine.

TEST PROGRAM

The overall test program for the IPU Engine Starter Demonstrator was conducted in three parts: Part 1, Gas Generator Checkout Tests (hot fire); Part 2, Cold-Gas Turbine Drive Checkout Tests; and Part 3, System Start Demonstration Tests. The planned test matrix of the test program is presented in Table 26. The test operation in each part progressed from short-duration checkout series to a full duration test. The overall test program closely followed the planned test matrix. The test conditions and the major results are summarized in Table 27.

Gas Generator Checkout Tests

The primary objective of the gas generator checkout tests was to determine the gas generator operating characteristics with a new facility propellant feed system. Principal information derived from the checkout tests was:

1. Flow resistance characteristics of the facility propellant feed system, especially on the fuel side.
2. Priming and emptying characteristics of both the fuel and oxidizer sides, reckoned from the valve actuation times. Finite dribble volumes between the facility main valves and the injector manifold inlets which may cause delayed priming at the start transient, viz, ~50 to 60 msec for the oxidizer and ~200 to 250 msec for the fuel priming. Priming times for both sides which were determined directly from the injection pressure traces, i.e., P_{IO} and P_{IF} as shown in Fig. 120.

TABLE 26. IPU STARTER DEMONSTRATOR TEST MATRIX

Test No.	Test Day	Objective	Duration, seconds	Conditions and Procedure
Gas Generator Checkout				Demonstrator propellant feed system. Gas generator only. Simulated turbine manifold (existing).
-	1	Establish System Characteristics	2	Blowdown each system. Use afterburner with fuel blowdown.
1	2	Previous Test Conditions	2	MR = 0.55 and full flow.
2-3	2	Adjust MR for 1650 F gas. Ignition and Shutdown Diagnostics	2	Nominal sequence
4-6	3	Coking Characterization at Planned Duration	23	Nominal sequence. Cool hardware between runs.
7-8	4	Off Design Flowrate	2	Nominal sequence.
Cold-Gas Turbine Drive				Demonstrator system without gas generator. Adapter with GH_2 inlet.
9	5	Dynamic Balance. Instrumentation Checkout. Gas Brake Checkout.	20	Open GH_2 valve and slowly increase pressure. Cutoff at 20,000 rpm. Use brake to slow.
10	5	Nominal Sequence Checkout	10	Set nominal GH_2 pressure. Cutoff at 30,000 rpm.
11	5	Full Speed Checkout. Verify Critical Speed.	23	Set nominal GH_2 pressure. Cutoff at 60,000 rpm.
12-13	6	Adjust GH_2 for Start Simulation	23	Set nominal GH_2 pressure. Cutoff at 60,000 rpm.
System Start Demonstration				Hot-fired system.
14-15	7	Verify Hot-Gas Drive	2 & 10	Nominal flow and mixture ratio.
16	7	Full Speed Checkout With Hot-Gas Drive	23	Nominal flow and mixture ratio. Cutoff at 60,000 rpm.
17-18	8	Simulate Start Time. Start Simualtion Characteristics	23	Nominal mixture ratio. Adjust flowrate for target start time. Cutoff at 60,000 rpm.
19-28	9-11	Duty Cycle Demonstration	23	Nominal mixture ratio. Selected flowrate. Cool hardware at start. Cutoff at 60,000 rpm.

TABLE 27. IPU ENGINE STARTER DEMONSTRATOR TEST SUMMARY

Run No.	Date	Configuration	Duration (sec.)	Max. N rpm	Comments*
1.01	5/23/78	GG Checkout	-	-	Ignition failure
1.02	5/23/78	GG Checkout	-	-	Ignition failure
1.03	5/23/78	GG Checkout	1.2	-	Increase O_2 lead
1.04	5/23/78	GG Checkout	1.2	-	
2.01	5/24/78	GG Checkout	4.0	-	
2.02	5/24/78	GG Checkout	3.4	-	
2.03	5/24/78	GG Checkout	2.3	-	
2.04	5/24/78	GG Checkout	3.1	-	
2.05	5/24/78	GG Checkout	23.2	-	
2.06	5/24/78	GG Checkout	23.1	-	
2.07	5/24/78	GG Checkout	22.6	-	Completion of G.G. checkout tests
3.01	5/30/78	GN_2 Turbine	11.4	3,750	Slow speed ramp
3.02	5/30/78	Drive	45.2	20,000	Slow speed ramp
3.03	5/30/78	GH_2 Turbine	24.2	19,800	Partial turbine drive flowrate
4.01	5/31/78	Drive	17.1	22,000	Partial turbine drive, manual cut
5.01	6/01/78	"	13.8	29,800	VSC cut with speed cut - increase VSC level
5.02	6/01/78	"	26.8	57,800	Completion of cold spin checkout tests
6.01	6/03/78	GG Turbine	3.9	11,600	
6.02	6/03/78	Drive	-	-	Ignition failure; cut-off by T_c overshoot at start; 80% supply pressures
7.01	6/05/78	"	9.1	25,200	
8.01	6/06/78	"	-	-	Cut, facility malfunction
8.02	6/06/78	"	-	-	Cut, low lub. oil pressure
8.03	6/06/78	"	25.2	60,100	
9.01	6/07/78	GG Turbine	25.1	60,200	
9.02	6/07/78	Drive	13.2	36,300	VSC cut

* Tests conducted at full power except as noted.

TABLE 27. (Concluded)

Run No.	Date	Configuration	Duration (sec.)	Max. N rpm	Comments*
10.01	6/15/78	GG Turbine Drive	24.3	60,180	
10.02	6/15/78	GG Turbine	-	-	Overtemp cut (at start transient)
10.03	6/15/78	Drive	-	-	Overtemp cut; no hardware discrepancy
11.01	6/16/78	"	25.5	60,090	Purge-lead used at start transient
11.02	6/16/78	GG Turbine	-	-	Overtemp cut
11.03	6/16/78	Drive	25.3	60,540	Purge-lead plus shorter GoX-lead
11.04	6/16/78	"	-	-	Overtemp cut
12.01	6/19/78	GG Turbine	25.7	60,270	Repeated 11.03 w/o purge-lead
12.02	6/19/78	Drive	27.0	60,811	Run at lower T_c & P_c
13.01	6/20/78	"	25.5	60,450	
13.02	6/20/78	"	25.7	60,133	
14.01	6/22/78	GG Turbine Drive	27.5	60,680	Run at lower T_c; completed 10 demonstration tests
15.01	6/23/78	"	25.4	60,130	Extra run to document (movie) self-estinguishing exhaust

* Tests conducted at full power except as noted.

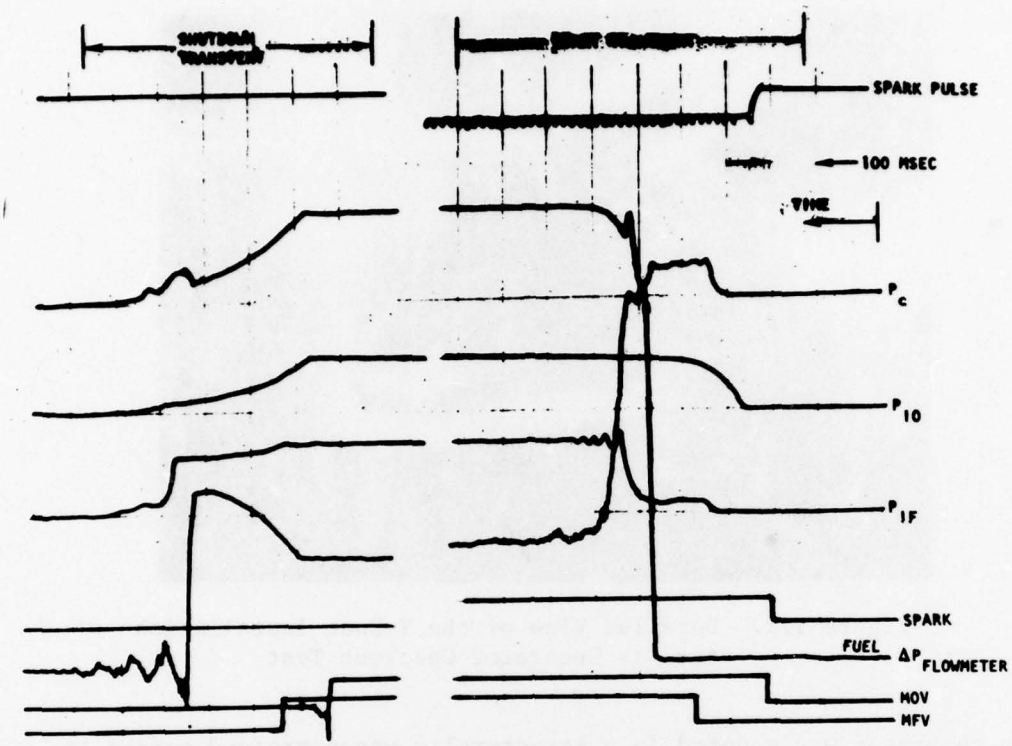

Figure 120. Oscillograph Showing Start and hutdown Transient (Test 2.06)

Test Setup. The test setup involved in the gas generator checkout tests consisted of the high-power gas generator (with oxidizer injector orifices modified) and the uncooled "Y-duct" section. The twin orifices at the ends of the Y-duct were enlarged to 0.50 inch in diameter each to closely simulate the effective flow resistance expected for the real turbine manifold. Figure 121 shows the Y-duct flange-coupled to the exhaust discharge pipe to preclude air entrainment and possible combustion in the exhaust during gas generator firing.

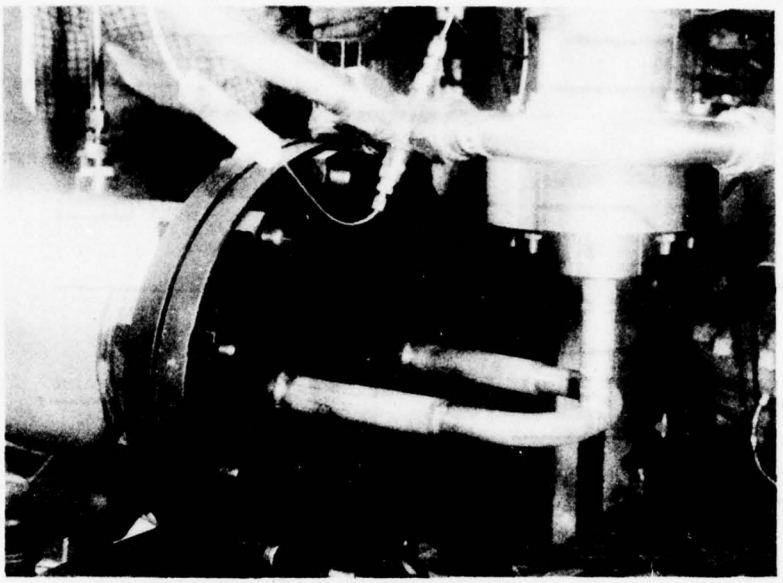

Figure 121. Detailed View of the Y-Duct Installation for Gas Generator Checkout Test

The gas generator was mounted in a structurally unconstrained manner to allow some degree of axial expansion of the gas generator during the test operation. This was largely achieved by letting the facility feed lines support part of the gas generator weight. This feature was particularly beneficial for the full demonstrator assembly in which excess load on the turbine manifold housing was avoided.

All the instrumentation related to the Phase I gas generator testing remained intact, as originally installed, for the starter demonstrator tests. A thermocouple was positioned at the upstream flange of the Y-duct for the hot-gas temperature measurement.

Short-Duration Tests. The "cold-flow" checkout tests were initiated on 23 May 1978 after a series of leak checks on the facility feed system and a detailed calibration of the pressure instrumentation. A series of blowdown runs then followed with the fuel side and oxidizer side separately actuated for preliminary checkout, followed by simultaneous valve actuations

without operation of either the gas generator spark igniter or the exhaust burner torch. The blowdown test with simultaneous valve openings revealed a significant difference in the priming times (~150 msec faster oxidizer prime) and a slight pressure rise ($\lesssim$10 psig) on the fuel side just prior to priming. This apparently was a combined result of compression by the advancing liquid fuel slug and by the backflow of the oxidizer gas from the combustion chamber.

The "hot-fire" checkout tests were initiated with presetting the automatic sequencer for a 1-second test duration (nominal). The sequencer was also preset for the simultaneous propellant priming at the start transient; that is, by energizing the fuel valve 150 msec earlier than the oxidizer valve. This was deemed necessary based on the results of the gas generator/facility checkout tests. The first two tests conducted encountered ignition failure. The hot-fire checkout firing was repeated with the sequencer reset for $\gtrsim$100 msec oxidizer lead at the start transient, flawless ignition was achieved for two tests in a row. The gas generator testing continued in order to obtain an accurate value of the fuel-side flow resistance coefficient ($\Delta P\rho/\dot{w}^2$) during the hot-fire operation. Typical traces of the short-duration gas generator firings are shown in Fig. 122. The fuel feed system flow resistance coefficient was determined to be 4×10^4 lbf-sec^2/lbm-ft^2, which is equivalent to a total system ΔP of 166 psid for a nominal fuel flowrate of 0.45 lbm/sec.

The hot-gas temperatures measured during the first two short-duration checkout runs did not reach the steady-state limits, but generally displayed a good correlation with the mixture ratio. Typical temperature vs mixture ratio relation obtained in the checkout tests is presented in Fig. 123 by flagged symbols. The results correlated very well with the LOX/RP-1 data reported in the past for the Rocketdyne H-1 and F-1 rocket engine gas generator studies.

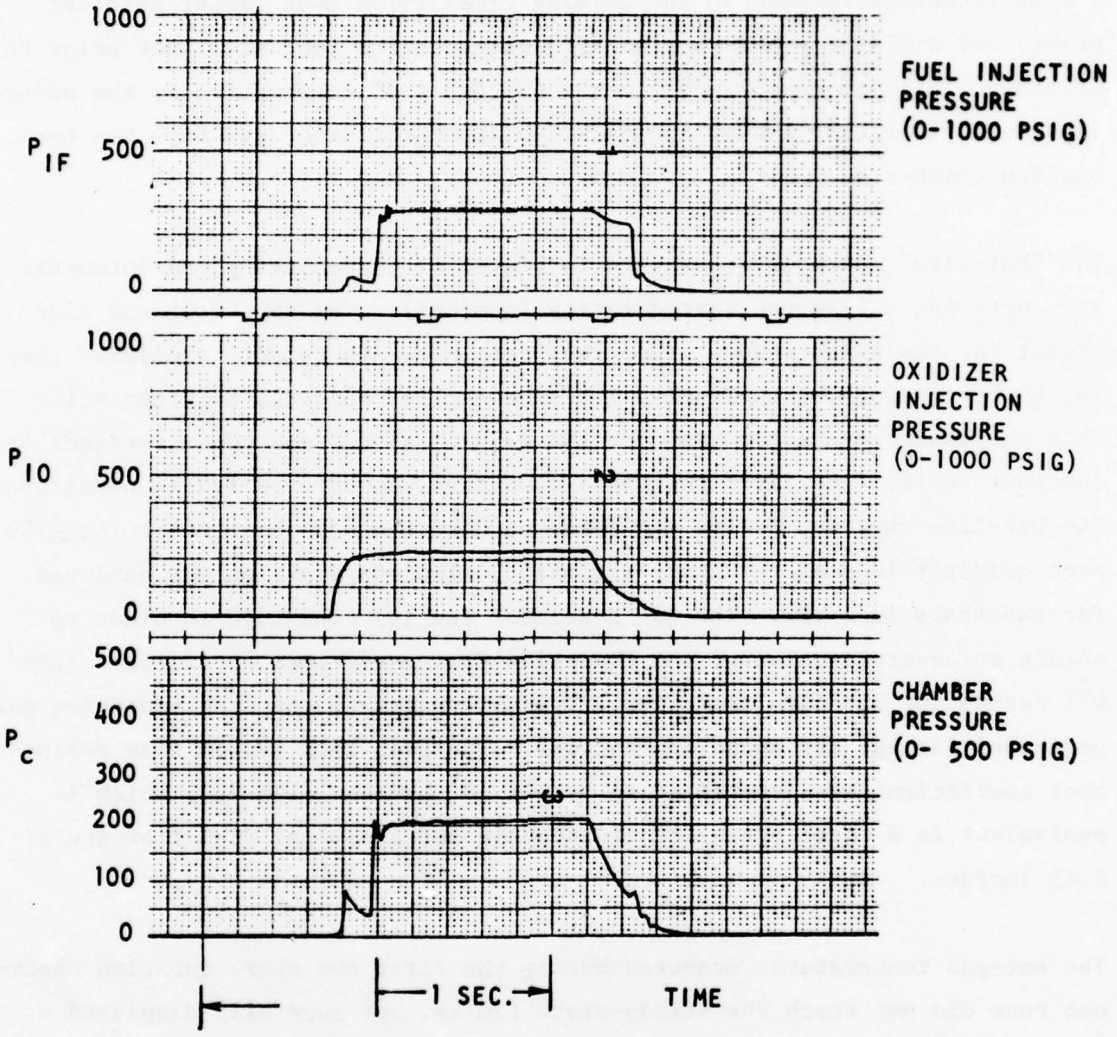

Figure 122. Gas Generator Checkout Test - 5/24/78

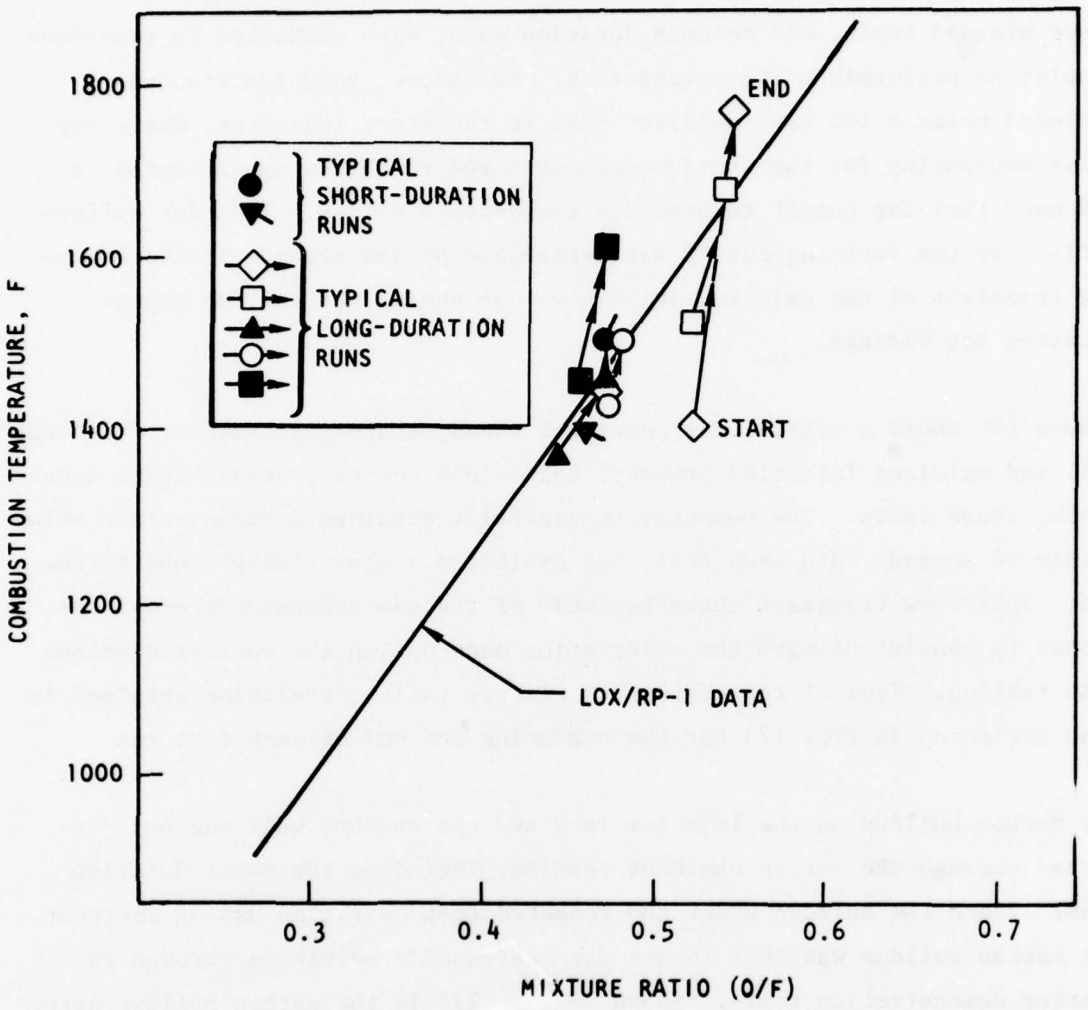

Figure 123. High-Power Gas Generator Performance Obtained During Checkout Tests

Long-Duration Tests. The purpose of the long-duration checkout tests was to evaluate the steady-state performance and the carbon buildup characteristics of the gas generator for the typical duration of the starter operation. Three planned tests, ~23 seconds duration each, were conducted to reproduce consistent performance characteristics. As before, good ignition was achieved using a 100 msec oxidizer lead at the start transient, while the valve sequencing for the shutdown was tailored to obtain approximately a 150 msec fuel-lag cutoff to preclude temperature spikes. The time differential for the fuel-lag cutoff was determined by observing a finite emptying transient of the oxidizer dribble volume during the earlier short-duration hot firings.

Figure 124 shows a typical gas generator steady-state performance. Both the fuel and oxidizer injection pressure maintained constant steady-state levels during these tests. The temperature generally attained a steady-state value within 10 seconds into each test, but exhibited a slow rising trend to the end. This slow transient characteristic of the gas generator thermal response is consistent with the observation made during the earlier development testing. Typical temperature vs mixture ratio correlation obtained is also presented in Fig. 123 for the beginning and end of each test run.

The carbon buildup on the injector face and the chamber wall was not disturbed through the entire checkout testing, including the short-duration runs. Since the buildup under the repeated test operation was of interest, the carbon buildup was left intact for continued observation through the starter demonstration tests. Shown in Fig. 125 is the carbon buildup after the long-duration (23.2 seconds) test plus the preceding 6 runs (totaling 15.2 seconds). The posttest inspection made after the third long-duration test showed practically the same buildup characteristics except for slightly added growth near the upper section of the chamber wall, near the injector face.

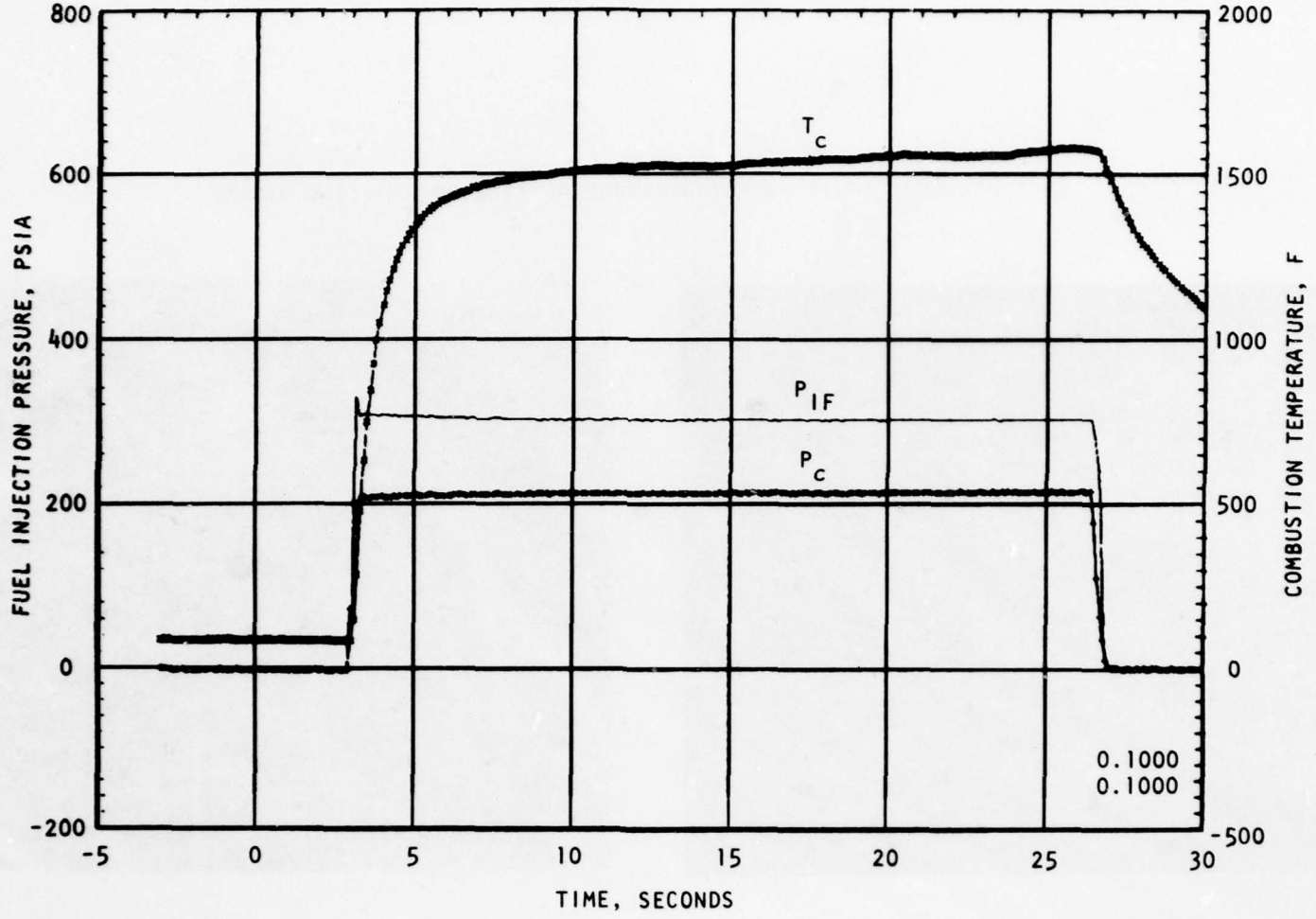

Figure 124. Combustion Performance of Gas Generator With Y-Duct Nozzle Installation

Figure 125. Carbon Buildup Characteristics After Test Run 2.05

Turbine-Flywheel Checkout Tests

The cold-flow spinup of the turbine-flywheel rotating hardware assembly was performed to determine the turbine vibration response and the mechanical integrity of the assembly. The test sequence used in the cold-flow tests is presented in Fig. 126. The checkout was completed in five runs using, initially, nitrogen as a drive gas for low-speed checkout. Hydrogen gas was used in the final three runs for higher acceleration spinup. The hydrogen flowrate was increased in steps before making a full-acceleration checkout at a power level equivalent to the gas generator operation. A summary of the hydrogen spinup test results is presented in Table 28. Except for the first checkout test made with nitrogen drive gas, the checkout tests were made by setting the redline speed at a predetermined level, and the tests were terminated by the automatic sequencer.

TABLE 28. SUMMARY OF GH_2 SPINUP DATA

Run	P_{Turb} Exhaust, psia	T_{Turb} Exhaust, F	N_{Turb}, rpm	N_{GB}, rpm	P_{H_2} Vent, psia	T_{H_2} Vent, F	P_{H_2} D/S, psia	Duration, seconds	c^* ft/sec	$\dot{w}_{H_2}$, lbm/sec	A^*_{Turb}, in.^{2}
3.03	14.9	24.1	20,120	19,813	98.1	63	72.3	24.2	5243	0.145	0.328
4.01	15.2	22.5	21,883	21,591	134.2	72	96.0	16.7	5288	0.197	0.338
5.01	15.6	0.5	30,134	29,832	201.3	82	146.0	13.8	5337	0.293	0.333
5.02	15.2	-44.5	57,962	57,457	193.1	68	139.3	26.8	5262	0.285	0.335

- Check on $\dot{w}$ calculation: P = 193.1 psia, T = 528 F, C^1 = 0.6858, c^* = 5261.8 ft/sec, A^*_{vent} = 0.2417 in.^{2}, $\dot{w}$ = 0.285 lbm/sec
- $A^*_{Turb/Effective}$ = 0.334

The vibration redline was initially set at an exceptionally low 10 g peak-to-peak with a 100 msec delay. This redline setting tripped the sequencer in one of the checkout runs (Run 5.01) at a speed of 30,000 rpm. The following full-acceleration test (Run 5.02) was conducted with the vibration redline set at a reasonable 25 g peak-to-peak with a 100 msec delay, and setting the redline speed at 60,000 rpm for both the turbine and the gearbox mounted pickups. No further problems were encountered. The results of the cold-flow, full-acceleration checkout tests are presented in Fig. 127.

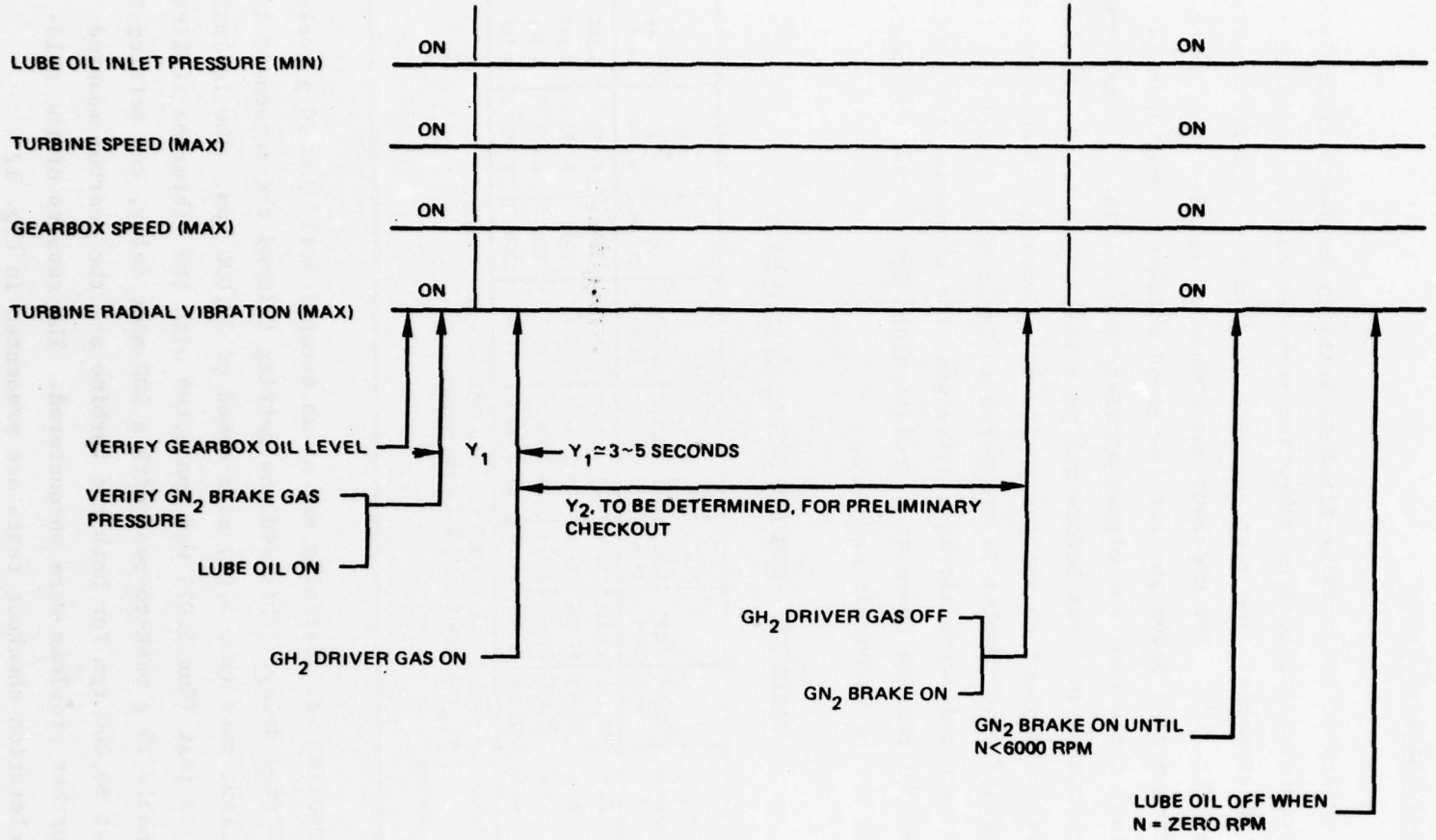

Figure 126. Sequence for Cold Spin (Test Series II)

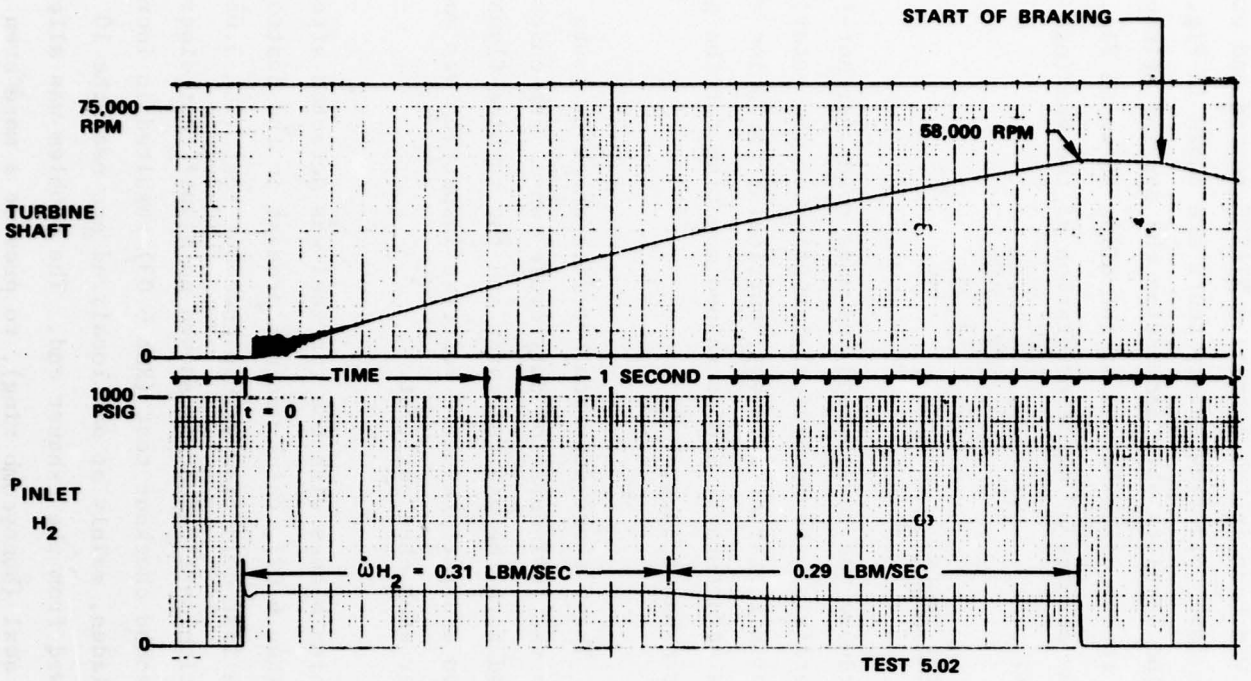

Figure 127. Full-Acceleration Cold-Flow Spinup of Turbine and Flywheel With Hydrogen Drive Gas

The vibration responses recorded on the FM tapes were processed and reviewed after each test day to monitor the performance of the turbine assembly. The vibration data reduction was made in two forms: a STATOS record and an isoplot obtained from the last cold-flow spinup tests are shown in Fig. 128 and 129, respectively. The isoplots obtained during the earlier spinup tests also exhibited the random distribution of the blips shown in Fig. 129. This was indicative of the absence of an deterioration of the bearings or other rotating components.

Engine Starter Demonstrator Tests

The full demonstrator hardware was reassembled and made ready for hot-fire checkout shortly after verifying the mechanical integrity of the rotating system. In restoring the full starter assembly, particular attention was directed to maintaining a structurally unconstrained mounting for the gas generator and the turbine exhaust duct.

Initial System Checkout. Three short-duration hot-fire checkout tests were made before proceeding to the full-duration duty cycle runs. The checkout tests generally reproduced both the gas generator and the turbine-flywheel design operating condition and performance. Posttest inspection was made on the turbine rotor after each checkout test.

Minor rubbing of the turbine blades with the tip seal was detected after the 10-second checkout test (Run 6.02), which was not present in the posttest inspection made after the last cold-flow spinup checkout test (Run 5.02). The results of the vibration data reduction showed no significant discrepancy. A subsequent 10-second checkout test (Run 6.03) resulted in increased rubbing of the turbine blades, mainly at one localized arc near the 10 o'clock position, as viewed from the exhaust end. The problem was alleviated by rotating the tip seal (honeycomb ring), to provide a more even clearance without any hardware rework.

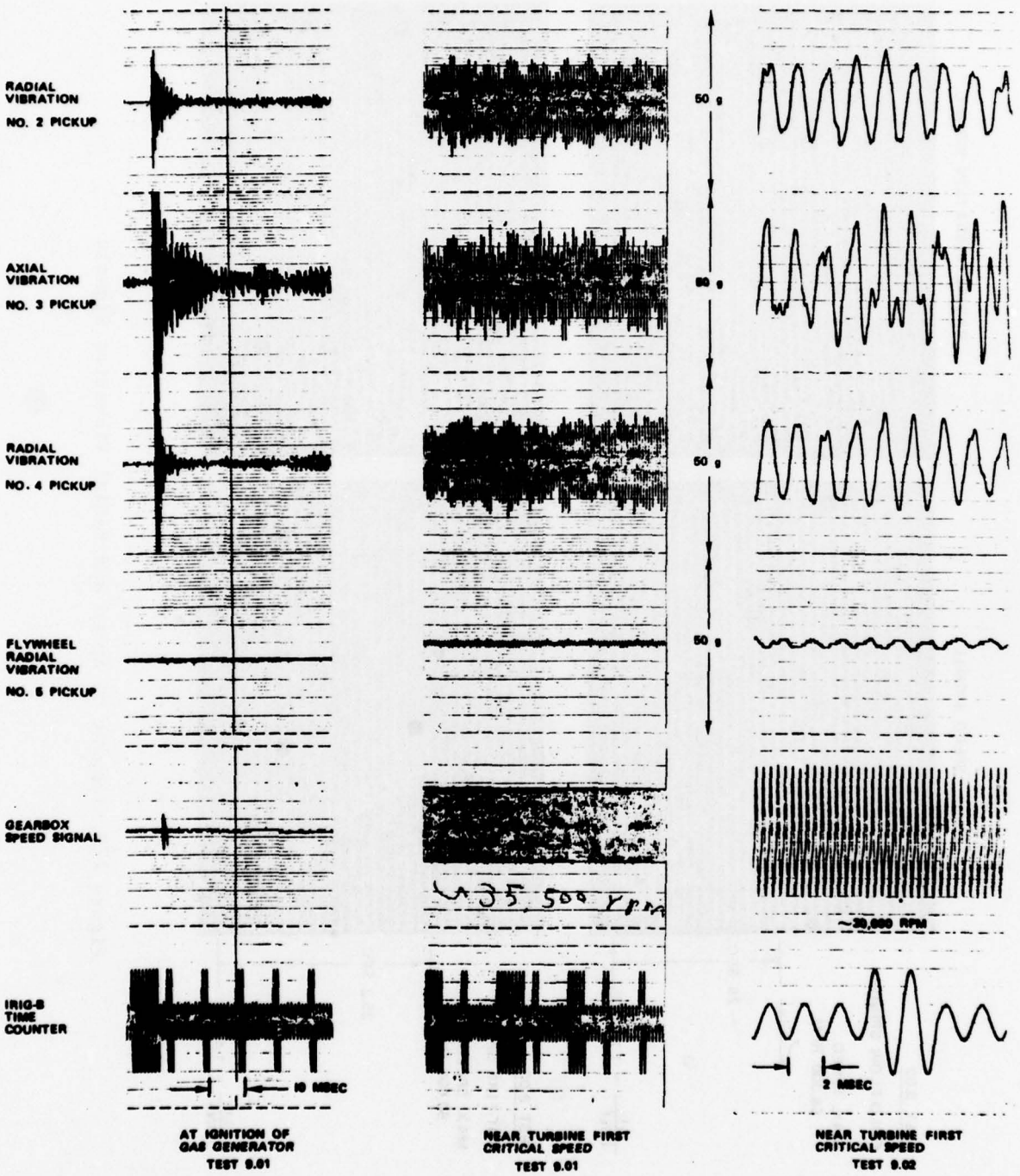

Figure 128. Typical Traces of STATOS Record

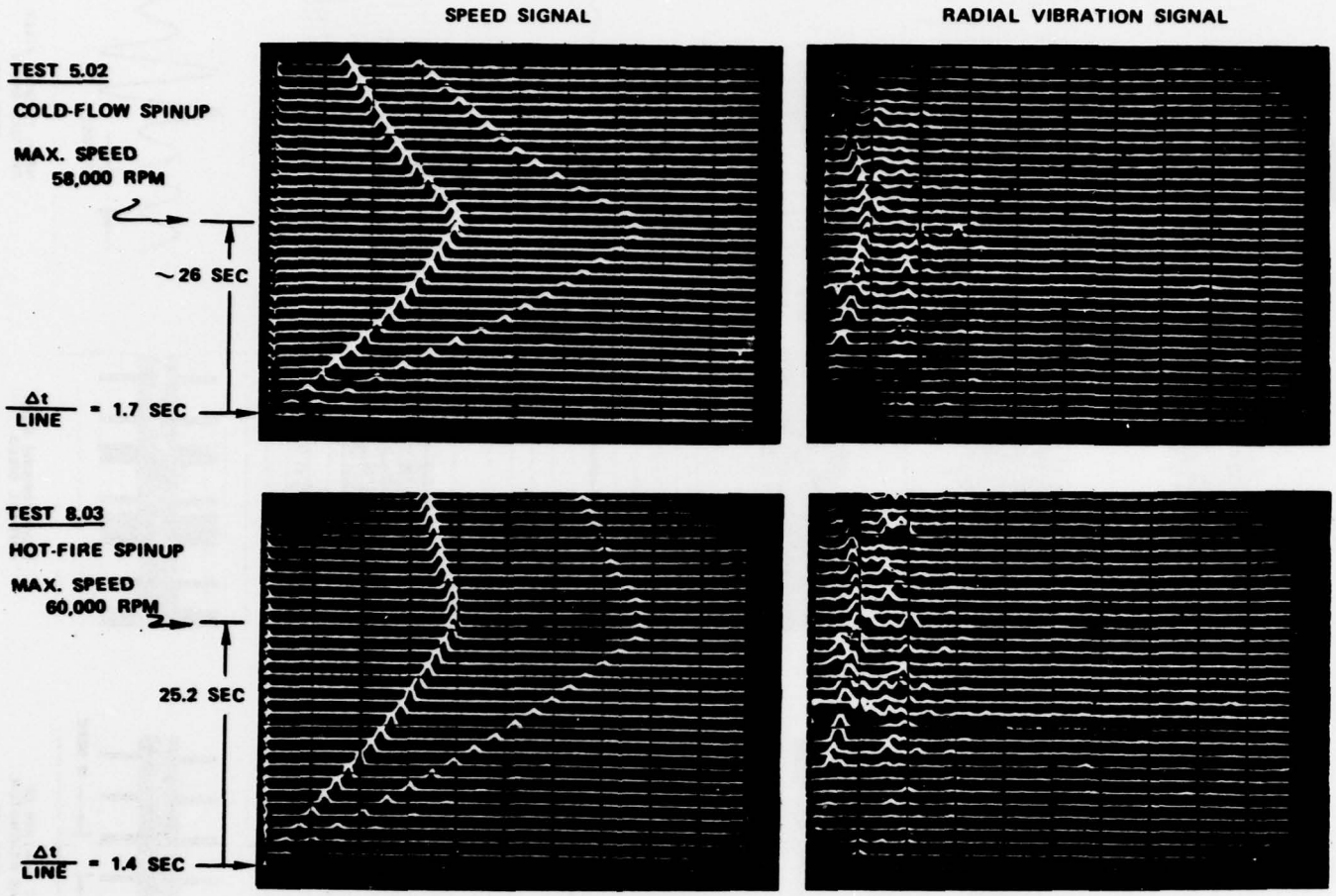

Figure 129. Isoplot of Speed and Radial Vibration Signals

Full Demonstration Tests. The demonstration tests for the complete engine starter assembly began on 6 June 1978, and 11 tests of full duty cycles were successfully completed on 23 June 1978. During initial runs, a redline cutoff was encountered due to a brief temperature overshoot at the start transient, usually in a form of a spike peaking at 1900 F. The overshoot transient, i.e., time lapse above the redline value of 1700 F, seldom exceeded 40 msec, and was readily detected by the sensitive thermocouples of 1/32-inch diameter used. The cause for the overshoot is due to ignition of combustible gas from the fuel-soaked carbon layer; it was not due to any irregularity associated with the propellant injection, and represented no operational problem. This problem also occurred during gas generator tests. The condition was simply rectified by replacing the old thermocouples with thermally less sensitive 1/16-inch diameter thermocouples.

A vibration-related cutoff was encountered once during Run 9.02. The redline (25 g peak-to-peak, 100 msec delay, was tripped at 36,000 rpm turbine shaft speed. Detailed review of all the vibration data obtained up to Run 9.02 did not disclose any conspicuous hardware discrepancy and testing proceeded through the entire remaining tests with a new redline (30 g peak-to-peak and 250 msec delay), with all other redline settings being unchanged.

A total of 11 hot-fired, full-acceleration start tests in succession were successfully achieved with the IPU engine starter demonstrator. Engine start was consistently demonstrated within 25.5 seconds with gearbox output power and speed of 228 horsepower and 7777 rpm, respectively. A typical starter performance during full-power acceleration (Run 13.01) is shown in Fig. 130 with smooth acceleration and steady-state combustion.

The test results, and test conditions of all starter tests are summarized in Table 29. The test results also are plotted in chronological order in Fig. 131. The test-to-test sawtooth trace of gas generator chamber pressure indicates an alternate buildup nd spalling of carbon formed in the turbine nozzles, causing an alternate decrease and increase in turbine nozzle inlet flow area. A trend of increasing carbon buildup is indicated. After

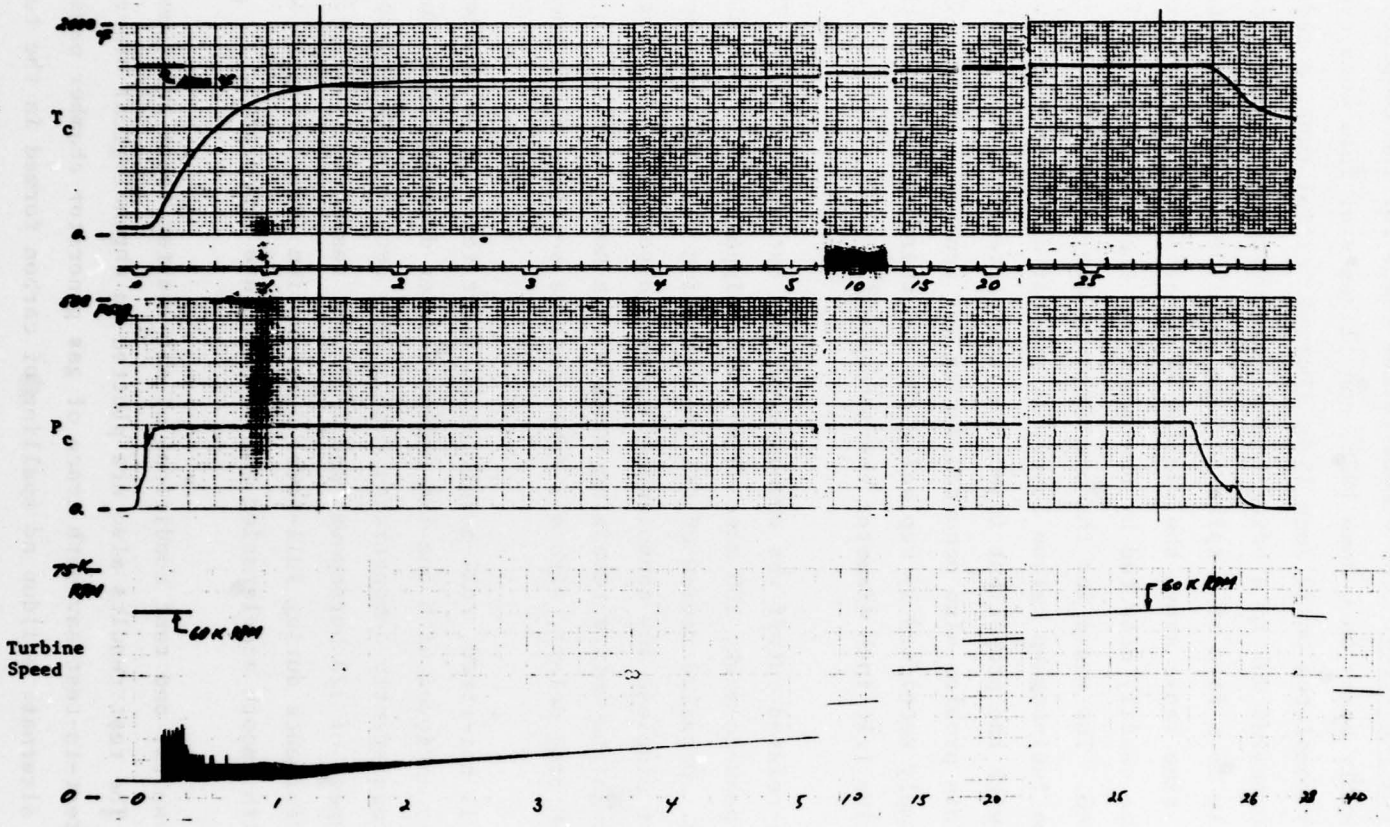

Figure 130. IPU Engine Starter Demonstrator Performance During Full-Power Acceleration (Run 13.01)

TABLE 29. IPU ENGINE STARTER DEMONSTRATOR TEST RESULTS.

Test	Hot-Fire Duration, seconds	GOX Flowrate, lbm/sec		Fuel Flowrate, lbm/sec		MR (o/f)		P_c, psia		T_{C1}, F		$\dot{w}_{CLNT}$, lbm/sec	N_{TURB}, rpm	N_{GB}, rpm
		Ignition + 1 sec Start	End	Start	End	Start	End	Start	End	Start	End			
6.01	3.9	0.208	0.208	0.435	0.433	0.476	0.481	200.	202.7	1430	1505	0.602	11,520	NG
7.01	9.1	0.205	0.305	0.445	0.436	0.445	0.470	199.5	204.3	--	--	0.578	24,935	24,698
8.03	25.2	0.204	0.204	0.444	0.431	0.461	0.473	200	210	1400	1474	0.646	60,042	59,033
9.01	25.1	0.204	0.204	0.426	0.413	0.477	0.486	204	211.8	1436	1490	0.636	60,350	59.700
9.02	13.4	0.205	0.2044	0.423	0.413	0.485	0.495	205.3	213.3	1450	1521	0.618	36,554	36,046
10.01	24.3	0.208	0.2084	0.438	0.427	0.477	0.488	211	212.6	1463	1531	0.640	60,178	59,843
11.01	25.5	0.205	0.205	0.428	0.419	0.480	0.489	207.2	213	1474	1580	0.615	60,087	59,483
11.03	25.3	0.207	0.207	0.424	0.414	0.488	0.479	213.1	216.2	1250	1326	0.617	60,540	60,068
12.01	25.7	0.200	0.2011	0.440	0.430	0.456	0.468	197.8	203.6	1318.8	1456	0.645	60,268	60,113
12.02	27.0	0.203	0.203	0.434	0.420	0.468	0.483	200	210.3	1346	1491	0.674	60,811	60,474
13.01	25.5	0.204	0.204	0.433	0.414	0.472	0.492	215.8	222.2	1335	1588	0.622	60,449	59,978
14.01	27.5	0.200	0.1984	0.432	0.430	0.460	0.461	223.2	225.7	1400	1439	0.636	60,675	60,068
15.01	25.4	0.202	0.202	0.387	0.372	0.523	0.544	239.5	251.2	1525	1684	0.644	60,133	59,978

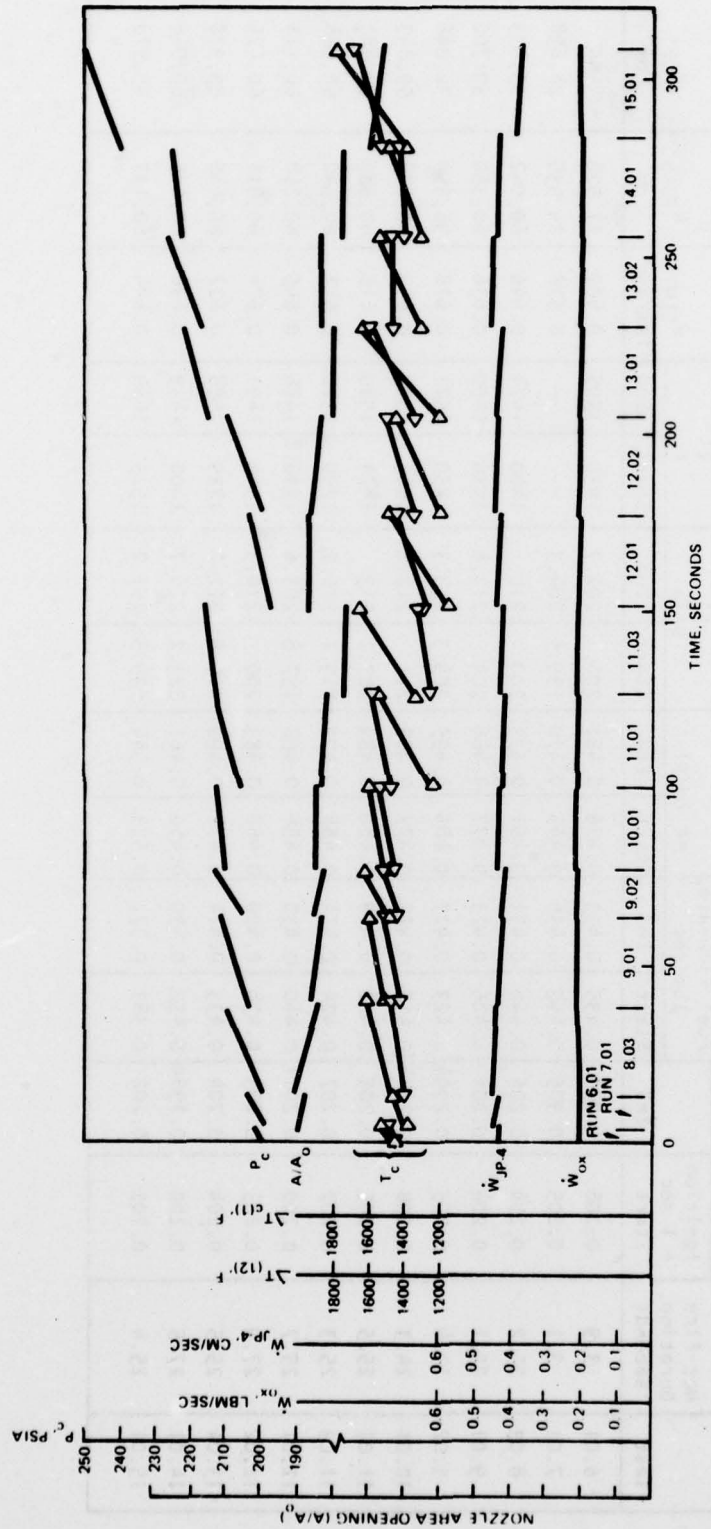

Figure 131. Variation of Test Parameters Through the Starter Demonstrator Test Series

completion of the entire demonstration test series, the gas generator and turbine were completely disassembled and were found in good condition. The gearbox and flywheel also were in good condition.

Gas Generator Performance. The gas generator performed satisfactorily throughout the entire demonstration test series. In general, both combustion temperature and pressure exhibited a slight updrift during each test. As indicated in Fig. 139, the combustion pressure varied between tests, and exhibited a "sawtooth" characteristic indicating a change in turbine nozzle area at each start.

The foregoing observation contrasted with the insignificant combustion pressure variation observed during the earlier gas generator checkout tests (Fig. 124). The combustion temperatuare practically attained a steady-state value within a few seconds after ignition, but continued to rise as a result of mixture ratio shift concurrent with fuel flow reduction caused by combustion pressure increase. The steady-state performance of the gas generator was evaluated by taking the combustion temperature and the mixture ratio near the end fo the test, and the results are shown in Fig. 132. Good correlation with LOX/RP-1 performance is evident again. The gas generator hardware was found to be in good condition.

Turbine Performance. The Mk 44F turbine power output was found satisfactory, and the spinup to the maximum speed consistently required approximately 25.5 seconds (average) instead of the estimated 23 seconds. The lower torque was, in part, due to finite pressure loss in the passage between the gas generator and the turbine inlet, which was estimated to be at least 20 psi at the typical mass flow operating condition of $\dot{w} \sim 0.65$ lbm/sec. Increased turbine blade tip rubbing during the hot-fire operation also contributed to lower torque, especially in view of slight binding of the turbine rotor against the tip seal observed in most of the posttest inspections.

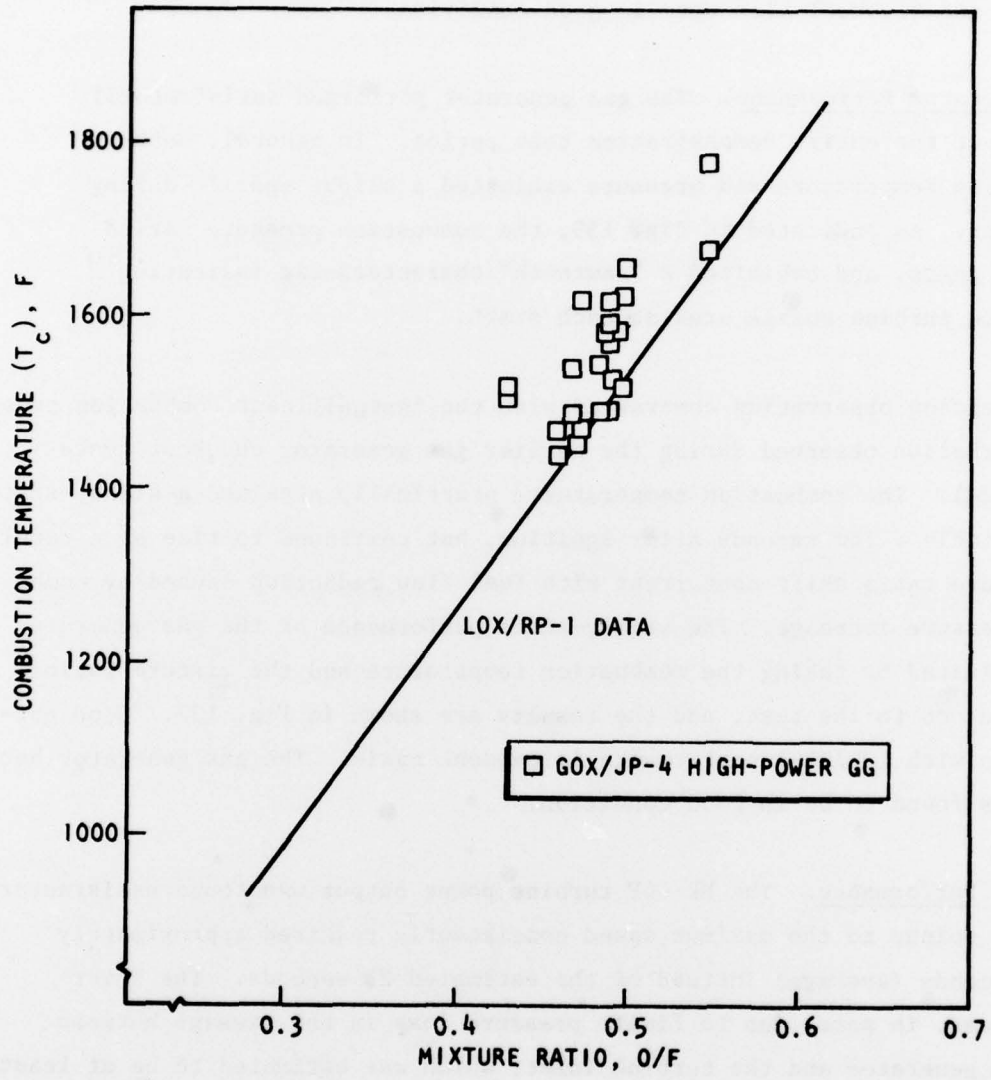

Figure 132. Gas Generator Performance in the IPU Engine Starter Demonstrator

The blockage of the turbine nozzles was calculated for each test by taking into account the effect of gas temperature and gas throughput, which varied from one test run to another, as well as during each test. The area change is presented in Fig. 131 in a normalized form with the effective nozzle area of 0.334 $in.^2$, used as the reference. The results indicate approximately 24% of the turbine total inlet nozzle area was affected by coking after 300 seconds of operation.

After the turbine was completely disassembled and visually inspected, no major hardware discrepancies were evident and only two minor problems were noted. These were rubbing of the turbine blades against the honeycomb tip seal and a localized flaking of the tungsten carbide, flame plating on the turbine wheel hub. Both problems are probably the result of using an existing turbine at conditions other than those for which it was designed.

Carbon Buildup. The physical characteristics of the carbon buildup in the gas generator appeared generally as expected and consistent with that observed earlier during the high-power gas generator upgraded test series. The carbon buildup throughout the entire gas generator interior was soft and flaky as shown in Fig. 133. A relatively heavier buildup (about 1/8-inch thick) appeared only near the injector end fo the combustor wall, extending about 2 inches below the injector face. Along with some discrete localized barewall exposure between the outer row injector elements, minor surface erosion was found in four hot-spot locations. These locations coincided closely with those developed during the earlier gas generator component tests. The observed erosion occurred only in the last test of the demonstration series (Test Run 15.01) during which marked drift of test conditions occurred causing sizable change of exhaust gas temperature, from approximately 1460 F at start to 1730 F at shutdown. (The thermocouple connected to a sequencer for safety cutoff read 1525 and 1684 F, respectively, at the corresponding time slices.)

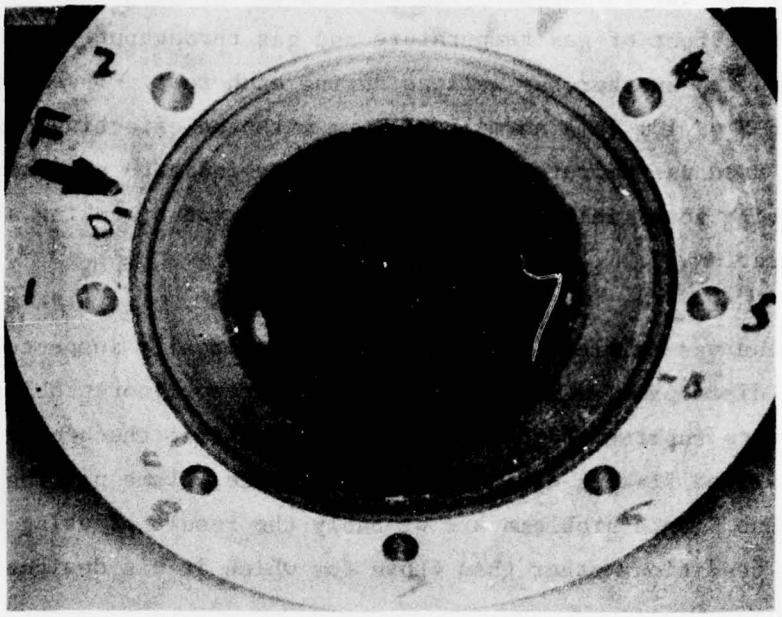

Figure 133. Gas Generator Combustor Wall After Starter Tests

The carbon buildup elsewhere on the combustor wall appeared quite thin (1/16 inch or less) and uniform. The carbon buildup on the chamber wall was partially cleaned only once for inspection during the hot-fire gas generator checkout test (after Test Run 2.05), and was kept undisturbed during all remaining tests for observation of continuous growth.

The carbon layer at the injector face shown in Fig. 134, which had not been disturbed throughout the entire test series (Run 1.03 to Run 15.01), was found to have accumulated to approximately 1/10-inch average thickness. The layer was quite uniform except for random formation of local buildup surrounding each of the injector elements. This localized carbon buildup crumbled quite easily by slight finger touch, and probably flakes off between test. The carbon buildup in the injector face observed during gas generator checkout tests (Run 2.05) is seen in Fig. 125. The injector was found to be free of any hardware discrepancy.

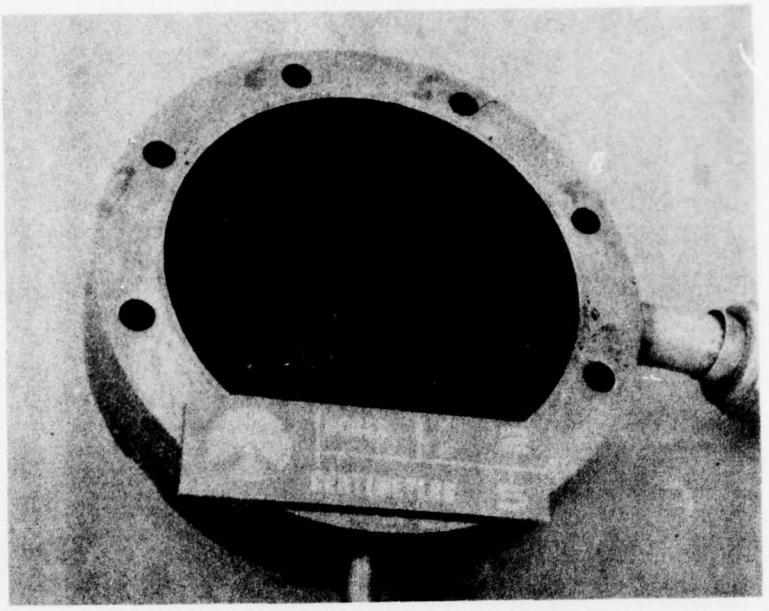

Figure 134. Injector Face After Starter Demonstrator Tests

The carbons found in the turbine manifold, nozzles, blades,and wheel are shown in Fig. 135 and 136. The carbon buildup is in the form of a thin soft layer that rubs off readily. The turbine components were also found to be covered with a film of bearing lubrication oil which may cause the soft carbon to adhere more tightly than it otherwise would. Oil leakage into the turbine manifold would not normally be encountered in an optimum flight system design.

PHASE II ASSESSMENT

The successful testing of the breadboard engine starter demonstrator, as a complete system with the gas generator, power turbine, and gearbox, clearly demonstrated the feasibility and practicality of a GOX/JP-4 IPU system for aircraft. As an aircraft engine starter, the demonstrator repeatedly achieved full acceleration of a typical aircraft engine (simulating the CFM56-2B) within sea level engine start time requirements of 26 seconds.

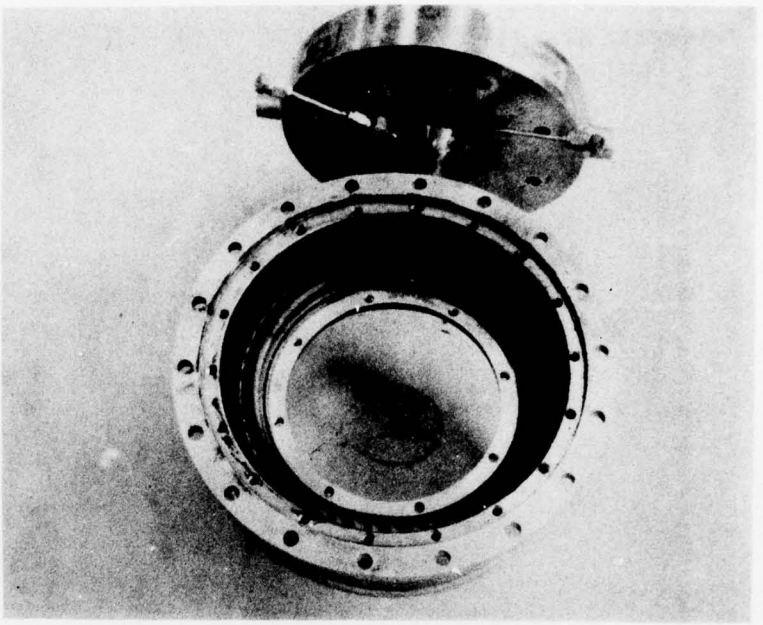

(a) Turbine Manifold

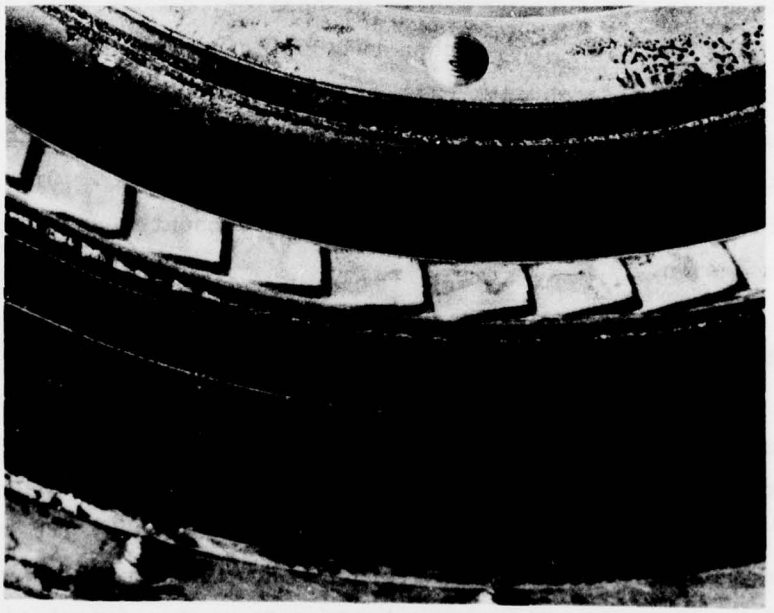

(b) Turbine Nozzles

Figure 135. Mk 44 Turbine Manifold and Nozzles After Starter Demonstrator Test

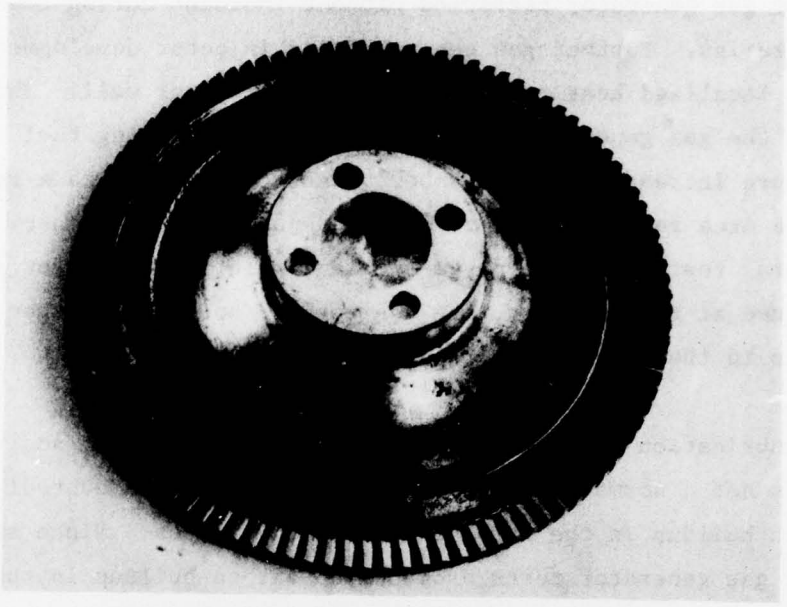

(a) Turbine Wheel

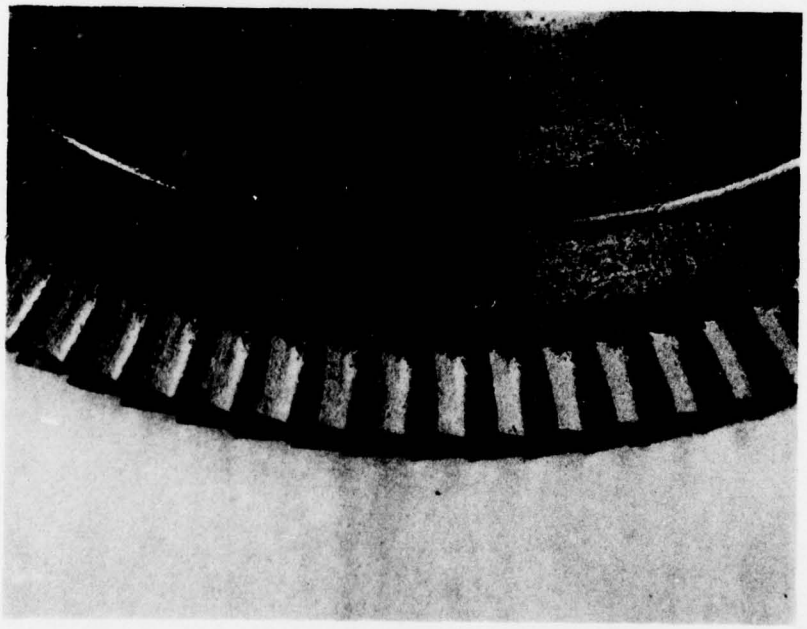

(b) Turbine Blades

Figure 136. Mk 44 Turbine Wheel and Blades After Starter Demonstrator Test

The high-power gas generator performed without incident during the demonstrator test series. Further gas generator and injector development will eliminate the localized heating problem on the combustor wall. The temperature rise in the gas generator was attributed to decreasing fuel flow as chamber pressure increased. The chamber pressure increase was a result of turbine nozzle area reduction due to carbon deposits. Preliminary analyses and experimental tests indicate purge-free and cold gas generator starts, with GOX assured at the injector, are achievable; however, further developmental efforts in these areas are recommended.

The bearing lubrication oil leakage into the turbine manifold and throughout the turbine is not a normal occurrence and the oil film undoubtedly contributed to carbon buildup in the turbine nozzles and blades. Since all previous long-duration gas generator tests produced no carbon buildup in the gas generator discharge nozzle, or in the Y-duct discharge nozzle, soft carbon buildup in the turbine nozzle probably would not occur with a clean dry surface.

CONCLUSIONS

Based on the successful experimental test results achieved in the development of the LOX/JP-4 low-power and high-power gas generators, and the subsequent successful demonstration of feasibility in using the LOX/JP-4, high-power gas generator in an IPU Engine Starter Demonstrator Unit, the following conclusions were reached:

1. In the experimental evaluation of the following types of LOX/JP-4 injectors in the low-power gas generator: augmented spark igniter (ASI), coaxial-element injector, and the triplet-element injector, reliable ignition, good combustion, throttleable operation, low carbon formation, and uniform hot-gas temperature was achieved by the triplet-element injector and, therefore, was selected for further development in the high-power gas generator.

2. The low-power gas generator, utilizing the LOX/JP-4, triplet-element injector, also demonstrated successful ignition and combustion with cold propellants (GOX at -240 F and JP-4 at -60 F); with hot propellants (GOX and JP-4 at 135 F); with low-cut JP-4 and JP-8 (Jet A) fuels; and at altitudes (simulated) over 74,000 feet.

3. The high-power gas generator utilizing the triplet-element injector and modified GOX injector orifice, which reduced GOX injection velocity and increased JP-4 fuel penetration for better mixing, achieved good ignition, stable combustion, throttleable operation and, in long-duration runs, stabilized formation of soft carbon. The 12-element injector spray pattern developed localized heating at the combustor wall near the injector, and the problem can be resolved through additional development testing.

4. The high-power gas generator, utilizing the LOX/JP-4 triplet-element injector, also demonstrated successful ignition and combustion with cold propellants (GOX at -170 F and JP-4 at -70 F) and with low-cut JP-4 and JP-8 (Jet A).

5. The IPU Engine Starter Demonstrator Unit, consisting of the LOX/JP-4 high-power gas generator, available power turbine, off-the-shelf gearbox, and a flywheel simulating an aircraft engine (CFM56-2B), has successfully achieved 11 hot-fired, full-acceleration start tests in succession. Engine starting was consistently demonstrated within 25.5 seconds with gearbox output power and speed of 228 horsepower and 7777 rpm, respectively. Posttest inspection indicated excellent hardware conditions. Soft carbon deposits were found in the turbine nozzles and rotor blades. The test-to-test "sawtooth" trace of gas generator chamber pressure indicated alternate buildup and spalling of the carbon formed.

6. The feasibility and practicality of using normally available, on-board aircraft LOX and JP-4 fuel for aircraft auxiliary power equipment have been amply demonstrated by the successful experimental testing performed on the LOX/JP-4 low-power and high-power gas generators and on the LOX/JP-4 IPU Engine Starter Demonstrator Unit. With the technical test results achieved, continued development of LOX/JP-4 power equipment for aircraft auxiliary power (APU), emergency power (EPU), and engine starter, or a super-integrated power unit (SIPU) which combines all of these functions, can be undertaken with confidence.

*U.S.Government Printing Office: 1979 — 657-002/454